



NEUTRONS
FOR SCIENCE®



ANNUAL REPORT
2012
INSTITUT LAUE-LANGEVIN

Publishing information

Editors: Giovanna Cicognani and Helmut Schober

Production team: Giovanna Cicognani, Alison Mader, Robert Corner and Susan Tinniswood

Design: www.synthese-eca.com - **Printing:** Imprimerie du Pont de Claix

Photography: Serge Claisse, ILL (unless otherwise specified)

Further copies can be obtained from Institut Laue-Langevin

Scientific Coordination Office (SCO)

BP 156 F-38042 Grenoble Cedex 9 (France)

Email: sco@ill.eu - web: www.ill.eu

DIRECTOR'S FOREWORD

1

4

WHAT IS THE ILL

2

6

SCIENTIFIC HIGHLIGHTS

3

8

MILLENNIUM PROGRAMME
AND TECHNICAL DEVELOPMENTS

4

72

EXPERIMENTAL
AND USER PROGRAMME

5

90



CONTENTS

ILL Annual Report 2012

CONTENTS

2
3

REACTOR OPERATION

6

100

MORE THAN SIMPLY NEUTRONS

7

104

WORKSHOPS AND EVENTS

8

110

ADMINISTRATIVE MATTERS

9

118

PUBLICATIONS

10

124



Endurance

It is now more than 40 years since the first neutron experiments were conducted at ILL, and although accounts vary over what was the first sample to be studied, and who carried out the measurement, there is no dispute that by the end of the 1970s the ILL had established itself as a world-leading centre for science. That remarkable success is a testament to the vision and skill of ILL's founding fathers and the band of pioneering scientists, engineers and technicians who created it. What is also remarkable is how well ILL has stood the test of time: it still leads the field of neutron science and technology and far from being an 'old' or even 'middle-aged institute', almost every technical component between the source and the detectors on our instruments has been upgraded at least once.

The latest cycle of reincarnation – the Millennium Programme - has brought astonishing gains, increasing the average detection rate across the instrument suite by a factor of more than 24 already, and transforming the scope and capacity of the science we support

The latest cycle of reincarnation – the Millennium Programme - has brought astonishing gains, increasing the average detection rate across the instrument suite by a factor of more than 24 already, and transforming the scope and capacity of the science we support. 2012 saw first neutrons on the third small-angle instrument D33, optimised for magnetic studies from day one, and with a time-of-flight option that enables

structure to be studied on an unprecedented range of length-scales in a single shot. We also welcomed back the greatly upgraded cold triple-axis CRG spectrometer IN12, which now contends with our public instrument IN14 as class-leader, and throws down the gauntlet to the team who will upgrade it to ThALES. And the cold-neutron Laue instrument LADI returns to a new position with a new guide, boosting its flux and pushing back the boundaries of biological crystallography way beyond what seemed reasonable 5 and more years ago.

The Millennium Programme still has two years to run, but the process of renewal should not end there. It is vital to the health both of our Institute and the broader scientific community that we continue to explore and exploit the limits of what is possible in instrumentation. To this end, four years of consultation and planning will deliver in 2013 the case for the next wave of our upgrade Programme, christened 'Endurance' to signal our aim to continue to lead for years to come. 2013 will therefore be crucial for ILL: approval and funding for the Endurance Programme will not only lever significant further improvements in performance, but much of the technical development we propose should also be applied further afield in other neutron centres. Not least among these will be the next-generation European Spallation Source in Lund as it ramps up to full scientific strength by the end of the next decade.

Elsewhere at the ILL other major projects abound. Post-Fukushima work is well underway to strengthen our defences further against yet more improbable circumstances: in this we are very fortunate to be able to receive prompt and generous




additional funding from our Associates, strong political support from our host country, France, and tremendous expertise and determination on the part of many ILL staff to deliver this project. We will also soon have a new 'Science Building', funded by the city of Grenoble and the Rhône-Alpes region, to house facilities shared with the ESRF: a common theory group, joint chemistry laboratories and the Partnership for Soft Condensed Matter will all be housed therein, together with members of both institutes to establish a vigorous new scientific community, particularly for large-scale structures. Further afield, the rest of the 'Presqu'île Scientifique' is also in the midst of major reconstruction, with new facilities for research, innovation and education promised for the members of the GIANT partnership (ILL, ESRF, EMBL, with the laboratories of the CEA and CNRS as well as local universities). The accent on 'innovation' marks a new departure for ILL, with additional funding to establish with ESRF new interface facilities for industrial users.

Of course the real strength of ILL is human – represented both by expert staff and a vibrant user community – and we paid tribute to some of them in 2012. We celebrated two 80th birthdays in 2012: that of the neutron itself – or rather its first public announcement by James Chadwick – as well as Philippe Nozières, the first head of our theory group and still playing a key role in the intellectual life of the ILL. We feted the remarkable contribution of his successor, Efim Kats, as well the many and varied contributions of Alan Hewat – one of that original pioneering band referred to above – and Joe Zaccai, whose has done so much to bring biology to the ILL, and vice versa. We also saw the departure of José Luis Martínez Peña,

who came to the end of his term of office as French Associate Director: José Luis brought great clarity and rigour to the planning and delivery of the Millennium Programme – indeed to all aspects of the life of ILL in which he was involved – and we salute him for that: muchas gracias y hasta pronto! He gives way to Charles Simon, a long-term user of ILL who brings much "savoir-faire" in matters scientific, technical and political. Finally, we note the passing of the "baton" from Martin Walter to Manuel Rodriguez-Castellano as Head of Administration. Martin held the fort magnificently during an unexpected interregnum period, while Manuel brings decades of experience working for our neighbours, the ESRF: bienvenido !

Of course this is all part of the much broader renewal of staff who have contributed in very different but no less crucial ways. This point is made most clearly each year at the General Assembly for retired ILL staff: looking out towards old friends and colleagues in our Chadwick Amphitheatre it is humbling to be reminded of the roles they have played in ILL's success. This success is all the more remarkable for the diversity of the actors, with very different skills and cultural backgrounds yet bound through the generations to a common purpose: truly an example of a 'Europe that works'.



Director of the ILL



About the ILL

Why neutron scattering is useful

About the ILL

The Institut Laue-Langevin (ILL) is an international research centre at the leading edge of neutron science and technology, where neutrons are used to probe the microscopic structure and dynamics of a broad range of materials at molecular, atomic and nuclear level.

The ILL is owned by the three founding countries - France, Germany and the United Kingdom. The three Associate member countries contributed a total of about 68 M€ to the Institute in 2012, a sum enhanced by significant contributions from the ILL's Scientific Member countries, Austria, Belgium, the Czech Republic, Hungary, India, Italy, Poland, Spain, Slovakia, Sweden and Switzerland. ILL's overall budget in 2012 amounted to approximately 106 M€.

The Institute operates the most intense neutron source in the world, based on a single-element, 58.3 MW nuclear reactor designed for high brightness. The reactor normally functions round-the-clock during four 50-day cycles per year, feeding

neutrons to a suite of 40 high-performance instruments that are constantly upgraded.

As a service institute, the ILL makes its facilities and expertise available to visiting scientists. Our user community is world-wide: every year, about 2000 researchers from more than 30 countries visit the ILL to perform over 800 experiments selected by a scientific review committee.

The ILL monitors the papers published as a result of the use of our facilities, of which there are more than 600 per year. We pay particular attention to papers published in high-impact journals. About 80 such papers are published per year from data taken on ILL instruments.

The Institute has a Director and two Associate Directors who represent each of the Associate countries and are appointed on short-term contracts, normally for five years. A Scientific Council, comprising external scientists from the member countries, advises the Directors on scientific priorities

Why neutron scattering is useful

When used as a probe for small samples of materials, neutron beams have the power to reveal what is invisible using other radiations. Neutrons can appear to behave either as particles or as waves or as microscopic magnetic dipoles and it is these specific properties which enable them to uncover information which is often impossible to access using other techniques.

WAVELENGTHS OF TENTHS OF NANOMETERS

Neutrons have wavelengths varying from 0.01 to 100 nanometers, which makes them an ideal probe of atomic and molecular structures ranging from those consisting of single atomic species to complex biopolymers.

ENERGIES OF MILLIELECTRONVOLTS

The associated energies of millielectronvolts are of the same magnitude as the diffusive motions of atoms and molecules in solids and liquids, the coherent waves in single crystals (phonons and magnons) and the vibrational modes in molecules. An energy exchange between the incoming neutron and the sample of between 1 μeV (even 1 neV with spin-echo) and 1 eV can easily be detected.

MICROSCOPICALLY MAGNETIC

Neutrons possess a magnetic dipole moment which makes them sensitive to magnetic fields generated by unpaired electrons



for the Institute and how to develop the instrument suite and technical infrastructure in order to best meet the needs of the user research programme. It also assesses the scientific output of the Institute. Our governing body is the Steering Committee, which meets twice yearly and is made up of representatives of the Associates and the Scientific Members together with the Directors and Staff Representatives. Within the framework of the Intergovernmental Convention, the Steering Committee has the ultimate responsibility for determining operational and investment strategies for the Institute.

NEUTRONS AND SOCIETY

The scope of the research carried out at the ILL is very broad, embracing condensed matter physics, chemistry, biology, materials and earth sciences, engineering, and nuclear and particle physics. Much of it impacts on many of the challenges facing society today, from sustainable sources of energy, improved healthcare and a cleaner environment to new materials for information and computer technology.

For example, neutron scattering experiments have given us new insights into the structure and behaviour of biological and soft condensed matter, important in designing better drug delivery systems or improving polymer processing. They also provide a unique probe into the phenomena that underpin high-temperature superconductivity or the molecular magnetism that may provide the technology on which the computers of the future are based.

PREPARING FOR THE FUTURE

In 2000, the ILL launched an ambitious programme to modernise its instruments and infrastructure called the ILL Millennium Programme, whose aim was to optimise the ILL's instrument suite (Phase M-0: 2000-2007; Phase M-1: 2008-2014). We are now looking forward to and setting the scene – in the framework of our Endurance programme - for developments still further into the future, in order to maintain the Institute's world-leading position for another 20 years.

in materials. Precise details of the magnetic behaviour of materials at the atomic level can be investigated. In addition, the scattering power of a neutron by an atomic nucleus depends on the orientation of the spin of both the neutron and the atomic nuclei in a sample, thereby providing a powerful tool for detecting the nuclear spin order.

ELECTRICALLY NEUTRAL

Neutrons are electrically neutral and so can penetrate deep into matter, while remaining non-destructive. This makes them an ideal probe for studying, for example, biological samples or engineering components under extreme conditions of pressure, temperature or magnetic field, or within chemical-reaction vessels.

HIGH SENSITIVITY AND SELECTIVITY

The variation of scattering power from nucleus to nucleus in a sample varies in a quasi-random manner, even in different isotopes of the same atom. This means that light atoms are visible in the presence of heavy atoms and atoms that are close to one another in the periodic table may be distinguished from each other. This introduces the possibility of using isotopic substitution (for example deuterium for hydrogen or one nickel isotope for another) to allow contrast to be varied in certain samples thereby highlighting specific structural features.

In addition, neutrons are particularly sensitive to hydrogen atoms and therefore they are a powerful probe of hydrogen storage materials, organic molecular materials, and biomolecular samples or polymers.



Magnetism
Materials
Soft matter
Biology
Liquids and glasses
Nuclear and particle physics
Modelling and spectroscopy
Theory

100 years ago Max von Laue, Walter Friedrich and Max Knipping, three young scientists from the University of Munich, dropped an envelope into the letterbox of the Bavarian Academy of Sciences. Along with a sketch of their experimental apparatus and a few clichés of their data, the envelope contained a one-page hand-written letter reporting the discovery of interference patterns produced when X-ray beams passed through crystals. The authors certainly had sufficient foresight to sense the importance of their work. In fact, just two years later the instigator of the experiment, Max von Laue, received the Nobel Prize. However, even the most daring visionaries could not have imagined just how much this discovery and the subsequent development of diffraction studies would change the world. At the time of Laue's experiment, details of the microstructure of matter were really only just emerging. The existence of atoms composed of electrons and nuclei was a brand new concept. The diffraction of X-rays not only made it possible to determine the exact position of atoms in space but also shed light on the physical nature of these hitherto mysterious waves.

The scientific highlights presented in this year's annual report demonstrate how research with neutrons continues to push back the frontiers of science

The idea put forward by Laue to justify the now famous experiment was erroneous and, recognising this, his peers tried to dissuade him from pursuing his plans. However, Laue's perseverance paid off in the end, demonstrating that science, not unlike other human endeavours, progresses along a winding road with many turns that do not always have to be taken for the right reasons. In any case, the time was ripe for the discovery and if it had not been Laue's obstinacy, sooner or later some other idea would have precipitated the event. The philosophers among us may wonder whether this same inevitability is inherent in all scientific discoveries.



In any event, the resulting experimental ability to scrutinise matter on atomic length scales, combined with the theoretical understanding developed in parallel, paved the way for the technological and scientific revolution of the 20th century. It is indeed difficult to imagine how transistors, integrated circuits and micro- and nanoelectronics could have come about without access to the structure and dynamics of matter at the atomic level. And the same deep level of understanding is needed when it comes to engineering materials at the molecular level or influencing the molecular processes that govern living organisms.

By giving science access to the technological progress it helped bring about, it has been possible to develop increasingly sophisticated experimental equipment, which in turn has stimulated still further technological progress. In particular, the seemingly never-ending increase in computing power has given a tremendous boost to the investigation of matter. Crystallography, for example, has reached a level of sophistication that no one could have anticipated even a few decades ago. Thanks to the use of modern database technology, we are fast approaching a situation where most structures are just a mouse click away.

For quite some time diffraction studies were the domain of X-rays, even if electrons did try to enter the game in the 1930s. Scientists realised the potential of neutrons as an ideal scattering probe, in particular in the field of magnetism and for the investigation of dynamics at the atomic level, soon after their discovery. However, it was only with the advent of dedicated powerful neutron sources, in which the ILL played a pioneering role, that routine neutron diffraction and spectroscopy became possible. The role of neutrons as a major player in modern analytical science has never been questioned since. By exploiting modern technologies to improve, in particular, neutron transport and detection, neutron sources have been able to retain their market share of research,

even in the face of stiff competition from a host of alternative techniques, including the latest generation X-ray sources.

The scientific highlights presented in this year's annual report demonstrate how research with neutrons continues to push back the frontiers of science by allowing scientists to decipher the structure and dynamics of ever more complex materials with steadily increasing precision. Highlighting the importance of neutrons in the field of magnetism, the report contains a number of fascinating stories about magnetic structures and excitations. Material properties are also covered over a wide range of applications, from graphene sheets in solution to active carbon and crack retarders in aircraft structures. Membranes and other biological molecular arrangements are explored from various angles, always with the aim of helping to further our understanding of biological functions. The broader field of liquids and soft matter holds the promise of exciting applications in molecular engineering, such as the production of organic electronic devices. Two particularly outstanding results from the area of fundamental physics are the measurement of the refractive index of silicon for gamma rays and the excitation of transitions between gravitational quantum levels of ultra cold neutrons. Finally, you should not miss the contributions from the ILL theorists, which provide fascinating insight into correlated electronic states, spin transport and membrane stability. 2012 has been a marvellous year for science at the ILL and I hope you enjoy reading about some of our successes.

Helmut Schober

Helmut Schober
Associate Director




ILL in the press

- 1 - Published in *Chemistry World* on 19 July 2012.
- 2 - Published in *LABOR PRAXIX* on 8 August 2012.

- 3 - Published in *WIRED* on 19 June 2012.
- 4 - Published in *Le Figaro* on 24 May 2012.

- 5 - Published in *Le Monde* on 6 October 2012.
- 6 - Published in *EL PAIS* on 5 June 2012.


1



Guided by the light of a neutron candle

19 July 2012 Philip Robinson

It is 80 years since James Chadwick discovered the neutral sub-atomic particle and 40 years since the Laue-Langevin Institute opened its doors. To celebrate, Philip Robinson visits the most intense neutron source in the world



On the outskirts of Grenoble, the Laue-Langevin Institute (ILL) sits at the junction of the Isère and Drac rivers, nestled at the foot of the French Alps. Although dwarfed by its Alpine surroundings, the ILL is a scientific colossus. Within its walls a nuclear reactor runs day and night solely to provide one of the most powerful analytical tools available to science: the neutron.

Just as today's physicists across the Alps at Cern are turning subatomic particles inside out to uncover the source of the universe's missing mass, their forebears were perplexed by a similar conundrum. The mismatch between the mass of an atom and its atomic number was only solved by James Chadwick's discovery of the neutron 80 years ago. Since then, the neutron has become one of scientists' most powerful allies, with researchers from around the globe flocking to sites such as the ILL to make use of neutrons in their research.

3



Haemoglobin's internal thermometer adapts to body temperature

By Liel Clark | 19 June 12



SCIENCE

Technology | Culture | Science | Business | Gaming | Ideas Bank | Geek Gad

HOME NEWS REVIEWS VIDEOS MAGAZINE PODCAST TOPICS

Technology | Culture | Science | Business | Gaming | Ideas Bank | Geek Gad

Home > News > Science > Haemoglobin evolution

SCIENCE

Haemoglobin's internal thermometer adapts to body temperature

By Liel Clark | 19 June 12

5



Des neutrons toujours percants

Depuis quarante ans, ces particules aident à explorer le cœur de la matière. Visite de l'un des fleurons mondiaux de cette technique, l'Institut Laue-Langevin à Grenoble

Science & Techno

Depuis quarante ans, ces particules aident à explorer le cœur de la matière. Visite de l'un des fleurons mondiaux de cette technique, l'Institut Laue-Langevin à Grenoble

Des chercheurs ont percé les secrets d'une molécule: ses interactions avec l'eau

2



Wie Myoglobin ohne Wasser auskommt

Mithilfe der Neutronenstreuung haben Forscher am Beispiel des Myoglobins herausgefunden, dass Proteine auch ohne wässrige Umgebung ihre grundlegenden biologischen Funktionen erfüllen können. Diese Erkenntnisse helfen bei möglichen Anwendungen von Protein in biochemischen Gassensoren oder neuartigen Wunderbinden

Die Wissenschaftler von links nach rechts: Martin Wahl, François-Xavier Gallet (Mitte) von ILL und Jérôme Cornet (rechts) (Foto: ILL/ILL)

Grenoble/Frankreich, Bristol/Großbritannien, Canberra/Australien, Garching, Jülich – Proteine können auch ohne wässrige Umgebung ihre grundlegenden biologischen Funktionen erfüllen. Dies fanden Wissenschaftler vom Institut de Biologie Structurale (IBS) in Grenoble, der Universität Bristol, der australischen nationalen Universität, dem Institut Laue-Langevin und dem Jülicher Zentrum für Forschung mit Neutronen heraus. In einem kürzlich veröffentlichten Beitrag zeigte das Team mithilfe der Technik der Neutronenstreuung, dass sich Myoglobin genau so bewegt, als ob es von Wasser umgeben wäre, wenn es in eine Hülle von Polymeren eingeschlossen ist. Myoglobin ist ein im Muskelgewebe von Wirbeltieren vorkommendes, Sauerstoff bindendes Protein. Diese Bewegungen sind für die Erfüllung der biologischen Funktionen eines Proteins wesentlich und die Ergebnisse machen Proteine zu einem entwicklungs-fähigen Material für neue Wunderbinden oder sogar chemische Gassensoren.

4



Le neutron «fête» ses 80 ans cette année

Notas clés : Neutron, Physique, Grenoble, James Chadwick, Institut Laue-Langevin

Par Marc Messier

Publié le 24/05/2012 à 22:27 Réactions (8)

Facebook 48 Twitter 18 LinkedIn 11 share 13 Recommander

L'Institut Laue-Langevin de Grenoble s'apprête à célébrer les 80 ans de la découverte du neutron. Cette étonnante particule subatomique a permis de réaliser des avancées considérables en physique mais aussi en biologie et en médecine.

Il y a 80 ans, le physicien britannique James Chadwick confirma l'existence du neutron, une particule subatomique dénuée de charge électrique (d'où son nom). Outre son importance capitale sur le plan fondamental, cette découverte qui valut à son auteur le prix Nobel de physique, a eu des répercussions considérables dans un très grand nombre de domaines scientifiques. En physique bien sûr mais aussi, et de plus en plus, en biologie et en médecine.

Du fait de leur charge électrique nulle, les faisceaux de neutrons, comme ceux produits à l'Institut Laue-Langevin (ILL) de Grenoble, ont la capacité de pénétrer très profondément dans la matière où ils viennent interagir avec les noyaux atomiques. En réaction, ces derniers les ralentissent et les dévient de leur trajectoire, ce qui permet de scruter la matière avec une précision hallucinante de l'ordre de l'ångström (soit 1 dixième de milliardième de mètre). De quoi déterminer la structure de molécules complexes, comme les protéines, mais aussi leur dynamique dans un milieu liquide par exemple.

La source la plus intense au monde

6



Rayos de neutrones para captar casi todo

El laboratorio europeo ILL utiliza un reactor nuclear para adentrarse en la materia sin destruir

MALEN RUIZ DE ELVIRA | Madrid | 5 JUN 2012 - 20:32 CET

Archivado en: I+D+I | Bases | Política | Cultura | Física | País Vasco | Ciencias exactas | España | Investigación científica | Ciencia

Experimento en uno de los instrumentos de la Fuente de neutrones del Instituto Laue-Langevin (ILL) en Grenoble, / 2012

7 - Published in *New Scientist* on 23 January 2012.

9 - Published in *EL CULTURAL* on 15 November 2012.

8 - Published in *La Stampa* on 4 June 2012.

10 - Published in *Science* on 8 May 2012.

11 - Published in *BBC NEWS* on 23 January 2012.

7

NewScientist
Home News In-Depth Articles Blogs Opinion TV Galleries Topic Guides Last Word Blog
SPACE TECH ENVIRONMENT HEALTH LIFE PHYSICS&MATH SCIENCE IN SC

One Per Cent
Taking the sweat out of technology

Magnetic soap could clean up oil spills
22:00 23 January 2012
Green Tech
Jacob Aron, technology reporter

(Image: KeystoneUSA-ZUMA/Rex Features)

A soap that responds to magnetic fields could be used to clean up oil spills without leaving behind detergents that can harm surrounding wildlife.

Researchers at the University of Bristol, UK dissolved iron particles in water that contained chlorine and bromine ions, materials which are commonly found in household products such as mouthwash or fabric cleaner. This created a metallic centre within the soap particles that could be influenced by a nearby magnetic field.

The team tried out their new soap by placing it in a test tube beneath layers of water and an oil-like substance. Using a magnet, they were able to overcome both gravity and surface tension to lift the soap through the layers and out of the tube.

This test shows that it is much easier to remove magnetic soaps from mixtures of other liquids, suggesting they could be used in response to environmental disasters such as oil spills, where

9

EL CULTURAL.es 15/11/2012 El Cultural en PDF Alta suscripciones Conectar Recibir boletín ELOMUNDO.es

Inicio | Libros | Arte | Escenarios | Entrevistas | Cine | Opinión

Blog: Agenda Premios Libros más vendidos Exposiciones Estrenos Arte internacional Álbumes Vídeos Editores Primeros capítulos RSS

CIENCIA
09/11/2012
Asteroides: ¿principio y fin de la vida? - Origen y composición de estos cuerpos ante la XII Semana de la Ciencia

¿Qué se puede hacer con los neutrones?
El 1 de junio se cumplen 80 años del artículo de James Chadwick confirmando su existencia

Resultados: ★★★★★

Antonio RUIZ DE ELVIRA | Publicado el 01/06/2012 | Ver el número en PDF

Verlos aniversarios recatan al neutrón de las profundidades de la materia. Hoy se cumplen 80 años del artículo del físico James Chadwick en el que confirmaba su existencia. Se celebran además los 40 de los primeros experimentos en el Institut Laue-Langevin, en Grenoble, y los 25 de la incorporación de España a la institución.

Microfotografía de un único átomo de oro. De "Cielo y Tierra" (Phaidon).

10

Science AAAS.ORG | FEEDBACK | HELP | LIBRARIANS

Daily News Enter Search Te

NEWS SCIENCE JOURNALS CAREERS BLOGS & COMMUNITIES MULTIMEDIA COLLECT

Home > News > ScienceNOW > May 2012 > Gamma-Ray Bending Opens New Door for Optics

Science NOW UP TO THE MINUTE NEWS FROM SCIENCE

Science LIVE
Every Thursday at 3:00 p.m. EST
Upcoming: The Genes We Eat 15 November

Gamma-Ray Bending Opens New Door for Optics
by Jon Cartwright on 8 May 2012, 4:20 PM | 0 Comments

Lenses are a part of everyday life—they help us focus words on a page, the light from stars, and the tiniest details of microorganisms. But making a lens for highly energetic light known as gamma rays had been thought impossible. Now, physicists have created such a lens.

RECENT ARTICLES

ENLARGE IMAGE

8

LA STAMPA.it SCIENZA

EDIZIONI LOCALI: TORINO • CUNEO • AOSTA • ASTI • NOVARA • VCO • VERCELLI • BIELLA • ALESSANDRIA

ATTUALITÀ OPINIONI ECONOMIA SPORT TORINO CULTURA SPETTACOLI MOTORI DONNE

HOME | POLITICA | ESTERI | CRONACHE | COSTUME | TECNOLOGIA | SCIENZA | AMBIENTE | LAZ

IL CIELO
04/06/2012

Buon compleanno al neutrone e alla luce X

PIERO BIANUCCI
TORINO
Nessuno lo ha festeggiato, ma il 1° giugno il neutrone ha compiuto ottant'anni. Circa la metà dell'universo che vediamo, o quindi anche del nostro organismo, è fatto di neutroni. Sarebbe una buona ragione per ricordarsi del compleanno.

Eppure nessuno si è accorto che proprio il 1° giugno del 1932 James Chadwick (foto) pubblicò

11

BBC NEWS SCIENCE & ENVIRONMENT

Home UK Africa Asia Europe Latin America Mid-East US & Canada Business Health Science

23 January 2012 Last updated at 23:09 GMT

Magnetic soap could help in oil spill clean-ups

An international team of scientists has demonstrated the first soap that responds to magnets.

This means the soap and the materials that it dissolves can be removed easily by applying a magnetic field.

Experts say that with further development, it could find applications in cleaning up oil spills and waste water.

More articles on:
<http://www.ill.eu/news-events/press-room/ill-in-the-media/>

COLLEGE 1 - APPLIED METALLURGY, INSTRUMENTATION AND TECHNIQUES

Authors: **D.J. Hughes** (Chair) and **G. Cuello** (Secretary)

It is often the case that neutrons are associated very closely to *fundamental* scientific investigations, pushing forward mankind's understanding of the behaviour of matter. However, studies that are closely aligned to applications in the *real world* are also feasible and these are the types of project that are generally assessed within the College. The scope of *Applied Science* at ILL is wide, varied and state-of-the-art, recently covering diverse subjects such as predicting lifetimes of weldments in nuclear power plants and manufacturing processes in 15th century gunshot. Indeed, recently accepted proposals are equally exciting, including turbocharger manufacturing techniques, *in-situ* aluminium casting experiments and an exciting investigation which may lead to the identification of a new species of extinct mammal by using inelastic scattering techniques. We look forward to reading about the results in the next Annual Report!

In this Annual Report we present three studies, all employing neutron scattering but each with an eye on important applications. The first highlight relates to crack retarding structures in aircraft airframes in a project in collaboration with Airbus and Alcoa (p. 30). The group from The Open University investigated a fibre-reinforced composite strap which was bonded to aluminium alloy. In particular the stresses arising during the adhesive bonding process were of concern as they can strongly affect the damage tolerance of the aircraft. Using SALS, they show that the stresses arising from the bonding process were low and that the beneficial stresses around cold-expanded holes were largely unchanged. A second highlight studied activated carbon in order to see how mixtures of gas/vapour are adsorbed in its micropores. Thanks to SANS experiments, the group led by the Budapest University of Technology and Economics observed that the interaction of adsorbed molecules is substantially modified by the confining walls, opening new perspectives for green chemistry (p. 34).

Graphene continues to stimulate enormous interest regarding potential applications based on its remarkable mechanical and electrical properties (just funded as EU flagship project). In another SANS experiment, a group led by Imperial College studied the morphology of graphene sheets in solution, and developed a method for producing bulk quantities of individually dispersed monolayer graphene sheets (p. 32).

The potential for ground-breaking applied science using instruments at ILL is continuing to gather momentum as key instruments come on-line or are improved as part of the *Endurance* programme. For example a proposed Super-SALS would utilise a polychromatic beam, significantly widening the range of application for the instrument and opening up the possibility of *in-situ* measurements during important manufacturing processes.

COLLEGE 2 - THEORY

Author: **T. Ziman** (ILL Theory Group)

Activity in the College was in subjects within a spectrum ranging from soft condensed matter, relevant to biological materials, to the physics of artificially nano-structured materials and to materials more accessible to conventional neutron diffraction in crystalline form. The methods were of analytical mathematics or more numerical approaches, which can relate microscopic parameters to observables, or a combination of the two.

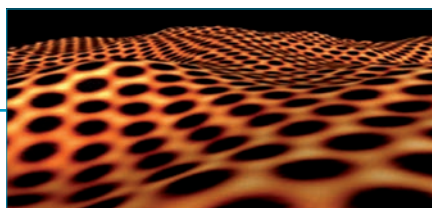
While we aim to relate our calculations to the experimental world, the relevance to neutron results is not necessarily immediate: for example in the case of the work on stress and rupture of fluid membrane vesicles (p. 68) the relevance is to the general issue of the relation of form (which is accessible to imaging by neutrons) and function (which is central to the biological functions in cells). More directly applicable to neutron experiments are calculations of thermal mean-square displacements of hydrogen in proteins and the structure and dynamics of short strong hydrogen bonds (in collaboration with Scientific Computing). A thesis recently initiated in the college is devoted to simulations of the structure and dynamics of water in proton-conducting membranes, relevant to ILL experiments by small-angle and quasi-elastic neutron scattering. Turning to "hard" condensed matter physics, in the discussion of the spin Hall effect (p. 70) in ferromagnetic nanowires, the ultimate aim is to identify the relevant bulk properties controlling skew scattering in metallic ferromagnets, in this case non-linear spin susceptibilities, which might then be studied in more detail microscopically using neutron scattering from larger samples. Other work involved the physics of Andreev currents in ferromagnetic-superconducting interfaces. The impetus of the study came from bulk electrical and thermal conductivity measurements on specially fabricated superconducting "spin-valves", *i.e.* superconducting/multidomain ferromagnet/metallic tunnel devices, but the results show that the current-voltage profiles depend primarily on the exchange field, accessible by neutron diffraction. The behaviour near the interfaces can be revealed by neutron reflectivity studies on ferromagnetic and superconducting films. As a final example, in bulk correlated systems (p. 66) a new interpretation has been provided for the boundary of the "pseudo-gap" phase of Copper-oxide-based high-temperature superconductors, which are extensively studied by neutron inelastic scattering. This advances the understanding of this phase, peculiar to the phenomenology of cuprate superconductors, and also relates the thermodynamics to a microscopic Hubbard model via state-of-the-art calculations of correlated electrons, which can be extended to materials with more general electronic structures.

COLLEGE 3 - NUCLEAR AND PARTICLE PHYSICS

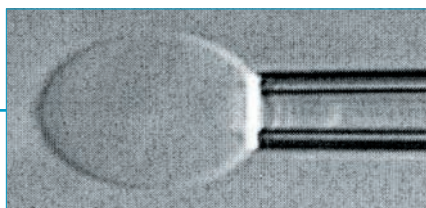
Authors: **W. Korten** (Chair) and **M. Simson** (Secretary)

Nuclear and particle physics at the ILL covers fundamental physics topics as searches for additional forces, but also ranges to applied physics topics like the production of radioisotopes for medical imaging and radio-nuclear therapy. Throughout the past years there is a strongly increasing demand to do nuclear physics experiments on a neutron beam. Albeit the intensity of a neutron beam is much lower than inside a reactor, it offers much cleaner conditions as well as access to nuclei with very short lifetimes. During the last reactor cycle in 2012 an array of 16 germanium detectors was installed at the cold neutron beam line PF1B in order to perform high-resolution gamma-ray spectroscopy. Several very successful (n, gamma) measurements as well as a neutron-induced fission campaign of ²³⁵U for the study of neutron-rich exotic nuclei were completed by a large user community of about 50 persons. A total of 20 TB of data was produced so far and is now available for analysis by the users. Measurements will continue in spring 2013.

A surprising discovery with huge potential impact in the field of gamma ray optics was made during the last year. While a non-zero refractive index for visible light is a well-known phenomenon it was thought to be going to



Applied metallurgy, instrumentation and techniques
cf. article "The structure and morphology of charged graphene sheets in solution" p. 32



Theory
cf. article "Rupture of a biomembrane under dynamic surface tension" p. 68



Nuclear and particle physics
cf. article "Measurement of the refractive index of Silicon for Gamma Rays" p. 56

zero for higher radiation energies for any material. Using the ultra-high resolution crystal spectrometer GAMS a deviation of the refractive index of silicon from zero was found for gamma ray energies above 700 keV in a recent measurement. This discovery may lead to the construction of optical devices for gamma rays (*e.g.*, lenses), which in turn would be a huge leap forward for medical imaging and cancer treatment, but also for characterisation of nuclear materials and radioactive waste.

Using ILL's long standing ultracold neutron source PF2, the qBounce collaboration measured the transitions between the quantum states of neutrons in earth's gravitational field with unprecedented accuracy. This result allows putting new limits on the nature of dark energy. The new beam position H172B for the development of a new source of ultracold neutrons was commissioned in autumn and the first measurements on UCN production performed. This new position allows optimising both UCN production and extraction.

COLLEGE 4 - MAGNETIC EXCITATIONS

Authors: **E. Blackburn** (Chair) and **E. Wheeler** (Secretary)

Inelastic neutron scattering is essential for studying magnetic and electronic excitations. This leads to high demand for experimental time on both time-of-flight instruments (TOF) and triple axis spectrometers (TAS), and provides interesting challenges for the selection panel. Single crystal experiments on the IN5 TOF spectrometer are now in strong demand, and the spectrometer was used to great effect by Baker *et al.* (p. 18) to map the four dimensional scattering function of single-crystal molecular nanomagnets. In their work on a Cr₈ antiferromagnetic ring, they showed that the dynamics of the system could be described without recourse to input from theoretical Hamiltonian models, demonstrating the fundamental role of neutron scattering to understanding magnetic systems. The wide coverage provided by IN5 was essential for this.

There has been strong growth in the area of frustrated magnetism, where the competing interactions that are a signature of frustration lead to the creation of exotic ground states with unusual excitations. For example, using the TOF spectrometer IN5, Fak *et al.* (p. 16) have observed novel spin correlations in a powder sample of kapellasite, which appears to have a 2D Kagome lattice. These correlations pointed towards a gapless quantum spin liquid ground state.

Quantum magnetism also continues to provide new fields of study. Here, we highlight the work of Mourigal, Enderle *et al.* (p. 22) in their investigation of LiCuVO₄ using IN14 and polarised neutron analysis on IN20. To understand the dynamics of this chiral system, polarised neutron analysis was indispensable. As a frustrated spin-chain system, it had previously been shown to be an interesting quantum magnet and now in an applied magnetic field they have evidence for a bond-nematic quantum state.

Long-term studies of unconventional superconductors and unconventional magnets continue to provide new insights. An exciting new result to come out of the TAS instrument IN14 is the work on the well-studied heavy fermion antiferromagnet CeB₆ by Inosov *et al.* (p. 20), where magnetic resonant mode was seen in the antiferromagnetic state, with strong similarities to that seen in some unconventional superconductors. The multi-detector Flatcone option allowed them to measure strong resonance peaks and weak streaks of scattering

simultaneously. IN14 will be upgraded to Thales during the long-shut down this summer and we look forward to an even higher performing instrument.

COLLEGE 5A - CRYSTALLOGRAPHY

Authors: **R. Walton** (Chair) and **M. Brunelli** (Secretary)

The College is concerned with the study of the atomic-scale structures of the solid state, both in the form of single crystals and polycrystalline powders, and considers applications for beamtime on a suite of diffractometers, each of which is optimised to provide data of the resolution and sample geometry required for specific experiments. The classical advantages of neutron diffraction are a vital tool in the crystallographic study of numerous functional solids; the accurate location of low atomic number elements in the presence of those with high atomic number, which is extremely difficult by X-ray diffraction. Neutron diffraction now forms the basis of the full characterisation of many important classes of materials for emerging applications. This is particularly important in the field of energy, where, for example, in solid-oxide fuel cell materials oxygen positions must be determined in the presence of metals, and in rechargeable battery materials the position of lithium ions in an oxide host must be defined. Single-crystal neutron diffraction studies of organometallic catalysts have similarly revealed the fine details of chemical bonding in intricate coordination complexes. As well as static studies of crystal structures, neutron crystallography at the ILL is increasingly concerned with studies of the activity and behaviour of a wide range of materials under non-ambient and chemically reactive conditions. Such experiments use the penetrating power of neutrons to probe materials contained in complex and bulky environmental cells. This has led to some striking studies of even the simplest materials, leading to new, fundamental insights into the structure of the solid state. For example, new polymorphs of ice have been discovered at high pressure and the nature of the hydrogen bonding forming these structures has been elucidated by refinement against neutron diffraction patterns. Some of these experiments at unusual combinations of pressure and temperature are of relevance to a deeper understanding of the properties of the Earth's atmosphere, for example in cloud formation, and in learning about the behaviour of molecules in outer space, such as on other planets. The use of rapid data acquisition, combining new detector technology and high neutron flux, now permits the routine use of time-resolved powder neutron diffraction to follow the chemistry of functional materials under operating conditions: for example, the formation and decomposition of hydrides leading to the storage and release of hydrogen gas, where kinetics and mechanisms can be efficiently mapped to fine tune properties of materials for future energy storage applications.

COLLEGE 5B - LIQUIDS AND GLASSES

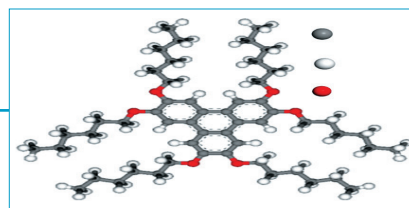
Authors: **R.K. Kremer** (Chair) and **C. Ritter** (Secretary)

Trying to unravel the fascinating complexity of magnetism in solids forms the central focus of the activities of the College. Apart from the classical but nevertheless successfully pursued applications of neutron diffraction for single crystal and powder magnetic structure determination, the latter is very often exploring new materials or magnetic systems



Magnetic excitations

cf. article "Metastable vortex lattice phases in MgB₂" p. 28



Crystallography

cf. article "Dancing discotic molecules for self-assembled electronic devices" p. 64

with the traditionally fruitful overlap to organic and inorganic chemistry efforts and to theory. In this context an increasing number of projects make use of the ILLs well developed portfolio of versatile sample environments. Low-temperature, high or very high magnetic fields, high-pressure environments or sophisticated combinations of these are increasingly asked for. Proposals exploiting the unique capabilities of ILL for providing very intense polarised neutrons beam over a wide energy range constitute another landmark of the activities in the College. Experiments employing polarised neutrons were especially in demand for the investigation of entangled magnetic structures in chiral or skyrmion magnets, in multiferroic systems, pnictides or cuprate superconductors. Small-angle neutron scattering is another focus of our activities, for example, to investigate vortex lattices in superconductors, the magnetism of spin-glasses or the properties of new nanomagnets. The commissioning of the new small-angle neutron scattering instrument, D33, considerably enabled the compliance with the increasing demands of the SANS community in the College. The highlights selected for this report from the multitude of successful experiments of the past year emphasises the diversity of magnetic problems tackled. The tetragonal heavy fermion superconductor URu_2Si_2 , in addition to the superconductivity phase below about 1.2 K, shows a transition to a hidden-order phase the character of which has remained in the dark until recently. Detailed polarised neutron diffraction experiments carried out to determine the magnetisation distribution of the $5f$ electrons combined with theoretical calculations revealed that the hidden-order transition is due to ordering of higher-rank magnetic multipoles of the $5f$ electrons.

Even a decade after the discovery of 40 K superconductivity in MgB_2 , SANS experiments are able to unveil still unknown features of its flux-line lattice. SANS measurements carried out on unprecedentedly tiny single crystals weighing a few hundred micrograms only, disclosed new non-equilibrium vortex configurations which differ substantially from theoretical predictions. Oxypnictides are interesting not only because of their outstanding superconducting properties but also may become important because they can exhibit colossal magnetoresistance as, for example, has been observed in $\text{NdMnAsO}_{1-x}\text{F}_x$. Powder neutron diffraction on $\text{NdMnAsO}_{1-x}\text{F}_x$ helped to determine the magnetic ordering of the Mn and Nd magnetic moments and assisted in optimising the synthesis of novel compounds with tailored magnetic and electric properties.

COLLEGE 6 – LIQUIDS AND GLASSES

Authors: **H. Holland-Moritz** (Chair) and **V. Cristiglio** (Secretary)

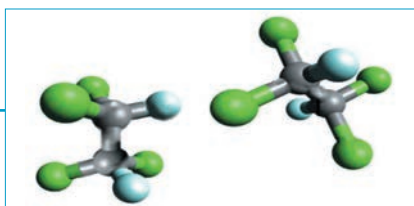
Different from crystalline materials, the structure of liquid and amorphous matter is characterised by the absence of any long-range order. Nevertheless, within the range of few atomic or intermolecular distances also liquids and amorphous solids exhibit some degree of topological and in many cases also some degree of chemical order. This short-range order determines most macroscopic physical properties of liquid and amorphous matter, as well as the solidification behaviour of melts when cooling the melts below the melting temperature. Neutron diffraction is a powerful tool for studying the short-range structure in liquids and amorphous materials. Due to the different scattering cross sections neutron scattering provides structural information complementary to that inferred from X-ray scattering. Moreover, isotopic substitutions techniques allow even tuning the neutron

scattering cross sections enabling *e.g.* the determination of partial structure factors of binary liquids. One example for structural neutron scattering investigations on molecular liquids is found at p.52. Another important issue when dealing with liquids and amorphous solids are dynamical aspects such as diffusion processes, vibrational modes or different kind of excitations. Inelastic and quasielastic neutron scattering offer unique opportunities for dynamical investigations taking advantage from the fact that, different from X-ray scattering, typical neutron energies are in the meV range. One reason for the special interest in studies on the dynamics in the field of liquids and glasses is motivated by the drastic change of the mobility of atoms or molecules at temperatures close to the glass transition temperature. Hence, inelastic and quasielastic neutron scattering experiments on the dynamics combined also with elastic neutron scattering studies on the short-range structure help finding a better understanding of the mechanisms of glass-formation, which are not well understood to date. Apart from investigations on structural and dynamical properties of bulk liquids and amorphous solids, during recent years there is growing research interest in investigations on the special properties of liquids confined in porous media. While most studies are concerned with confinement of a liquid in a solid medium, a special kind of confinement effect has been predicted to occur also for fully miscible systems if a component of high mobility relaxes within a slower matrix. In a recent work indications for such intrinsic confinement effects were found in a binary glass-forming system (p. 54).

COLLEGE 7 – MODELLING AND SPECTROSCOPY

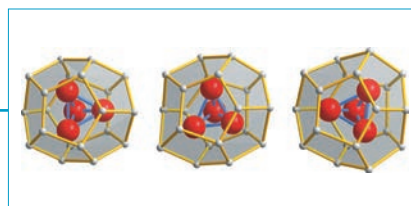
Authors: **D. Djurado** (Chair) and **M. Zbiri** (Secretary)

Over the last few years the field of 'Spectroscopy in solid-state physics and chemistry', covered by College 7 activities, has demonstrated its efficient versatility by conjugating diversity and common themes through its increasingly varied research topics. Mostly located within a societal framework the related research proposals are at the boundaries of different domains ranging from materials science and condensed matter to energy and life science. This is well reflected by typical applications whose proposals were ranked as highlight during the last two subcommittee rounds in 2012. One can cite ferroelectricity in molecular materials, molecular quantum dynamics of confinement within fullerenes and nanotubes, electron-phonon coupling in the Co analogue of cuprates, conformations of peptides in molecules, phonons in DNA, catalytic formation of hydrogen, magneto-elastic excitations in pyrochlores, Li diffusion in electrolytes, phonons in multiferroic materials, spectroscopy of new metal organic frameworks, critical pretransitional dynamics within crystallographic superspaces, anharmonicity and dynamics of thermoelectrics, negative thermal expansion in molecular framework solids and proton dynamics in perovskite type oxides. Basically a good mix between polycrystalline or powder and single crystal samples is observed. The requested instruments systematically concern most of the ILL spectrometers along with some demand of relevant diffractometers (structure and dynamics). Presently, the multifaceted science done within the framework of college 7 is exemplified by three highlights using the neutron time of flight spectroscopy as a common technique to study the quasi-elastic scattering for works on different subjects, which are of prime importance to fundamental research as well



Liquids and glasses

cf. article "Propagating structure: from molecules to short range ordering" p. 53



Modelling and spectroscopy

cf. article "A switchable molecular rotator: a spin-crossover compound comes into the field of molecular machines" p. 61

as to technological applications. The first highlight focuses on studying periodic approximants to quasicrystals, which would offer a unique opportunity to better understand structure and physical properties of their quasicrystal counterparts. This field is being boosted further thanks to the regain of interest induced by the attributed 2011 Nobel prize in chemistry. On a different scale of mosaicity, the second highlight deals with a potential candidate material targeting at energy sustainability to build electronic devices including photoconverters for practical solar cell applications. This is based on the morphological and dynamical properties of the organic-based discotic liquid crystals. By keeping the same interest in functionalized materials, the last article in this section presents an investigation of a spin-crossover compound by studying its molecular bistability towards a possible construction of crystalline molecular rotators, in the quest for artificial molecular machines.

COLLEGE 8 – BIOLOGY

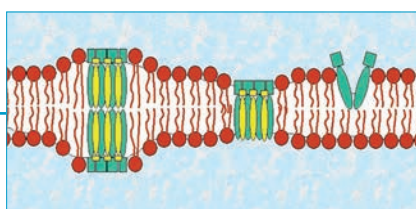
Authors: **C. Cardin** (Chair) and **M. Blakeley** (Secretary)

The use of neutrons in biology continues to increase at the ILL with biological studies covering a broad range of length scales and accounting for 12% of all applications in 2012, compared with 11% the year before. The scientific themes of the submitted proposals were divided rather evenly among 'biological membranes', 'solution structure of biological macromolecules', and 'dynamics of biological macromolecules', rather less proposals were submitted for 'macromolecular crystallography' (10%) with 'methodological studies in biology and biophysics' (4%) again falling behind somewhat.

A highlight this year from D16 (*p. 44*) was the study of how amphotericin, a widely used drug in the treatment of fungal infections, is incorporated into human and fungal cell membranes. The results of the diffraction studies by researchers from King's College London have provided important details towards comprehension of the drug's anti-fungal activity.

The motion of a protein in its native intracellular aqueous environment is a complex superposition of atomic vibrations, the diffusion of molecular subunits, as well as the rotational and translational diffusion of the entire protein. It is challenging to separate these different contributions to the observable neutron scattering signal. A highlight from studies performed using IN10 and IN16 (*p. 48*) has been the development of a new and general approach to the analysis of backscattering data that allows one to extract accurate information solely on the internal molecular motions, opening up new perspectives for future dynamics experiments on protein solutions.

In pharmaceutical science and biopharmaceutics, the characterisation of therapeutic agents is primarily based on chemical purity with little attention paid to their physical properties such as conformational states or the flexibility of molecular subunits. However, a recent study of phenacetin, a pain-relieving compound, which combined inelastic neutron scattering experiments (using IN10 and IN6) with computational analysis has demonstrated that this type of approach offers unprecedented advantages to describing the dynamics of hydrogen atoms in solid drugs (*p. 50*).



Biology

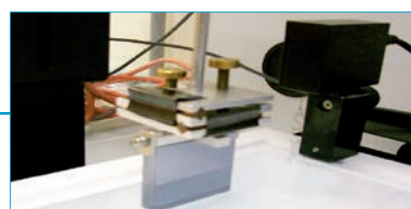
cf. article "Structural studies of amphotericin's incorporation within model human and fungal cell membranes" p. 44

A final highlight for 2012 was that from Rondelli and co-workers (*p. 46*) which describes pioneering work towards the preparation of complex mimics for cell membranes and their characterisation with neutron reflectometry using D17. Raft forming molecules GM1 and cholesterol are included in the model membranes. The presence of the ganglioside GM1 is experimentally shown, for the first time, to force asymmetry in the lipid bilayer with a preferential GM1 and cholesterol distribution supposed to have a key role for membrane functionality.

COLLEGE 9 – SOFT CONDENSED MATTER

Authors: **J.T. Cabral** (Chair), **R. Campbell** (Secretary) and **L. Porcar** (vice secretary)

Soft condensed matter remains an important growth area at the ILL with the number of proposals submitted to the College hitting a record high of 178 in the second proposal round of 2012. The scientific topics cover a broad range of fundamental to applied soft matter, at the interface of physics, chemistry, and biology, which comprises colloids, micelles, surfactants, polymers, bio-systems and their complexes and mixtures. Neutrons are a unique probe for soft matter structure and dynamics, spanning a considerable range of its intrinsically broad length- and timescales, and permitting key contrast variation via isotopic substitution. Polymeric systems remain an important focus in soft matter. Recently, time-resolved small-angle neutron scattering measurements on D22 have elucidated the mechanisms and the kinetics of complex collapse and intermicellar aggregation processes of triblock copolymers (*p. 40*). In terms of mixed systems, work on FIGARO, involving a novel comparison of reflection up/down measurements, allowed the distinction of molecular adsorption effects from gravity-driven transport of particles with internal molecular structure to certain interfaces providing an improved understanding of interfacial multilayers in a polymer/surfactant mixture (*p. 36*). Continued interest on bio-related soft matter has resulted in several highlights. The loss of asymmetry in the inner and outer leaflets of lipid bilayers in the fluid phase has been probed on FIGARO (*p. 38*), while a comparative protein dynamics, within the pico-nanosecond timescales, was carried out on IN16 indicating a protein structure-dependent dynamic landscape (*p. 42*). Industrially relevant research, building upon self-assembly of soft matter has also seen a considerable growth, encompassing functional devices (including photovoltaics and storage), to personal care (including foods and detergents), environment (aerosols, recycling, pollution containment) and biomedicine (materials and drugs). From a sample environment perspective, considerable effort is dedicated to enabling science by combining in-situ techniques, including dynamic light scattering/small-angle neutron scattering experiments taking place on D11, and infrared spectroscopy/neutron reflectometry experiments taking place on D17; in addition, custom experimental devices, for fast (ms) time-resolved studies, advanced rheological and environmental cells, including microfluidic devices, as well as industrially relevant fuel cells modules, are increasingly employed. Our community further benefits from the Partnership for Soft Condensed Matter which progressively provides a key platform to support scientific visitors in the pre-characterisation, analysis and interpretation of scattering data from ILL and ESRF.



Soft condensed matter

cf. article "Lipid flip-flop mechanism: loss of asymmetry in a model membrane system" p. 38

Magnetism

Time-of-flight spectrometer IN5

Kapellasite - a geometrically frustrated two-dimensional gapless quantum spin liquid showing exotic chiral spin correlations

Kapellasite has the same chemical formula ($\text{Cu}_3\text{Zn}(\text{OD})_6\text{Cl}_2$) but a different crystallographic structure from the well-studied mineral herbertsmithite [2]. The Cu^{2+} ions in kapellasite carry a spin of $1/2$ and form flat layers of a regular arrangement of corner-sharing equilateral triangles (see **figure 1a**). This highly frustrated two-dimensional lattice is called kagome after a Japanese basket weaving pattern and is known closer to us since the Roman times (**figure 1b** shows a 2000 year old mosaic in Catalonia). In kapellasite, the kagome layers are separated by weak O-H-Cl bonds assuring a high degree of two dimensionality. Kapellasite is not a stable end product in a chemical reaction and only powder samples are available, but once formed it is stable and has a beautiful baby-blue color. Kapellasite does not show any magnetic ordering down to the lowest temperatures (50 mK for neutron scattering and 20 mK for muons). The static susceptibility exhibits a

Frustrated magnets are materials where competing interactions between localised spins on a lattice cannot be simultaneously satisfied. The ground state of such a system is highly degenerated and predicted theoretically to show exotic phenomena, in particular for quantum spins [1].

However, there are only a few experimental realisations of such materials available.

We have used inelastic neutron scattering to study a newly synthesised frustrated quasi two-dimensional material, kapellasite, where the ground state is a gapless quantum spin liquid, characterised by highly correlated spins that fluctuate strongly down to zero temperature.

weakly ferromagnetic Curie-Weiss constant, but the dominating interactions are actually antiferromagnetic. Indeed, fitting an 11th order high-temperature series expansion to the susceptibility shows that the nearest-neighbour interaction J_1 (see **figure 1a**) is ferromagnetic while further-neighbour interactions are antiferromagnetic. The high-temperature series

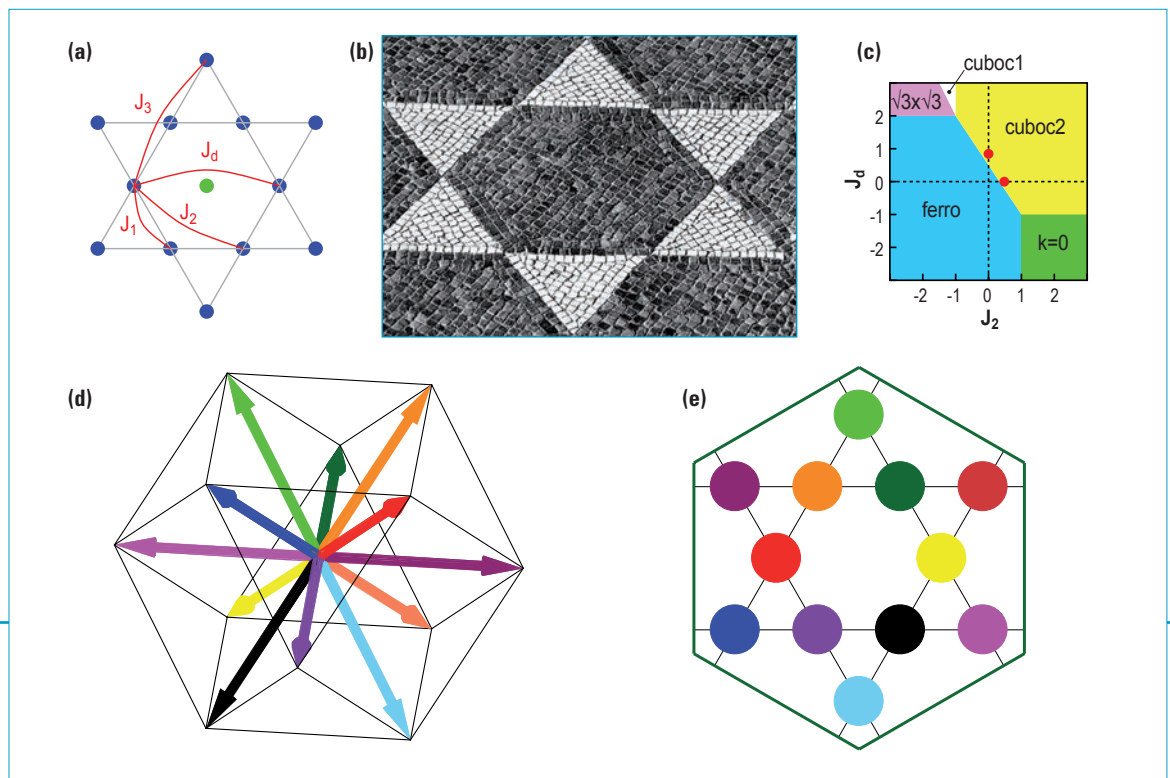


Figure 1: (a) Kagome plane of kapellasite with Cu^{2+} $S=1/2$ spins in blue. The main exchanges are shown in red. (b) Roman floor mosaic showing the kagome lattice (Empuries, Catalonia, ca. 60 BC). (c) Classical J_2 - J_d phase diagram for ferromagnetic nearest-neighbour coupling J_1 . Red points correspond to various high-temperature series-expansion fits to the magnetic susceptibility and clearly situate kapellasite in the cuboc2 part of the phase diagram. (d-e) The cuboc2 structure can be visualised by taking each colored spin arrow in the cubocta-hedron of (d) and place it (keeping its direction) on the correspondingly colored spot on the kagome lattice in (e).

expansion also explains the peak at 2 K in the magnetic specific heat C/T . In all cases, the exchange interactions are such that the system, if it consisted of classical spins, would order in the so-called cuboc2 phase, as illustrated in the phase diagram of **figure 1c**. The cuboc2 structure is a non-collinear twelve-sublattice magnetic structure, best visualised by a cartoon, but we have tried to illustrate it in **figures 1d-e**. This structure was first predicted theoretically only a few years ago [3], but has never been observed hitherto.

Inelastic neutron scattering measurements were performed on a 3 g fully deuterated powder sample on the time-of-flight spectrometer IN5 [4]. The neutron scattering intensity is shown color-coded on a logarithmic scale versus wavevector and energy in **figure 2a**. Clearly, there are no spin-wave like sharp dispersive features, but a dispersionless strong scattering at a wave vector of 0.5 \AA^{-1} , with no further magnetic scattering until about 1.7 \AA^{-1} . This is more clearly seen in **figure 2b**, where the energy-integrated quantity $S(Q)$, the static structure factor, is shown as a function of Q . Of all possible regular magnetic structures, only the cuboc2 structure can describe this highly unusual pattern. Hence, there is a tremendous agreement between our high-temperature series expansion of the magnetic susceptibility and the short-range magnetic correlations. As is also seen from the color map in **figure 2a**, the scattering from kapellasite is purely inelastic, and the system is thus a spin liquid with dynamic short-range correlations of cuboc2 type. The energy response obtained after Q -integration, shown in **figure 2c**, is well described by a Lorentzian at high temperatures, as expected for a classical spin liquid with a single energy scale. Below a temperature of 5 K, deviations are seen from the single Lorentzian, signalling the onset of quantum spin-liquid correlations. Such fluctuations are also seen in the muon measurements, which rules out any spin freezing and confirms the absence of a spin gap down to 20 mK, *i.e.* $J_1/10$.

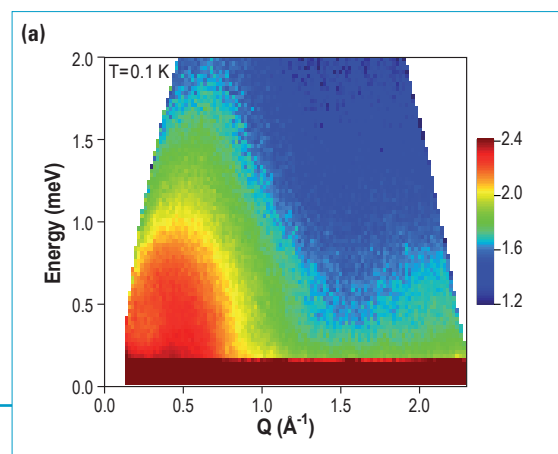


Figure 2: (a) Neutron scattering intensity on a logarithmic scale as a function of wave vector Q and energy of kapellasite at a temperature of 0.1 K. The diffuse inelastic magnetic scattering is centered at $Q=0.5$ and 2.0 \AA^{-1} . (b) Wave-vector dependence of the inelastic magnetic scattering integrated over energy for different temperatures. The line is the theoretical calculation using the Schwinger-boson mean-field approach at $T=5$ K. (c) Energy dependence of the magnetic scattering integrated over wavevector for different temperatures. The data show deviations from a quasi-elastic Lorentzian (lines) at low temperatures.

Theoretical calculations using the Schwinger-boson mean-field approach show that the cuboc2 structure is preserved even in the case of strong quantum fluctuations and reproduce the specific form of the static structure factor $S(Q)$ (see **figure 2b**) as well as the muon spin-relaxation time, but do not describe well the dynamics seen in the neutron scattering experiment. Qualitative theoretical considerations point to the importance of chiral spin correlations.

In conclusion, our inelastic neutron scattering measurements show that the mineral kapellasite is a kagome quantum spin liquid exhibiting novel short-range dynamic spin correlations. This exotic ground state is a direct consequence of the geometric frustration of a 2D kagome lattice combined with competing exchange interactions in the quantum limit. Several experimental results are well described by a bosonic approach, but a full theoretical understanding would probably require the development of fermionic chiral methods.

Authors

B. Fåk (SPSMS, CEA, Grenoble, France)

E. Kermarrec, F. Bert, P. Mendels, B. Koteswararao and F. Bouquet (CNRS-Paris Sud University, Orsay, France)

L. Messio (Institute of Theoretical Physics, Lausanne, Switzerland)

B. Bernu and C. Lhuillier (CNRS-Pierre and Marie Curie University, Paris, France)

J. Ollivier (ILL)

A.D. Hillier (ISIS, UK)

A. Amato (PSI, Villigen, Switzerland)

R.H. Colman and A.S. Wills (University College London, UK)

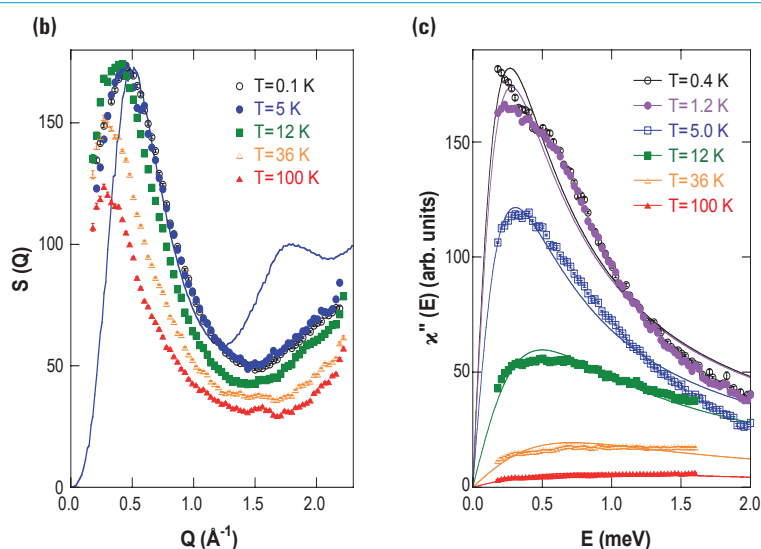
References

[1] L. Balents, Nature 464 (2010) 199

[2] P. Mendels and F. Bert, J. Phys. Soc. Jpn. 79 (2010) 011001

[3] J.-C. Domenge, P. Sindzingre, C. Lhuillier and L. Pierre, Phys. Rev. B 72 (2005) 024433

[4] B. Fåk, E. Kermarrec, F. Bert, P. Mendels, B. Koteswararao, F. Bouquet, L. Messio, B. Bernu, C. Lhuillier, J. Ollivier, A. D. Hillier, A. Amato, R.H. Colman and A.S. Wills, Phys. Rev. Lett. 109 (2012) 037208



Magnetism

Time-of-flight spectrometer IN5

Spin dynamics of molecular nanomagnets unravelled at atomic scale by four-dimensional inelastic neutrons scattering

Magnetic characterisation of molecular nanomagnets is generally performed by fitting experimental measurements, for example inelastic neutron scattering (INS) spectra, to an appropriate spin Hamiltonian model. However this method meets severe computational limitations with increasing system size or when a large number of model parameters make the fit ambiguous. We used the Cr_8 antiferromagnetic ring as a benchmark system for the demonstration that recently developed instrumentation on the cold neutron time-of-flight spectrometer IN5 yields the possibility to obtain three dimensional neutron momentum vector and energy transfer analysis in vast portions of reciprocal space [4] the result of which is a wealth of information concerning the quantum dynamics within the Cr_8 ring. The Fourier components of dynamic spin pair correlations within the Cr_8 ring modulate the neutron scattering intensity with respect to neutron wave-vector and hence can be extracted directly from the inelastic neutron scattering results without relying on a model dependent analysis.

The eight Cr(III) ions ($3d^3$, $s=3/2$) within the Cr_8 molecule are arranged forming a near regular octagon (**figure 1**). Nearest neighbour Heisenberg antiferromagnetic exchange interactions result in a total spin singlet ground state. At 1.5 K neutrons of 5 \AA probe a weakly non degenerate triplet excited state at 0.8 meV and 3.1 \AA neutrons access additional triplet excited states at 4 and 5.5 meV. Successive measurements are performed for multiple crystal orientations and combined using

Molecular nano-magnets are finite sized magnetic clusters chemically synthesised in a crystalline arrangement of magnetically isolated units. The collective magnetic properties of exchange coupled ions within the molecule are investigated for a variety of fundamental concepts in quantum mechanics such as quantum tunnelling and entanglement [1]. Quantum coherence presents potential for tailoring molecular nanomagnets suitable for quantum information processing [2,3]. With increasingly sophisticated molecules exhibiting properties suitable for such applications, a significant challenge is met for their detailed physical characterisation.

the HORACE software suite to give the full four-dimensional scattering function $S(Q,E)$. **Figure 2** shows the wave-vector dependence of the cross-section in the plane of the Cr_8 ring for the three low temperature excitations of the molecule. These three transitions account for all the low temperature excitations exhibited in Cr_8 . The Fourier components of the dynamical spin correlations between spins within the molecular unit are extracted for each excitation by fitting the measured three dimensional neutron momentum transfer intensity to a general magnetic scattering equation. The obtained dynamical terms agree excellently with calculated Heisenberg Hamiltonian values. The results prove that the essential information in the form of low temperature dynamic spin correlations can be extracted experimentally and a complete description of the low temperature quantum dynamics of the internal spin structure within the molecule is obtained without the necessity

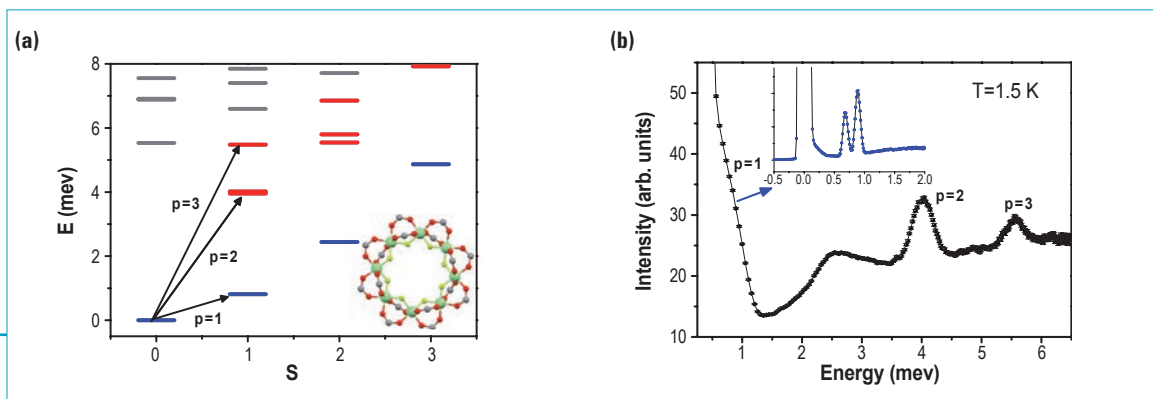


Figure 1: Magnetic energy spectrum of Cr_8 and zero-temperature INS transitions. **(a)** Low-lying energy multiplets as a function of their total spin for the isotropic exchange Hamiltonian of Cr_8 . The arrows indicate the three transitions seen by INS at zero temperature. All other transitions have negligible cross-section. The blue and red symbols indicate L- and E-band states, respectively. The inset shows the core of Cr_8 (Cr_{80} , Cr_8 , F_8 , D_{144} , O_{32} ; green, Cr; yellow, F; red, O; dark grey, C; D omitted). **(b)** Measured low-T INS spectra for a powder Cr_8 sample, with an incident neutron wavelength $\lambda = 3.1 \text{ \AA}$. The labels indicate the three peaks corresponding to the transitions reported in **(a)**. The $p = 1$ transition is partially hidden by the elastic signal. The inset reports higher-resolution measurements with $\lambda = 5 \text{ \AA}$ showing the $p = 1$ transition split by magnetic anisotropy.

of a Hamiltonian model. The measurement of the full set of low temperature Fourier coefficients allows the evaluation of important quantities such as the correlations within the ground state, and the dynamical response that describes how quantum fluctuations propagate within the molecule. As example, **figure 3** shows the time evolution of the local magnetisation s_z following a delta magnetic field pulse disturbance applied on (the red) spin site 1 of the Cr_8 molecule. Graphical visualisation of the dynamics provides an intuitive picture into particular regimes characteristic of the molecule. For example, comparison with a hypothetical Cr_8 exhibiting properties putting it into the Néel vector tunnelling regime, show clear differences in the response to a delta pulse, confirming the low temperature dynamics of Cr_8 cannot be described by Néel vector tunnelling.

In conclusion, wide coverage position sensitive detectors for inelastic neutron scattering provide new opportunities for characterising dynamic spin correlations within single crystal molecular nanomagnets. This method is demonstrated successfully for the Cr_8 antiferromagnetic ring. The level of information obtained by this experimental method gives a unique model-free means to examine elusive physical phenomena such as Néel vector tunnelling, quantum entanglement of

wavefunctions and magnetic frustration effects. More generally, the possibility to characterise the low temperature dynamics of molecular nano-magnets at the atomic scale without reliance on theoretical, calculated Hamiltonian models is demonstrated.

Authors

M.L. Baker (ILL and now Tohoku University, Japan)

H. Mutka and **J. Ollivier** (ILL)

T. Guidi (ISIS Facility, UK)

S. Carretta, **G. Amoretti** and **P. Santini** (University of Parma, Italy)

H.U. Güdel (University of Bern, Switzerland)

G.A. Timco, **E.J.L. Mc Innes** and **R.R.E.P. Winpenny** (University of Manchester, UK)

References

[1] D. Gatteschi, R. Sessoli and J. Villain, *Molecular Nanomagnets*, Oxford University Press (2006) 1086

[2] M.N. Leuenberger and D. Loss, *Nature* 410 (2001) 789

[3] F. Troiani *et al.* *Phys. Rev. Lett.* 94 (2005) 207208

[4] M.L. Baker, T. Guidi, S. Carretta, J. Ollivier, H. Mutka, H.U. Güdel, G.A. Timco, E.J.L. McInnes, G. Amoretti, R.E.P. Winpenny and P. Santini, *Nature Phys.* 8 (2012) 906-911

[5] C. Rüegg, *Nature Phys.*, 8 (2012) 859-860

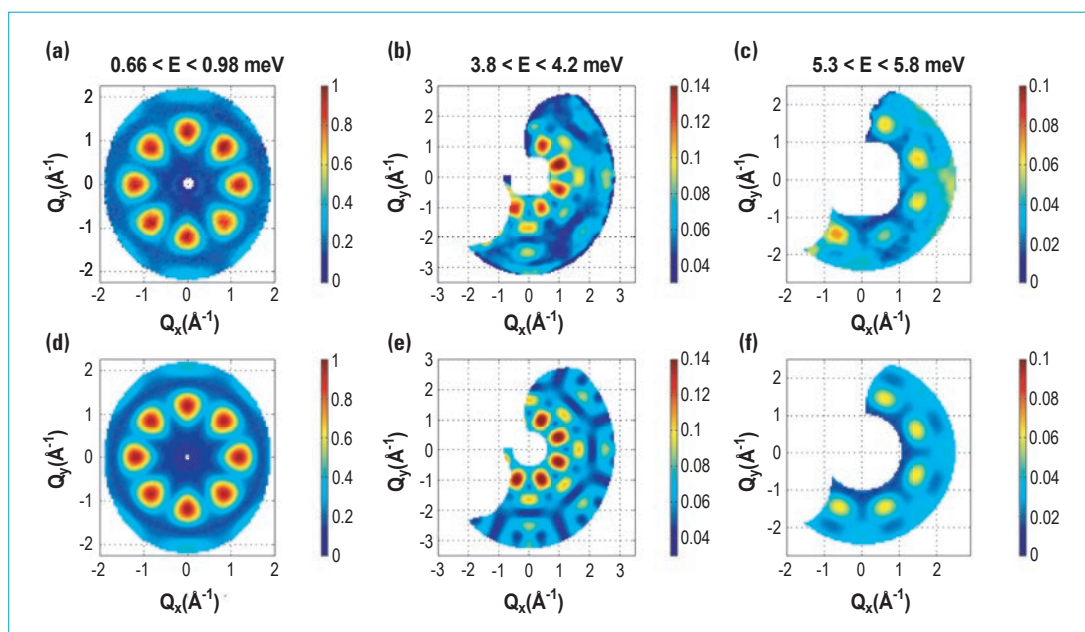


Figure 2:

Constant-energy plots of the neutron scattering intensity showing all of the possible magnetic excitations in Cr_8 at 1.5 K. The dependency of intensity on two wave-vector components $Q_x - Q_y$ lying in the ring's x-y plane, integrated over the full Q_z data range. (a) Data from transition $p = 1$, measured with a 5.0 Å incident neutron wavelength. b,c, Data from transitions $p = 2$ (b) and $p = 3$ (c), measured with a 3.1 Å incident neutron wavelength. d-f, Fits to the scattering law equation for excitations 1 (d), 2 (e) and 3 (f), [4].

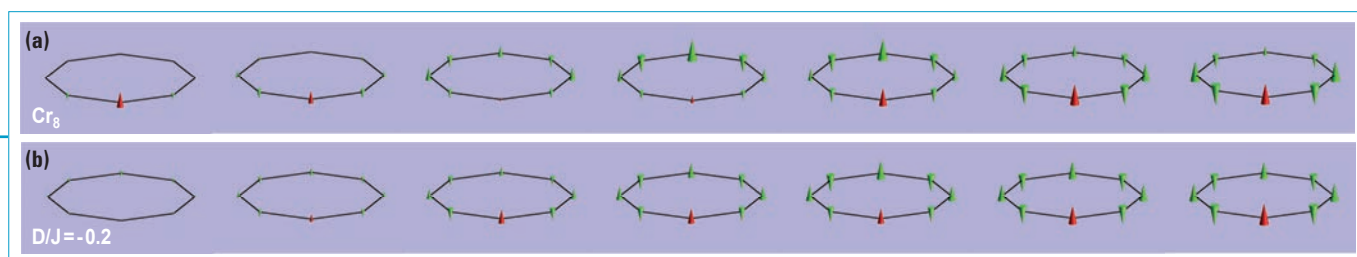


Figure 3: For details see [4]. Propagation of a local disturbance deduced from the present INS spectra and in a NVT regime. The frames show the time evolution of $\langle s_z(i) \rangle$ in an eight-spin ring after a delta-pulse perturbation $-bs_z(1)\delta(t)$ applied on the red ($d = 1$) spin. Note that with the ground state being a singlet, $\langle s_z(i) \rangle = 0$ just before $t = 0$ (frame not shown). (a) Dynamics as deduced using the experimental Fourier coefficients and frequencies. The delay between two frames is 1.9×10^{-13} s, that is, 1/32th of the longest oscillation period $2\pi/\omega_1$. (b) Results for a hypothetical ring in a NVT regime, that is, $D/J = -0.2$ corresponding to a tunnel action $S_0 \sim 7.6$. The delay between two frames is 1/32th of the tunnelling oscillation period $2\pi\hbar/\Delta$, with Δ being the tunneling gap.

Magnetism

Three-axis spectrometer IN14

Resonant magnetic exciton mode in the heavy-fermion antiferromagnet CeB₆

In many unconventional superconductors, including the famous high- T_c copper oxides, heavy-fermion superconductors such as CeCoIn₅ and CeCu₂Si₂, and the recently discovered iron pnictides, the spin fluctuation spectrum at low temperatures is dominated by an intense mode of resonant magnetic excitations. This resonant mode has several characteristic features. It is usually comprised of the magnetic spectral weight associated with fluctuations of an antiferromagnetic order parameter, whenever static antiferromagnetism is present in the close vicinity in the phase diagram. As the system enters the superconducting state below its critical temperature, T_c , the formation of Cooper pairs leads to an energy gap, Δ , in the electronic density of states near the Fermi level. As a result, particle-hole scattering is suppressed at energies lower than 2Δ , allowing for the formation of an exciton mode in this energy window, which is characterised by a narrow width in energy (or long lifetime). In the absence of an energy gap, as well as at energies higher than 2Δ , the lifetime of any magnetic excitation would be reduced dramatically by coupling to the particle-hole continuum, precluding the formation of a sharp resonant mode. We therefore expect the energy of any such mode to reduce with increasing temperature, following the closure of the superconducting gap, until it becomes overdamped and fully vanishes above T_c .

One important question is whether superconductivity is really indispensable for the formation of a magnetic resonant mode, or whether some other order parameter could open an energy gap equally well and thus enhance the lifetime of the resonant excitation. Indeed, as follows from the above description, we could expect the same mechanism in any material with a proximity of two different order parameters — one of them offering the magnetic “juice” of its spin fluctuations for the formation of an intense mode, the other responsible for reducing the electron density of states near the Fermi level and for the suppression of particle-hole damping, making this mode sharp in energy. Our recent experiment performed at the ILL cold-neutron spectrometer IN14 suggests that the non-superconducting heavy-fermion antiferromagnetic metal CeB₆ with a simple cubic crystal structure could be a good example of such a system [1].

The electronic states near the Fermi level of CeB₆ are composed of localised cerium-4f¹ levels hybridised with itinerant cerium-5d and boron-2p electrons, closely analogous to those of the superconductors CeCoIn₅ and CeCu₂Si₂. In contrast to these compounds, however, CeB₆ exhibits antiferromagnetic

Heavy-fermion metals continue to attract attention due to their anomalous low-temperature properties, such as unconventional superconductivity and exotic magnetic phases. Among rare-earth hexaborides, CeB₆ is unique as it develops a mysterious “hidden order” at temperatures between 2.3 and 3.2 K in zero magnetic field. It has been attributed to the ordering of magnetic quadrupole moments, although its true origin is still being debated.

This phase is found in close proximity to antiferromagnetism, which sets in below 2.3 K. Our study of spin excitations in this compound has revealed a magnetic resonant mode in the antiferromagnetic state, suggesting unexpected parallels with unconventional superconductors.

order below $T_N=2.3$ K. It is preceded by another phase transition at $T_Q=3.2$ K, whose order parameter has long remained hidden to standard experimental probes such as neutron diffraction. Theoretical work has attributed it to interactions between the multipolar moments of the Ce-4f electrons mediated by the itinerant conduction electrons, which break the large ground-state degeneracy of the cerium ions in their cubic crystal field and stabilise an antiferroquadrupolar (AFQ) order with the $(\frac{1}{2} \frac{1}{2} \frac{1}{2})$ propagation vector [2].

We show in **figure 1** two energy scans measured at this wave vector above and below T_N in the conventional triple-axis configuration of the spectrometer. In the antiferromagnetic state ($T=1.6$ K), an intense resonant peak dominates the spectrum at an energy of 0.5 meV. It is sharp in energy and is characterised by an intrinsic (resolution-corrected) width of only 0.2 meV. As the temperature is increased above T_N , the resonant peak becomes overdamped and transforms into a broad quasielastic response that is typical for the paramagnetic state of heavy-fermion metals. We can therefore associate the formation of this resonant peak with the opening of a spin gap in the low-energy part of the quasielastic spectrum upon cooling and the consequent spectral-weight transfer from below 0.35 meV to higher energies.

To visualise the momentum structure of the new excitation, we used the *FlatCone* multianalyser installed at the IN14 spectrometer to map out the reciprocal space at the resonance energy, as shown in **figure 2**. One can see that the maximum of intensity coincides with the propagation vector of the

“hidden order” phase. The intense resonance peak can be observed at two equivalent R points, $(\frac{1}{2} \frac{1}{2} \frac{1}{2})$ and $(\frac{1}{2} \frac{1}{2} \bar{\frac{1}{2}})$, which are additionally connected by weaker streaks of intensity that surround the M point.

Our observation of the magnetic resonant mode in CeB₆ has led to a substantial rethinking of the theory underlying the magnetic excitation spectrum of this compound. It emphasises the dominance of itinerant spin dynamics in the ordered low-temperature phases of CeB₆, throwing new light on the interplay between antiferromagnetism, superconductivity, and “hidden” order parameters in correlated-electron materials. A recent theory [3] has offered a description of the spin-exciton mode in the framework of a fourfold degenerate Anderson lattice model, which treats both order parameters in CeB₆ as particle-hole condensates of itinerant heavy quasiparticles. According to this theory, the exciton peak forms from spin fluctuations associated with the AFQ order parameter, which determines its position in the momentum space. However, a sharp exciton mode is only enabled below T_N due to the opening of an energy gap that suppresses the particle-hole damping, in close resemblance to the formation of a resonant mode in unconventional superconductors.

Future experiments addressing the magnetic-field dependence of the resonant excitation, as well as its dispersion and complete three-dimensional structure in the reciprocal space could clarify its origins and offer a direct way to verify the newly proposed theory. We expect these experiments to provide a long-awaited clue to the puzzle of the “hidden order” phase in CeB₆, as well as to the mechanisms underlying the formation of similar resonant excitations in a broad class of correlated metals, including unconventional superconductors.

Authors

G. Friemel, B. Keimer and **D.S. Inosov** (Max Planck Institute for Solid State Research, Stuttgart, Germany)

A.V. Dukhnenko, N.Y. Shitsevalova and **V.B. Filipov** (Institute for Problems of Material Sciences, Kiev, Ukraine)

N.E. Sluchanko (General Physics Institute, Moscow, Russia)

A. Ivanov (ILL)

References

- [1] G. Friemel *et al.*, Nature Commun. 3, 830 (2012)
- [2] Y. Kuramoto *et al.*, J. Phys. Soc. Jpn. 78, 072001 (2009)
- [3] A. Akbari and P. Thalmeier, Phys. Rev. Lett. 108, 146403 (2012)

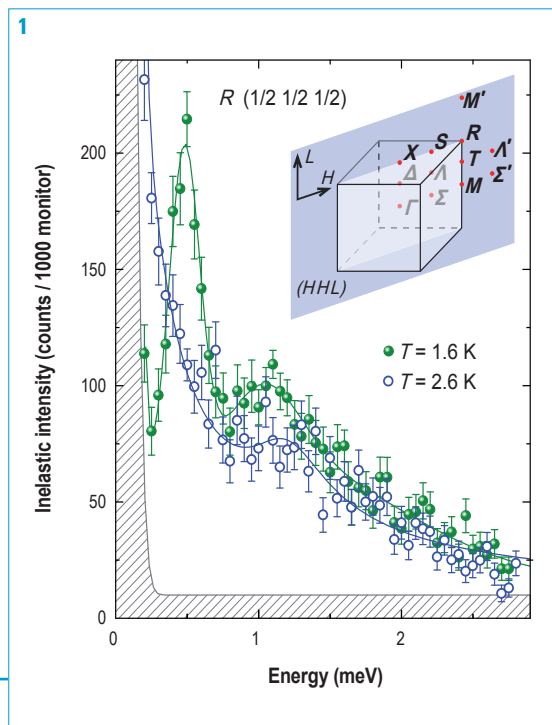


Figure 1: Energy dependence of the inelastic neutron-scattering signal above and below the antiferromagnetic transition temperature of CeB₆, T_N=2.3 K, measured at the corner of the cubic Brillouin zone, Q = $(\frac{1}{2} \frac{1}{2} \frac{1}{2})$. This point is marked as R in the sketch of the Brillouin zone shown as an inset.

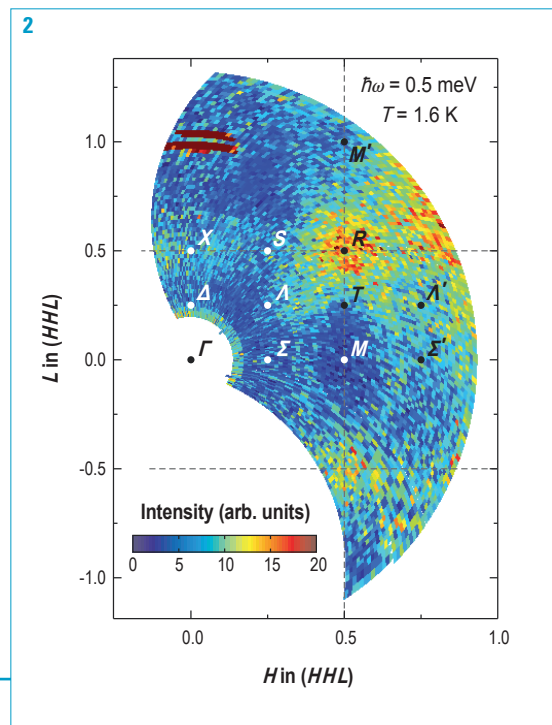
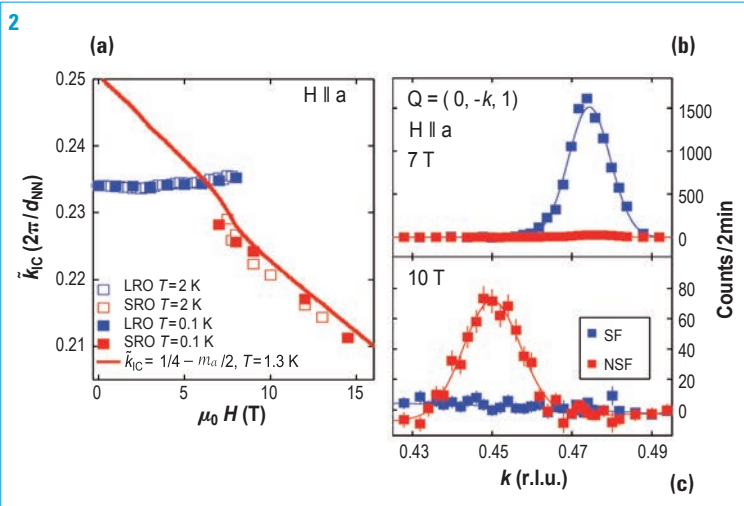
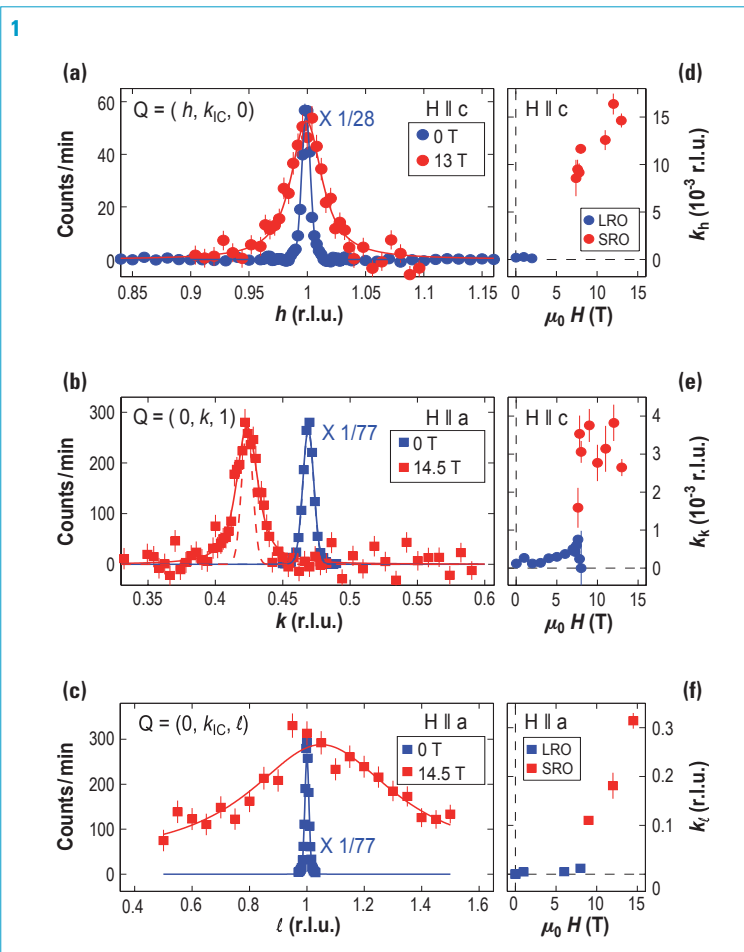


Figure 2: Inelastic signal at 0.5 meV energy transfer along the (hhl) plane in the reciprocal space, which is shown in the inset of **figure 1**. The measurement was done in the low-temperature antiferromagnetic phase (T=1.6 K) in a zero magnetic field. The labels represent different high-symmetry points, and the dashed lines mark Brillouin zone boundaries. The measurement was done at the ILL using the IN14 spectrometer equipped with the FlatCone multianalyser.

Magnetism

Three-axis spectrometers
IN14 (ILL), IN20 (ILL)
PANDA (FRM-II, Munich, Germany)

Evidence of a bond-nematic phase in LiCuVO_4



Spin nematic states are novel exotic quantum phases related to nematic phases in liquid crystals. Intense ongoing theoretical work predict that these new quantum phases should be present in a variety of models, relevant to topological insulators, pnictide superconductivity, and quantum spin liquids. For one-dimensional periodic arrays of spins $1/2$ with ferromagnetic and additional frustrating interactions, an extended multipolar-nematic phase should exist above a small critical magnetic field [1]. In this multipolar-nematic phase a spin-liquid like character coincides with multipolar spin order defined on bonds between the spin sites which contribute to the spin-multipole moment [2]. Our neutron scattering results provide the first comprehensive experimental evidence for the existence of the hitherto unobserved bond-nematic quantum state [3].

In spite of the perfectly regular lattice of spin $1/2$ sites, the bond-nematic phase displays no periodic order of the spin-dipole moment. This absence of long-range order is characteristic for a spin liquid.

Our unpolarised neutron scattering experiments show this important signature of the liquid character: all dipolar correlations in the frustrated ferromagnetic spin- $1/2$ chain compound LiCuVO_4 become suddenly short-ranged above a critical magnetic field of about 9 Tesla, **figure 1** (the saturation field is over 40 T). The characteristic wave vector of this dipolar short-range order is field dependent, and we show without employing a priori models that the field dependence of this wave vector follows precisely the relation for the spin-quadrupolar nematic state, see **figure 2a**.

Figure 1:

(a) - (c) Scans of the dipolar correlations at $T=0.1$ K for the three reciprocal space directions are resolution limited at zero field and broadened above the critical field of about 8 T. (d) - (f) Magnetic field dependence of the inverse dipolar correlation length $K=\xi^{-1}$. The onset of short-range order at the critical magnetic field is clearly seen for all three reciprocal space directions [3].

Figure 2:

(a) Incommensurate propagation vector k_{1C} in units of $2\pi/d_{NN}$ as a function of the applied field compared to the theoretical prediction for the quadrupolar-nematic phase, using the experimental magnetisation normalised to $1/2$ at the saturation field. (b) - (c) Polarised cross sections measured at $T=0.07$ K for the magnetic reflection $Q=(0, k_{1C}, 1)$ (b) in the cone-phase below the critical field, and (c) in the bond-nematic phase above the critical field [3].

Polarised neutrons and polarisation analysis evidence that the short-ranged incommensurate dipolar correlations involve only spin components parallel to the applied magnetic field (**figure 2c**), exactly as predicted for the bond-nematic phase, and opposite to a cone-structure (observed below the critical field, **figure 2b**), where the incommensurate dipolar correlations are transverse to the magnetic field and long-range ordered.

At zero-magnetic field LiCuVO_4 orders into a three-dimensionally correlated long-range ordered cycloid structure with resolution-limited magnetic Bragg peaks. Here, the anomaly of the heat capacity is attributed to the three-dimensional dipolar long-range order. However, above 9 Tesla, the heat capacity still evidences a phase transition, in spite of only short-ranged dipolar correlations found by neutron scattering. Like at zero-field, this phase transition is certainly driven by the interchain coupling in LiCuVO_4 , however, contrary to a wide-spread assumption, the zig-zagged interchain interaction that we identified in LiCuVO_4 [4] does not lead to amplitude-modulated (dipolar) long-range order. We therefore conclude that there must be an order parameter of higher than dipolar order. Since the field dependence of the short-range correlations follows precisely the relation for spin-quadrupolar bond-nematic order, this order parameter is probably of spin-quadrupolar character and hence invisible to neutron scattering.

We relate our surprising findings to an intuitive picture of low-density fermionic particles that are topological excitations with respect to the incipient dipolar order [3], and illustrated by red arcs and numbers ± 1 in **figure 3**. In this picture the exotic quantum phase is characterised by antiferromagnetic order of the low-density fermionic particles, while there is neither periodic positional order of these fermions nor a pairing

into multi-fermion bound states (**figure 3bc**). At zero-magnetic field, the zig-zagged interchain interaction favors long-range cycloid order by binding the fermionic particles into quartets (**figure 3d**), but above the critical field the zig-zag interchain interaction has no binding effect (**figure 3e**). Here the fermionic particles are free, deconfined, and so can efficiently destroy dipolar long-range order.

In view of the novelty and general relevance of our experimental results, we believe that our discovery of a new quantum phase of matter will trigger considerable theoretical attention, as it connects two very active fields of hard- and soft-condensed matter.

Authors

M. Mourigal (ILL and Johns Hopkins University, USA)

M. Enderle (ILL)

A. Hiess (ILL and now ESS, Sweden)

B. Fåk (CEA/UJF, France)

R.K. Kremer and **J.M. Law** (Max Planck Institute for Solid State Research, Germany)

A. Schneidewind (HZB–TU Dresden, Germany)

A. Prokofiev (Johann Wolfgang von Goethe University, Germany and Vienna University of Technology, Austria)

References

[1] J. Sudan, A. Lüscher and A.M. Läuchli, Phys. Rev. B 80 (2009) 140402(R)

[2] L. Kecke, T. Momoi and A. Furusaki, Phys. Rev. B 76 (2007) 060407(R)

[3] M. Mourigal, M. Enderle, B. Fåk, R.K. Kremer, J.M. Law, A. Schneidewind, A. Hiess and A. Prokofiev, Phys. Rev. Lett. 109 (2012) 027203

[4] M. Enderle, C. Mukherjee, B. Fåk, R.K. Kremer, J.-M. Broto, H. Rosner, S.-L. Drechsler, J. Richter, J. Malek, A. Prokofiev, W. Assmus, S. Pujol, J.-L. Ragazzoni, H. Rakato, H.M. Ronnow and M. Rheinstädter, Europhys. Lett. 70 (2005) 237

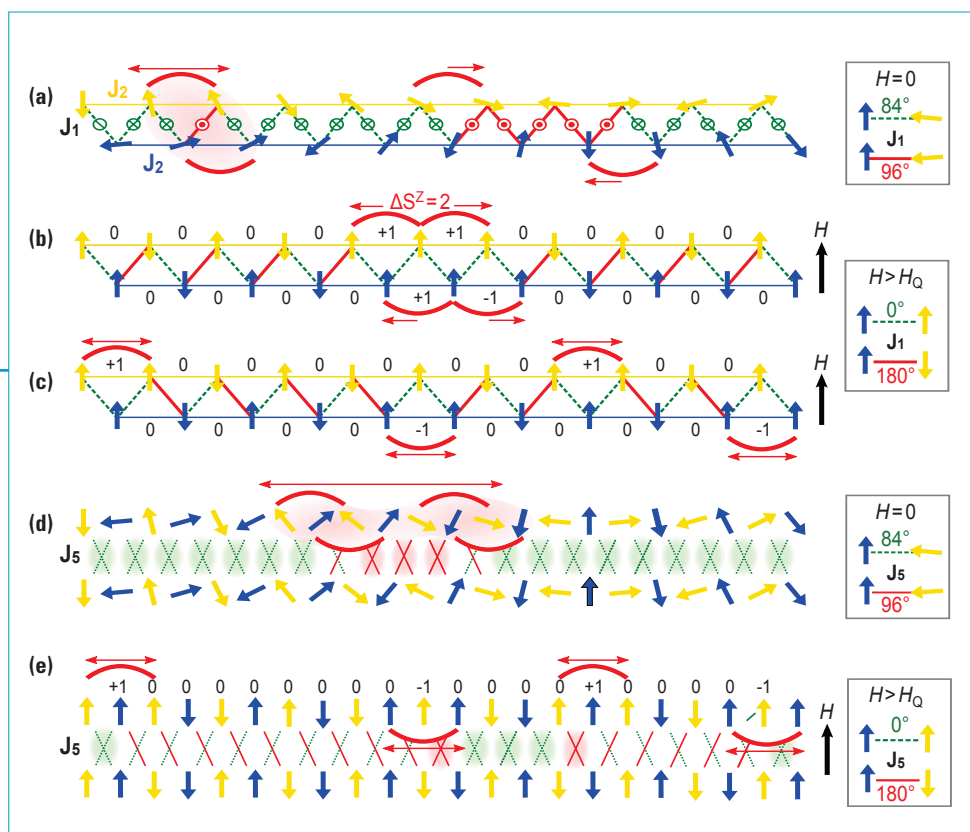


Figure 3:

(a) One frustrated ferromagnetic chain seen as two intercalated Heisenberg antiferromagnetic chains (closed and open arrows), the vector chirality on the nearest-neighbor bond is shown as green cross or red dot. At $H=0$, the ferromagnetic nearest-neighbor interaction binds the fermions (red arcs and numbers ± 1) into pairs. (b-c) Above the critical field, individual propagation of the fermions costs no extra energy, as long as they keep a non-local, nematic "antiferromagnetic" order of their "numbers". (d) The largest interchain interaction in LiCuVO_4 , J_5 , favors four-fermion bound states at $H=0$, (e) but allows for free propagation of the fermions above the critical magnetic field, as long as the non-local "nematic" "antiferromagnetic" order of the fermion-numbers is kept [3].

Magnetism

High-intensity two-axis diffractometer D20

Colossal magnetoresistance in Mn²⁺ oxypnictides NdMnAsO_{1-x}F_x

Magnetoresistance is defined as the change in electrical resistivity, ρ , which occurs upon applying a magnetic field, H , so that $MR = (\rho(H) - \rho(0)) / \rho(0)$, where $\rho(0)$ and $\rho(H)$ are equal to the resistivity in zero and applied field respectively. Colossal magnetoresistance (where the electrical resistivity reduces by orders of magnitude upon application of a magnetic field) has previously been reported in perovskite manganites such as $\text{La}_{1-x}\text{Sr}_x\text{MnO}_3$ [3]. **Figure 1a** shows the temperature variation of the 7 T magnetoresistance of $\text{NdMnAsO}_{1-x}\text{F}_x$ for $x = 0.050, 0.065$ and 0.080 . For all samples $-MR$ is observed below about 75 K and its magnitude increases exponentially as the temperature is reduced. Below 20 K the magnitude of the magnetoresistance rises sharply and increases further as the temperature is lowered.

In order to elucidate the mechanism of CMR in $\text{NdMnAsO}_{0.95}\text{F}_{0.05}$ we performed a variable temperature and field neutron diffraction study (at 4 K) on the high intensity D20 diffractometer. The neutron powder diffraction pattern confirms that $\text{NdMnAsO}_{0.95}\text{F}_{0.05}$ is phase pure and crystallises in the ZrCuSiAs crystal structure previously reported for the parent compound at both temperatures [4]. Neutron powder diffraction data reveals antiferromagnetic order of the Mn²⁺ moments below 356 (2) K in which the electron spins are

The recent discovery of high temperature superconductivity in pnictides such as $\text{LnFeAsO}_{1-x}\text{F}_x$ has led to great interest in these materials [1]. This is the first time that so-called high temperature superconductivity has been observed for a non-cuprate material. We have recently discovered the counterpart, colossal magnetoresistance (CMR) in Mn²⁺ based oxypnictides, so that both manifestations of correlated electronic behaviour are now found in these new materials [2]. Future spintronic devices will capitalise on the CMR mechanism for smaller, faster, cheaper and more efficient computing applications.

aligned antiparallel in the ab plane, but ferromagnetically along c with the moment ordered parallel to the c axis (**Figure 1b**). Upon cooling to 23 K antiferromagnetic order of the Nd³⁺ moments is detected with spins aligned parallel to the basal plane. At the same time the Mn²⁺ moments reorient into the ab plane as previously reported for NdMnAsO_4 , so that at 20 K, T_{SR} , the Mn²⁺ moments are fully aligned parallel to the basal plane.

Figure 2a shows a portion of the 4 K neutron diffraction pattern recorded on D20, where upon applying a magnetic field, it is apparent that the intensity of the [100] magnetic diffraction

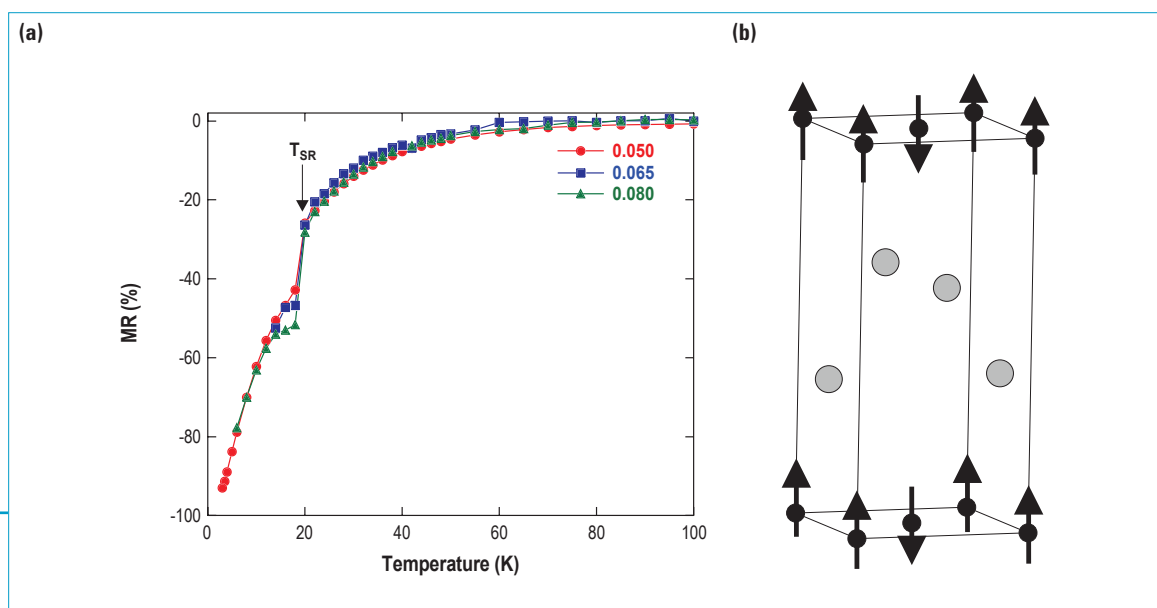


Figure 1: (a) The temperature variation of the magnetoresistance (MR) for $\text{NdMnAsO}_{1-x}\text{F}_x$ ($x = 0.05, 0.065, 0.08$) evidencing CMR at low temperature. (b) The high temperature magnetic structure.

peak decreases. There is no change in intensity of any of the other magnetic or nuclear peaks and hence there is no evidence of a ferromagnetic component upon increasing the field. The field variation of the magnetic structure was determined by structural Rietveld refinement of the neutron diffraction data, so that the decreased intensity of the [100] magnetic peak can be modelled by a reduction in both the antiferromagnetically ordered Nd^{3+} and Mn^{2+} moments with increasing field. The Nd^{3+} and Mn^{2+} moments are reduced from 2.09 (3) μ_B to 1.36 (3) μ_B and from 3.83 (2) μ_B – 3.56 (2) μ_B respectively upon increasing $\mu_0 H$ from 0 – 5 T. Upon returning the field to 0 T, the Mn^{2+} and Nd^{3+} moments refine to 3.86 (2) μ_B and 2.10 (3) μ_B respectively so that the reduction in magnetic moments with field is reversible. The results show that there is a second order phase transition from antiferromagnetic order of the Mn^{2+} and Nd^{3+} spins in zero field to paramagnetism at higher fields.

Figure 2b shows that there is in fact a correlation between the field variation of the ordered Mn^{2+} moment and the observed magnetoresistance across the field range measured (0 – 5 T) at 4 K. The magnetoresistance observed is related to the magnitude of the Mn^{2+} moment, so that -

$$\text{MR} = \left(\frac{\Delta M}{C} \right); \Delta M = M(0) - M(H), \text{ where } M(H) \text{ is the } \text{Mn}^{2+}$$

moment in a field, $M(0)$ is the Mn^{2+} moment when $\mu_0 H = 0$ T, and C is a constant (0.4 μ_B at 4 K) which equates to the moment reduction that would theoretically result in a -MR of 100 %. The same relation is not detected with the field reduction of the Nd^{3+} moment. The results clearly demonstrate that it is the field-suppression of the basal plane Mn^{2+} moment which is the origin of the CMR observed in $\text{NdMnAsO}_{1-x}\text{F}_x$ below T_{SR} , so that the electron correlations are weaker in the paramagnetic phase, resulting in dramatically increased electron transport.

In conclusion the variable temperature and field neutron diffraction study of $\text{NdMnAsO}_{0.95}\text{F}_{0.05}$ recorded on diffractometer D20 has established a novel CMR mechanism, further highlighting the exotic properties of transition metal pnictides. CMR in manganite perovskites arises when a magnetic field enhances ferromagnetic alignment of spins at the paramagnetic – ferromagnetic (magnetic disorder – order) boundary. Here we show that CMR is also possible in Mn_{2+} pnictides at the antiferromagnetic – paramagnetic (magnetic order-disorder) transition in a field. In future work we aim to tune the CMR to higher temperatures for technical applications by selected chemical substitutions.

Authors

E.J. Wildman, J.M.S. Skakle and A.C. McLaughlin

(University of Aberdeen, UK)

N. Emery (CNRS- Paris-Est Créteil University, France)

M. Brunelli (ILL)

References

- [1] Y. Kamihara, T. Watanabe, M. Hirano and H. J. Hosono, *J. Am. Chem. Soc.* 130 (2008) 3296
- [2] E.J. Wildman, J.M.S. Skakle, N. Emery and A.C. McLaughlin, *J. Amer. Chem. Soc.* 134 (2012) 8766
- [3] C.N.R. Rao and B. Raveau (Eds.), *Colossal Magnetoresistance, Charge Ordering and Related Properties of Manganese Oxides*, (World Scientific, Singapore, 1998)
- [4] N. Emery, E.J. Wildman, J.M.S. Skakle, R.I. Smith, A.N. Fitch and A.C. McLaughlin, *Phys. Rev. B* 83 (2011) 14429

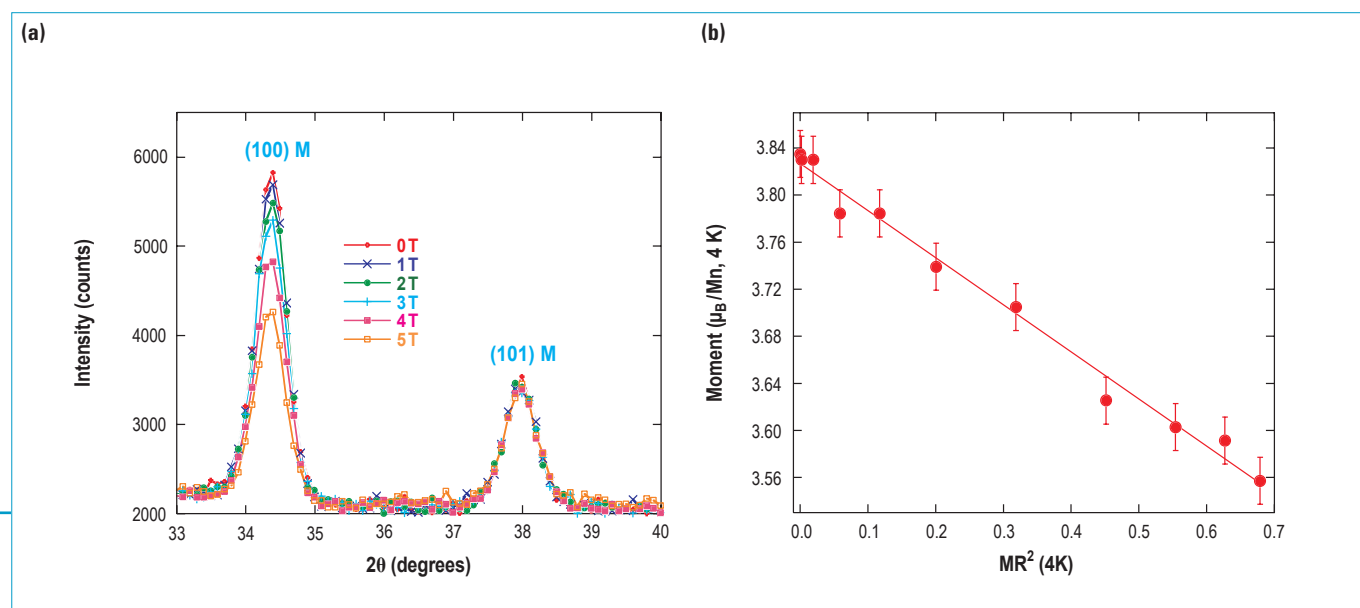


Figure 2: (a) A portion of the 4 K neutron diffraction pattern showing a reduction in intensity of the (100) magnetic diffraction peak with increasing magnetic field ($\mu_0 H$) from 0 – 5 T. (b) The results show an empirical correlation between the observed -MR and the field-reduced Mn^{2+} moment recorded at 4 K with $H = 0 - 5$ T (every 0.5 T) for $\text{NdMnAsO}_{0.95}\text{F}_{0.05}$.

Magnetism

Four-circle diffractometer D9 Two-axis spin polarised diffractometer D3

Hidden order in URu₂Si₂ unveiled

The tetragonal heavy fermion superconductor compound URu₂Si₂ is a good example of such materials. It has been puzzling physicists for more than two decades. Its specific heat presents two anomalies: the first one, at T_{SC} = 1.2 K, is ascribed unambiguously to a superconducting transition. The second one, at T₀ = 17.5 K, is referred to as a transition to an hidden order, because it is easily recognised in many other macroscopic measurements (non-linear magnetic susceptibility, thermal expansion, electrical resistivity, ...), but gives no clear microscopic signal to elastic scattering neither by neutrons nor by X-rays.

In spite of impressive experimental efforts, the mystery of the hidden order in URu₂Si₂ still remains unsolved. No order parameter has been determined so far for this transition. Dozens of microscopic models, including multipole ordering, have been successively proposed over the years to account for the wide variety of experimental results, without being able to conclude the story. A definitive identification of this hidden order would be one of the most exciting results in the field of heavy-fermions, but this task remains an experimental challenge. The fact, for instance, that it could originate in a freezing of high-rank multipoles cannot be evidenced directly by neutron scattering. Nonetheless, it was reasonable to anticipate that the magnetisation distribution, that is the distribution of unpaired electrons, induced under an applied magnetic field, might depend on the otherwise invisible ground state. It became thus highly desirable to study URu₂Si₂ by polarised neutron scattering in both the paramagnetic phase and in the mysterious phase, to probe potential relevant changes when entering the hidden order. Precision measurements of the Fourier components of a magnetisation distribution, more commonly called (scalar) magnetic structure factors, can indeed be achieved by using polarised neutrons, with the help of the classical polarised beam technique, at the condition that the nuclear structure is determined with a good precision. An unpolarised neutron diffraction experiment

Uranium and uranium-based materials are an endless source of unconventional and exotic physical properties. Their 5f electrons are intermediate between itinerant and localised and experience several interactions without clean-cut hierarchy, resulting in a large variety of novel phenomena. In particular, associated with the large orbital angular moments of these electrons, exists the possibility for high order electromagnetic multipoles to form and order.

is thus a necessary preliminary step. This unpolarised neutron experiment was carried out on the four-circle diffractometer D9, whereas the flipping ratio measurements have been performed on the two-axis diffractometer D3. After data treatment, a set of 50 independent magnetic structure factors were extracted at respectively 25 K (paramagnetic state) and 2 K (hidden order phase).

To recover the magnetisation distribution in real space from the set of magnetic structure factors, one has to solve an inverse Fourier problem. Several methods can be used, in particular the Maximum Entropy technique (MaxEnt), which provides the most probable magnetisation distribution map compatible with the observations and their uncertainties. **Figure 1** shows the reconstructed magnetisation distributions projected along the [001] axis at the two investigated temperatures, and the corresponding projection of the crystal structure. These reconstructions immediately reveal a clear feature that concerns the shape of the magnetisation distribution around the uranium site: whereas this distribution looks elongated along the [110] and [1-10] direction at T = 2 K, a change of symmetry is visible when crossing T₀, resulting in a distribution elongated along [100] and [010] at T = 25 K.

In order to get deeper insight into this shape change, magnetic structure factors were computed using the tensor operator formalism in an ionic model where only uranium is magnetic. From the calculated structure factors, magnetisation

Figure 1:

- (a) Projection of the MaxEnt reconstructed experimental magnetisation distribution in URu₂Si₂ along the [001] axis at T = 2 K.
- (b) Same MaxEnt projection at T = 25 K.
- (c) Projection of the unit cell of URu₂Si₂ along the crystallographic [001] axis, in the (a,b) plane. Uranium atoms in green, ruthenium atoms in red.
- (d) Projection of the magnetisation distribution calculated from a strong $\Gamma_1^{(1)}$ contribution.
- (e) Projection of the magnetisation distribution calculated from the strong $\Gamma_1^{(2)}$ contribution.

distributions were generated by inverse Fourier transform and compared to the experimental ones. A crucial point of the calculations was the choice of the relevant wavefunctions. First-principle electronic structure calculations suggested that the states with highest weight at the Fermi level correspond to combinations of 3 Crystalline Electric Field (CEF) singlets, $\Gamma_1^{(1)}$, $\Gamma_1^{(2)}$ and Γ_2 , built over the states $|M\rangle$ of the ground multiplet $J = 4$ of the $5f^2$ electrons of the U^{4+} ion within the Russel-Saunders coupling scheme. Modifications of the shape of the calculated magnetisation distributions in agreement with the observed ones were only obtained by changing the mixing parameter between $\Gamma_1^{(1)}$ (dominant term at low temperature in the hidden order phase) and $\Gamma_1^{(2)}$ (dominant term in the paramagnetic regime). Such a change can only be produced by a dotriacontapole operator (rank 5, product of 5 angular momentum operators), which supports the conclusion that the mysterious phase could be associated with an order of dotriacontapoles as recently proposed in the literature.

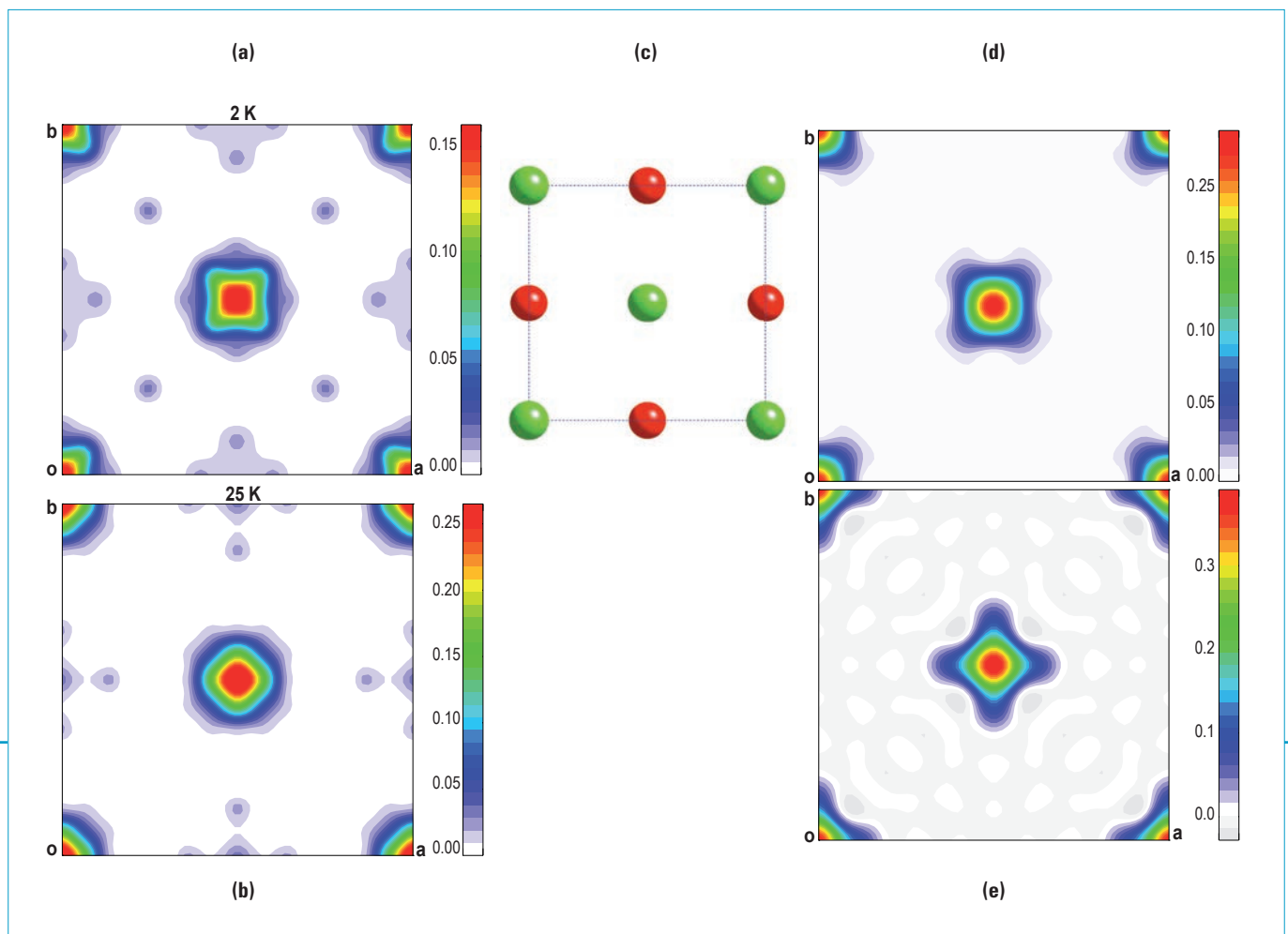
To summarise, a shape change in the field induced magnetisation distribution in URu_2Si_2 has been evidenced by accurate polarised neutrons measurements on decreasing the temperature. Within a simple ionic model, this shape change is interpreted as a microscopic fingerprint of an order of dotriacontapoles. Although confrontation to more sophisticated theoretical approaches might be awaited, this new experimental result certainly unveil a part of the mystery of the hidden order in URu_2Si_2 .

Authors

E. Ressouche, F. Bourdarot, D. Aoki and J. Flouquet (CEA/UJF-Grenoble, France)

R. Ballou and V. Simonet (Néel Institute, CNRS and Joseph Fourier University, Grenoble, France)

M.T. Fernandez-Diaz and A. Stunault (ILL)



Magnetism

Small-angle scattering diffractometer D22

Metastable vortex lattice phases in MgB₂

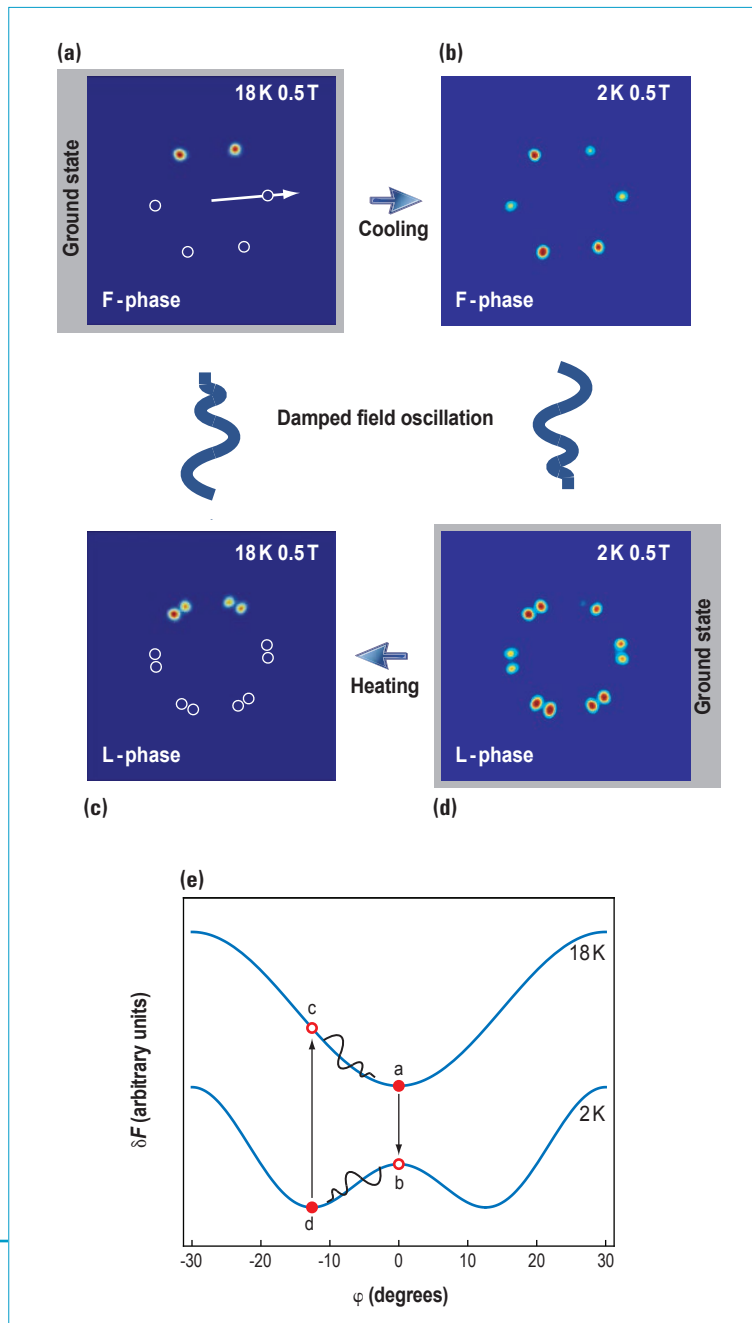


Figure 1: Vortex lattice metastability. Panels (a)-(d) show SANS diffraction patterns following heating/cooling and application of a field oscillation to induce vortex motion. Panel (e) shows free energy curves corresponding to the VL configurations above.

Metastable phases of matter are well known, and include famous examples such as the supercooling and superheating of liquids and diamond which is one of the many allotropes of carbon. Recently we have discovered an unprecedented degree of metastability in connection with a second-order vortex lattice (VL) reorientation transition in MgB₂.

This cannot be understood in terms the single domain VL free energy, and instead we speculate that is due to a jamming of ordered but counter-rotated VL domains.

Superconductors hold great promise for practical applications such as quantum interference devices for brain imaging and in powerful magnets used for MR imaging. However, to fully live up to the potential it is critical to understand the behavior of the vortices, induced by an applied magnetic field, as they can lead to dissipation even within the superconducting state. At the same time, vortex matter presents a rich system for fundamental investigation, bridging from "hard" to "soft" condensed matter physics. Studies of the vortex lattice (VL) are therefore important, both from a basic scientific as well a practical perspective.

Prior studies of MgB₂ with $H \parallel c$ found a triangular VL which undergoes a field-driven 30° reorientation transition bounded by two second-order transitions [1]. At the endpoints of this

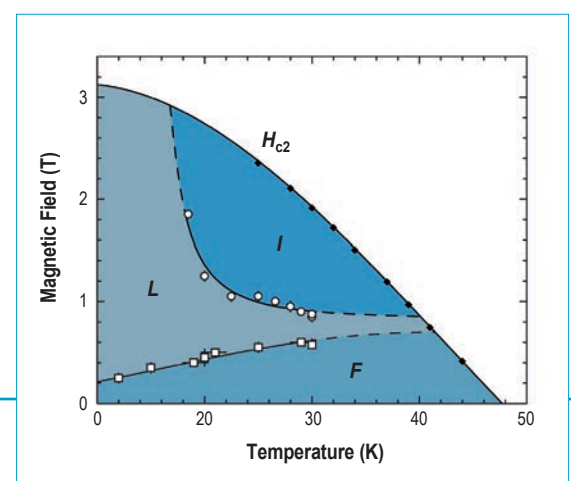


Figure 2: Ground state vortex lattice phase diagram for MgB₂. The VL in the F- and I-phases are aligned along the α and α^* crystalline axes respectively. In the intermediate L-phase the VL undergoes a continuous 30° rotation.

transition the VL is aligned with a high symmetry direction in the hexagonal crystalline basal plane. **Figure 1(a)-(d)** show diffraction patterns for two of the VL phases obtained at the small-angle scattering (SANS) instrument D22 [2]. These show a striking result, namely the existence of highly ordered nonequilibrium VL configurations and the observation of hysteresis in connection with a second-order phase transition. Simply cooling or heating in a constant field will trap the VL in a metastable configuration, as shown in **figures 1(b) and (c)**. At any field and temperature the ground state VL, shown in **figures 1(a) and (d)**, is only obtained by inducing significant vortex motion (here by a damped, small-amplitude field oscillation).

The VL metastability leads to a revised ground state VL phase diagram, shown in **figure 2**. In the *F*- and *I*-phases a single VL domain oriented was observed. In the intermediate *L*-phase, we observed 12 VL Bragg peaks corresponding to domains rotated in opposite directions. We note that VL metastability is observed both in connection with the *FL* and *LI* phase transitions. The continuous rotation of the VL and the second-order transitions means that the VL free energy as a function of the orientation angle is given by

$$\delta F = K_6 \cos 6\varphi + K_{12} \cos 12\varphi$$

with $K_{12} > 0$ [2]. The δF -curves in **figure 1(e)** show how the metastable *L*-phase **(c)** corresponds to an unstable equilibrium ($d(\delta F)/d\varphi \neq 0$). This demonstrates that the VL metastability cannot be understood from the single-domain free energy.

We propose that the origin for the VL metastability is a jamming of counter-rotated VL domains, which prevent these from rotating to the equilibrium orientation with respect to the

crystalline lattice, shown schematically in **figure 3**. The concept of jamming is mostly associated with granular materials, often exhibiting glassy dynamics when subjected to external excitations [3,4]. Our results indicate that the VL can be used as a model system to study jamming, and that neutron scattering is uniquely suited for such measurements.

In conclusion we have discovered pronounced metastability in connection with the VL rotation transition in MgB_2 . This phenomenon cannot be understood based on the single domain free energy but is speculated to be due to a jamming of VL domains. As a result we expect that the transition to the VL ground state configuration will exhibit slow (glassy) dynamics, similar to what is observed in granular materials. Preliminary measurements carried out at ILL, using a small AC field to perturb the VL, indicate that this is the case. These results have opened up a new direction for vortex lattice studies.

Authors

M.R. Eskildsen, C. Rastovski and P. Das (University of Notre Dame, USA)
C.D. Dewhurst (ILL)
N.D. Zhigadlo and J. Karpinski (ETH Zurich, Switzerland)

References

- [1] R. Cubitt *et al.* Phys. Rev. Lett. 91 (2003) 047002
- [2] P. Das *et al.*, Phys. Rev. Lett. 108, (2012) 167001
- [3] A.J. Liu and S.R. Nagel, Annu. Rev. Condens. Matter Phys. 1 (2010) 347
- [4] E. Corwin, Physics 5, 97 (2012)

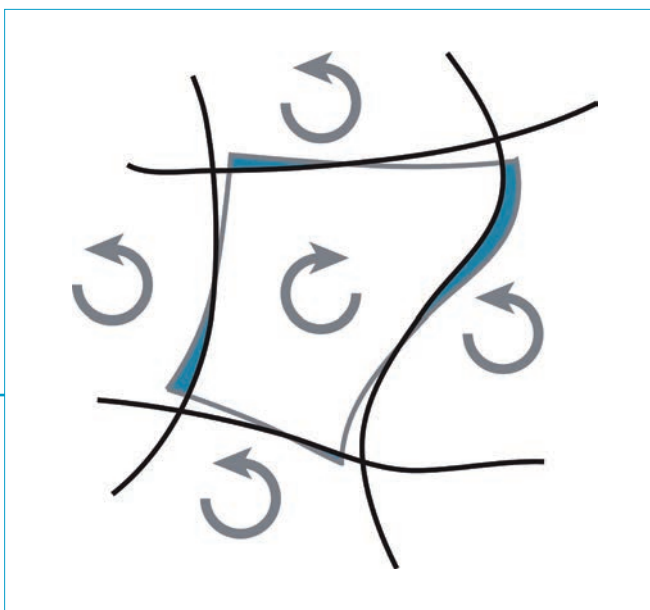


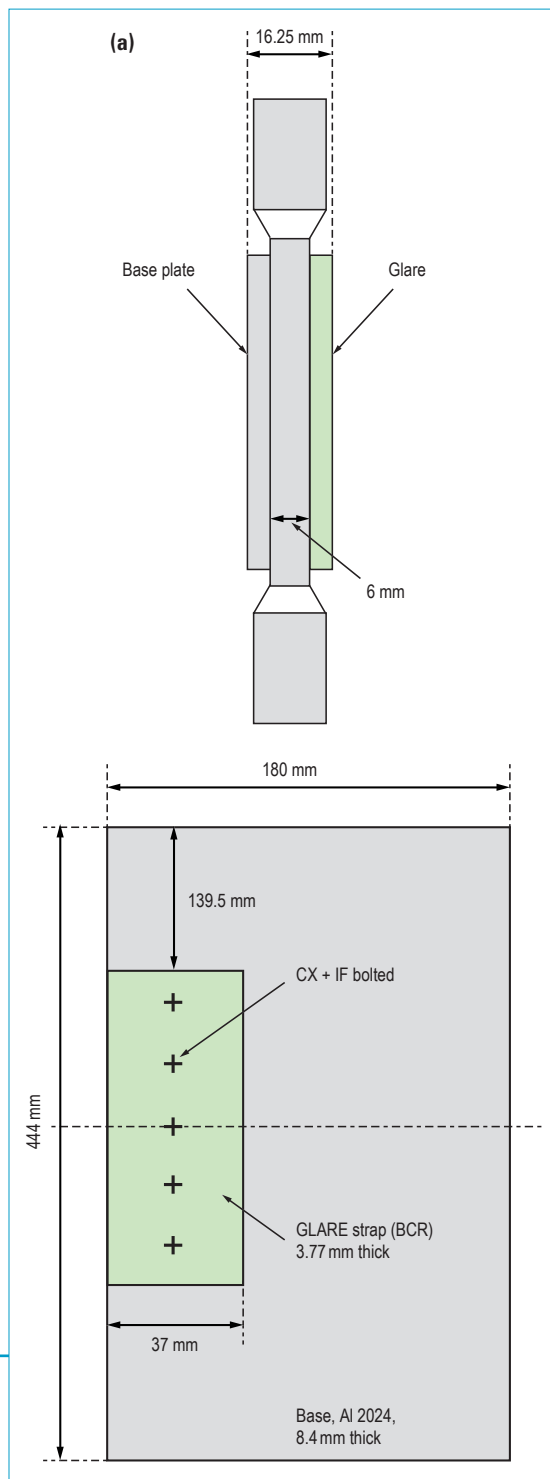
Figure 3:

Schematic of the proposed domain jamming. Counter rotated VL domains are prevented from rotating to the ground state orientation by the shaded regions.

Materials

Strain imager for engineering applications SALSA

Effect of thermal residual stresses in an aircraft manhole structures containing bonded crack retarder and interference bolts



In recent years bonded crack retarder (BCR) technology has attracted considerable interest in increasing the fatigue life and structural integrity within the airframe. The principle is to adhesively bond a stiffening "strap" in regions where crack propagation can be expected. The local increase in stiffness reduces crack growth consequently enhancing the fatigue life. However, thermal residual stresses developed during the bonding process are the drawback in BCR. In practice a reinforcing strap will require additional fixing by means of riveting or bolting to increase the fail safety and these holes will be cold worked to generate beneficial radial compressive stresses [1, 2]. Thermal residual stresses generated due to adhesive bonding may affect these beneficial compressive stresses which can then affect fatigue life of the secondary fixings. Therefore the quantification of these residual stresses is essential to improve the fatigue life and subsequently the damage tolerance of the aircraft.

The experiment was carried on SALSA at the ILL. The high flux available at SALSA allowed us to penetrate into the assembly, using a sufficiently small gauge volume for high resolution mapping of the strain field. Because of the stress discontinuities in the assembly, destructive techniques are not effective and X-rays do not have sufficient penetrability.

Figure 1a and **1b** shows the geometrical details of the Manhole specimen. The base material is made of Al 2024 and the BCR

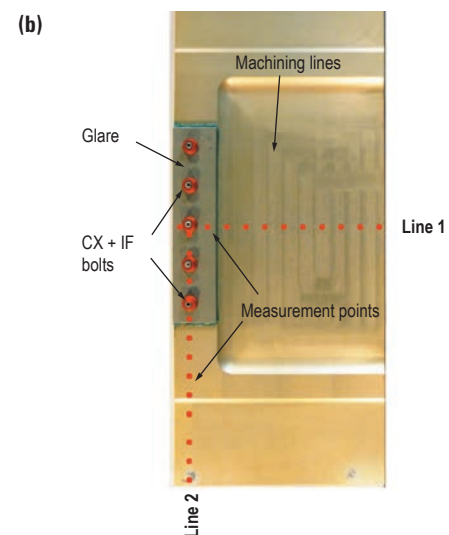


Figure 1: (a) Schematic representation of Manhole specimen; (b) Actual specimen used for the measurements.

is of glass reinforced composite sandwich (GLARE 6/5) made of 6 layers of aluminium sheets (Al 2024 T351) and 5 layers of adhesive impregnated with glass fibres. The measurements were carried out, in three principal strain directions, which were inferred from the geometry and symmetry around the holes, with a $2 \times 2 \times 2 \text{ mm}^3$ gauge volume. A far field measurement was carried in the base material and considered as a stress free reference measurement. Measurements were performed in two different locations *i.e.* line 1 and line 2 as shown in **figure 1b**. All the measurements were carried in the base material (Al 2024) at a distance of 1.5 mm through the thickness direction on the BCR side.

The data obtained was analysed in depth and **figure 2** shows the results obtained from the measurements. In line 1, measurements were performed starting from the edge of the strap (glare) and progressed towards the far edge of the specimens as shown in **figure 1b**. From **figure 2**, line 1, it can be seen that radial compressive stresses were present up to 3-4mm from the edge of the hole on both the sides of the bolted hole which results from the cold expansion process.

As the measurements progressed away from the hole compressive stresses are diminished and balancing tensile stresses were observed. Away from the strap, tensile stresses of 50 to 90 MPa can be observed in all the directions which may be attributed to the machining process on the specimen surface which can be seen in **figure 1b**.

In line 2, measurements were started from the lower edge of the specimen to the centre of the specimen as shown in **figure 1b**. In these measurements, from **figure 2**, line 2, the presence of radial compressive stresses can be observed around

the three bolted holes resulting from the cold expansion process. The tensile stresses (30 – 40 MPa) at the beginning of the measurements may be attributed to material texture as the base material is rolled along the longitudinal direction during the manufacturing process. In both the measurements thermal stresses are very low and have no significant effect on the cold expanded stresses.

In conclusion, the novel technique of neutron diffraction has been used and the high neutron flux at ILL allowed us to measure the residual stresses in the complex geometry.

Thermal residual stresses arising due to the elevated temperature adhesive bonding process are very low which attributed to the similar thermal expansion coefficients of both the base material and strap (BCR).

The results reveals that cold expansion process results in beneficial radial compressive stresses around the bolted hole and distributed up to 3-4mm from the edge of the hole. The results also reveal that there is no significant effect of thermal stresses on the cold expanded stresses.

Authors

A.K. Syed, M.E. Fitzpatrick and J.E. Moffatt (The Open University Milton Keynes, UK)
T. Pirling and A. Evans (ILL)

References

- [1] B. Nadri, L. Edwards, M.E. Fitzpatrick and A. Lodini, Journal of Neutron research 12 (2004)
- [2] A.T. Ozdemir and L. Edwards, Journal of strain analysis 31 (1996)

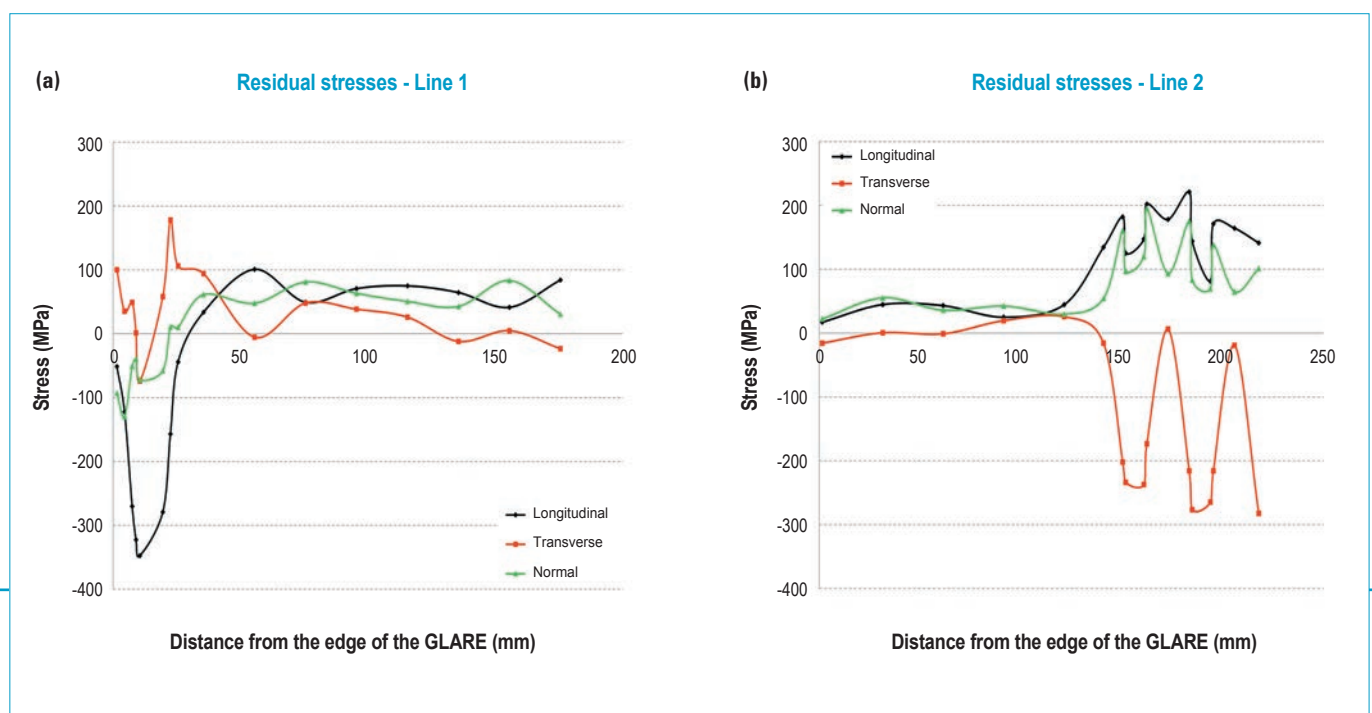


Figure 2: Residual stress measurements on the Manhole specimen (a) line 1 (b) line 2.

Materials

Small-angle scattering diffractometer D11

The structure and morphology of charged graphene sheets in solution

Graphene is perhaps the most exciting discovery in materials science in the last decade. Its experimental emergence in 2004 has inspired a surge in research and development, and its discoverers were awarded the Nobel Prize in Physics in 2010 [1]. Graphene is of immense interest as one of the few known 2-dimensional materials, providing us with free-standing atomic crystals with extraordinary physical properties and potential applications.

Graphene sheets have been isolated by a number of methods, including micromechanical cleavage of bulk graphite using sticky tape, epitaxial growth on surfaces, and thermal decomposition of silicon carbide [1,2]. However, these methods are low yield and rather labour intensive, and so they are less than ideal for industrial scale-up. For this reason there is great interest in graphene production and manipulation via liquid phase routes (inks), which can be used for the scalable production of functional films and composites.

Current methods for preparing graphene solutions include the dispersion of graphite powders in organic solvents via sonication,

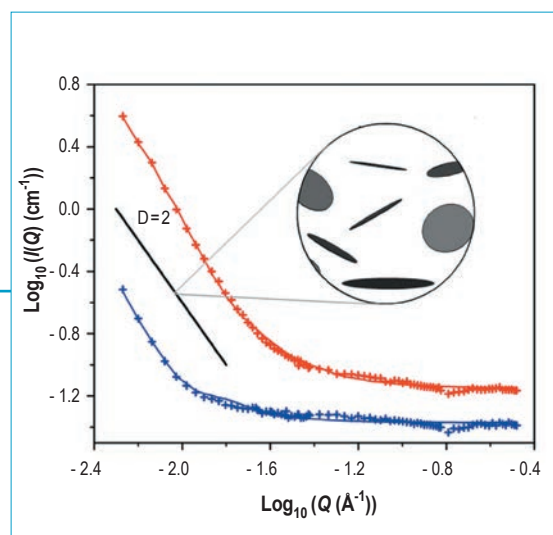
Graphene is a truly remarkable material, formed by a honeycomb lattice of carbon that is just one atom thick. It is stronger than steel, a better conductor of heat and electricity than copper, and almost completely transparent to light. Graphene therefore has numerous potential applications, from ultra-thin displays and touch screens, to transistors and solar panels. We have used neutron scattering to understand how individual graphene sheets can be dissolved in solution, paving the way for many new graphene-based processes and products.

polymer and surfactant wrapping, and reduction of soluble graphite oxides [3]. Another approach is to start with graphite intercalation compounds, which are formed by inserting arrays of atoms or molecules between the individual graphene sheets of graphite. In addition to providing increased concentration of pristine (unfunctionalized) graphene, intercalated graphite starting materials have the further advantage of providing us with control over the solution phase species, to yield a predominance of mono-, bi- or tri-layer graphene.

Small-angle neutron scattering data obtained on D11 from solutions of charged graphene platelets (of composition KC_{48}) dissolved in a solution of ammonia and tetrahydrofuran, at concentrations of 0.1wt% (red) and 0.01wt% (blue). The crosses are the experimental data, and the solid lines are the best fits obtained using the model shown in **figure 2**.

For guidance, the solid black line has a gradient $D = 2$ as expected for a solution of randomly oriented thin discs, as illustrated in the schematic.

Figure 1:



Our work has sought to address the problem of graphene dissolution, and we have developed a two-stage method for producing bulk quantities of individually-dispersed monolayer graphene sheets. In this process graphite is first charged and intercalated in liquid metal-ammonia solution, and second it is then dissolved in an organic solvent such as tetrahydrofuran.

Crucially, *in situ* small-angle neutron scattering (SANS) experiments conducted on the D11 instrument have provided us with detailed information about the structure and morphology of our graphene sheets in solution. SANS has proved an extremely powerful probe of these systems, and has allowed us to determine for the first time whether the graphene is present as single layers or agglomerates, as well as investigating the morphology of the monolayer graphene (for example, whether it is flat or rippled or folded).

Detailed analysis of our D11 data (**figure 1**) reveals that single layer graphene is indeed the dominant species in our solutions (> 95% by volume of dissolved particles), and demonstrates that the charged graphene platelets are flat over length scales >100 Å. The results also indicate a strong solvation shell around the charged graphene, which is quantitatively consistent with the picture that emerges from computer simulations (**figure 2**). A striking finding is that the size and shape of the original graphitic discs appears to be retained during the dissolution. Finally, the presence of single graphene sheets has been corroborated by using *ex situ* atomic force microscopy and Raman spectroscopy of drop-coated films.

Small-angle neutron scattering has provided us with the first detailed picture of the structure and morphology of graphene sheets in solution. The data show us that the use of electrostatic charging combined with appropriate mixed solvents leads to successful graphene dissolution. The physical structure of the graphene is unaffected by this processing, unlike methods relying on oxidation, functionalization or intense sonication, thereby offering significant benefits in a wide range of applications. Future work is aiming to dissolve much larger graphene sheets, and to systematically control the layer thicknesses.

Authors

E.M. Milner, C.A. Howard, N.T. Skipper, D.J. Buckley and **P.L. Cullen**
(University College London, UK)

M.S.P. Shaffer (Imperial College London, UK)

R.K. Heenan (ISIS)

P. Lindner and **R. Schweins** (ILL)

References

- [1] K.S. Novoselov, A.K. Geim, S.V. Morozov, D. Jiang, Y. Zhang, S.V. Dubonos, I. Grigorieva and A.A. Firsov, *Science* 306 (2004) 666
- [2] X. Li, W. Cai, J. An, S. Kim, J. Nah, D. Yang, R. Piner, A. Velamakanni, I. Jung, E. Tutuc, S.K. Banerjee, L. Colombo and R.S. Ruoff, *Science* 324 (2009) 1312
- [3] A.A. Green and M.C. Hersam, *J. Phys. Chem. Lett.* 1 (2010) 544

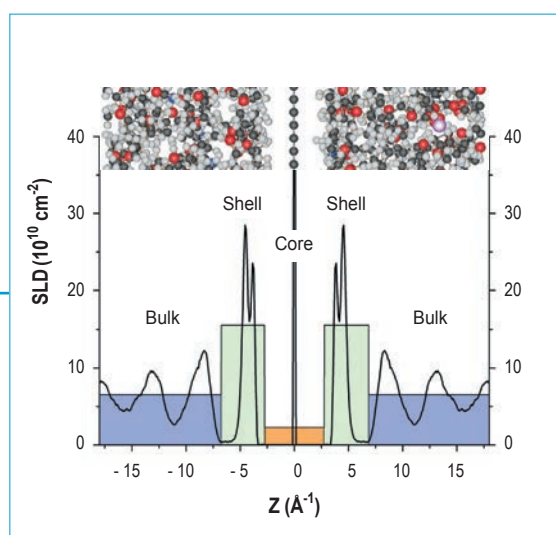


Figure 2:

The solvation structure of charged graphene platelets. Our small-angle neutron scattering data in **figure 1** is best fitted using a “core-shell-bulk” model, in which the core (orange block) denotes the graphene sheet, the shell (green block) the solvent molecules that directly solvate it, and the bulk (blue block) is the more distant solvent. The solid black line shows the neutron scattering length density (SLD) normal to the *ab*-plane of a single charged graphene platelet as obtained by Monte Carlo simulation. A representative molecular configuration is shown above (atomic color scheme: K – pink, H – light grey, N – blue, O – red, C – dark grey).

Materials

Small momentum transfer diffractometer D16 ESRF diffraction and multi-wavelength anomalous dispersion beamline BM02

Immiscible liquid vapour adsorption on a high-surface-area carbon

The adsorption of binary gas/vapour mixtures, of polar and non-polar molecules in particular, by high-surface-area activated carbon is not completely understood. With certain target molecules where efficiency of capture is vital (*e.g.* toxic substances), this could be an issue if water vapour is also present. Here we study the organisation of the condensed phase adsorbed in micropores from binary mixtures of two model molecules, toluene and water, using small-angle neutron scattering with contrast variation.

Activated carbon is a general adsorbent and was already prized by the ancient Egyptians. Today it occupies a commanding position in this respect, both as an adsorbent of impurities from liquids and from gases. It is used in the vapour phase for a range of applications, from air purification in gas masks to vapour retention in vehicle fuel tanks, plus a host of others.

In practice, the organic molecules targeted for adsorption compete with the relative humidity of the atmosphere, and this compromises the purification process.

The adsorption of binary gas/vapour mixtures, of polar and non-polar molecules in particular, by high-surface-area activated carbon is not completely understood. With certain target molecules where efficiency of capture is vital (*e.g.* toxic substances), this could be an issue if water vapour is also present. Here we study the organisation of the condensed phase adsorbed in micropores from binary mixtures of two model molecules, toluene and water, using small-angle neutron scattering with contrast variation.

Activated carbon owes its efficiency to its large surface area and high porosity (the surface area of one gramme of activated carbon often exceeds a thousand square metres). Its 'activity' comes from its hierarchical pore structure (a nanoreplica of a tree's root system) and its surface chemistry. The width of the narrowest pores is comparable to the size of the molecules of gas to be adsorbed (usually less than 1 nm). The molecules trapped inside the pores are in a state close to that of the bulk liquid, but their molecular interactions may be strongly influenced by the pore walls. As a consequence, if the adsorbed material consists of two species immiscible in the bulk state, spectacular differences in macroscopic behaviour could arise.

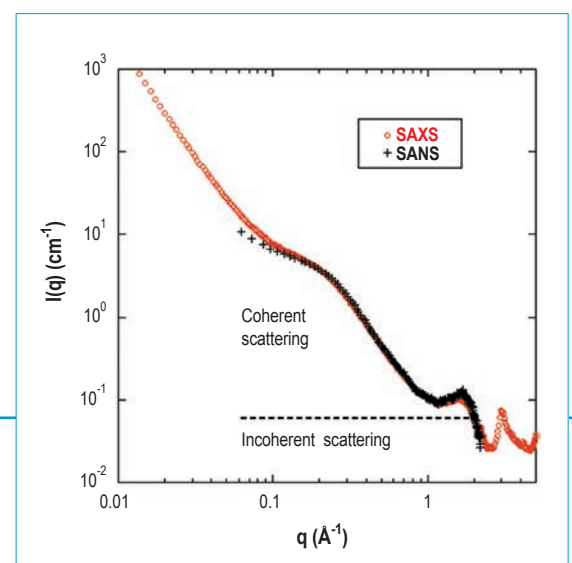


Figure 1:

A comparison of the SANS (+) and SAXS (o) signals from the dry activated carbon as a function of momentum transfer q yields the incoherent scattering intensity, which is related to the number of protons in the system.

When bulk liquid water and toluene are shaken together, they remain immiscible: the toluene dissolves no more than 0.033 % of its own weight of water. The question is: what happens when a mixture of these vapours enters the pores of an activated carbon? Is one species expelled, or are they adsorbed as separate phases? These questions are of practical importance, as they address a vital issue when dealing with toxic substances, the question of desorption.

Whilst macroscopic “break-through” measurements provide information on the overall adsorption pattern of binary mixtures of gases, they are unable to yield any indication of the spatial distribution of each species within the adsorbed layers [1, 2]. Neutron scattering with contrast variation can help here. It can reveal the different components in the adsorbed layer separately, if the neutron contrast of the probe molecules is modified by substituting deuterium for hydrogen.

The SANS measurements on D16 using contrast variation on an oxidized nanoporous carbon exposed simultaneously to water and toluene vapour showed that both solvents are adsorbed [3]. The intensities of the coherent and incoherent parts of the scattered signal (obtained with the aid of small-angle X-ray scattering measurements at the ESRF (figure 1) [4]) both show that the water volume fraction in the mixture inside the pores is about 0.12, *i.e.*, the toluene contains about 12 % v/v of water; this greatly exceeds the solubility of water in bulk toluene. Moreover, the values of the partial structure factors $S_{jk}(q)$ calculated for the ternary system (water + carbon + toluene) are only physically acceptable if the density of the adsorbed layer

is lower than its value in the bulk (figure 2). Thus, although the overwhelming majority of the adsorbed phase consists of toluene, the structure factors of the water, the toluene and the carbon components all have the same shape. This means that no distinct water phase (such as drops or inclusions) develops within the adsorbed fluid. Therefore, on the length scale of the observations, the mixture is uniform.

The activated carbon acts as a compatibilizer between toluene and water. The interactions between the adsorbed molecules in the confined space of the narrow pores are substantially modified by the surface of the confining walls. This opens a promising new avenue towards “green chemistry”, *i.e.*, chemical reactions under milder physical conditions.

Authors

K. László (Budapest University of Technology and Economics, Hungary)
O. Czakkel (ESRF, France)
B. Demé (ILL)
E. Geissler (UJF, Grenoble, France)

References

- [1] P.J. Reucroft, P.B. Rao, G.B. Freeman, Carbon 21 (1983) 171
- [2] A.W. Heinen, J.A. Peters, H. van Bekkum, Appl. Catalysis A: General 194 (2000) 193
- [3] K. László, O. Czakkel, B. Demé, E. Geissler Carbon 50 (2012) 4155
- [4] K. László, O. Czakkel, G. Dobos, P. Lodewyckx, C. Rochas, E. Geissler, Carbon 48 (2010) 1038

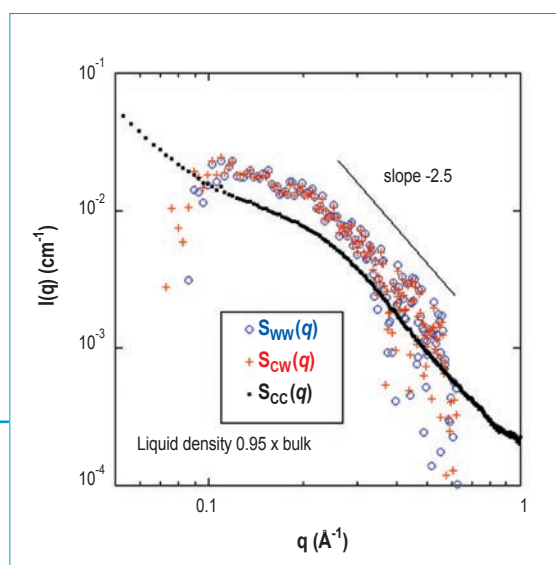


Figure 2:

Partial structure factors $S_{CC}(q)$ of the carbon and $S_{WW}(q)$ of the water are positive and proportional in the range, $q > 0.1 \text{ \AA}^{-1}$ (*i.e.*, where the micropores are filled with solvent). At $q > 0.6 \text{ \AA}^{-1}$ the signal is too small to give meaningful results. The density of the adsorbed liquid phase was taken to be 95 % of the bulk value.

Soft matter

Horizontal reflectometer FIGARO

Multilayers at interfaces of an oppositely charged polyelectrolyte/surfactant system resulting from the transport of bulk aggregates under gravity

Spontaneous multilayer formation at air/liquid and solid/liquid interfaces has been reported in a range of soft matter systems [2]. In many cases the mixed systems in question involve macromolecules. Repeating structures within the multilayer may be identified by the presence of a Bragg diffraction peak in specular neutron reflectometry measurements of a surface [3] or by off-specular neutron scattering [4]. A common interpretation of such observations is surface-induced self assembly, *i.e.*, spontaneous ordering of molecules induced by the presence of an interface in order to minimise its free energy.

Polymer/surfactant mixtures, which are used ubiquitously in formulations of countless household products such as detergents, have been shown to be extremely good candidates in the formation of multilayered interfaces [5]. It is also known that in the bulk solution strongly interacting mixtures form aggregates with internal molecular structure. The scope of the present work was to scrutinise whether the bulk aggregates could be involved in the formation of multilayered structures at interfaces and then determine the mechanism unequivocally.

We chose the strongly interacting mixture poly (diallyldimethylammonium chloride) /sodium dodecyl sulfate (Pdadmac/SDS) which had received recent attention because of a striking peak in its surface tension isotherm. Nevertheless it had been categorised as a system where interfacial multilayers were not expected, which prompted us to test whether any possible mechanism of formation of interfacial multilayers could be related to dynamic changes in the bulk phase behavior.

Some relevant visual observations concerning the bulk phase behavior of the system are represented in **figure 1**. For samples close to the charge match point of the oppositely charged polymer and surfactant, there is a suspension of bulk aggregates immediately upon mixing. With time the aggregates grow due to their lack of colloidal stability and under gravity the phase separation process becomes more evident. Depending on the isotopic contrast, the aggregates either float for polymer

Potential has been realised to make functionalised multilayered interfaces for use in electronic devices by molecular self assembly. Using neutron reflectometry measurements on FIGARO we have demonstrated a new mechanism of interfacial multilayer formation involving the self assembly of particles with internal molecular structure and their transport under gravity to surfaces of particular locations [1]. These findings may lead to optimised production of nanostructured interfaces involving a range of synthetic and biological macromolecules such as proteins or DNA.

with hydrogenated surfactant in deuterated water (left) yet they sink for polymer with deuterated surfactant in hydrogenated water (right). This difference arises due to changes in the relative densities between the aggregates and the bulk liquid when changing isotopic contrast. The same processes occur even for normal mixtures containing purely hydrogenated materials but here switching isotopic contrast was used as a tool to allow us to investigate the underlying physical chemistry more closely. These observations made us intrigued about the implications on the interfacial properties of these particles travelling in one direction or the other.

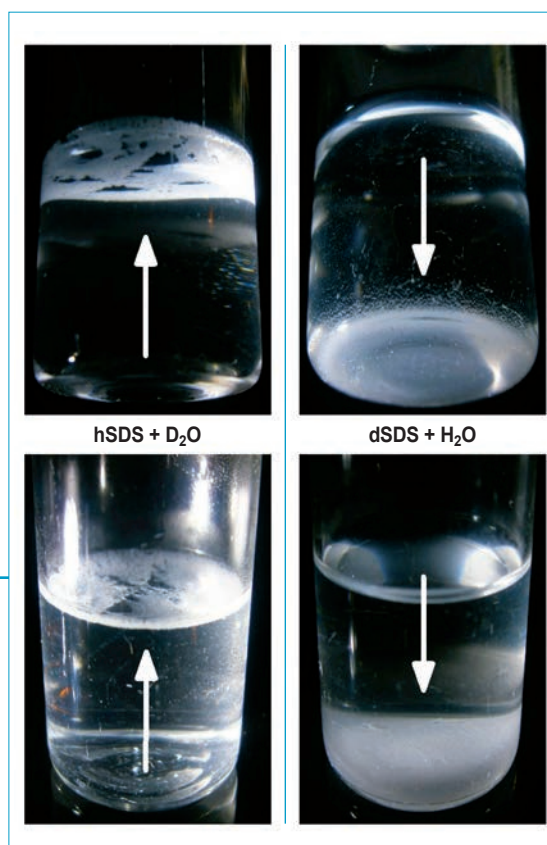


Figure 1:

Photos that highlight the directionality of the bulk aggregate transport for aged samples of Pdadmac/hSDS/D₂O (**left**) and Pdadmac/dSDS/H₂O (**right**). Perspectives are shown both from below the bottom surface (**top**) and above the top surface (**bottom**). The samples all contained 100 ppm Pdadmac, 0.82 mM SDS and 0.1 M NaCl which matched charge neutralisation of the bulk aggregates.

A series of measurements on FIGARO's adsorption troughs showed us that a strong Bragg peak and clear off-specular scattering – both indicative of interfacial multilayers – were present under three strict conditions: (1) only for samples in the phase separation region, (2) only for fresh samples where a suspension of bulk aggregates was still present in solution, and crucially (3) only where the aggregate transport process occurs upwards in the direction of the air/water interface. The data were modelled to show that the relative sizes of the diffraction peak recorded in different isotopic contrasts were not consistent with a surface-induced self assembly mechanism. Instead the data were consistent with a mechanism where the interesting surface structures were observed only under conditions when the aggregates floated. Nevertheless, we lacked direct proof of this proposed mechanism involving bulk self-assembly and transport of aggregates under gravity because we could not make measurements with bulk air beneath the liquid for obvious practical reasons!

As a result we formulated a proof-of-principle experiment where we substituted air for hydrophobic solid crystals. This had the advantage that confined surfaces in different locations could be measured both above and below the liquid. Different isotopic contrasts were also measured: one involving polymer with hydrogenated surfactant in deuterated water where the aggregates floated (left) and one involving polymer with deuterated surfactant in hydrogenated water where the aggregates sank (right). This experiment involved the comparison of reflection up and down measurements in time-of-flight mode on FIGARO, which is a unique capability.

The hypothesis under test was that if the mechanism of interfacial multilayer formation were surface-induced self assembly driven by the minimisation of the free energy of the surface then the pair of experiments involving the same sample at different orientations should produce equivalent data, yet if the data are not equivalent then gravity may be a critical missing factor in tuning the interfacial properties. **Figure 2** shows unequivocally that the surface structure – shown here as off-specular scattering images of the neutron detector with baseline-corrected Bragg peaks from the specular reflectivity – is present only when the structured particles were travelling under gravity in the direction of the interface in question.

The bulk transport mechanism determined in this work [1] is an alternative route of formation of interfacial multilayers to surface-induced self-assembly. Clearly the two processes give rise to interfaces with very different structural and morphological properties. Also, while it is most intuitive to consider an air/liquid interface with air above a flat liquid surface this is not the situation in droplets and foams, which emphasizes the need to understand the link between dynamic changes in the bulk phase behavior and the interfacial properties of such systems more clearly.

We believe that our findings may be relevant to the functional properties of macromolecule/surfactant mixtures in a range of systems.

Authors

R.A. Campbell (ILL)
M. Yanez Arteta and **T. Nylander** (Lund University, Sweden)
A. Angus-Smyth (ILL and Durham University, UK)
I. Varga (Eötvös Loránd University, Hungary)

References

- [1] R.A. Campbell, M.Y. Arteta, A. Angus-Smyth, T. Nylander and I. Varga, *J. Phys. Chem. B* 116 (2012) 7981–7990
- [2] D.J.F. Taylor, R.K. Thomas and J. Penfold, *Adv. Colloid Interface Sci.* 132 (2007) 69–110
- [3] H.S. Nalwa, "Handbook of Polyelectrolytes and their Applications", Vol. 1, American Scientific Publishers, 1st edition (2002)
- [4] D.E. Savage, J. Kleiner, N. Schimke, Y.-H. Phang, T. Jankowski, T. Jacobs, R. Kariotis and M.G. Lagally, *J. Appl. Phys.* 69 (1991) 1411–1424
- [5] P.M. Saville, I.R. Gentle, J.W. White, J. Penfold and J.R.P. Webster, *J. Phys. Chem.* 98 (1994) 5935–5942

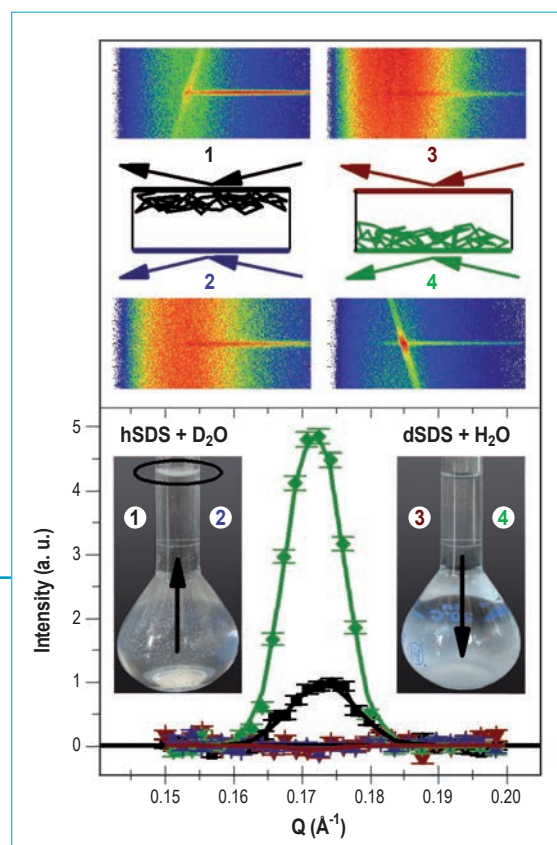


Figure 2:

(a) Neutron detector images comprising a color map of scattering for reflection angles of $\pm 1.5^\circ$ (vertical axis) with respect to the wavelength over a range of $1.5 - 10 \text{ \AA}$ (horizontal axis) from neutron reflectometry measurements on FIGARO of Pdadmac/SDS solutions at the hydrophobic solid/liquid interface.

(b) Bragg peak in the specular reflectivity profiles each with Gaussian fits, and additional illustrative photos of aged samples of Pdadmac/hSDS/D₂O (left) and Pdadmac/dSDS/H₂O (right). The samples all contained 100 ppm Pdadmac, 0.82 mM SDS and 0.1 M NaCl, and the data were recorded with a surface age of 27–36 hours.

Soft matter

Horizontal reflectometer FIGARO

Lipid flip-flop mechanism: loss of asymmetry in a model membrane system

Lipid translocation in membranes is a crucial process in biological science still far from being understood and characterised. In nature the lipid distribution across the inner and outer leaflet of cell membranes is asymmetric [1] and this asymmetry plays a prominent role

The nature of the process, its timescale and the necessary condition for its activation are not only far from being understood in natural cell membranes but also in simpler model systems. For example several discrepancies about the occurrence of the process and its characteristic time scale are present in the literature [3,4]. With the experiment performed on the neutron reflectometer FIGARO we provided a clear interpretation of

during cell fusion, activation of the coagulation processes, recognition and removal of apoptotic cell corpses by macrophages [2]. Lipid asymmetry in natural membranes is hypothesised to be promoted by the action of specific enzymes and by retentive mechanisms that trap lipids in one leaflet of the bilayer. The experiment performed showed that for a reconstituted system, where traps and enzymes were not present, it is not possible to keep the original asymmetric structural composition once all the lipids are in the fluid phase.

the structural conditions necessary to activate this process in a model membrane system. Among all the available techniques neutron reflectivity is a unique tool for the investigation of the absolute composition and the relative location of the molecules within the bilayer and at its interfaces. Using Langmuir-Blodgett and Langmuir-Schaefer deposition techniques (made available at the PSCM* facility of the ILL) we could prepare

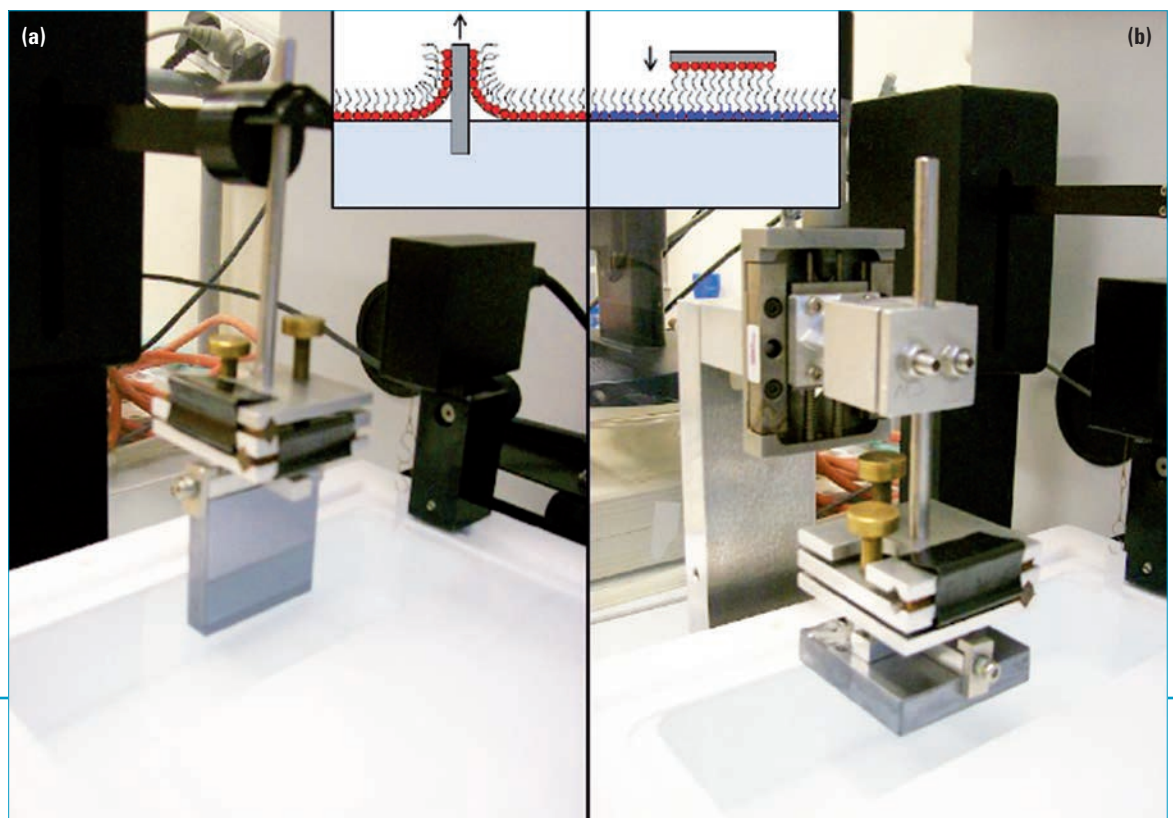


Figure 1: Langmuir-Blodgett (a) and Langmuir-Schaefer (b) stages used to produce the asymmetric starting bilayer. The NIMA trough is part of the PSCM equipment.

an asymmetric lipid bilayer with deuterated phospholipids in the gel phase and hydrogenated ones in the fluid phase in the inner and outer leaflet, respectively. The preparation steps are summarized in **figure 1**. In both phases the lipid molecules are constrained to the two dimensional plane of the membrane, but in liquid phase the molecules diffuse freely within this plane, being the packing of the molecules less ordered. The transition temperature between the two phases is indicated as melting point and this is different for different lipid types.

Crossing both of the phase transition temperatures activates the flip-flop process resulting in a structural rearrangement of the molecules toward complete mixing.

The reflectivity data and the resulting structural profiles are compared in **figure 2 (a)** panels for starting deposition, **(b)** ones for the final structure).

The temperature dependence of the reflectivity signal indicates that the asymmetry is maintained when at least one side of the bilayer is composed by lipids in the gel phase; the molecules mix completely when the melting point of both the lipid species is crossed [5].

Natural membranes are commonly composed by lipid in the fluid phase together with an asymmetric distribution of lipid species between the two leaflets. The experiment performed clearly demonstrates that is not possible to keep the asymmetric structural composition in a model bilayer once all the lipids are in the fluid phase. Therefore more complex systems have to be developed in order to mimic properly a natural asymmetric membrane.

* Partnership for Soft Condensed Matter, see p. 107.

Authors

Y. Gerelli, L. Porcar and G. Fragneto (ILL)

References

- [1] P.F. Devaux, *Biochemistry* 30 (1991) 1163
- [2] Fadeel B. and D. Xue, *Crit. Rev. Biochem. Mol. Biol.* 44 (2009) 264
- [3] M. Nakano and M. Fukuda and T. Kudo and H. Endo and T. Handa, *Phys. Rev. Lett.* 98 (2007) 238101
- [4] T. Anglin and M. Cooper and H. Li and K. Chandler and J. Conboy, *J. Phys. Chem. B* 114 (2010) 1903
- [5] Y. Gerelli, L. Porcar and G. Fragneto, *Langmuir* 28 (2012) 15922

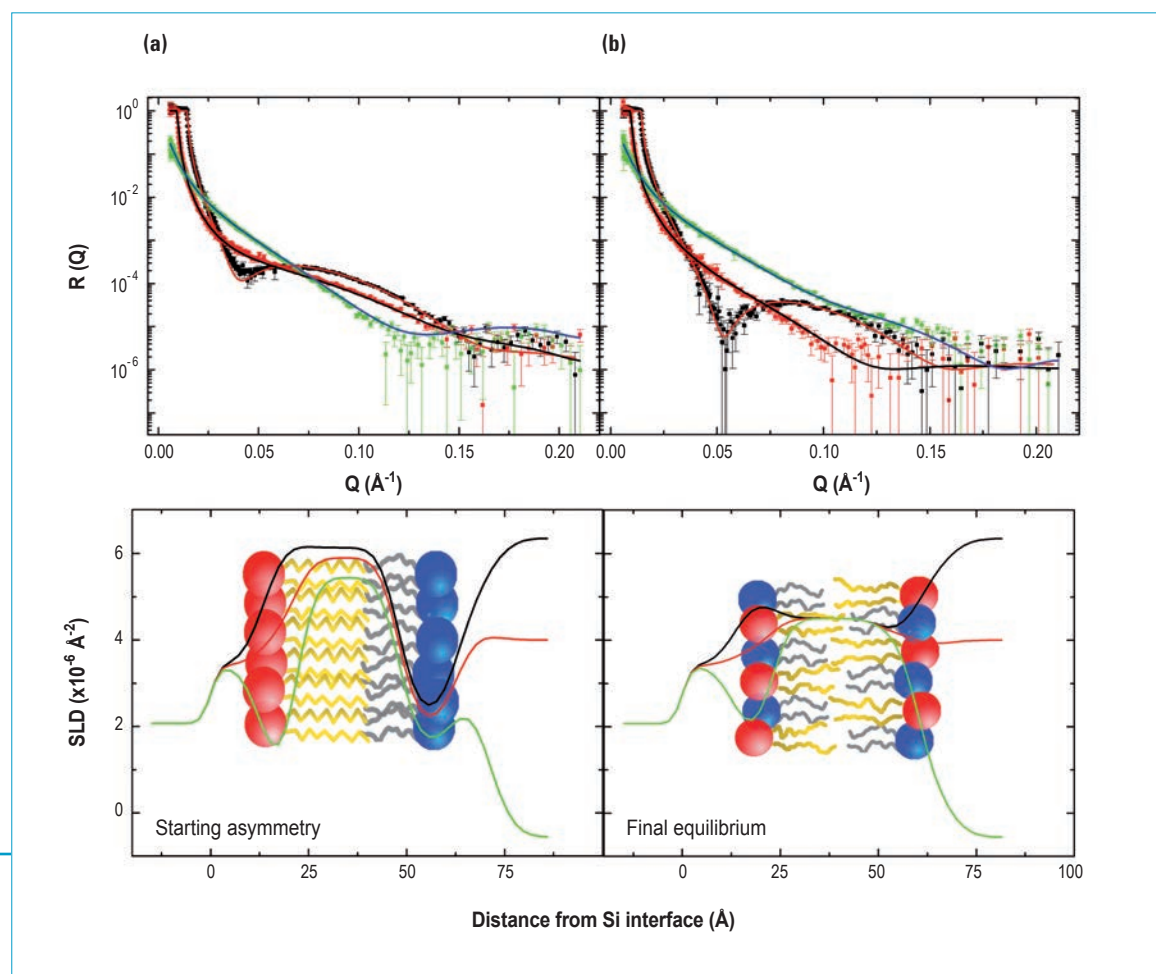


Figure 2: Reflectivity curves measured in different solvents before **(a)** and after **(b)** the phase transition. The resulting scattering length density profiles are shown in the lower panels. A pictorial sketch of the corresponding structures is reported as well.

Soft matter

Small-angle scattering diffractometer D22

Elucidating the kinetics of collapse transition and cluster formation in a thermoresponsive micellar solution induced by a temperature jump

The majority of thermoresponsive polymers in aqueous solution show lower critical solution temperature (LCST) behaviour. Below the LCST, they are water-soluble and the sample is optically transparent; above the LCST, at the so-called "cloud point", the polymer coils collapse and phase separate [1] and the system becomes optically turbid. We have investigated solutions and hydrogels from symmetric triblock copolymers which have long thermoresponsive poly(N-isopropylacrylamide) (PNIPAM) middle blocks and short and very hydrophobic polystyrene (PS) end blocks. Such block copolymers form flower-like micelles with a small PS core and a thermoresponsive PNIPAM shell and physically cross-linked thermoresponsive hydrogels by virtue of the hydrophobic aggregation of the end blocks.

Compared to classic chemically cross-linked thermoresponsive gels, they offer much higher structural variability. In previous temperature-resolved experiments, we found that, at the cloud

In aqueous solutions, triblock copolymers with a thermoresponsive middle block and hydrophobic end blocks form core-shell micelles with a thermoresponsive shell. Such systems may, for instance, be used for controlled gelation and ultrafiltration, as in microfluidic set-ups. At the cloud point of the shell block, the micellar shell collapses, and the micelles form large aggregates. Time-resolved small-angle neutron scattering (TR-SANS) has helped to elucidate the mechanisms and the kinetics of the complex collapse and intermicellar aggregation processes.

point (31.5 °C), the micellar shell collapses and the micelles form large aggregates in which they are tightly packed [2,3]. Yet, the process seemed to be highly complex.

To elucidate the pathways in this process, we carried out a fast temperature jump across the cloud point and followed the structural changes using time-resolved small-angle neutron scattering (TR-SANS) [4,5]. We used a modified stopped-flow cell at instrument D22 (**figure 1a**). The polymer solution (50 mg/ml in D₂O) was kept in the reservoir at 29.6 °C,

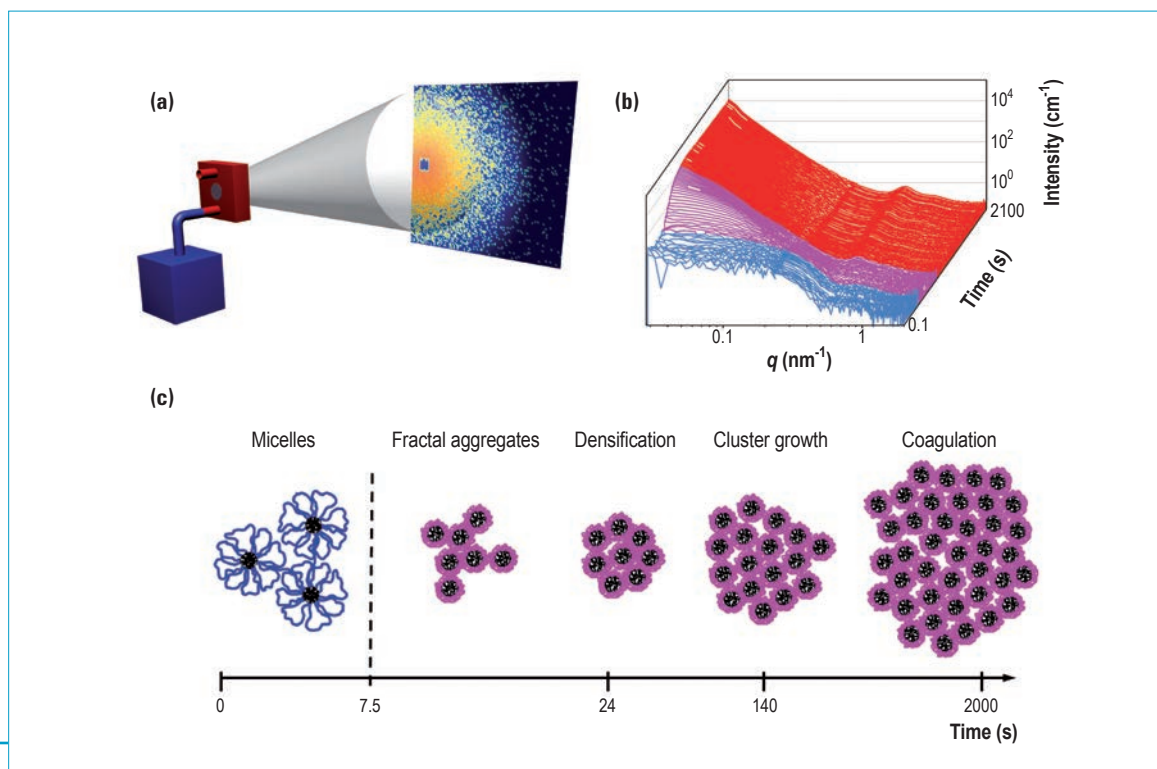


Figure 1: (a) Schematic set-up. The polymer solution is kept in a reservoir at 29.6 °C (blue) and is injected into the cell which is preheated to 34.6 °C (red). Data acquisition is started remotely upon injection. (b) SANS curves dependent on time. The different colours denote different time regimes. (c) Model of the structural reorganisation during the temperature jump. Black: PS blocks. Blue: swollen PNIPAM blocks. Pink: collapsed PNIPAM blocks.

thus below the cloud point. The sample cell in the neutron beam was pre-heated to 34.6°C, *i.e.* slightly above the cloud point. When the polymer solution was transferred from the reservoir into the cell, SANS measurements were started. Measuring times were increased from 0.1 s to 30 s. The cloud point was crossed after 7.5 s, and the target temperature was reached after about 100 s.

The SANS curves (**figure 1b**) initially show form factor scattering, reflecting the core-shell structure of the spherical micelles, together with a very weak structure factor indicating their correlation, which is partly due to intermicellar bridging (blue curves). With time, the forward scattering increases and the peak of the structure factor vanishes (pink curves). After 27 s, a correlation peak appears at a higher momentum transfer than in the swollen state. The distance between the micelles is again, thus, well-defined, but it has decreased compared to below the cloud point. The clusters first grow by attachment of additional micelles and, later, by coagulation (red curves).

We analysed the curves by fitting a model describing spherical core-shell micelles that are correlated in a liquid-like manner. This approach worked well below the cloud point and again far above. In contrast, just after crossing the cloud point, the collapsed micelles were found to form small, imperfect aggregates, which could be described by an expression for small fractal clusters of micelles [6]. In the later stages, the aggregates had grown and densified and could be described as large spheres which contain closely packed collapsed micelles.

The most important findings are summarised in **figure 2**. Whereas the radius of the PS cores stays constant, the micellar radius decreases abruptly at the cloud point because of the collapse of the PNIPAM shell. The collapse occurs within less than 1 s. Right above the cloud point, the collapsed micelles instantaneously form small fractal aggregates which

first densify – as evident from the increase of the fractal dimension to a value of 3 – before continuing to grow. Growth initially occurs by the attachment of single micelles to the existing aggregates, which is diffusion-limited; at later stages, the existing aggregates grow by coagulation (not shown). These structural changes are summarised in **figure 1c**. They are significantly more complex than those observed in a concentrated solution of PNIPAM homopolymers in D₂O [7].

In conclusion, TR-SANS provided a detailed picture of the complex structural changes and their kinetics when physically cross-linked thermoresponsive hydrogels are heated above their cloud point. These results are of great importance for designing the switching procedure in applications.

Authors

J. Adelsberger, E. Metwalli, A. Diethert, P. Müller-Buschbaum and **C.M. Papadakis** (TU Munich, Germany)

A.M. Bivigou-Koumba and **A. Laschewsky** (Potsdam University, Germany)
I. Grillo (ILL)

References

- [1] V. Aseyev, H. Tenhu and F.M. Winnik, *Adv. Polym. Sci.* 242 (2011) 29
- [2] A. M. Bivigou-Koumba, E. Görnitz, A. Laschewsky, P. Müller-Buschbaum and C. M. Papadakis, *Colloid Polym. Sci.* 288 (2010) 499
- [3] J. Adelsberger, A. Kulkarni, A. Jain, W. Wang, A. M. Bivigou-Koumba, P. Busch, V. Pipich, O. Holderer, T. Hellweg, A. Laschewsky, P. Müller-Buschbaum and C. M. Papadakis, *Macromolecules* 43 (2010) 2490
- [4] J. Adelsberger, E. Metwalli, A. Diethert, I. Grillo, A.M. Bivigou-Koumba, A. Laschewsky, P. Müller-Buschbaum and C.M. Papadakis, *Macromol. Rapid Commun.* 33 (2012) 254
- [5] J. Adelsberger, I. Grillo, A. Kulkarni, M. Sharp, A.M. Bivigou-Koumba, A. Laschewsky, P. Müller-Buschbaum, C.M. Papadakis, *Soft Matter* 9 (2013) 1685
- [6] J. Teixeira, *J. Appl. Crystallogr.* 21 (1988) 781
- [7] A. Meier-Koll, V. Pipich, P. Busch, C.M. Papadakis and P. Müller-Buschbaum, *Langmuir* 28 (2012) 8791

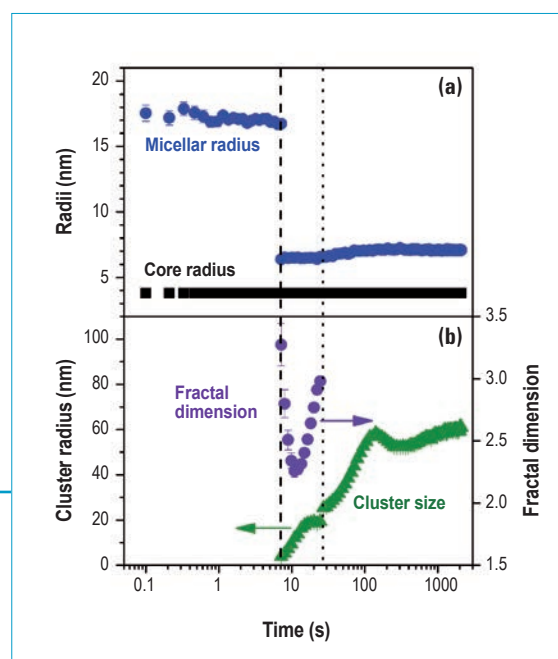


Figure 2:

(a) Core radius and micellar radius and (b) cluster radius and fractal dimension of the clusters. The dashed line denotes the cloud point, the dotted line the end of the near-transition regime.

Soft matter

Cold neutron backscattering spectrometer IN16

Lyophilised protein dynamics: more than just methyls?

Protein dynamics play a pivotal role in biological functions such as enzyme catalysis, ligand binding and protein folding. As a result, detailed appreciation of the relationships between dynamics and biological function require analysis based on models that realise the full complexity of macromolecular material. Neutron spectroscopy is an ideal tool with which to gain insight into the dynamics of bio-molecules since it not only is a non-destructive and selective technique but also provides simultaneously spatial and temporal information; parameters extracted from experimental neutron studies being akin to those calculated in molecular dynamic (MD) simulations. The range of bio-macromolecular problems addressed using neutron spectroscopy is considerable. However, it is clear that there is a need for further complete dynamical data given the complexity and diversity of bio-macromolecules.

The high energy resolution backscattering spectrometer, IN16, allows unique insight into the dynamic landscape of lyophilised proteins on the ps-ns time scale. Previously, we used the instrument to demonstrate that in the iron-storage protein apoferritin, between 100 K and 300 K, fast molecular motion

The movement of molecules on the fast pico- (ps) to nano- (ns) second time scale in proteins affects the slower, larger length-scale dynamics involved in protein folding and biological function [1].

As a result, detailed understanding of structure–dynamics–function relationships requires the use of theoretical models that incorporate the full dynamic complexity of a bio-material. To advance such models we have used neutrons to probe protein dynamics on the ps-ns timescale in a series of proteins: apoferritin (Apo), insulin (Ins), superoxide dismutase (SOD) and green fluorescent protein (GfP). Our results hint at a protein structure dependent dynamic landscape.

is dominated by the movement of methyl (CH_3) side groups. We observe a distribution of CH_3 activation energies consistent with the expected environmental heterogeneity which exists around methyl species in a protein. A mean activation energy of 17 kJ mol^{-1} was determined, with a width (σ) of 4 kJ mol^{-1} .

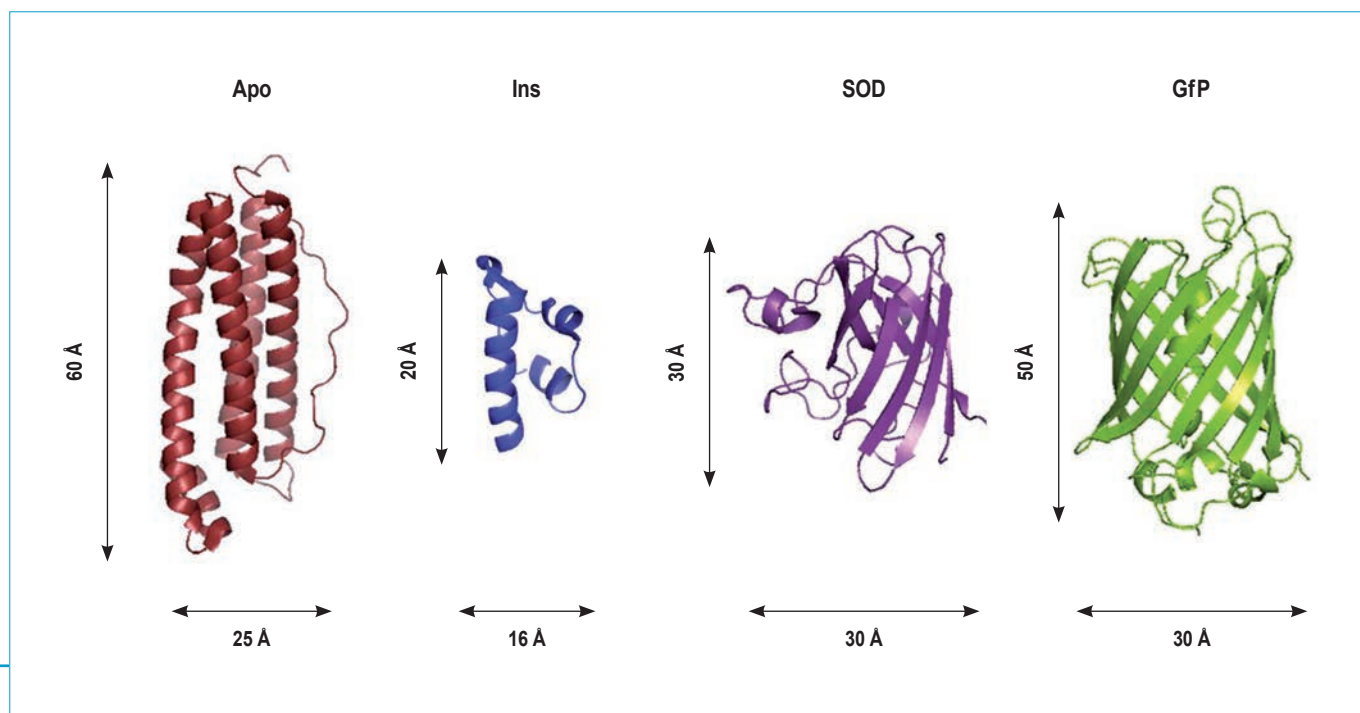


Figure 1: Representative tertiary structures for Ins, SOD, GfP and a single Apo subunit. The structures shown were generated in Pymol from the Protein Data Bank (PDB) wet crystal XRD entries.

Recently, however, we focussed our attention on the influence of protein structure on molecular dynamics. For this study we chose GfP and SOD as representative non-helical β -sheet proteins and Ins as an example of a protein with a helical structure (**figure 1**). The results were linked to those from the tightly bound helical assembly of apoferritin. The proteins were chosen since they all have approximately 25 % of their protons associated with methyl groups. For this study, we used IN16 operating in complementary elastic fixed window scan (EFWS) and inelastic fixed window (IFWS) scan modes. While the former is a well established experimental neutron method, the IFWS mode of operation is a novel technique and applied by us for the first time for the study of dry protein dynamics [2]. Our IFWS results are shown in **figure 2**.

Unlike Apo, neutron data from GfP, SOD and Ins cannot be described satisfactorily using a simple CH_3 -activation model alone. Instead, a second dynamic contribution, with a mean activation energy and distribution width comparable to that of methyl species, is required to fully describe the experimental data (**figure 2**). Unfortunately, no information about the geometry of the motion associated with this second process could be inferred from the data collected and further measurement and analysis is required. Molecular dynamic simulations are currently underway, in collaboration with the Computation - Lab (C-Lab, *p.106*) at the ILL, to identify the origin, or origins, of this additional dynamic response. However, our results are in line with early experimental NMR studies which suggest that CH_3 group reorientations may only account for 60 – 90 % of observable relaxation [3] and with the suggestion [4] that in homomeric polypeptides (*e.g.*, polyalanine) non-methyl side-chain motions may contribute to neutron elastic intensity changes of the order 10 – 20 %. In addition, reorientations of side groups containing exchangeable protons (*e.g.*, amino groups) may be expected

since no H/D exchange of the labile hydrogen atoms was performed during sample preparation.

In conclusion, we have successfully exploited the recently developed IFWS method on the IN16 spectrometer to study ps-ns dynamics in four structurally different lyophilised proteins [5]. The IFWS method has proven particularly useful for this work since it has allowed us to separate, with certainty, the extremely weak quasi-elastic scattering intensity arising from mobile atoms, from the sizable and dominant elastic scattering signal originating from immobile species. There is a clear difference in dynamical modes which cannot be solely described by the rotations of methyl groups. We note that, despite the limited number of proteins studied so far, the increase in IFWS intensity correlates with α -helix and β -sheet composition; higher inelastic intensities, hence mobility, being observed from the β -sheet rich species.

Authors

M.T.F. Telling (ISIS and University of Oxford, UK)
L. Clifton, S. Howells and **V. García Sakai** (ISIS, UK)
B. Frick (ILL)
J. Combet (ILL and now CNRS, Strasbourg, France)

References

- [1] K.A. Henzler-Wildman, M. Lei, V. Thai, S.J. Kerns, M. Karplus and D. Kern, *Nature* 450 (2007) 913-927
- [2] B. Frick, J. Combet and L. van Eijck, *NIM in Physics Research Section a-Accelerators Spectrometers Detectors and Associated Equipment*, 669 (2012) 7-13
- [3] E. R. Andrew, D.N. Bone, D.J. Bryant, E.M. Cashell, R. Gaspar and Q.A. Meng, *Pure and Applied Chemistry* 54 (1982) 585-594
- [4] G. Schiro, C. Caronna, F. Natali and A. Cupane, *J. Am. Chem. Soc.* 132 (2010) 1371-1376
- [5] M.T.F. Telling, L. Clifton, S. Howells, B. Frick, J. Combet and V. García Sakai, *Soft Matter Communication* 8 (2012) 9529-9532

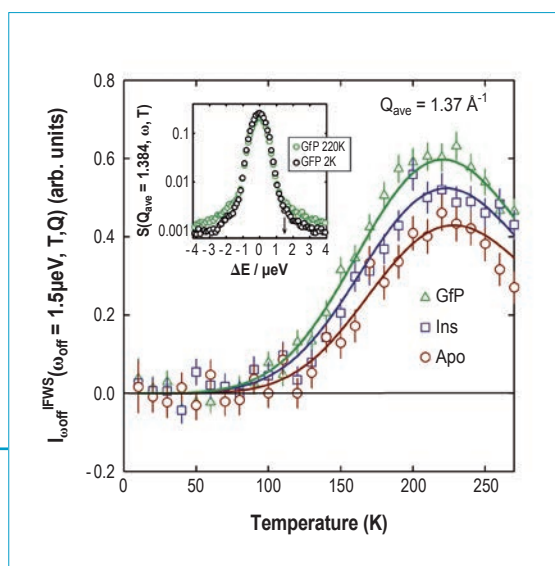


Figure 2: Inelastic fixed window intensities (IFWS) from Apo, GfP and Ins at an energy offset of 1.5 μeV and $Q_{\text{ave}} = 1.37 \text{ \AA}^{-1}$. The solid lines are a fit to the data using model functions.

Biology

Small momentum transfer diffractometer D16

Structural studies of amphotericin's incorporation within model human and fungal cell membranes

The clinical usefulness of amphotericin has always been circumscribed by the kidney-damaging side effects that arise when the drug is used in high doses [1], and the need for higher doses is now becoming more commonplace because of fungal strains that have developed resistance to the drug [2]. The way forward in tackling these problems would involve designing new drugs that work in the same way as amphotericin, but which are sufficiently different in their chemistry that the disease-causing fungi are not able to counteract their effects. Such an approach, of course, requires that we fully understand how amphotericin works, and unfortunately this is not the case. We do know that the drug has little effect on the cells in a human because these cells are surrounded by membranes containing cholesterol. We also know that the drug exerts its effects on fungi because their cells do not contain cholesterol, but instead have a related sterol, ergosterol. Quite how this difference between human and fungal cell membranes is important in the working of amphotericin, however, remains unclear.

Amphotericin is widely used in treating fungal infections in particular the life-threatening infections that affect chemotherapy patients and those suffering from AIDS.

Lately, however, there have been reports of infections that prove to be amphotericin-resistant. Combating this resistance through the development of new anti-fungal agents requires detailed knowledge of the drug's molecular mechanism but unfortunately this is far from clear. Neutron diffraction studies of the drug's incorporation within model cell membranes have here been performed to shed light on this problem.

The received wisdom is that the drug forms pores in the cell membranes, thus causing the cells to become leaky and then die. What these pores look like, whether they involve both sterol and drug or just drug, and whether those formed in fungal cell membranes are different from the ones formed in human cell membranes is not yet established.

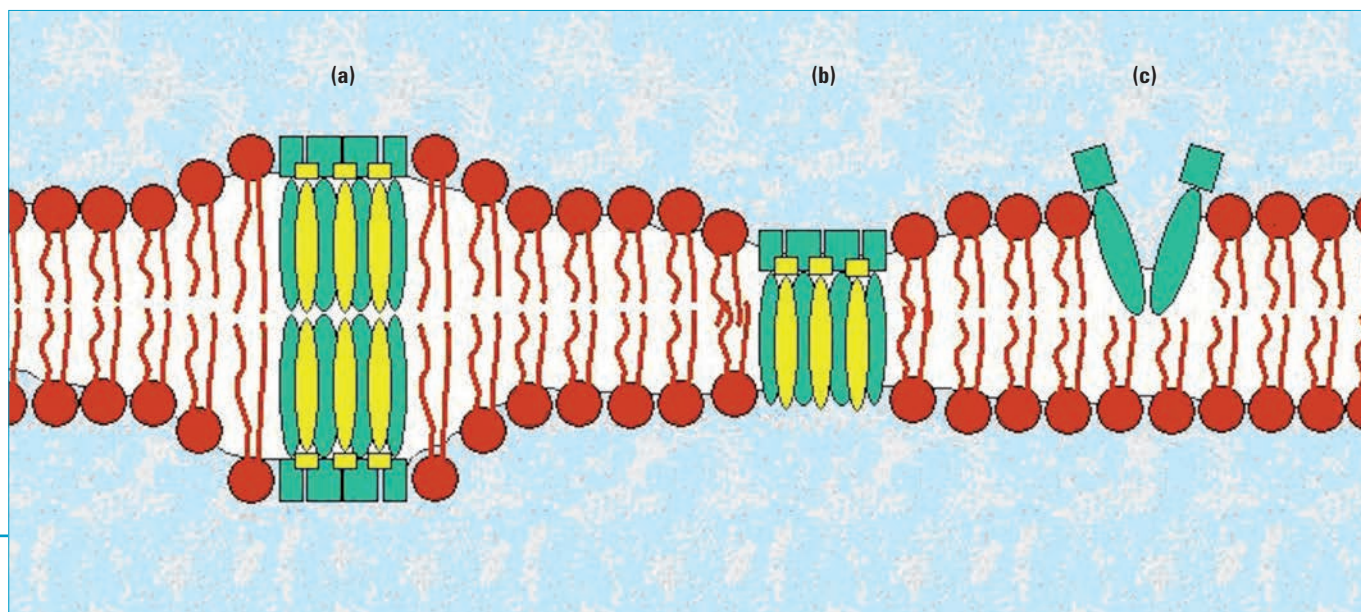


Figure 1: Schematic illustration of the various different structures proposed for the pores formed by amphotericin in lipid bilayers: aligned half-pores/ion channels **(a)**, half-width pores **(b)** and half-pores **(c)**. Amphotericin molecules are shown in green, sterols, yellow, and phospholipids, red.

In our research at King's College London, our aim was to find out precisely why this difference between cholesterol-containing and ergosterol-containing cell membranes is critical, and why, therefore, amphotericin is so damaging to fungi and not to humans.

In order to establish how amphotericin interacts with cell membranes and how its interaction differs between fungal and human cell membranes, we carried out neutron diffraction studies using the ILL diffractometer D16.

These studies (involving use of deuterated membrane lipids) allowed us to 'visualise' the position and orientation of the (hydrogenous) drug inside (model) human and fungal cell membranes, allowing us to discriminate between the different possible models that have been hypothesised to account for its anti-fungal activity. More specifically, the diffraction experiments allowed us to determine (1) whether the drug formed pores spanning the entire width of the membranes, (2) whether it formed pores spanning only half of the membrane, (3) whether such pores involved ergosterol and cholesterol as well as amphotericin (**figure 1**, [3]).

The results obtained were consistent with the model of amphotericin forming pores across the full width of the membrane, these pores comprising both sterol and drug molecules (**figure 1a**). There were subtle differences seen in

the position and orientation of the drug inside the fungal and human cell membranes, and this may be significant as regards the drug's anti-fungal activity (**figure 2**).

These first neutron diffraction experiments provide only a relatively low level of detail about the interaction between amphotericin and cell membranes. More detailed studies are planned for the future which will hopefully provide sufficient information to explain precisely (*i.e.*, at a sub-molecular level) why the drug behaves differently inside fungal versus human cell membranes. This will allow us to determine the part(s) of its chemical structure that give rise to this differing behaviour, and thus provide us with the knowledge to be able design new anti-fungal drugs that have the same specificity as amphotericin, but lack its kidney-damaging side effects.

Authors

D.J. Barlow, F. Foglia and M.J. Lawrence (King's College, London, UK)
G. Fragneto and B. Demé (ILL)

References

- [1] C. Lass-Flo, *Mycoses* 52 (2009) 197
- [2] M.A. Pfaller, *Am. J. Med.* 125 (Suppl. 1) (2012) S3
- [3] B.E. Chohen, *Biochim. Biophys. Acta – Biomembranes* 1108 (1992) 49

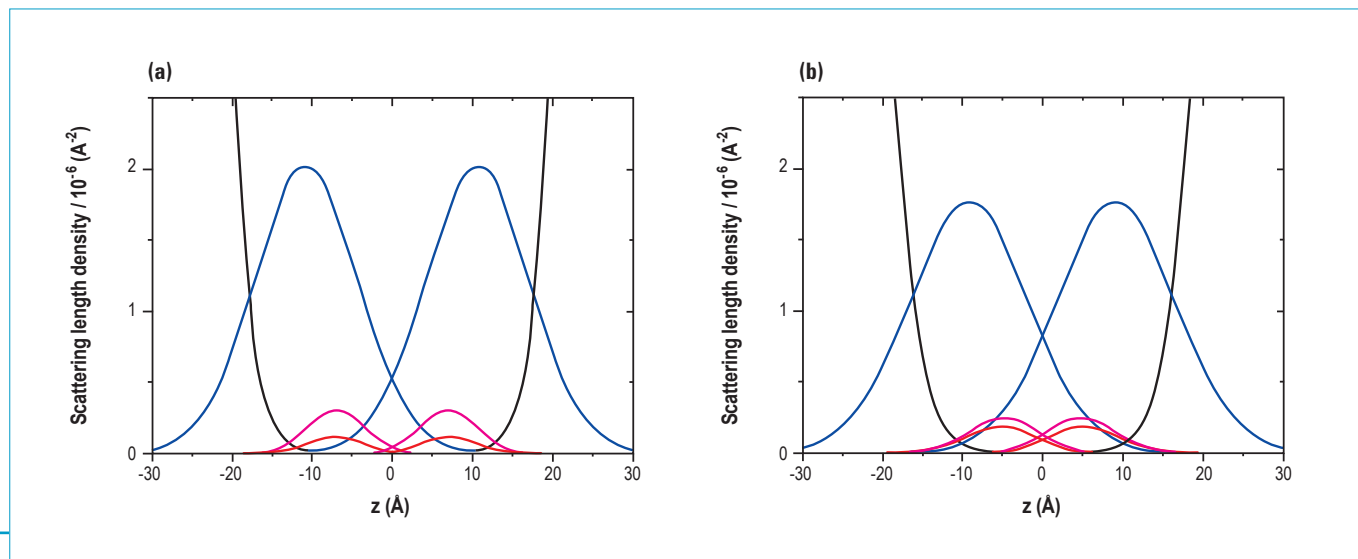


Figure 2: Fitted scattering length density profiles for the bilayer constituents: POPC (blue lines), cholesterol or ergosterol (red lines), amphotericin (magenta lines), and solvent (black lines). **(a)** POPC-cholesterol-amphotericin system; **(b)** POPC-ergosterol-amphotericin system. The scattering length density (in \AA^{-2}) is plotted as a function of z , the distance along the normal to the bilayer (in \AA), with the bilayer centre assigned as $z = 0 \text{\AA}$. Note that for clarity in display of the AmB and sterol distributions, the scale on the ordinate is expanded, and so only the in-facing tails of the solvent distributions are seen.

Biology

Reflectometer D17

Reflectivity from floating bilayers: an insight in the asymmetric structuring of biomimetic membranes

Lipid rafts [1] are membrane domains with a very specific lipid composition, high in cholesterol and host to special proteins or receptor molecules. Certain lipid rafts are enriched with gangliosides, sialic-containing glycosphingolipids which are only found in the outer layer of the membrane. Glycosphingolipids have a special link with cholesterol, regulating the membrane structure [2]; they are involved in many biological processes. In lipid rafts, strong cholesterol enrichment (about 70 % of the total) is hypothesised in their inner leaflet, *i.e.* in the opposite layer with respect to the glycosphingolipids that enrich the outer leaflet [3]. The asymmetric distribution of ganglioside-cholesterol may be reflected in both the asymmetric distribution of other molecules within the raft and in specific local mechanical properties. In this view, the ganglioside-cholesterol pair could constitute a structural unit across the membrane. Our aim is to validate an experimental model for the study of the internal structure of lipid rafts. There are numerous experimental difficulties; the challenge is to couple nanoscale probing and the construction of asymmetric model membranes with a template-free, defined heterogeneous composition (a particularly interesting artificial system).

We developed a protocol for the preparation of lipid floating membranes using a combination of Langmuir-Blodgett and Langmuir-Schaefer techniques (**figure 1**), replicating asymmetry and mimicking the composition of the lipid rafts (phospholipid: cholesterol: glycolipid = 10: 2.5: 1 molar ratio).

The distribution of components in biomembranes is uneven in both the transverse and the longitudinal directions, modulating the membrane tridimensional structure and dynamics. Spatial selection of components is essential for membrane functionality. Components leading to inhomogeneities in the two leaflets of a membrane can also couple within functional domains such as lipid rafts [1]. We used neutron reflection technique to examine ganglioside-cholesterol structural coupling, which is widely considered to be determinant for membrane rafts structure, although never experimentally confirmed.

We then took neutron reflectivity measurements, using the D17 reflectometer, to study the effect of monosialo-ganglioside GM1 on the distribution of cholesterol within the membrane.

We investigated two different model systems, assessing **(a)** the distribution of cholesterol in GM1-free floating membranes, and **(b)** the response of the cholesterol distribution with GM1 asymmetrically inserted, whether by incubation with a GM1 solution or by inclusion of the GM1 in the floating-membrane deposition protocol. Fully deuterated DPPC was used to highlight the cholesterol and GM1 within the phospholipid matrix. All of the membranes were observed in three water solvents, for contrast variation.

We can first of all confirm that we did indeed succeed in building for the very first time a complex multicomponent asymmetric floating membrane system.

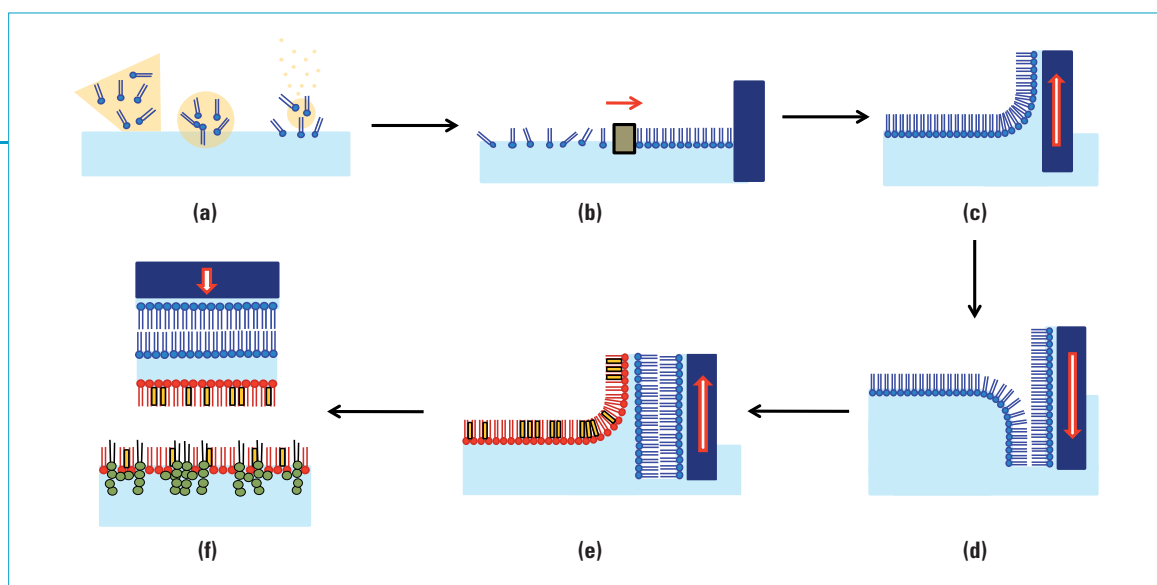


Figure 1: Schematic representation of the bilayer deposition technique: **(a)** spreading of lipid monolayer on water surface; **(b)** compression of monolayer; **(c), (d), (e)** Langmuir-Blodgett depositions of the first three layers; **(f)** Langmuir-Schaefer deposition of fourth monolayer.

Secondly, we were able to observe that if the DPPC-cholesterol sample is annealed, the cholesterol is redistributed symmetrically. This is an important finding, also in view of the use of cholesterol-containing model membranes. In fact, standard procedures often involve annealing (heating and cooling the sample to melt and gel the lipid chains), in order to remove any inhomogeneities due to sample preparation. Based on our observation, we suggest carefully reconsidering whether annealing is appropriate when dealing with asymmetric samples.

We found that the presence of GM1, on the other hand, forces an asymmetric distribution of cholesterol, even after annealing (**figures 2 and 3**). The extent of cholesterol in/out asymmetry is indeed the same, whatever the initial distribution of cholesterol and the technique used for GM1 insertion (whether included during the deposition procedure or incubated onto a DPPC+cholesterol symmetric membrane). The distribution obtained is very close to the hypothesised physiological distribution (*i.e.* roughly 80 % in the inner layer of the membrane and 20 % in the outer, together with GM1). This is an important finding, as ganglioside-cholesterol structural coupling is considered by many to determine the membrane rafts structure, although this has never been experimentally confirmed.

We owe this experimental demonstration to the association of highly advanced neutron reflectivity techniques with the asymmetric Langmuir Blodgett deposition protocol. This is an extremely promising combination, as it allows biologically significant model membranes to be constructed with distinctive features such as asymmetry; it also allows their internal structure to be examined at nanometric scale.

Authors

V. Rondelli, S. Motta, E. Del Favero, P. Brocca, S. Sonnino and L. Cantù
(University of Milan, Segrate, Italy)
G. Fragneto (ILL)

References

- [1] K. Simons and E. Ikonen, *Nature* 387 (1997) 569–572
- [2] H. Ohvo-Rekilä, B. Ramstedt, P. Leppimäki and J.P. Slotte, *Prog. Lipid Res.* 41 (2002) 66–97
- [3] W.G. Wood, U. Igbavboa, W.E. Muller, G.P. Eckert and J. Neurochem. 116 (2011) 684–689

Original contributions

- [4] V. Rondelli *et al.*, *J. Phys.: Conf. Ser.* 340 (2012) 012083
- [5] V. Rondelli *et al.*, *BBA* 1818 (2012) 2860–2867

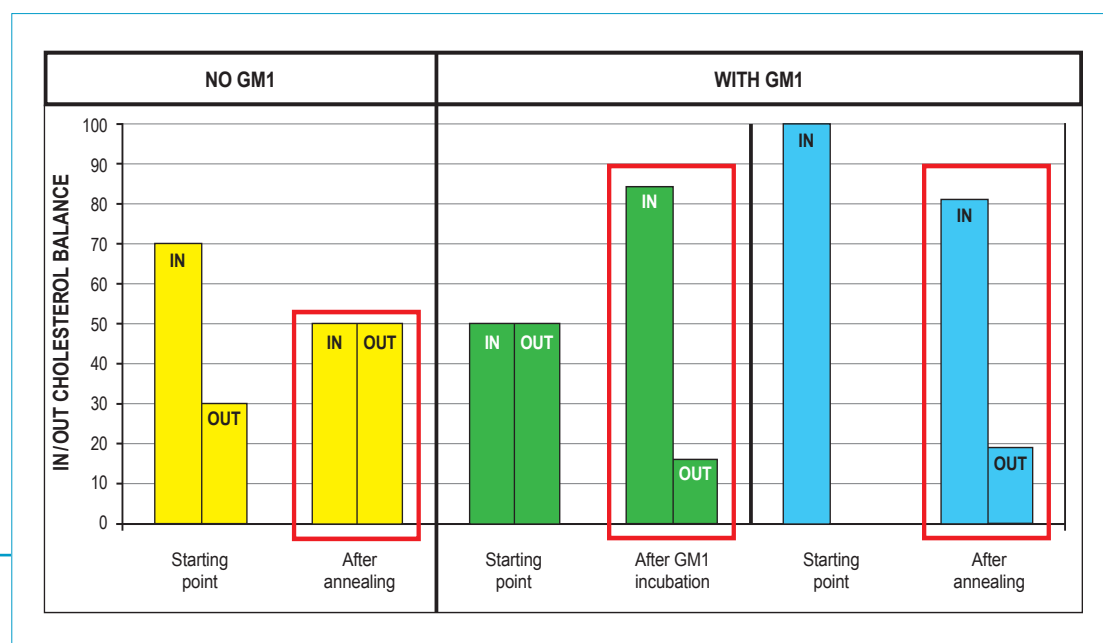


Figure 2:

Cholesterol positioning in the inner and outer leaflets of the floating membranes.

Left panel: without GM1, casted asymmetric positioning of cholesterol is destroyed by annealing. **Central and right panels:** GM1 forces redistribution of cholesterol in an optimal coupling ratio.

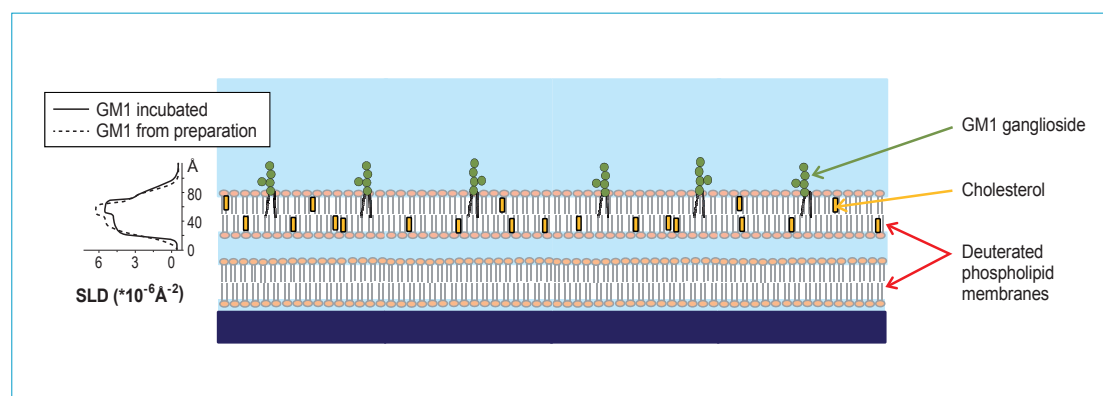


Figure 3:

Schematic representation of the samples investigated. The lipid matrixes consist of fully deuterated phospholipids. The floating membrane composition is asymmetric in cholesterol and gangliosides distribution. **Left graph:** contrast profiles of the floating bilayers of the two samples at $T=22^\circ \text{C}$ in H_2O . **Straight line:** GM1 was incubated; **dashed line:** GM1 inserted from preparation.

Biology

Backscattering spectrometers IN10 and IN16

Dynamics of proteins in solution around the denaturing transition: separation of global and internal modes

Side-chain and subunit motions are of particular interest to understand the biological function of proteins or potential applications of other nanometer-scale soft-matter systems in solution such as suspensions of grafted colloids or polymers. Incoherent neutron spectroscopy provides an optimal tool to record the unperturbed dynamics of hydrogen-rich macromolecules suspended in solution. Ideally, the solvent molecules – typically water – are deuterated to enhance the scattering contrast and sensitivity to the solute molecules.

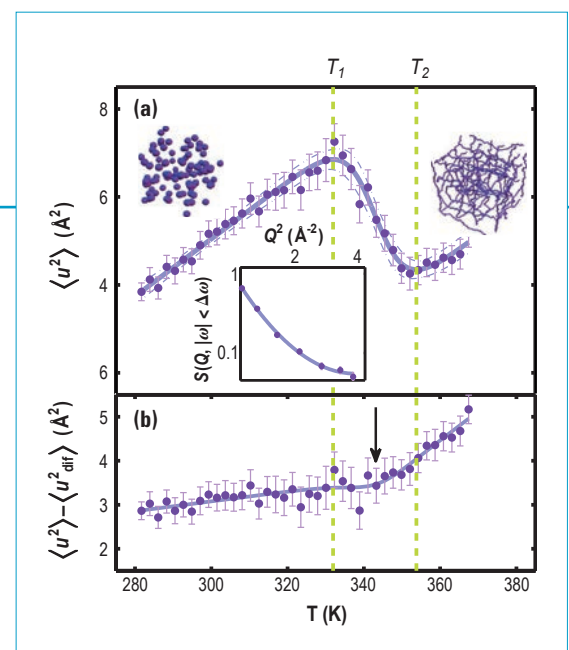
A significant difficulty, however, arises when it comes to separating the different types of motion of the solute molecules which contribute to the observable dynamic scattering function $S(Q, \omega)$. These different types of motion include the global center-of-mass diffusion D of the solute molecules, the internal diffusion characterised by an average confinement length scale Δr , and vibrations. To circumvent this analytical problem, internal dynamics of macromolecules have been studied often

The motion of a protein in its native intracellular aqueous environment is a complex superposition of atomic vibrations, the diffusion of molecular subunits, as well as the rotational and translational diffusion of the entire protein. It is challenging to separate these different contributions to the observable neutron scattering signal. A new and general approach to the analysis of backscattering data now allows to extract accurate information on the internal molecular motions and to for instance infer on the thermal unfolding of side chains.

not on solution samples, but on samples in a dry or hydrated state, thereby suppressing the center-of-mass diffusion [1]. Our new general approach [2] simplifies similarly comprehensive investigations of solution samples as described in the following. We thereby refer to our benchmarking experiment using an aqueous (D_2O) solution of the globular model protein Bovine Serum Albumin (BSA).

Using fixed elastic window neutron backscattering spectroscopy, we observe the scattering function $S(Q, \omega)$ within the very narrow elastic energy window $\Delta\omega$, *i.e.* $S(Q, |\omega| < \Delta\omega)$. We define the apparent total mean-squared

Figure 1:
(a) Total mean-squared displacement $\langle u^2 \rangle$ (circles) of an aqueous BSA (500 mg/ml) solution versus temperature T . The solution was heated at 0.074 K/min. Using a phenomenological transition model [2] we describe the data (solid line) and determine the denaturing interval $T_1 < T < T_2$ (dashed vertical lines). The upper inset images illustrate a colloidal suspension of native proteins (**left**) and the cross-linked network of denatured proteins (**right**). Lower inset: Measured elastic intensity $S(Q, |\omega| < \Delta\omega)$ versus Q^2 (circles) for the same sample at $T=290$ K recorded at IN10. A quadratic fit (solid line) was used to determine $\langle u^2 \rangle$.
(b) $\langle u^2 \rangle - \langle u_{diff}^2 \rangle$ (circles). The vertical dashed lines denote the transition regime. At $T_0 = (T_1 + T_2) / 2$ a transition occurs, characterised by a kink in the curve (arrow).



displacement $\langle u^2 \rangle$ observable in backscattering as $\langle u^2 \rangle = -3 \lim_{Q \rightarrow 0} \{ \log [S(Q, |\omega| < \Delta\omega)] / Q^2 \}$. We display the experimental result for $\langle u^2 \rangle$ as a function of temperature T recorded on BSA (500mg/ml) in D_2O in **figure 1a**. Subsequently, we employ the analytical separation of the different contributions to $\langle u^2 \rangle$ [2] and our existing knowledge on the global diffusion of the proteins [3] (**figure 2**). We write $\langle u^2 \rangle = \langle u_{\text{vib}}^2 \rangle + \langle u_{\text{sub}}^2 \rangle + \langle u_{\text{dif}}^2 \rangle$ with the contributions due to vibrations $\langle u_{\text{vib}}^2 \rangle$, protein subunit diffusion $\langle u_{\text{sub}}^2 \rangle$ and the global protein diffusion $\langle u_{\text{dif}}^2 \rangle$ [2]. As a result, we obtain the mean-squared displacement arising solely from the internal motions of the proteins (**figure 1b**). We point out that the heuristic approach of separating the different contributions to the total mean-squared displacement into a sum can be justified more rigorously based on the general form of the elastic incoherent structure factor [2]. Our experimental example serves to identify the denaturing temperature T_0 of BSA (arrow in the lower part of **figure 1**). T_0 can be obtained from a phenomenological transition model [2] within a broad transition regime (vertical dashed lines in **figure 1**), where the thermal unfolding of the proteins occurs. Beyond the denaturing temperature, the unfolding protein side groups cross-link and form a gel-like network at a sufficiently high protein concentration. Remarkably, $\langle u^2 \rangle$ (**figure 1**) strongly decreases within the transition regime $T_1 < T < T_2$ due to the slowing-down of the global motions. For $T_2 > T$, $\langle u^2 \rangle$ increases again due to the thermally enhanced internal motions in the gel-like entangled network of protein chains.

Our new study opens up perspectives for future experiments on protein solutions. Notably, molecular crowding is expected to have an impact on the thermal stability of proteins [4].

Crowding can therefore be assumed to influence the slope in $\langle u^2 \rangle - \langle u_{\text{dif}}^2 \rangle$ as well as the denaturing temperature. Our new framework can, hence, be applied to systematically investigate thermal stability properties of proteins in their native solution environment as a function of the level of macromolecular crowding. Further, the influence of salt added to the protein solution may be investigated, which can also influence the thermal stability of proteins. Finally, our new approach to the analysis of elastic window neutron scattering data from solution samples is not limited to protein systems, but can be applied to suspensions of other nanometer scale soft matter systems such as polymers or other macromolecules

Authors

M. Hennig, F. Roosen-Runge, F. Zhang, S. Zorn and F. Schreiber

(University of Tübingen, Germany)

M.W.A. Skoda (ISIS, UK)

R.M.J. Jacobs (University of Oxford, UK)

T. Seydel (ILL)

References

- [1] F. Gabel, D. Bicout, U. Lehnert, M. Tehei, M. Weik and G. Zaccai, Q. Rev. Biophys. 35 (2003) 327
- [2] M. Hennig, F. Roosen-Runge, F. Zhang, S. Zorn, M. W. A. Skoda, R. M. J. Jacobs, T. Seydel and F. Schreiber, Soft Matter 8 (2012) 1628
- [3] F. Roosen-Runge, M. Hennig, F. Zhang, R. M. J. Jacobs, M. Sztucki, H. Schober, T. Seydel, and F. Schreiber, PNAS 108 (2011) 11815
- [4] L. Stagg, S.-Q. Zhang, M.S. Cheung and P. Wittung-Stafshede, PNAS 104 (2007) 18976

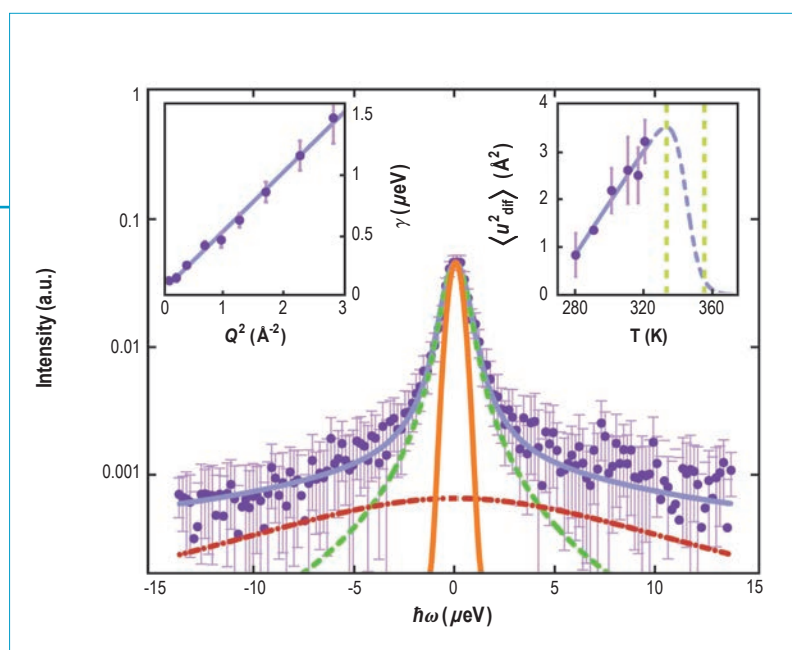


Figure 2:

Example spectrum $S(Q, \omega)$ (symbols) recorded on IN16 for BSA in D_2O (concentration 500 mg/ml, volume fraction 27 %, $T=301$ K, detector at $Q=0.6 \text{ \AA}^{-1}$). The solid line superimposed on the data indicates the fit. The two Lorentzian contributions are denoted by the dashed and dash-dotted lines, respectively, and the Gaussian resolution by the solid line in the center.

Inset left: Lorentzian width γ due to global diffusion (symbols) fitted to the signal from grouped detectors versus Q^2 .

Inset right: Temperature dependence of $\langle u_{\text{dif}}^2 \rangle$ due to global diffusion (symbols). The solid line is a linear fit for $T \leq 320$ K, namely $\langle u_{\text{dif}}^2 \rangle = aT + b$. For $T > 320$ K we assume that the diffusion is hindered by entanglement and we therefore postulate $\langle u_{\text{dif}}^2 \rangle = (aT + b)[1 - \Theta(T^*)]$ with the smeared-out step-function $\Theta(x) = [1 - \exp(-x)]^{-1}$.

The vertical dashed lines denote the transition regime.

Biology

Backscattering spectrometer IN10 Time-of-flight spectrometer IN6

Hydrogen bonds, molecular dynamics, and conformational flexibility in pharmaceuticals

If drugs are just chemicals, why, then, do they have such an impact on a structure as large and complicated as the human body? The answer lies in the way our bodies function. If we could see ourselves at a molecular level we would see a marvelous display of chemical reactions taking place, keeping the body healthy. A drug entering this world interacts with these processes via mechanisms common to solution chemistry, including hydrogen bonding, dipole-dipole interactions, charge-transfer and covalent bonding. There is therefore nothing surprising or peculiar in the fact that substrate-receptor interactions, drug metabolisms within cells, and phase stability are all linked to the dynamics of molecular fragments and the properties of hydrogen bonds. Moreover, understanding the relationships at a molecular level between intermolecular hydrogen bonds, intramolecular dynamics, and conformational flexibility can help identify how chemical reactions occur in molecular drugs. In pharmaceutical

BEX [1] was a very popular drug in the 1950s, containing 42% aspirin, 42% phenacetin and a dose of caffeine or codeine.

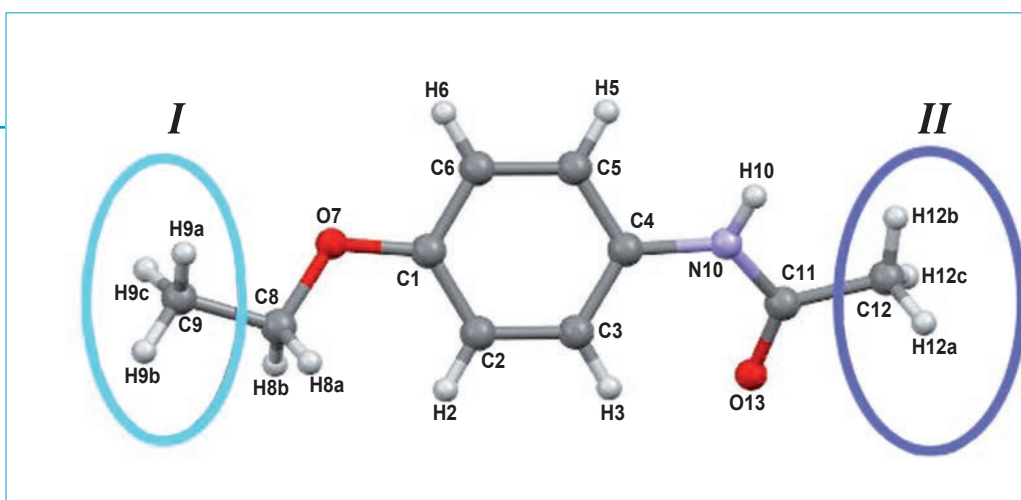
Australian sheep shearers used it every day as a stimulant, as did factory workers before each shift. It became an Australian icon: "A cup of tea, a BEX and a good lie-down".

This article is about neutron spectroscopy in pharmaceutical research, taking phenacetin as an example.

science and biopharmaceutics, however, the characterisation of therapeutic agents is still primarily based on chemical purity alone; there has been little attention paid to their physical properties such as conformational states or the motional flexibility of molecular subunits.

It was in this context that we decided to combine inelastic neutron scattering experiments with computational analysis, with a view to demonstrating that this type of approach offers unprecedented advantages for describing the dynamics of hydrogen atoms in solid drugs. The main benefits of using neutrons arise from the absence of selection rules and the access they provide to both spatial and time correlations captured via

Figure 1:
Left: Molecular structure and atom numbering scheme of phenacetin, where the different methyl groups are highlighted.
Right: (a) Experimentally determined generalised density of states, GDOS, of phenacetin at 80K, compared to the **(b)** DFT-derived total and partial density of states, PDOS, below 40 meV.



the dynamic structure factor. We selected phenacetin for the study ($C_{10}H_{13}NO_2$), a pain-relieving compound often delivered as aspirin-phenacetin-caffeine (APC).

The history of phenacetin and paracetamol ($C_8H_9NO_2$) goes back to 1887, when Bayer began to manufacture them both. Paracetamol, however, was overlooked as a commercial prospect in preference to phenacetin [2]. When phenacetin was removed from the market in 1983 after long-term studies showed it to be carcinogenic, paracetamol returned to favour. This example is just one of the many encountered in pharmaceutical science, where a minor difference in molecular structure can explain major differences in therapeutic effect.

We used ILL's backscattering instrument IN10 to evaluate the mean-square displacement of the hydrogen atoms obtained from the elastic fixed-window approach and observed a crossover of the molecular fluctuations between harmonic and non-harmonic dynamical regimes around 75 K. Using the temperature dependence of the quasi-elastic line-width accessed by the time-of-flight instrument IN6, we were able to attribute the onset of this anharmonicity to methyl group rotations. Finally, we calculated the lattice vibrations in the harmonic approximation using density functional theory-based methods (DFT). By focusing on the low-energy spectrum, we extracted critical information about the motions that can be activated under physiological conditions, involving, for instance, alkyl and peptide methyl group rotations, methyl group I and methyl group II, respectively in **figure 1**.

Our analysis demonstrated that in phenacetin the main molecular flexibility is associated with methyl group II.

On the basis of these results [3], we were able to characterise the low-energy vibrational motions and link the correlation times of the methyl-group rotations to the recorded molecular mean-squared displacements. We could assign the hopping process of the peptide methyl group II (**figure 1 left**) to the librational band observed in the inelastic signal. This implies that the different methyl groups in phenacetin encounter different chemical and crystallographic environments, thus inducing different dynamic environments. We concluded that phenacetin can assume different conformations; knowing this can facilitate our understanding of how chemical reactions occur. In the future, using biochemistry and molecular biology approaches, such work may improve our insight into how molecules interact with each other in living systems.

Authors

H.N. Bordallo (Niels Bohr Institute, Denmark)

B.A. Zakharov and **E.V. Boldyreva** (Novosibirsk State University & Institute of Solid State Chemistry and Mechanochemistry, Russia)

M.M. Koza, **T. Seydel** and **M.R. Johnson** (ILL)

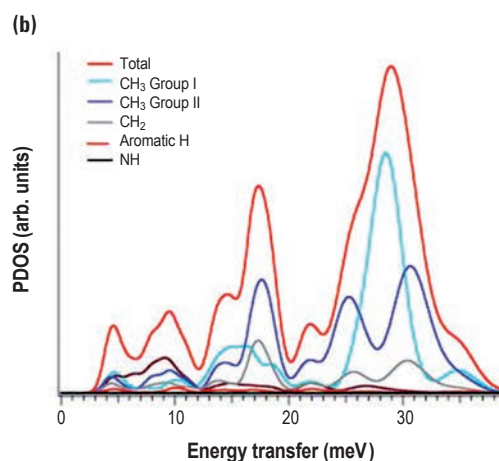
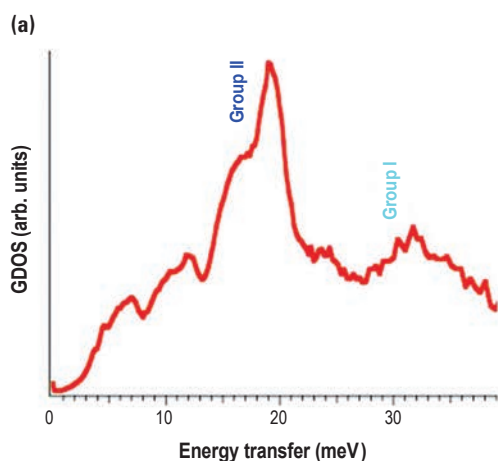
J. Fischer (Forschungszentrum Jülich, Germany)

References

[1] <http://bexandaliedown.wordpress.com/about-bex/>

[2] A. W. Jones, *Drug Test. Analysis* 3 (2011) 337

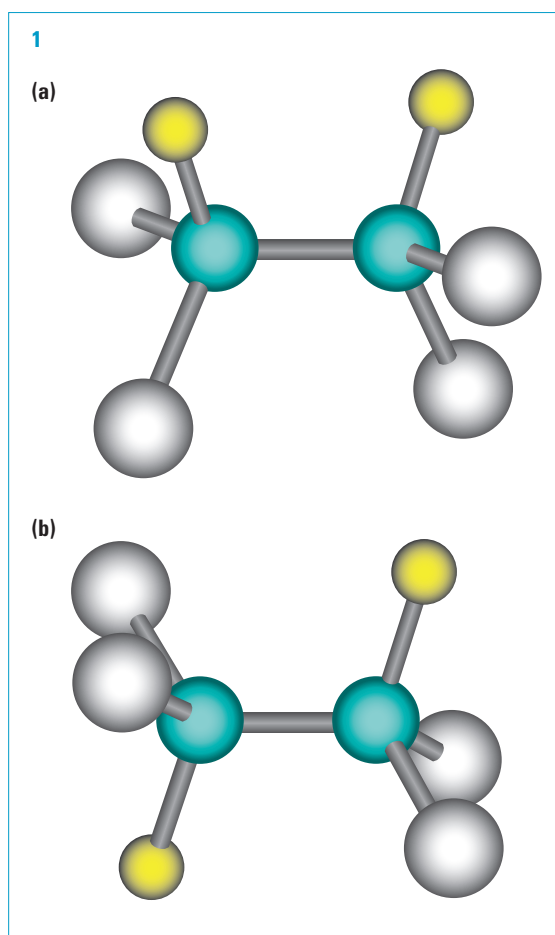
[3] H.N. Bordallo *et al.*, *Mol. Pharmaceutics* 9 (2012) 2434



Liquids and glasses

Liquids and amorphous diffractometer D4

Propagating structure: from molecules to short range ordering



Among the classical states of matter, liquids still lack a general framework explaining the entire complexity of their dynamics and structure. The physics of gases is well understood: the interaction between molecules is negligible and they therefore lack structure; their dynamics might be described by simple ballistic motions.

Tools for the study of crystalline solids have a long history: crystallography is used to determine the structure of solids and the cooperative dynamics of molecules in a solid are well described by the collective excitations named phonons. Liquids, however, are found in between these two states of matter: they have structure, but only at short length scales, and their dynamics and its relation to their structure is still not understood despite the efforts made by a great number of scientists. Nor is it clear how intra-molecular degrees of freedom might affect the liquid structure and its dynamics.

In a study of a molecular system at the ILL we focused on how changes in molecular shape, and therefore at very short length scales, affect the short-range ordering of molecules in a liquid, *i.e.* at intermediate length scales. We chose Freon112 for the study, since the two sides of its molecules can rotate along the C-C axis, with the result that they occur in two

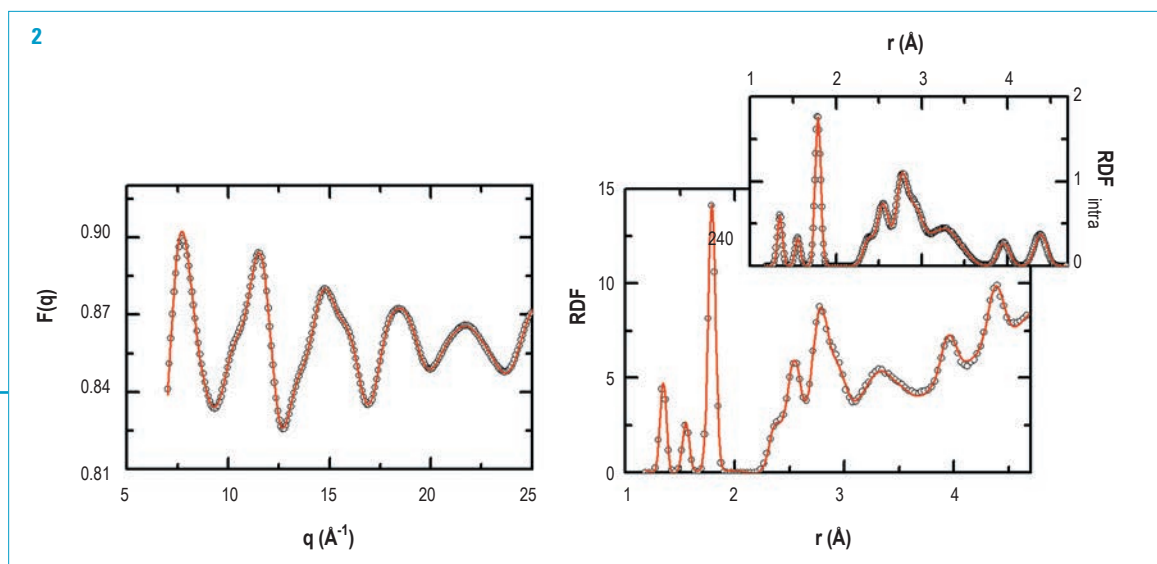


Figure 1:
The two conformations trans **(a)** and gauche **(b)** of the Freon112 molecule.

Figure 2: Reciprocal and direct space curves produced by the D4 diffractometer, together with the fits associated to the proposed molecular model.

conformations: trans and gauche (see **figure 1**). The relative concentration of the two conformers is expected to be that of the gas, *i.e.*, determined by the relative energy of the two conformers; given the high energy barrier between them, the number of molecules in an intermediate state is negligible. Experiments were performed on the ILL D4 diffractometer, to obtain structural information on the compound at different length scales in its liquid phase. This instrument gives access to the high momentum transfer region in reciprocal space, minimising any undesirable effects when trying to resolve the structure.

We first sought to determine in a robust way the structure of the molecule. This involved determining all the angles and distances, and, since the molecule has two conformers, identifying their relative amounts in the liquid phase. The first trial using standard procedures failed, as it was impossible to obtain satisfactory fits, given the high number of parameters required to describe the molecular geometry. We therefore resorted to a Bayesian method [1], to identify the molecular model best describing the experimental data. The results were excellent, as can be seen in **figure 2**. Note that we performed the fit in both direct and reciprocal space, as our fits of a simple test molecule showed that the model obtained is more reliable. The relative amounts of trans and gauche molecules, however, did not match the calculations, taking into account the different energies of trans and gauche molecules. We therefore carried out a molecular dynamics simulation, to examine whether the proportions corresponded to that of the gas phase (*i.e.* without molecular interaction), and whether each conformer had a different molecular environment.

Various molecular simulations were performed, fixing the pressure and the temperature close to the experimental one. Since both the density and the structure factor obtained were compatible with the experimental data, we concluded that the intra- and inter-atomic potentials chosen described our system. Once the equilibrium was reached, a simple calculation

showed that the gauche population was greater than expected, as the experimental data fit showed. We wished to determine whether this could be related to a different ordering of the molecules around trans and gauche conformers; we therefore studied the position of the centre of mass around each conformer. This was done by fixing the axis coordinates to the molecule: the polar axis was set along the C-C bond, and the angle φ was therefore the equatorial angle with a fluorine atom at the origin (**figure 3**). In **figures 3b** and **3c** we show the map characterising the local molecular ordering.

The colour map shows the probability of finding a molecule with a certain equatorial angle φ as a function of the molecular coordination number (the number of the neighbouring molecule, when ordered by increasing distance from the central molecule). We can see that molecules arrange themselves in different ways around trans or gauche molecules, and that these differences in ordering extend, at least, to the first coordination shell formed by the 12 molecules closest to the central one.

We have therefore demonstrated that differences at intra-molecular scales can propagate to quite long distances and that this must be taken into account by theories seeking to describe the complex physics of liquids.

Authors

L.C. Pardo, J.LI. Tamarit, M. Rovira-Esteva, N.A. Murugan and Sz. Pothoczki
(Politechnical University of Catalunya, Spain)

S. Busch (FRM II, Technical University of Munich, Germany)

G.J. Cuello (ILL)

F.J. Bermejo (Material Structure Institute, CSIC, Spain)

Reference

[1] The fitting software can be found at <http://gcm.upc.edu/members/luis-carlos/bayesiano>

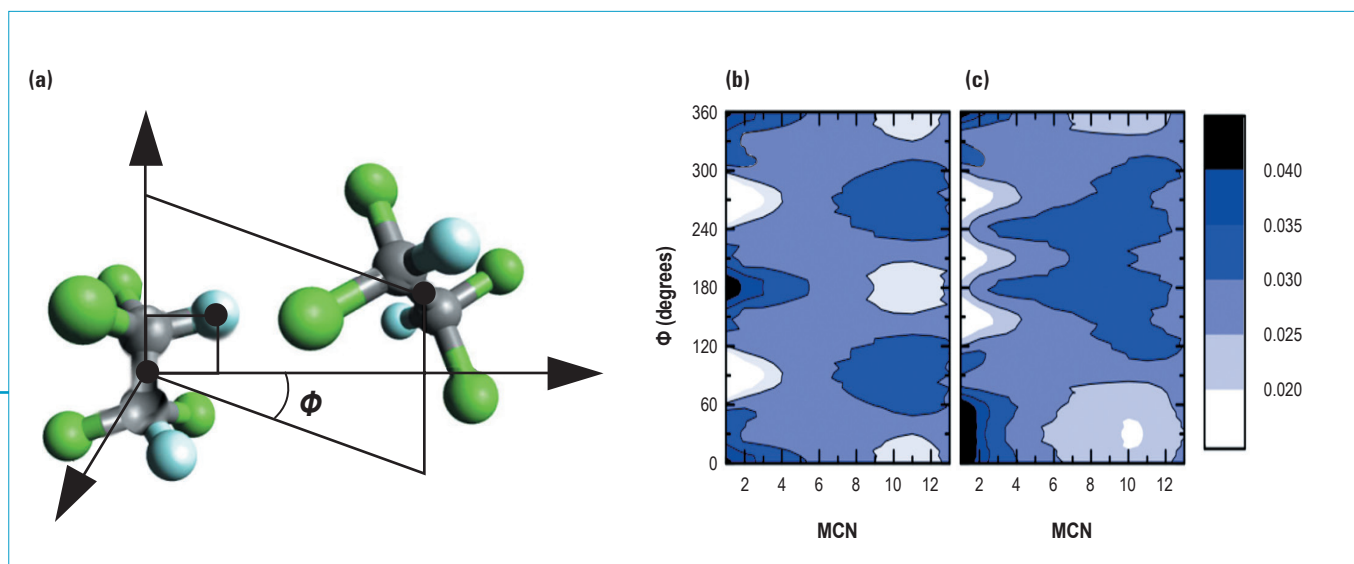


Figure 3: (a) Definition of the axes chosen to characterise the molecular ordering around a central molecule. In figures (b) and (c) we show this ordering around trans and gauche molecules, respectively.

Liquids and glasses

Time-of-flight spectrometer IN5 Backscattering spectrometer IN16

Intrinsic confinement effects in binary glass-forming systems

Traditionally it was assumed that two components mix well only if the binary system shows a single glass transition. Recent studies, however, identified two calorimetric glass transition temperatures, and thus a separation of time scales, in many fully miscible systems [1]. In that case so-called intrinsic confinement effects have to be expected, when a more mobile component relaxes in a matrix of slow or even frozen larger molecules. In the present study we look at the dynamic properties of such a more mobile component in a dynamically highly asymmetric system.

With incoherent quasielastic neutron scattering we selectively monitor the dynamics of a small organic glass former methyl-tetrahydrofuran (MTHF) in a matrix of perdeuterated polystyrene. A combination of neutron time-of-flight (IN5) and backscattering spectroscopy (IN16) reveals high mobility of the small component even several tens of Kelvin below the glass transition of the matrix. An example is given in **figure 1** (left), where the intermediate scattering function $S(q,t)$ derived from the quasielastic backscattering and neutron time-of-flight spectra is shown, that to first approximation selectively reflect the motions of the hydrogen atoms of the small molecules MTHF in the mixture. For example at 170 K, which is 15 K below the matrix glass transition in that particular system, a significant part of correlations of the small molecules monitored by $S(q,t)$ decay on the time scale of the neutron scattering experiment.

To study the dynamics in more detail we combined the neutron scattering techniques with depolarised dynamic light scattering, NMR and dielectric spectroscopy. It turns out that despite

Binary glass forming mixtures offer the possibility to tailor material properties by adapting the composition for a desired application. Particularly interesting in this respect are systems that mix well on a macroscopic scale but where its components evidence very different dynamic behaviour, so that one of the components is slow or even static, which then strongly influences the dynamics of the other, smaller and more mobile component. The microscopic behaviour of such interesting materials, like polymer plasticisers systems or hydrated proteins is so far not well understood.

In particular it is still unclear to what extent the observations are due to particular interactions at the liquid-solid interface or to the spatial restrictions imposed by the larger molecules. For example, for water in protein matrices a crossover in the temperature dependent correlation times was vigorously debated recently. In the present study the use of model mixtures with only van-der-Waals interactions allows to clarify whether the observed effects have to be regarded as general confinement induced phenomena.

the high mobility the slow or even static matrix strongly affects the dynamics of the small molecules in ways that are similar to confinement effects observed for liquids in nanoporous

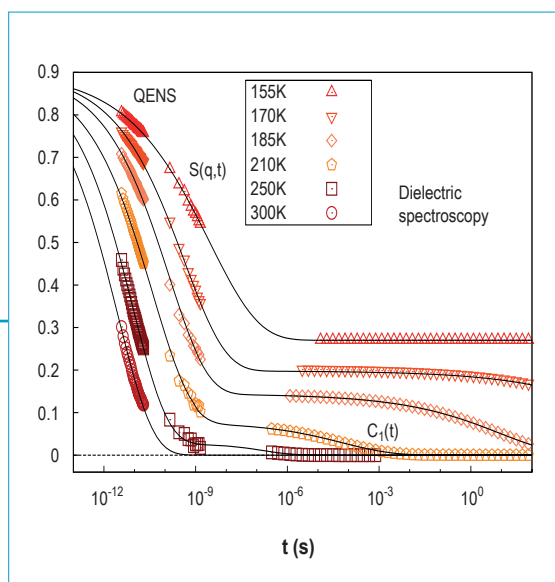


Figure 1: The dynamics of the small molecule methyl-tetrahydrofuran in a deuterated matrix of polystyrene. In the time-domain a combination of the intermediate scattering function $S(q,t)$ from quasielastic neutron scattering (QENS, data from IN5 and IN16) and the reorientational correlation function $C_1(t)$ from dielectric spectroscopy (DS) are shown, both of which reflect motions of the small molecules. The dielectric correlation function reveals a growing plateau in the μ s regime indicating a so-called type-A transition.

matrices. In **figure 2** we combine the time constants from neutron scattering at $q \approx 1 \text{ \AA}^{-1}$ with those of dielectric spectroscopy. Although such a combination is non-trivial it works well for bulk MTHF (blue symbols) as well as for MTHF in the mixture (red symbols).

While the bulk data follow a so-called Vogel-Fulcher behaviour typical for the dynamic slowing down at the glass transition, one identifies a so-called fragile-to-strong transition for the dynamics of intrinsically confined MTHF in the mixture, as the temperature dependence becomes Arrhenius-like below T_g of the matrix.

Recently, such a transition was fiercely debated in the context of hydration water in protein matrices [3], where it is argued that such a crossover might indicate the existence of a second critical point in supercooled water [4]. However, in our experiments the crossover turns out to be a simple confinement effect, which also occurs when hydrogen bonds are entirely absent.

Moreover, a detailed analysis of the dielectric and the NMR data shows that small molecules close to the solid matrix undergo an unusual type of glass transition [2]. Such a "type-A" transition was recently predicted in the framework of the mode coupling theory for binary systems and for glass transitions in confinement [5]. The hallmark of such a behaviour is a plateau in the microsecond range of the intermediate scattering function that evolves continuously out of zero below a certain critical temperature.

To demonstrate this behaviour, in **figure 1** the dipole autocorrelation function $C_1(t)$ extracted from dielectric experiments is shown together with the intermediate scattering function from neutron scattering.

Additional NMR data reveal, that this transition is connected with an increasingly anisotropic reorientation of the small molecules close to the hard wall formed by the polymer matrix upon lowering the temperature. Close to the intrinsically confining surface the correlation decay is only completed on a time scale where the slow matrix itself relaxes [2].

In conclusion, the simultaneous existence of fast and slow molecules in dynamically asymmetric mixtures leads to so-called intrinsic confinement of the more mobile component in a certain temperature range.

Among these confinement effects we identify a so-called fragile-to-strong transition, where the temperature dependence of the time constants crosses over from the well-known glassy behaviour at high temperatures to a simple Arrhenius law at low temperatures.

Moreover, small molecules are observed to perform anisotropic reorientation close to the confining wall, which leads to an unusual type of glass transition that was recently predicted in the framework of mode coupling theory.

While we observe all of these effects in mixtures of simple van-der-Waals molecules, the results have important implications for a much wider range of materials, where in many cases additional Coulombic or hydrogen bonding interactions complicate the behaviour.

Authors

T. Blochowicz, S. Schramm, S. Lusceac, M. Vogel and **B. Stühn**,
(Technical University of Darmstadt, Germany)
P. Gutfreund and **B. Frick** (ILL)

References

- [1] T. Blochowicz, S. Schramm, S. Lusceac, M. Vogel, B. Stühn, P. Gutfreund and B. Frick, *Phys. Rev. Lett.*, 109 (2012) 035702
- [2] T. P. Lodge, E. R. Wood and J. C. Haley, *J. Polym. Sci., Part B: Polym. Phys.*, 44 (2006) 756
- [3] W. Doster, S. Busch, A. M. Gaspar, M.-S. Appavou, J. Wuttke and H. Scheer, *Phys. Rev. Lett.* 104 (2010) 098101
- [4] S.-H. Chen, L. Liu, E. Fratini, P. Baglioni, A. Faraone and E. Mamontov, *Proc. Natl. Acad. Sci. USA* 103 (2006) 9012
- [5] V. Krakoviack, *Phys. Rev. Lett.* 94 (2005) 065703

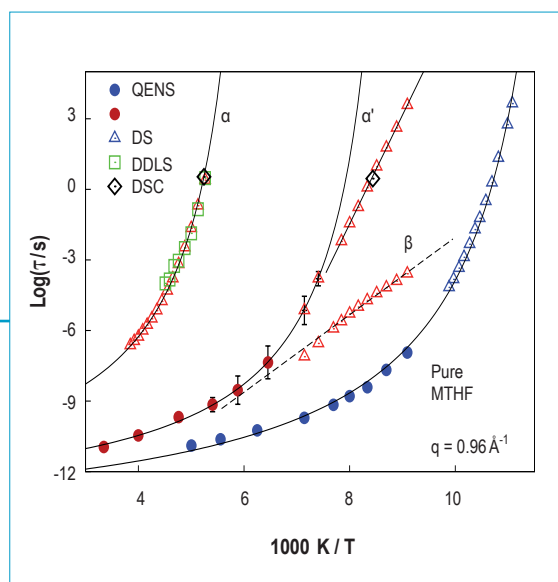


Figure 2: The time constants of quasielastic neutron scattering and dielectric spectroscopy for bulk MTHF (blue symbols) and MTHF in a binary mixture, where intrinsic confinement is observed.

In addition relaxation times of depolarised dynamic light scattering (DDLS) and calorimetry (DSC) are shown. Below the matrix glass transition monitored by light scattering a fragile-to-strong crossover for the relaxation times (α') of the small molecules occurs.

Nuclear and particle physics

Gamma-ray spectrometer PN3

Measurement of the refractive index of Silicon for Gamma Rays

The deviation from a value of one of the refractive index decides on how strong and in which direction radiation is deviated from its original direction. For visible light it is known to be larger than one. Going up in energy (equivalent to much shorter wavelengths) from visible light to X-rays it was known that the refractive index becomes smaller than one and more over that this deviation was very small. Since the effect was so tiny, refraction has not been used for X-ray instrumentation for long times. Only at the end of the 20th century researchers realised that by combining many hundreds of optical elements one could still constructively build focusing systems [2].

This and the combination with crystals for wavelength selection have given a strong boost to X-ray science. The energy dependence of the refractive index was studied for X-rays and it was found that with increasing energy the refraction effect becomes smaller and smaller. Therefore, for radiation energies at even much higher energy, namely for gamma rays, scientist expected to find no measurable refraction anymore.

For a long time the research in this field was not pushed since there were no sources of gamma rays comparable to intense

Refraction is the process describing how electromagnetic radiation is deviated when it is passing matter and the quantity, which summarises the interaction process, is the so called refractive index. Refraction is well known for light, allowing the construction of optical elements like lenses, prisms, and so on. While the effect for light is used in everyday life its existence for higher energy radiation such as X-ray or gamma rays was not considered for a long time.

In a very recent experiment scientists from the ILL and Munich found that even for very high radiation energies refraction is not zero and could be possibly used to build optical elements for this kind of radiation [1].

light sources like lasers or to X-ray sources like synchrotrons. However, the project of building a new generation gamma ray sources (based on Compton backscattering of an electron bunch in an intense laser pulse) has re-triggered the interest [3]. If one would have the possibility to manipulate the gamma rays

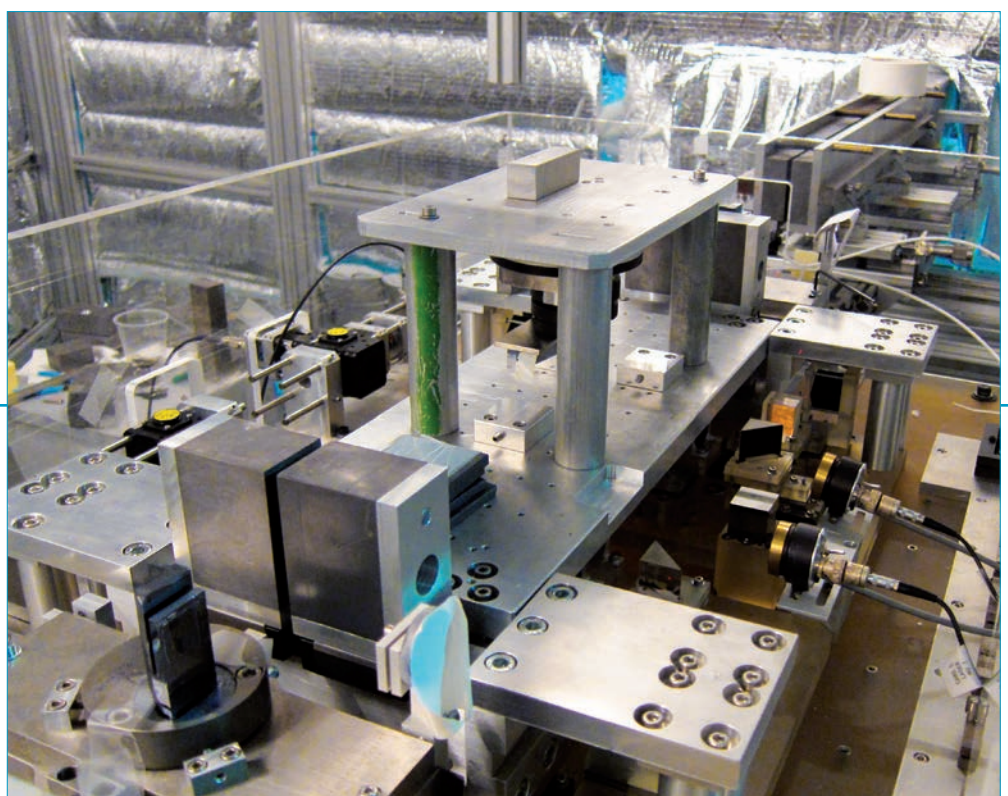


Figure 1:

View on the double crystal spectrometer GAMS5 used for the measurement of the refractive index.

In the foreground one of the two spectrometer crystals can be seen, which is producing an extremely monochromatic and low divergent beam. This beam is hitting a prism mounted to deviate the upper part of the beam. The second spectrometer crystal (hidden behind the lead collimation) is analysing the angular deviation of lower and upper beam.

further such that one could choose a very narrow energy band – equal to the excitation energy of a particular isotope – one could imagine building very selective tools and techniques. A key component for this is again the availability of refractive optics for gamma rays, which was triggering the according research.

The scientists were using the PN3-facility of the ILL. This installation consists of a beam tube tangentially passing the neutron high flux reactor and allowing to place samples in a very intense neutron flux. The samples are capturing the neutrons, due to which they are excited and emit gamma rays. The installation represents one of the most intense gamma ray sources available today.

At the exits of the beam tube the ultra-high resolution crystal spectrometer GAMS is installed. This device consists of two goniometers, controlling each the orientation of a perfect silicon crystal.

The first crystal pre-selects via Laue diffraction the energy of the gamma rays from the sample in the reactor, defining at the same time a very low divergent monochromatic gamma ray beam. It is so well defined that over a distance of 1000 m it would diverge not more than one cm. The direction of this beam is analysed by the second crystal. The scientists placed on half-height between the crystals a prism of silicon, which was deviating the upper half of the beam due to refraction.

The second crystal does now measure two beams – one deviated by refraction and one with refraction. Comparing the two directions allowed studying the effect for gamma ray energies.

Surprisingly the researchers found that the refractive index does not converge to a value of one for increasing energy. Starting from values slightly smaller than one it crosses the limit of one

and becomes larger. The unexpected finding was theoretically explained by the scientist extending earlier works to include effects of radiation matter interaction that had not been considered so far. This theoretical work allows the scientists to predict that for heavier materials the refraction effect is becoming even much stronger, which of course needs to be validated experimentally.

The practical impact of this finding could be quite immense. Having in mind that within the next decade the technology of very intense gamma ray sources becomes more commonly available one could expect to build devices that allow focusing and to energy selecting gamma rays. This allows a number of quite unique applications. Gamma rays are selective for specific isotopes, chemically identical atomic nuclei the difference of which is only their different nuclear mass. This would allow carrying out isotope specific tomography, which together with high penetration power of gamma rays would allow scanning for nuclear weapon material in ships or trucks as well as for nuclear waste in containers. Last but not least it would give a large boost to science too: similar as we are now manipulating atoms with light and X-rays, we could start to do this on a nuclear level with gamma rays. This opens a complete new field of activity, which can be named Nuclear Photonics.

Authors

D. Habs (Ludwig-Maximilians University, Munich, Germany)

M.M. Günther (GSI Helmholtz Centre for Heavy Ion Research, Darmstadt, Germany)

M. Jentschel and **W. Urban** (ILL)

References

[1] D. Habs *et al.*, Phys. Rev. Lett. 108 (2012) 184802

[2] A. Snigirev *et al.*, Nature 384 (1996) 49 - 51

[3] <http://www.eli-np.ro/>

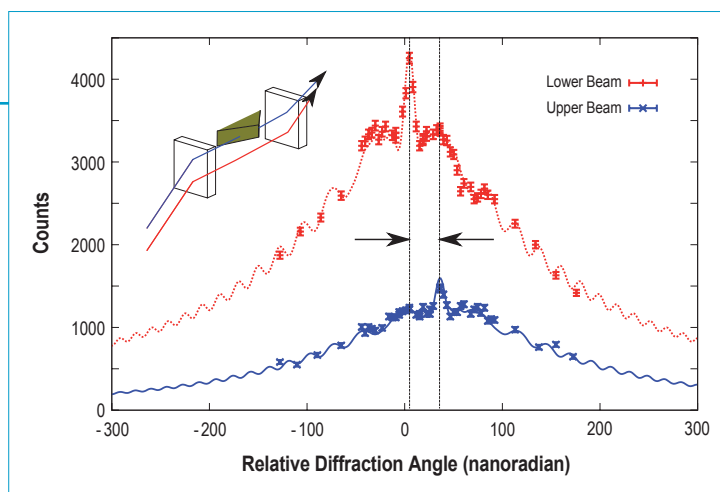


Figure 2:

Plot showing the relative angular deviation of the two partial beams as measured by the second spectrometer crystal. From these angular deviations the refractive index was deduced.

Nuclear and particle physics

Ultra-cold neutron facility PF2

Improving our knowledge on dark matter and dark energy using ultra-cold neutrons

We present a novel search strategy with neutrons based on the quantum bouncing ball. The experiment qBounce and its new resonant spectroscopic measurements make a search in the earth's gravity potential a powerful way to search for dark matter and dark energy contributions directly.

Specifically, the new development at ILL and Vienna University of Technology in collaboration with Heidelberg University and TU Munich brings together theoretical developments and experiments. Our task here is to push new experiments to a point, where a particular new idea can be compared with observation. This should help to select sustainable concepts among many interesting speculative ideas.

As far as dark energy is concerned, nobody knows what kind of dark energy the cosmological constant is. One possibility is the idea that we have not detected a nonzero cosmological constant, but rather a dynamical component that closely mimics the properties of vacuum energy. In other words, the vacuum energy is a field, assumed for simplicity's sake to be a fundamental scalar field. Quintessence is such a theory and is considered to be a new force. qBounce has access to several quintessence models. One of them is the so-called chameleon field. It provides explicit realisations of a quintessence model, where the quintessence scalar field couples directly to baryons and dark matter with gravitational strength. With the 2010 and 2011 data set, we performed a direct search for such a chameleon field [1]. We improve the exclusion limits for dark matter/energy particles by up to a factor of 100 000 in comparison to other methods [2] and by a factor of 100 in comparison with our previous measurement done in collaboration [2, 3].

Another puzzle in physics is the existence of dark matter. While many astronomic observations show evidence for their existence, their content is unknown. The axion is one hot-topic dark-matter particle, which would introduce a spin-mass coupling and thereby also solve the strong CP problem. Experiments with slow neutrons have the ability to restrict the parameter space of axions in a region that is non-accessible for other experiments. The idea behind these experiments is that so far hypothetical and unknown particles might interact with the neutron. Such an interaction would cause an energy shift in our resonant system [4]. Therefore, we perform a search for spin-dependent forces at short distances.

Gravitation is a conundrum to us: on the one hand, Newton's Inverse Square Law has been proven to be valid from the 50 μm scale up to inter-galactic distances, on the other hand, at very long range, the presence of an unknown dark and accelerating energy is observed; at intermediate range, the rotation curves of galaxies point to an unknown form of so-called dark matter, and at very short distances, unknown hypothetical extra-dimensions of space-time may be required. So far, observations have failed to find a force contributing to this dark energy or dark matter.

Resonant transitions are for this purpose measured with polarised neutrons. Our experiment improves the limits on such particles by a factor of 30 [1].

The long term aim of qBounce is to search for specific deviations from Newton's Law of Gravity provoked by dark energy or dark matter particles. The clarification of the role of dark matter and dark energy will have a decisive impact on future research in particle physics, astrophysics and cosmology. Such fundamental research addresses key questions asked by humankind: What is the universe made of? What was the past and what will be the future of the universe? What are the forces of nature that rule the world and keep it together?

Our solution is to use the interaction of a macroscopic system, here a mirror for neutron reflection, with a purely quantum mechanical system, *i.e.*, the excitation of bound quantum states of a neutron in the gravity potential of the Earth. The neutron matter waves can be excited by a mechanical oscillator coupled to these states in order to drive transitions between state $|p\rangle$ and state $|q\rangle$, see **figure 1**. A frequency measurement determines the energy difference with unprecedented accuracy, see **figure 2**.

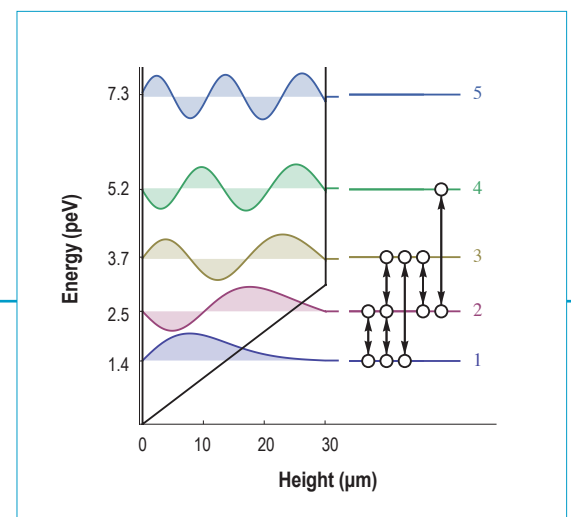


Figure 1:

Gravity Resonance Spectroscopy, based on energy eigenvalues of a neutron in the gravity potential of the earth with confining mirrors at the bottom and at the top separated by $l=30.1 \mu\text{m}$. Also shown is the neutron density distributions for energy levels $|1\rangle$ to $|5\rangle$. The Gravity Resonance Spectroscopy technique allows to drive transitions between these states. Quantum transitions $|1\rangle \leftrightarrow |2\rangle$, $|1\rangle \leftrightarrow |3\rangle$, $|2\rangle \leftrightarrow |3\rangle$, $|2\rangle \leftrightarrow |4\rangle$ have been observed [1,5,6].

This new technique is called Gravity Resonance Spectroscopy [5,6]. It is a Rabi-type spectroscopy method and consists of a state selector, where the initial state $|p\rangle$ is prepared. By applying a so-called π -pulse, transitions into a second state $|q\rangle$ are induced. A detector at the end measures these neutrons, which were accepted by the state selector. On resonance, a sharp decrease in count rate is found. The frequency width of the resonance is given by the time the neutron spends in the resonator. In our case the resonant transitions $1 \leftrightarrow 2$ and $2 \leftrightarrow 3$ are not separated; there exists a frequency band, where transitions $1 \leftrightarrow 2 \leftrightarrow 3$ can simultaneously be driven, but they are in frequency space well separated from $1 \leftrightarrow 3$ transitions.

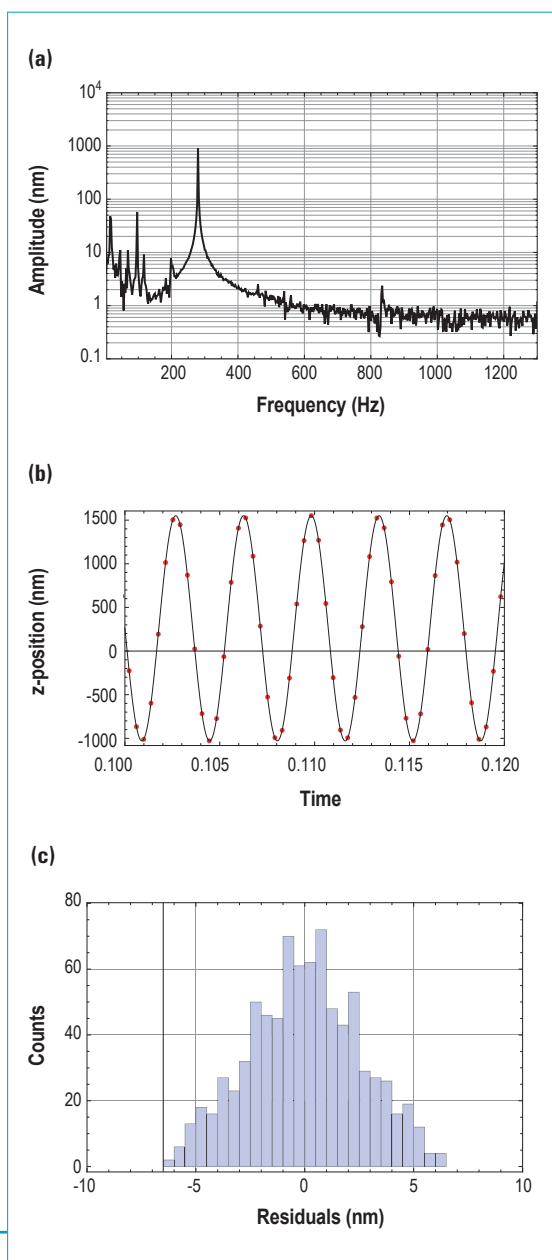


Figure 2: (a) Fourier spectrum of a typical frequency measurement. The vibration frequency is 280 Hz at an amplitude of 2.1 mm/s. Resonant frequencies of the mirror setup at 120 Hz and of the turbomolecular pump at 833 Hz are visible. (b) Inverse Fourier spectrum and a fit to vibration scan. (c) Residuals for amplitude measurement.

The set up is consisting of a polished mirror on bottom and a rough scatterer on top. In addition a third mirror serves as reference. Vibrations are controlled with 3-beam laser interferometer, see **figure 3**. A neutron entering this system is in a superposition of different eigenstates φ_n . The wavefunctions between the mirrors with distance l , acceleration g and height z , as a solution of the Schrödinger equation, are shown in **figure 1**.

Authors

T. Jenke, G. Cronenberg, A.N. Ivanov, H. Saul and H. Abele (Atominstut, TU Vienna, Austria)
P. Geltenbort (ILL)
T. Lauer (FRM II and TU, Munich, Germany)
T. Lins (TU Munich, Germany)
U. Schmidt (Heidelberg University, Heidelberg, Germany)

References

- [1] T. Jenke *et al.*, arXiv:1208.3875
- [2] P.Brax, G.Pignol, Phys. Rev.Lett. 107 (2011)111301
- [3] V.V. Nesvizhevsky *et al.*, Nature 415(2002) 299
- [4] H. Abele *et al.*, Phys. Rev. D81 (2010) 065019
- [5] T. Jenke, P. Geltenbort, H. Lemmel, H. Abele, Nature Physics 7 (2011) 468
- [6] T. Jenke, Dissertation, Vienna University of Technology (2011)
- [7] T. Lins, Diplomarbeit, Technische Universität München (2011)

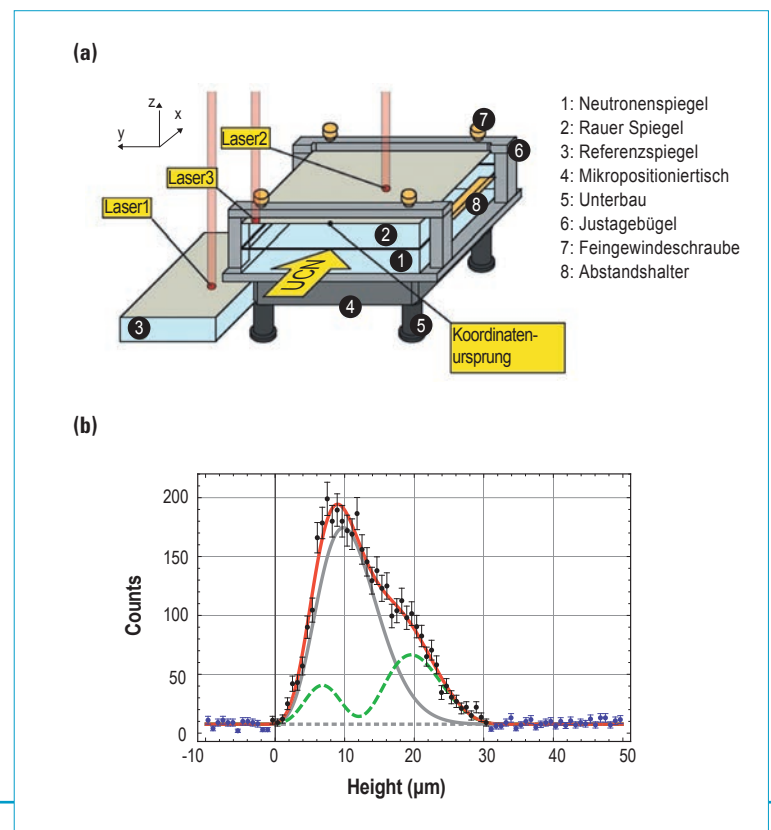


Figure 3: (a) a schematic diagram of the GRS set up. 1: bottom neutron mirror; 2: top rough mirror; 3: reference mirror; 4: micro-positioning table; 5: piezo-control; 6: adjustment; 7: fine pitch thread; 8: spacer (taken from [7]). (b) neutron density distribution above the mirror in front of the detector, measured by a track detector. A fit to the data (red) is compatible with a population of 67 % for state $\langle 1 \rangle$ (grey solid) and 33 % for state $\langle 2 \rangle$ (green).

Modelling and spectroscopy

Time-of-flight spectrometers IN4 and IN5

The Zn_6Sc periodic quasicrystal approximant: an exceptional dynamical flexibility

Periodic approximants to quasicrystals offer a unique opportunity to better understand structure and physical properties of their quasicrystal counterparts.

Both the icosahedral quasicrystal i-MgZnSc and its cubic approximant Zn_6Sc are built up from the same atomic clusters.

Zn_6Sc can be described as a packing of so-called 'Tsai-type' clusters, which are large atomic clusters consisting of successive shells with high (icosahedral) symmetry. For the periodic approximants, these cluster units are located on the vertices of a bcc lattice with space group $Im\bar{3}$ (lattice parameter 1.38 nm), whereas they lie on a quasiperiodic lattice in the quasicrystal*. At the center of these clusters one finds a central, symmetry-breaking, tetrahedron (**figure 1**) [1]. In the approximant an order-disorder transition from the cubic high temperature (HT) phase to the monoclinic low temperature (LT) phase takes place at about 160 K and is attributed to the ordering of the central tetrahedra. Above T_c , these tetrahedra appear as disordered, randomly occupying six equivalent orientations under the cubic symmetry group.

To investigate the static or dynamic nature of the tetrahedra disorder in the HT phase, QENS experiments - a powerful technique to study diffusive processes - were conducted at the time-of-flight spectrometers IN4 and IN5. **Figure 2** displays

In the approximant, an order disorder phase transition occurs at 160 K, going along with the ordering of the central tetrahedra in an antiparallel way. With quasielastic neutron scattering (QENS) and molecular dynamics (MD) simulations we evidence that the disorder above T_c is dynamic in nature, resulting in a model of tetrahedra behaving as single objects, 'jumping' between almost equivalent positions.

These rapid reorientations are accompanied by strong distortions of the surrounding cluster shells, conferring a unique dynamical flexibility to this system.

the temperature evolution of the Q-integrated signal, measured at IN5. Of particular importance is the comparison of measurements carried out just above and below T_c (first panel). While at 175 K a clear QENS signal is evidenced, this contribution has vanished at 150 K, with the remaining signal being due to the instrumental resolution. This is clear evidence for the QENS signal stemming from tetrahedron motions. A careful fitting procedure was applied to extract the quasielastic contribution from the measured $S(Q,E)$ signal. Analysing the entire data set we find that the QENS signal is Lorentzian in shape with its width Γ independent of Q at a given temperature, in agreement with a spatially limited jump process. At room temperature the width (FWHM) is found to be equal to about 0.5 meV, corresponding to a timescale of the order 1 ps. When looking at the T -dependence of the Lorentzian, a clear broadening is observed for increasing T , as illustrated in **figure 2a**. The temperature dependence of the width follows an Arrhenius law (**figure 2b**), yielding an energy barrier of about 60 meV. Moreover the integrated intensity of

* A quasiperiodic structure does not consist of a periodic arrangement of atoms as found in conventional crystals. However, long-range order is present and the atoms are arranged in a deterministic - but non-periodic - way.

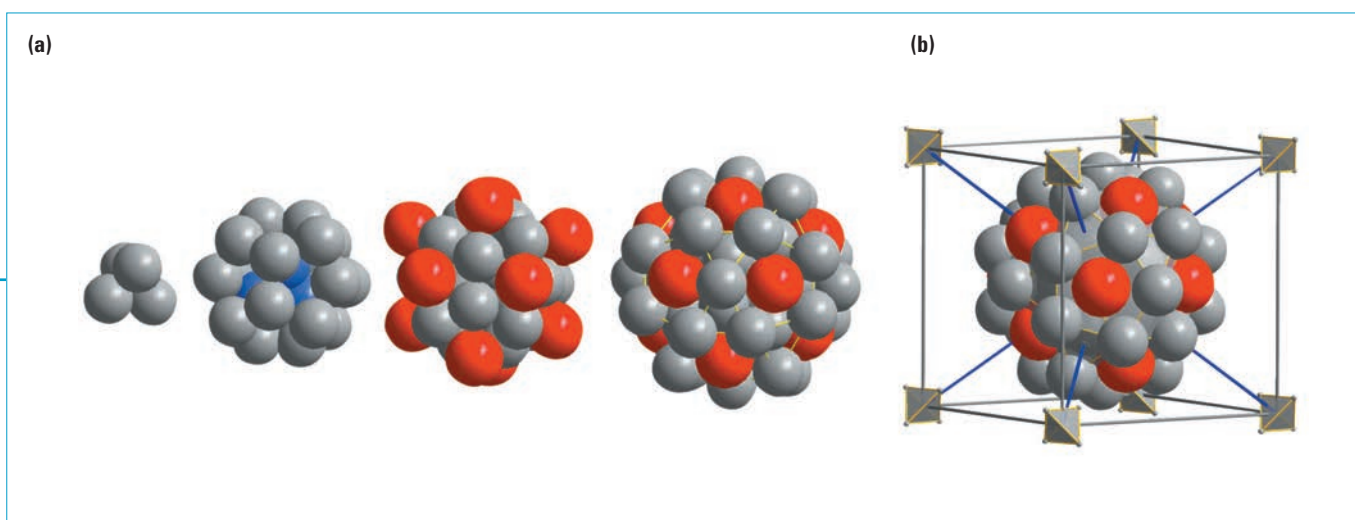


Figure 1: (a) Shells of the Tsai-type cluster in ZnSc 1/1 approximant. Light grey (blue) and red colours stand for Zn and Sc atoms respectively. (b) Tsai-type cluster in its bcc environment.

the QENS signal doesn't change with varying T , as expected for a thermally activated process. Finally the intensity evolution as a function of Q , which is related to the exact geometry of the jump process, displays an abrupt variation as a function of Q (**figure 2b**), with a maximum at Q equal to 2.9 \AA^{-1} . The position of I_{max} indicates a characteristic jump distance of about 1.6 \AA with the rather steep evolution of the intensity being a signature of collective motions.

These results are the characteristics of a jump process, with tetrahedra behaving as single molecules 'jumping' between different orientations, on a ps timescale, with an activation energy of about 60 meV and a characteristic jump distance of 1.6 \AA .

Using adapted oscillating pair potentials for atomic scale MD simulations we could reproduce the experimental observations yet, with a time scale of about three times the experimental one. The simulated width is increasing with temperature, following an Arrhenius law, with the same energy barrier as found experimentally, *i.e.* about 60 meV (**figure 2b**). Finally, the Q variation of the signal intensity is abrupt, and reproduces rather well the observed tendencies also shown in **figure 2b**. In particular the position of the maximum of the intensity is located at the same Q value for both experiment and simulation.

We could thus evidence that above T_c the central Zn tetrahedra behave as single molecules which reorient dynamically between different positions, on a time scale of a few ps, with distances 1.6 \AA and an energy barrier of 60 meV , in good agreement with atomic scale simulation. Although the system is a close-packed structure with a large (Sc) and a small (Zn) atom, the tetrahedron orientations above T_c induce strong distortions of the successive shells, which therefore lose the perfect icosahedral symmetry. This is exemplified in **figure 3**, where the dodecahedron

distortion is clearly visible as the tetrahedron reorients. Zn_6Sc thus displays an extremely large dynamical flexibility, to our knowledge unique for such intermetallic compounds. This specific dynamics together with the validated atomic scale simulations offer thus new perspectives for the understanding of the mechanisms underlying the stability of quasicrystals and approximants.

Authors

H. Euchner (University of Stuttgart, Germany and INP, UJF, Grenoble, France)

M. de Boissieu (CNRS, INP, UJF, Grenoble, France)

H. Schober and **S. Rols** (ILL)

References

- [1] A.P. Tsai, J.Q. Guo, E. Abe, H. Takakura and T.J. Sato, *Nature* 408 (2000) 6812
- [2] M. de Boissieu, S. Francoual, M. Mihalkovic, K. Shibata, A.Q.R. Baron, Y. Sidiq, T. Ishimasa, D. Wu, T. Lograsso, L.P. Regnault, F. Gähler, S. Tsutsui, B. Hennion, P. Bastie, T.J. Sato, H. Takakura, R. Currat and A.P. Tsai, *Nature Materials* 6 (2007) 977
- [3] Q.S. Lin and J.D. Corbett *Inorganic Chemistry* 43 (2004) 1912
- [4] T. Ishimasa, Y. Kasano, A. Tachibana, S. Kashimoto and K. Osaka, *Phil. Mag.* 87 (2007) 2887

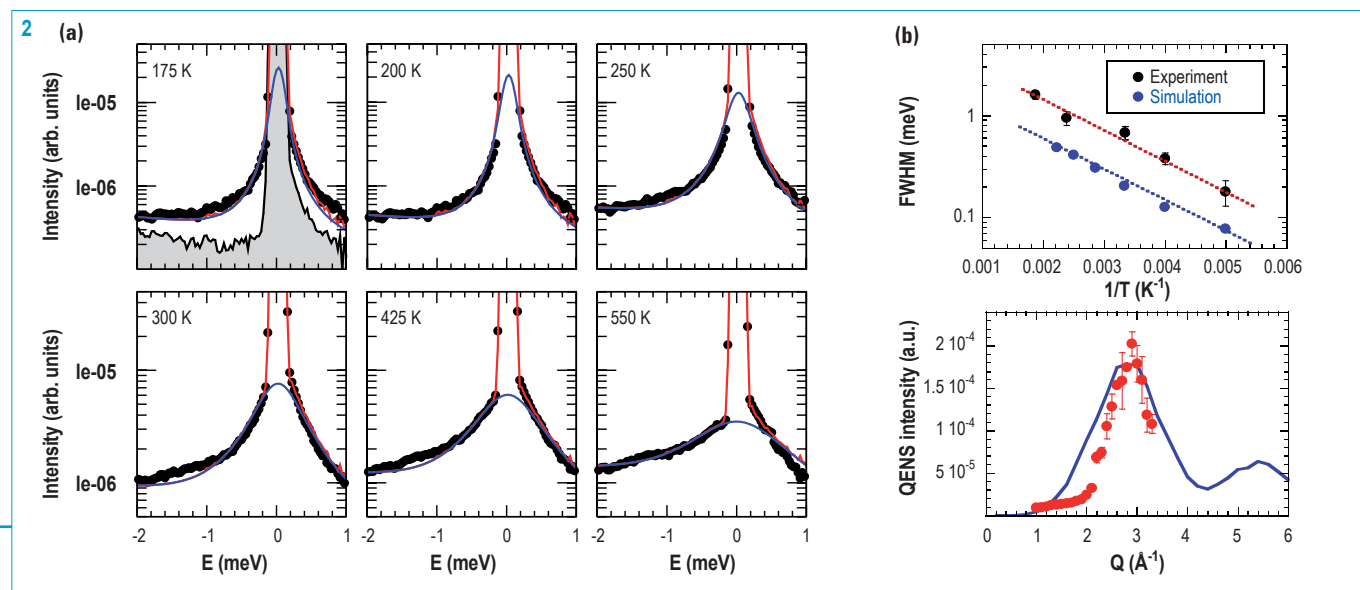
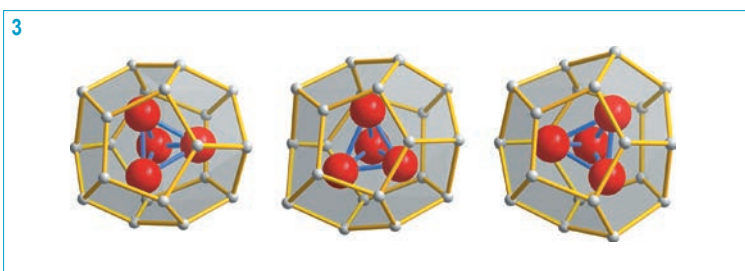


Figure 2: (a) Evolution of the QENS signal measured at $T = 175, 200, 250, 300, 425$ and 550 K . Filled circles stand for the measured data; error bars are smaller than the size of the circles. Blue and red lines stand for the Lorentzian plus background contribution and the total fit, respectively. In the first panel the grey curves corresponds to the measurement carried out at 150 K .

(b) Top panel: T -dependence of the FWHM of measured (black circle) and simulated (blue circle) quasielastic signal, displayed on an Arrhenius plot.

Bottom panel: Q -dependence of the quasielastic intensity as measured at 550 K (dots). The blue line is the quasielastic intensity variation as obtained from the simulation.

Figure 3: Configuration of tetrahedral and dodecahedral shell taken at $t = 0, 1.0$ and 2.6 ps from the simulation. The displacement of the tetrahedron is almost a clock-wise rotation around a 3-fold axis passing through the atom in the back. Notice the strong distortion of the dodecahedron as the rotation proceeds. From qualitative investigation of the tetrahedron motion the central configuration is found to have a somewhat shorter lifetime.

Modelling and spectroscopy

Time-of-flight spectrometer IN5

A switchable molecular rotator: a spin-crossover compound comes into the field of molecular machines

The possibility of designing systems that synergically combine different properties giving a multifunctional material is one of the most exploited advantages of molecular compounds. An example of this approach is the use of the well known spin-crossover phenomenon as a switch for a second physical property. Spin-crossover occurs in some transition metal compounds, where the electronic configurations can interconvert (switch) between high-spin and low-spin states under external stimuli, affording changes in magnetic, optical, dielectric, and structural properties. When the spin-crossover phenomenon occurs in a cooperative way, these compounds may present a first order spin transition with hysteretic behavior, conferring bistability and a memory function to the material [3].

In our porous polymeric spin-crossover compound $\{\text{Fe}(\text{pyrazine})[\text{Pt}(\text{CN})_4]\}$ we take advantage of its structural characteristics for meeting the main requirements in the design of artificial molecular machines [2]: a rigid framework ("stator"), the molecular motility of an internal rotary element ("rotator") and - what makes our system more interesting - the possibility of having a certain control of the motion (switching) thanks to its bistability. In this compound the rigid framework can be significantly modified by inducing

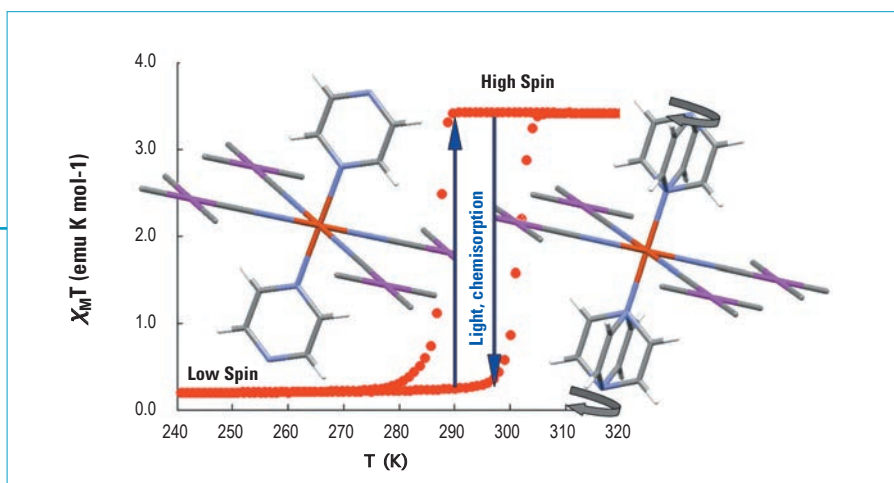
The molecular bistability that characterises spin-crossover compounds can be used for designing multifunctional materials where a second physical property is switched on and off by applying an external perturbation (temperature, pressure, light irradiation or chemical stimuli). In our case, we use this feature to switch on and off the rotation of a molecular fragment.[1]

Therefore, coming from the field of spin-crossover compounds, our system meets other of the most exciting branches of crystal engineering: the one dedicated to the construction of crystalline molecular rotators, in the quest for artificial molecular machines.[2]

the spin transition, and hence the switching of the motion of the rotary elements becomes possible and occurs in combination with the changes in magnetic, optical, dielectric, and structural properties that characterise the spin-crossover phenomenon.

$\{\text{Fe}(\text{pyrazine})[\text{Pt}(\text{CN})_4]\}$ displays a first-order spin transition between a $S=2$ paramagnetic high-spin state and a $S=0$ diamagnetic low-spin state, with a hysteresis of about 25 K wide (figure 1). The conversion can be achieved by changing

Figure 1: Temperature dependence of $\chi_M T$ for $\{\text{Fe}(\text{pyrazine})[\text{Pt}(\text{CN})_4]\}$ and representation of the structure with the rotation of the pyrazine rings.



the temperature, by light irradiation in the hysteresis loop [4a], or even by chemical stimuli [4b]: the adsorption of benzene produces the blocking of the system in HS state. A structural hint suggest that the pyrazine ligands, which are rotationally disordered in both spin states, could be moving in the high-spin state: the thermal ellipsoids of the carbon atoms are elongated in the rotation plane; but an evidence of the nature - static or dynamic - of the disorder is needed.

A quasielastic neutron scattering (QENS) spectroscopy study performed at IN5 (together with solid-state deuterium nuclear magnetic resonance, $^2\text{H-NMR}$) has allowed us to demonstrate that the switching of the rotation of a molecular fragment - the pyrazine ligand - occurs in association with the change of spin state. The QENS technique consists of the analysis of the broadening of the elastic line (associated with neutrons scattered without energy transfer) produced by interactions of the neutrons with particles diffusing or reorienting in the probed material.

With its characteristic energy scale and its high sensitivity to incoherent scattering from hydrogen nuclei, it is the ideal technique to probe the pyrazine motions. The measurement of $S(Q, \omega)$ in the bistability region allowed us to directly observe the motion in the high-spin state and its practical disappearance in the low-spin state.

As shown in **figure 2**, (where the sum over Q , $S(\omega)$, of the quasielastic spectra is represented), while the width in LS practically corresponds to that of the resolution function (given by the measurement of a vanadium sample), a clear broadening is observed in HS state, proving unambiguously that part of the system is moving.

When the system incorporates benzene guest molecules, the quasielastic broadening is still less pronounced than in the LS state, indicating the practical absence of mobility of the aromatic rings in this system. Further analysis shows that the motion in the high-spin state consists of a 4-fold jump rotation of the pyrazine rings about the coordinating nitrogen axis, as expected from the structural characterisation.

In summary, we have demonstrated by quasielastic neutron scattering the combination of molecular rotation and spin transition under external stimuli (temperature and chemical), showing that the correlation between molecular rotation and change of spin state in spin-crossover systems can be a practical element for creating artificial molecular machines.

Authors

J.A. Rodríguez-Velamazán (ICMA, CSIC-University of Zaragoza, Spain)

M. González (ILL)

J.A. Real (ICMol, University of Valencia, Spain)

M. Ohba (Kyushu University, Fukuoka, Japan)

References

- [1] J.A. Rodríguez-Velamazán *et al.*, *J. Am. Chem. Soc.*, 134 (2012) 5083–5089
- [2] *Molecular Machines*, Vol. 262, in *Topics in Current Chemistry* (Ed. T. R. Kelly), Springer, Berlin, (2005)
- [3] *Spin-Crossover in Transition Metal Compounds*; Vols. I–III, in *Topics in Current Chemistry* (Eds. P. Gütllich, H.A. Goodwin), Springer, Berlin, (2004)
- [4] (a) D. Ostrovskii *et al.*, *J. Am. Chem. Soc.*, 130 (2008) 9019–9024;
(b) M. Ohba *et al.*, *Angew. Chem., Int. Ed.* 48, (2009) 4767–4771

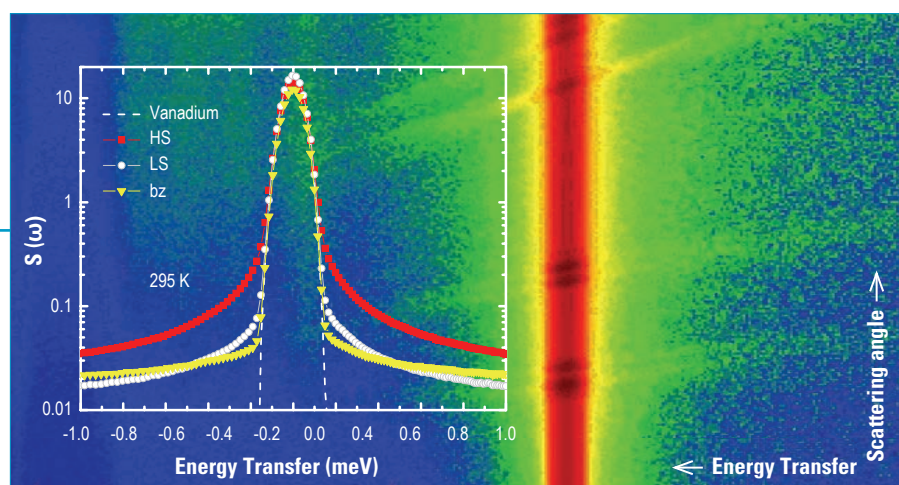


Figure 2:

Colour map showing the scattered intensity of $\{\text{Fe}(\text{pyrazine})[\text{Pt}(\text{CN})_4]\}$ as a function of the energy transfer and scattering angle and quasielastic spectra at 295 K, summed over Q , in both the HS (squares) and LS (circles) states, and in the sample incorporating benzene (triangles), together with the instrumental resolution (dashed line).

Modelling and spectroscopy

Time-of-flight spectrometer IN6
Small momentum transfer diffractometer D16

Dancing discotic molecules for self-assembled electronic devices

When disc-shaped poly-aromatic molecules are decorated with aliphatic side chains, they may self-assemble into columnar superstructures with both solid and liquid-like properties arising from the cores and tails, respectively. These discotic mesophases offer the potential for low cost, easy processing electronics with favorable properties, including self-healing of defects and tunable alignment of the conducting columns [1]. However, charge transport in these systems requires adequate intermolecular π -orbital overlap of the poly-aromatic cores along the entire columnar wire. The overall conductivity is therefore strongly dependent on the local conformation of the molecules, the presence of structural defects and thermal motions induced by the fluidic side chains [5,6]. Knowledge of how each of these three factors limits the hopping of charge carriers is valuable for rational design of discotic compounds with optimal device performance.

Neutron scattering is a convenient tool to study the dynamic structure of these systems. Neutron diffraction on deuterated samples generally achieves complementary information to X-ray diffraction. Considering the dynamics, quasi-elastic neutron scattering (QENS) is well suited to probe the picosecond timescale molecular motions of the discoids. We combined these techniques with classical molecular dynamics (MD) simulations to reveal the dynamic morphology of HAT6, one of the most basic compounds forming a discotic liquid crystalline

Discotic liquid crystals are a promising class of materials for molecular electronic devices, such as light emitting diodes, field-effect transistors and solar cells [1]. These disk-like molecules with poly-aromatic cores stack on top of one another to form stable columns, providing one-dimensional 'molecular wires' for charge-carrier transport, via a π - π overlap. Nevertheless, for widespread application the conductivity properties of discotics require optimisation. We have successfully elucidated the fundamental mechanisms that limit charge transport in discotics, by linking neutron diffraction and quasi-elastic neutron scattering (QENS) experiments directly with classical molecular-dynamics simulation. This enabled us to calculate the effect of dynamical disorder on conductivity [2-4].

phase [2-5]. MD simulations were performed on different initial model structures, which were built from a hexagonal superlattice of 12 columns each consisting of six molecules (**figure 1**).

The initial lattice parameters were determined from the observed reflections in the neutron powder-diffraction pattern and the measured density of HAT6. During MD pre-relaxation of

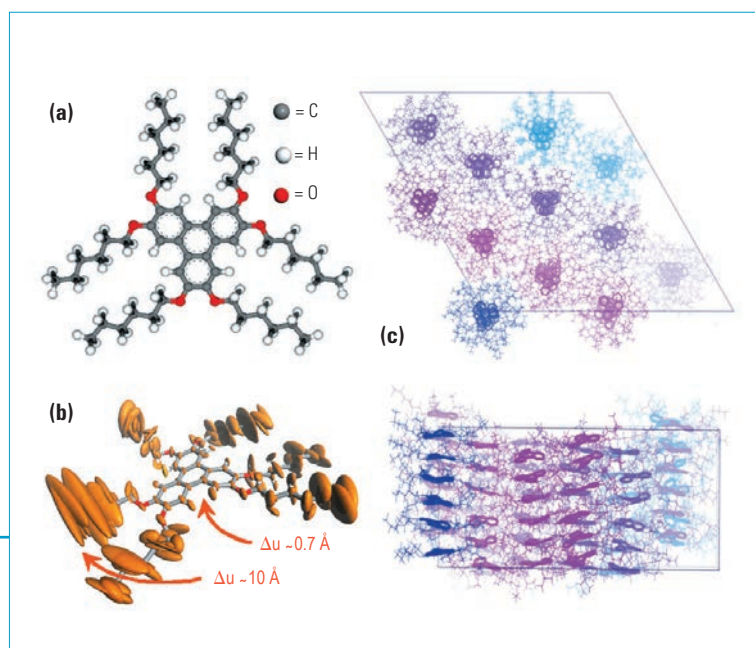


Figure 1: (a) 2,3,6,7,10,11-hexakis(hexyloxy)triphenylene (HAT6) in its initial D3h symmetric configuration, (b) average structure and thermal fluctuations for a HAT6 molecule and (c) snapshot of the MD simulation illustrating the hexagonal packing of the columnar stacks.

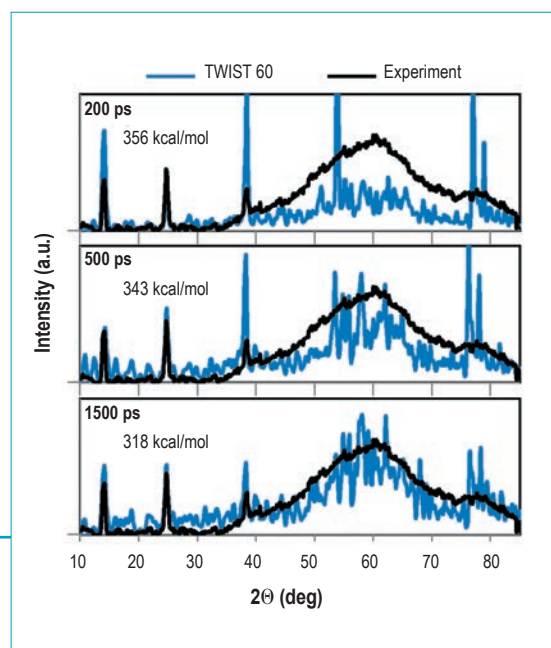


Figure 2: Comparison of the calculated diffraction pattern from MD simulations with the experimental pattern (D16). For longer simulation times the agreement improves.

the model structures, the evolution of the simulated diffraction pattern was followed and compared with experimental data (**figure 2**) obtained at the diffractometer D16. We found that different initial models converged towards a comparable overall minimum in configuration space, and consistently resulted in a satisfactory agreement with the experimental diffraction pattern. After the long pre-relaxation run a second MD simulation of about 0.5 ns was performed on the fully relaxed structural models. The diffraction patterns retained their good agreement with experiment during this time evolution, and thermally-averaged structure parameters were obtained (**figure 1c**). In addition, the incoherent-scattering function extracted from these MD simulations showed good agreement with the measured QENS data (**figure 4**) using the cold neutron time-focusing time-of-flight spectrometer IN6.

The agreement with experiment allowed us to identify the average structural and dynamical parameters by analysis of the simulation trajectories. We found that the local conformation of HAT6 molecules is characterised by a mutual rotation (twist) angle of about 37° and typically an average separation between aromatic-cores of 3.65 Å. This is a remarkable observation consistent with the shoulder at about $2\Theta = 77^\circ$ in the diffraction pattern. It should be noted that due to a considerable disorder in the core-core distances, about 20 % of the aromatic cores are separated by more than 4 Å, with a tail extending in excess of 5 Å (**figure 3**). These displacements act as structural traps because they persist for several tens of picoseconds, which is longer than the characteristic timescale for charge hopping. Considering the QENS spectra, two characteristic timescales can be observed at about 0.2 and 7 ps (**figure 4**). It was found that molecular translations ("in-plane" motions) are the dominant contribution to the spectral component of 0.2 ps in the QENS spectrum, whilst the 7 ps component mainly stems from both tilt and twist motions of the whole molecule.

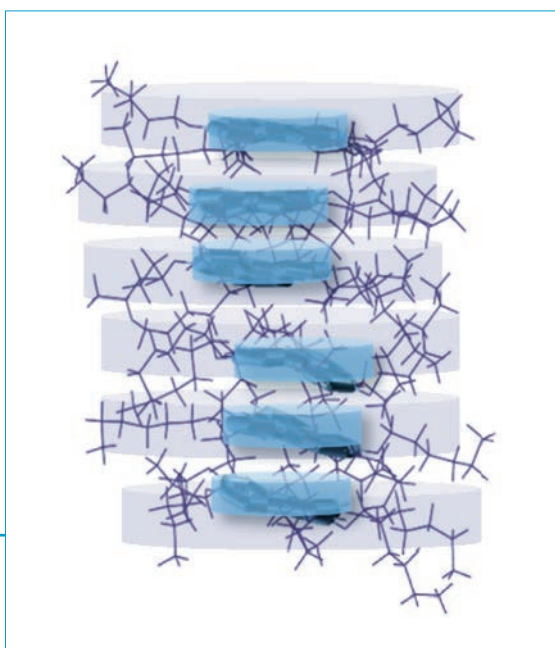


Figure 3: Disorder in columnar separations.

So what is the effect of local conformation, structural defects and thermal motions on charge transport?

To answer this, the situation for HAT6 was compared with that of larger discotic molecules exhibiting higher conductivities. It turns out that the large disorder in core-core distances is the major factor limiting the conductivity of HAT6. The charge hopping rate decreases exponentially as a function of core-core separations [5]. As a result, we consistently found that the structural defects in core-core distances account for a decrease in the mobility by a factor of about 100 in going from larger discotics to HAT6. The combination of MD simulations with neutron scattering is clearly of a key value for the study of liquid-crystalline phases [2-4].

Authors

L.A. Haverkate and **F. Mulder** (TU Delft, The Netherlands)

M. Zbiri, **M. Johnson** and **B. Demé** (ILL)

G.J. Kearley (ANSTO, Australia)

References

- [1] B.R. Kaafarani, *Chemistry of Materials*, 23 (2011) 378
- [2] L.A. Haverkate, M. Zbiri, M.R. Johnson, B. Deme, F.M. Mulder, G.J. Kearley, *Journal of Physical Chemistry B* 115 (2011) 13809
- [3] L.A. Haverkate, M. Zbiri, M.R. Johnson, B. Deme, F.M. Mulder, G.J. Kearley, *Journal of Physical Chemistry B* 116 (2012) 3908
- [4] L.A. Haverkate, M. Zbiri, M.R. Johnson, B. Deme, H.J.M. de Groot, F. Lefeber, A. Kotlewski, S.J. Picken, F.M. Mulder, G.J. Kearley, *Journal of Physical Chemistry B* 116 (2012) 13098
- [5] M. Zbiri, M.R. Johnson, G.J. Kearley, F.M. Mulder, *Theoretical Chemistry Accounts* 125 (2010) 445
- [6] X.L. Feng, V. Marcon, W. Pisula, M.R. Hansen, J. Kirkpatrick, F. Grozema, D. Andrienko, K. Kremer, K. Mullen, *Nature Materials* 8 (2009) 421

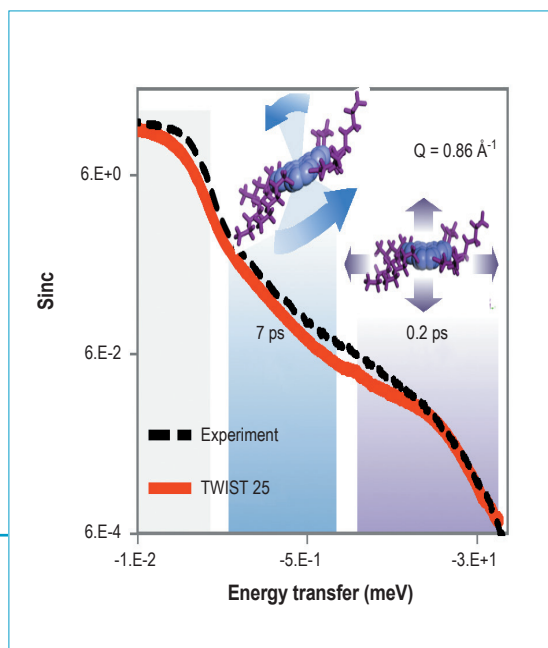


Figure 4: Simulated and observed (IN6) incoherent scattering function on a log scale. The coloured areas indicate the regions of dominant rotational (7ps) and translational (0.2 ps) motions.

Theory

An analogy with water comes to the rescue of superconductors

It is a common experience that liquid water is denser than its vapor. However, at sufficiently high pressure, liquid water and vapor cannot be distinguished by their density and there is no boiling point. Yet, there is a narrow temperature-pressure range where viscosity changes rapidly from water-like to vapor-like upon heating. The temperature pressure range where this rapid change occurs is called a Widom line.

Our work unveils an unexpected analogy with electrons in materials that become high-temperature superconductors. In these materials, it is known that there is a density-dependent temperature, the pseudogap temperature, where the electronic properties change rapidly.

The temperature-density line where electronic properties change rapidly, T^* in **figure 1**, can be understood as the Widom line that emanates from two distinct metallic phases with different densities at low temperature, one of which is the pseudogap phase that has been puzzling physicists for a long time.

Understanding often proceeds through unexpected analogies. Such an analogy has arisen between the properties of water and those of electrons in high-temperature superconductors, materials that conduct electricity without resistance at unusually high temperatures. More precisely, at high-temperature the difference between liquid water and water vapor gradually disappears, but not completely. Similarly, the electrons in a high-temperature superconductor can form a liquid-like phase and a vapor-like phase whose difference is apparent even at temperatures above those where one expects no difference.

In liquid water, molecules tend to stay close to their neighbours that attract them. In vapor a more disordered state is favored by thermal motion. Similarly, in high-temperature superconductors, the strong repulsion between electrons somewhat prohibits

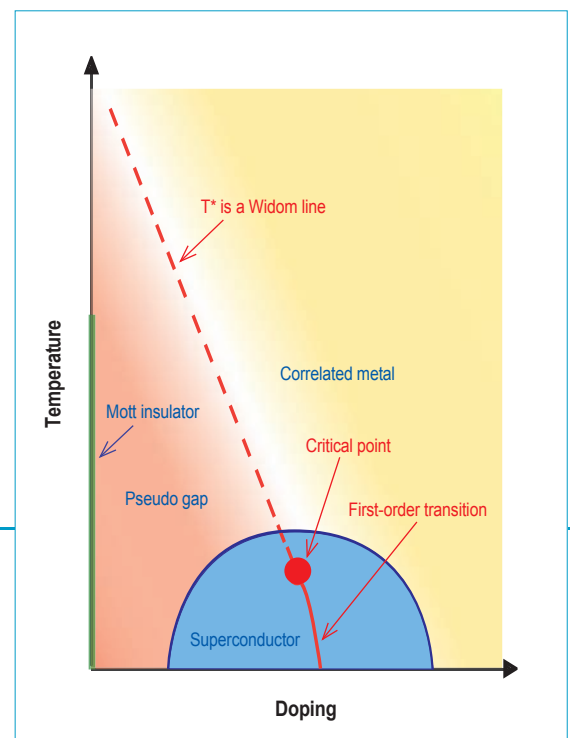


Figure 1:

Schematic temperature versus hole doping phase diagram based on the cellular dynamical mean-field solution of the two-dimensional Hubbard model. The pseudogap characteristic temperature T^* corresponds to the Widom line arising above a first-order transition. (Image credit: Virginie Guérard, ILL).

their motion in the pseudogap phase. A more disordered state, akin to ordinary metals, is favored by thermal motion and can also exist at higher-temperature.

Previous theories envisioned that the pseudogap needed to be a manifestation of a new ordered state. Such ordered states are called broken-symmetry states.

Contrary to common theories, this work shows that the pseudogap can occur solely because of strong electronic repulsion and short nonlocal correlations.

No additional broken symmetry is necessary to explain the phenomenon. Broken symmetry states, such as superconductivity, appear in the pseudogap and not the other way around.

Since the superconducting state is born out of the pseudogap over much of the phase diagram, the nature of the pseudogap is a fundamental issue in the field and it is under intense theoretical and experimental scrutiny.

These results were obtained by solving the archetypal model of interacting electron systems with state of the art numerical methods using the most powerful computers available.

The Widom line emerges from a first-order transition that arises in the presence of strong interactions when there is less than one conduction electron per copper atom, providing a new and generic mechanism for the pseudogap (see **figure 2**).

The interrelation between the pseudogap temperature T^* and the Widom line is the main finding.

Thus T^* appears in a new light: it is an unexpected example of a phenomenon observed in fluids, namely a sharp crossover between different dynamical regimes along a line of thermodynamic anomalies that appears above a first-order phase transition, the Widom line.

Authors

G. Sordi (ILL and now University of London, UK)

P. Sémon and **A.-M. S. Tremblay** (Sherbrooke University, Canada)

K. Haule (Rutgers University, US)

References

[1] G. Sordi, P. Sémon, K. Haule and A.-M.S. Tremblay, *Sci. Rep.* 2 (2012) 547

[2] G. Sordi, P. Sémon, K. Haule and A.-M.S. Tremblay, *Phys. Rev. Lett.* 108 (2012) 216401

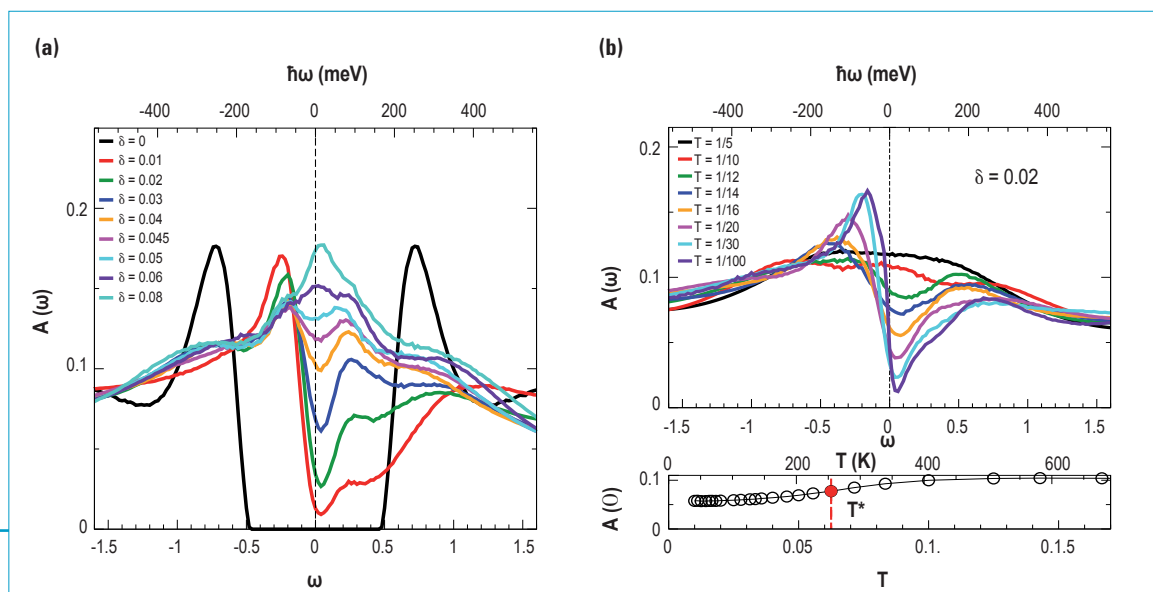


Figure 2: (a) Evolution of the electronic density of states with hole doping at a fixed temperature above the first-order transition.

One can distinguish 3 phases: Mott insulator ($\delta = 0$), pseudogap metal ($0.01 \leq \delta \leq 0.05$), and ordinary metal ($\delta \geq 0.06$).

(b) Temperature evolution of the density of states at constant doping. The inflection point in the density of state at the Fermi level, indicated by a red circle, is our estimate of T^* .

Theory

Rupture of a biomembrane under dynamic surface tension

Many aspects of biological activities and functioning crucially depend on stability of cell membranes for which several properties are not understood yet. Pores in such systems play an important role in the diffusion of small molecules across biomembranes. Likewise, dynamical properties of biological membranes, as related to molecular motions, are important since they are associated with biological functions and life.

A closed vesicle without pores can survive for a very long time. Pores can form and grow in the fluid-lipid membrane in response to thermal fluctuations and external influences. Several techniques (mechanical stress, electroporation, optical tweezers, imploding bubbles, adhesion at a substrate, sharp tip puncturing) are available for observing transient permeation and pore opening. In all instances, the resulting transient pore is usually unstable and leads to membrane rupture for some surface tension level. The challenge of the Dynamic Tension Spectroscopy (DTS) is to identify and quantify relevant parameters that govern the dynamics of membrane rupture and thereby characterize the membrane mechanical strength. Evans *et al.* [1] used DTS in experiments of rupturing membrane vesicles with a steady ramp of micropipette suction (**figure 1**). Motivated by these experimental observations, we developed a theoretical framework for the DTS to describing the kinetics of membrane breakage within the general framework of Kramers reaction rate theory.

How long a steadily stressed membrane vesicle lasts before rupture? Or conversely, how high the surface tension should be to rupture such a membrane? To answer these challenging questions we have developed a theoretical framework allowing description and reproduction of Dynamic Tension Spectroscopy observations. In this approach, the rupture of a membrane under surface tension stress is described as a dichotomy of a pore formation followed by a Brownian process of the pore radius crossing a time-dependent energy barrier.

Our description treats the membrane as a two-dimensional elastic continuum medium, and describes the membrane rupture kinetics by two successive processes: an initial pore nucleation followed by a diffusion dynamics of the pore size over a barrier height to membrane rupture.

Pore Formation: The pore nucleation in a membrane is described as a first-order activated process with a rate $q(\sigma)$, function of membrane surface tension σ as, $q(\sigma) = q_0 \exp\{\alpha(\sigma - \sigma_0)/\sigma_0\}$, where σ_0 is the unstressed surface tension and $q_0 = q(\sigma_0)$.

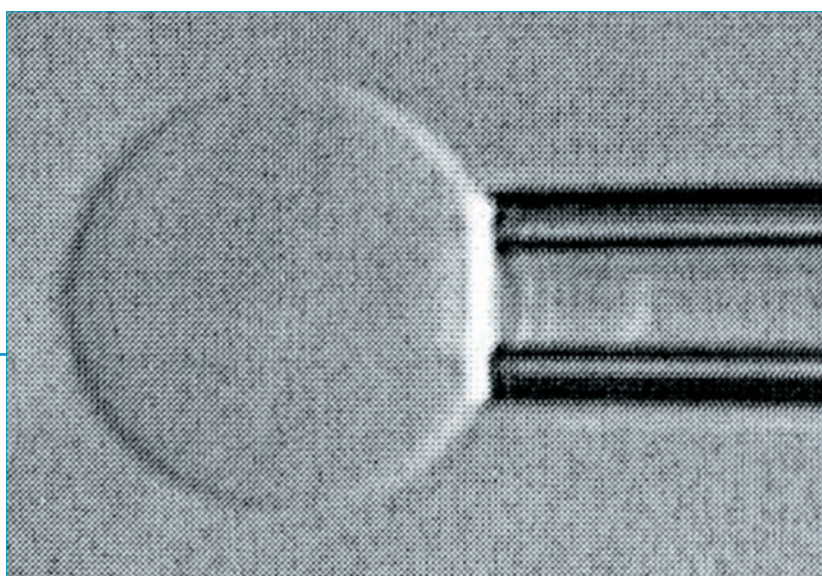


Figure 1: Image of a 20-nm bilayer vesicle aspirated in a micropipette (from [1]).

Pore Diffusion Dynamics: Once a pore is formed, the energy $V(r)$ of such a membrane with a circular pore of radius r consists of two opposed terms: the surface tension $\sigma > 0$, favoring the expansion, and the energy cost (line tension) $\gamma > 0$ of forming a pore edge, favoring the closure: $V(r) = 2\pi\gamma r - \pi\sigma r^2$. In DTS experiments [1] (**figure 1**), the membrane is steadily stressed such that (provided that γ remains constant) σ grows linearly with time as, $\sigma = \sigma_0 + vt$, where v is the dimensionless loading rate constant. The pore growth and membrane rupture dynamics is described as a two-dimensional (in pore size and tension spaces) Markovian stochastic process crossing a time-dependent energy barrier [2].

We have derived sets of stochastic and dynamical equations and performed simulations of the membrane rupture kinetics [2]. Results of simulations are illustrated in what follows.

As a successive process, the membrane mean lifetime $1/k(\epsilon|v)$, (where $k(\epsilon|v)$ is the membrane rupture rate), results from the summation of two contributions as, $1/k(\epsilon|v) = 1/k_{n,eff} + 1/k_d$, where $1/k_{n,eff}$ is the effective membrane lifetime due to pore formation and k_d is the rupture rate for a membrane initially with a pore in it, and $\epsilon = \gamma^2/(\sigma_0 k_B T)$ is the energy barrier height (with $k_B T$ the thermal energy). Two regimes can be distinguished.

Diffusion controlled limit ($q \rightarrow \infty$): This limit corresponds to the situation where membrane under tension stress has already a pore in it (or the formation of a pore is very fast) and, therefore, $k(\epsilon|v) = k_d$. In this case, the distribution $Q(y)$ of tensions $y = \sigma/\sigma_0$ at rupture broaden from the delta function at $y=1$ to a wider distribution when both v and ϵ increase [2]. Likewise, the mean tensions $\langle y(\epsilon|v) \rangle$ for membrane rupture also increase with both v and ϵ [2].

Finite pore nucleation rate $q \neq 0$ limit: **Figure 2** displays $k(\epsilon|v)$ (the reverse of membrane mean lifetime) as a function of the pore nucleation rate q_0 , where $k_{n,eff} = q_0$. As expected, $k(\epsilon|v)$ grows linearly with q_0 in the nucleation controlled limit $q_0 \ll k_d$ and saturates to k_d in the diffusion controlled limit $q_0 \gg k_d$. This illustrates how parameters can be tuned to follow the transition between the nucleation and diffusion controlled limits. **Figure 3** displays $Q(y)$ profiles corresponding to $q_0 \ll k_d$ limit and toward $q_0 \gg k_d$ limit.

We have developed a theory, in agreement with DTS experiments, which describes the membrane rupture kinetics by dichotomic processes: an initial pore nucleation followed by a diffusion dynamics of the pore size over a time-dependent barrier height to membrane rupture. Several aspects can be addressed as well using our model including transient pores in vesicles with leaking-out, membrane rupture with a non-circular but an arbitrary shaped pore, and the case of fluctuating membranes.

Authors

D.J. Bicout (ILL and UJF Grenoble and VetAgro Sup Lyon, France)

E. Kats (ILL and now Landau Institute for Theoretical Physics, Russia)

References

- [1] E. Evans, V. Heinrich, F. Ludwig and W. Rawicz, *Biophys. J.* 85 (2003) 2342
 [2] D.J. Bicout and E. Kats, *Phys. Rev. E* 85 (2012) 031905

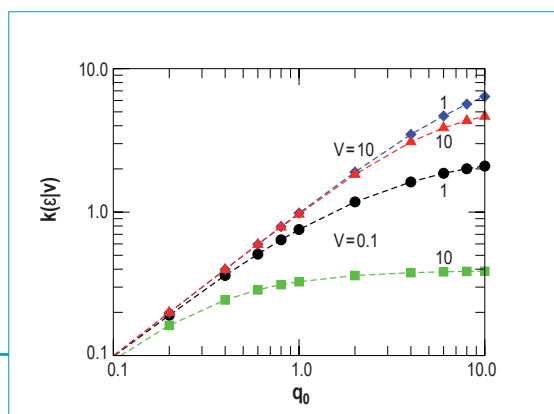


Figure 2: Rupture rate $k(\epsilon|v)$ as a function of the pore nucleation rate q_0 for various barrier heights ϵ (quoted numbers) and loading rates $v=0.1$ (circles and squares) and $v=10$ (diamonds and triangles). Filled symbols correspond to simulations and dashed lines are guide eyes.

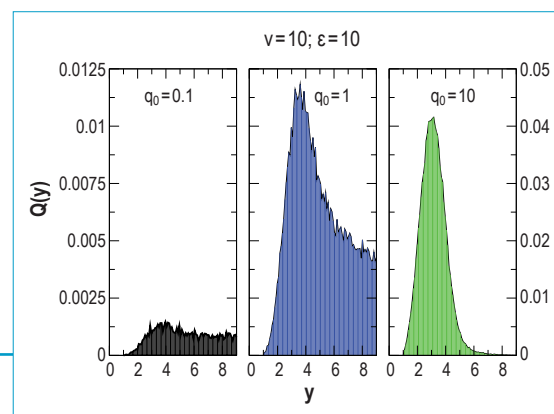
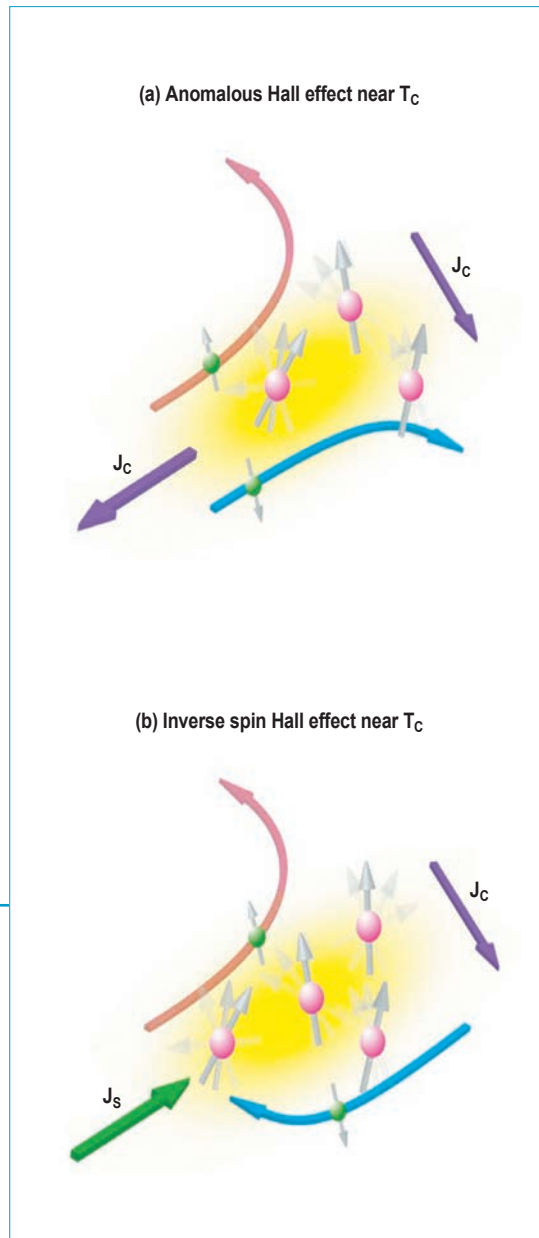


Figure 3: Distribution, $Q(y)$, of rupture tensions, y , for various values of the pore nucleation rate, q_0 . The panels with $q_0=1$ and $q_0=10$ have the same scales in both x and y axes.

Theory

The spin Hall effect as a probe of nonlinear spin fluctuations



The spin Hall effect (SHE) enables us to create spin current in non-magnetic materials without using ferromagnetic materials. It is a crucial element in the central idea behind spintronics. We have proposed a new way to harness the inverse process of SHE (ISHE), by which spin currents become observable by reconversion to charge, to probe non-linear spin fluctuations in the vicinity of the magnetic phase transition of a magnetic metal. This provides a new probe which has shown to be applicable to nanowires, with a sensitivity to a tiny magnetic moment orders of magnitude smaller than that which could be seen by a conventional SQUID magnetometer.

The field of spin electronics or "spintronics" is based on the idea of exploiting the spins of electrons, rather than their charges, in order to make circuits that would be smaller and consume less energy than conventional devices. The practical difficulties are that spin "currents" in which the two different polarisations of electron spin would move in opposite directions

Figure 1: Representation of the Anomalous **(a)** and Inverse Spin Hall Effects **(b)** in a ferromagnetic metal near the Curie temperature. The conduction electrons (green balls) carrying spin are scattered by fluctuations of local moments (red balls). The two effects are predicted to depend on higher correlations of third and fourth order respectively (than the longitudinal resistance, which is of second order).

must be made, and then detected, by some conversion from conventional charge currents. The fundamental processes which are key to this, are the spin Hall effect and its inverse, the inverse Spin Hall effect -see **figures 1 and 2** for schematic and real experimental definitions of these concepts. The inverse effect is essential since it enables us to convert a spin current, which is not an electrically detectable quantity, into a charge current. The aim is to find efficient ways of doing this, but also finding interesting applications to study other physical phenomena.

In recent work we proposed a way to harness the ISHE as a probe of nonlinear spin fluctuations in the vicinity of the magnetic phase transition. In general, to probe the spin fluctuation near the critical temperature T_C , the linear response to an applied magnetic field, *i.e.* linear magnetic susceptibility χ_0 is studied. However, χ_0 alone is not sufficient to understand all physical properties. For example, in the anomalous Hall effect (AHE) in a ferromagnet such as pure Ni and Fe, there is a sharp peak below T_C in the Hall resistivity that is related to χ_1 , the first non-linear coefficient of susceptibility.

We study the ISHE in weakly ferromagnetic NiPd alloys near their Curie temperatures, and found a new relation between the ISHE and the nonlinear spin fluctuation, which is impossible to be observed in non-magnetic materials. We observed an anomalous temperature variation of spin Hall resistance for the NiPd alloys near T_C . Our theoretical results imply that

the anomaly near T_C is related to the second order nonlinear spin fluctuation, unlike the AHE where it was of the first order.

The essential difference between the AHE and ISHE is that the incident current is a charge current in the former and a spin current in the latter. The difference in symmetry is sufficient to change the order of fluctuations. This conceptually important aspect has essentially been hidden for the 50 years since Kondo first calculated the effects of skew scattering in transport.

More importantly, it provides a new probe (at $Q=0$) applicable to nanowires, with a much higher sensitivity to the net magnetic moments than even a conventional SQUID magnetometer. This presents a challenge for neutrons: higher order correlations are not directly measurable by neutrons especially in such tiny samples.

Authors

T. Ziman (ILL, LPMMC, University Joseph Fourier and CNRS, Grenoble, France)

B. Gu and **S. Maekawa** (JAEA, Tokai, Japan)

References

[1] D.H. Wei *et al.*, Nature Communications 3 (2012) 1058

This work is in collaboration with the experimentalists D.H. Wei, Y. Niimi, Y. Otani of the ISSP, University of Tokyo

[2] B. Gu, T. Ziman, S. Maekawa, Phys. Rev. B 86 Rapid Comm., (2013) 241303 (R)

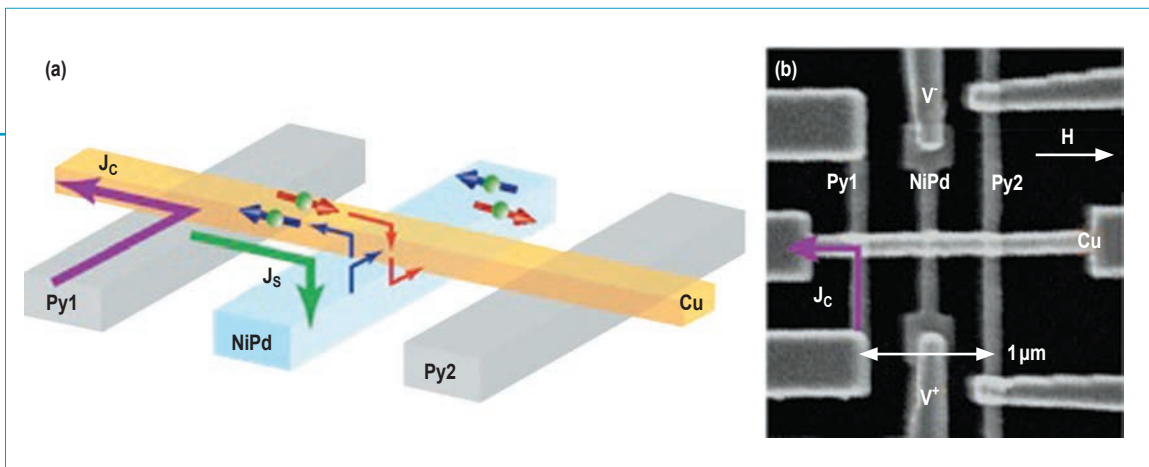


Figure 2:

The experimental device (as made in the laboratories of the group of Y. Otani, ISSP, Tokyo) both schematic and in reality. The skew scattering takes place in a Ni Pd nano-wire.

Millennium programme New experimental techniques Technical and computing developments

In the early years of neutron scattering experiments, the neutrons produced in the ILL's reactor travelled to the samples along a free flight (or "ballistic") trajectory. Nowadays, the guides and other focusing devices developed as a result of advances in neutron optics have dramatically increased the neutron flux on samples. It was in this tradition of continual improvement that the ILL launched its ambitious modernisation programme, known as the Millennium Programme. Involving a total investment of around 91 M€ over the period 2001 to 2014, the Millennium Programme has already produced not only a substantial number of new or upgraded instruments but also a vast range of technical improvements covering everything from neutron guides, monochromators and detectors to sample environment equipment and velocity selectors. The Millennium Programme has played a major part in allowing the ILL to retain its position as world leader in neutron sciences despite the emergence of some very challenging competitors.

The Millennium Programme has played a major part in allowing the ILL to retain its position as world leader in neutron sciences

During the period 2001-2012, many instruments were renewed, leading to impressive gains in counting rates thanks to more modern neutron guides and to larger and more efficient




monochromators and detectors. In addition, the increased concentration of the neutron flux has made it possible to use smaller and smaller samples, making life easier for our users. By way of an example, the number of protein crystallography experiments carried out at the ILL has increased significantly following the upgrade of the instrument LADI. On the triple axis CRG IN12, the gain is even more impressive bringing this instrument to the first place in the world. Of course, our CRG instruments are also regularly improved, thanks to the excellent partnerships the ILL has established with outside institutes and universities. For example, D1B (CSIC in Spain and the CNRS in France) now has a new detector, while the instruments GRANIT and SuperADAM have also been extensively improved.

In the past few years, the ILL's Projects and Techniques Division (DPT), in particular, has achieved many successes across all of its services: sample environment (high temperatures, low temperatures, magnetic fields), instrument control, data storage and processing. And of course the ever growing neutron user community has continued to benefit enormously from the commitment and expertise of the different ILL teams. For example, the ILL is a recognised expert in the domain of polarised neutrons. The Institute has its own polarisation station for helium-3, which is in operation every day to supply neutron analysers and polarisers. In 2012, the ILL installed a similar station at both ISIS in the UK and ANSTO in Australia (*p. 84*).

The years 2013-2015 promise to be a time of extremely intense activity on a host of projects, including the commissioning of IN16B and the mammoth task of replacing the guide H5. At the same time, work on the three-axis spectrometer ThALES and the spin-echo spectrometer WASP will be completed. The installation of the new state-of-the art guide and the commissioning of these two new instruments will bring to a close the final phase of the Millennium Programme.

As for the future, the Institute's technical and scientific teams are now facing another major challenge, that of keeping the ILL at the forefront of neutron scattering for the next decade and beyond. To achieve this ambitious goal, we are currently preparing a new modernisation programme which, in addition to further instrument upgrades, will include guide renewals and major investment in sample environment, laboratories and software. Appropriately baptised 'Endurance', this new upgrade programme will allow the ILL to continue to set the pace in neutron-based science in the years to come.



Charles Simon
Associate Director



Millennium programme

Millennium Programme 2012

2012 also saw the completion of the new **D33** small-angle scattering (SANS) diffractometer and the arrival of its first users (**figure 1**). D33 is now a fully commissioned world-class SANS instrument offering a wide range of interesting options (for more information, see *p. 76*). With its specially designed ^3He detector (built at the ILL), a very open space for sample environment, and extremely convenient collimation with a host of different options (including polarised neutrons), this spectrometer has taken up a well-earned place alongside D11 and D22 in the ILL's extremely competitive SANS instrument suite. In addition, a time-of-flight option will allow to access in a single measurement to an unprecedented range of Q (a factor of 1000). Due to the state-of-the-art design of its guide, the flux available at D33 is comparable to that of D22, despite its distance from the reactor. Four additional detectors to extend the Q range still further will be added at the very beginning of 2013.

The new backscattering spectrometer **IN16B** is also now in place (**figure 2**). The first neutrons have been delivered on the instrument, which has now been tested in all of its many possible configurations. The new and extremely challenging phase space transformer is ready for use and six full-size analysers specially designed for the chamber will be constructed and installed in 2013. After many years spent in the design and construction phases, IN16B is set to become a highly efficient backscattering spectrometer. The fixed-window technique employed on the instrument will facilitate detection of the dynamic precursors of phase transitions in the nanosecond time range, allowing scientists to determine the activation energy of the process.

In 2012, activity on the Millennium Programme was once again extremely intense.

The new design of the H14 guide has increased the neutron flux at the sample by a factor of 2. As a result, the performance of the instruments fed by this guide (D33, IN11, LADI and IN12) has improved considerably. On the three-axis spectrometer IN12 (operated as a CRG), the gain is most impressive and will change the type of science to be addressed using this instrument. IN12 is now the best three-axis spectrometer on a cold source in the world, D33 is now one of the world's best small-angle instruments and IN11 has once again become extremely competitive in its field.

The three-axis spectrometer **ThALES**, developed in collaboration with Charles University of Prague, will be the ILL's new TAS instrument. In this next-generation instrument, the focusing monochromator will concentrate the neutron beam on a smaller sample.

The high-intensity spin-echo spectrometer **WASP** aims to provide users with both a wide Q range and a wide time range. Work on this extremely challenging project is progressing well and a call for tenders is about to be issued for the precession coils.

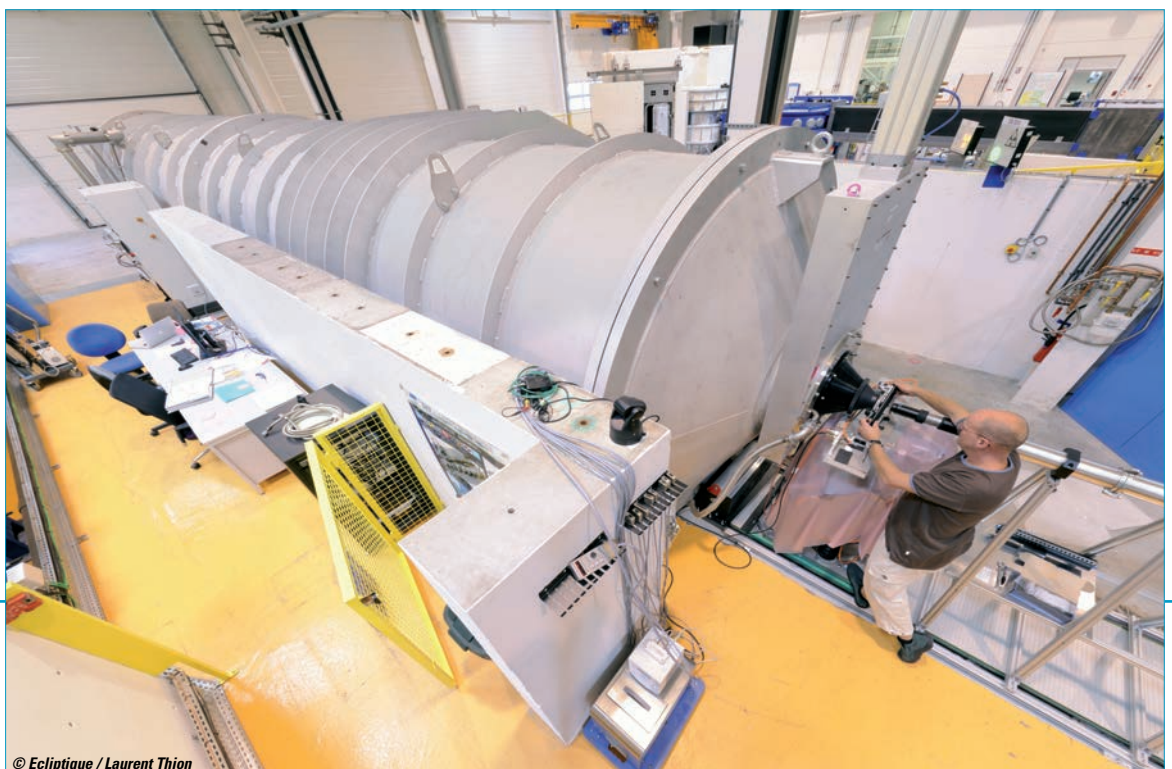


Figure 1:
The new small-angle
scattering
instrument D33.

© Ecliptique / Laurent Thion

WASP will be installed in the extension of the guide hall ILL 22 completed at the beginning of 2013. The instrument's analysing supermirrors are being produced at the ILL using thin-film sputtering techniques. The whole deposition process is expected to take several years, owing to the large surface area involved (a few square metres). By the end of 2014, about 180 degrees will have been covered. The cooling circuit and the additional electrical power needed for the coils (0.5 MW) will be ready in 2013.

The year 2012 was also devoted to preparing the long reactor shutdown (August 2013 - June 2014) during which, among other things, **the guide H5** will be replaced. The new guide will improve significantly the performance of the instruments D16, SuperADAM and CryoEDM and will also feed the new spin-echo spectrometer WASP. This new guide will be one of the more complex of ILL with four different branches after a common part (**figure 3**).

The neutron guide hall which houses H5 (ILL 22) is currently being extended in order to create room for WASP as well as an additional free instrument position. H5 will also feed the new spectrometer Thales, which will be sited on Level C of the reactor hall. Work on replacing H5 will involve dismantling the old guide and installing and commissioning the new guide in time for the reactor restart in 2014.

The millennium programme is now entering in its last phase with the guide H5 and the instruments ThALES and WASP. Thanks to the excellence of ILL teams, it will offer to users unique and challenging opportunities to imagine new challenges in neutron science.

Author
C. Simon (ILL)



Figure 2:
The new
backscattering
instrument IN16B.

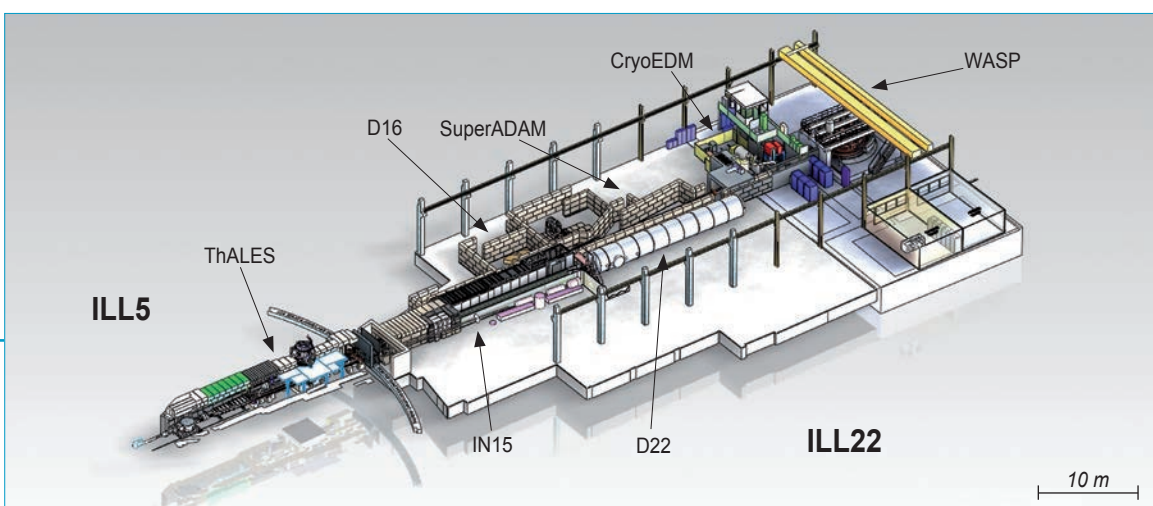


Figure 3:
CAD presentation
of the new guide
H5, and of the
instruments which
will be fed by it.

Millennium programme

D33 – Massive dynamic q -range time-of-flight SANS instrument

D33's primary goal is to enable measurements over a wide dynamic q -range (q_{max}/q_{min}), or range of material lengths scales observable in a single measurement. By equipping D33 with two independent detector arrays, a 64 x 64 cm (256 x 128 pixels) rear detector and a front detector made from four 16 x 64 cm panels (32 x 256 pixels), large and flexible solid angular coverage can be achieved. In time-of-flight (TOF) mode, instead of selecting a single incoming neutron wavelength with a monochromator or velocity selector, 'white' pulses of neutrons are shaped by the 4-chopper system and wavelength discrimination is made by their arrival time at the detector. The advantage of using the TOF method is that a wide band of neutron wavelengths illuminate the sample and hence simultaneously sample a massive dynamic q -range in excess of $q_{min}/q_{max} \sim 1000$. D33 can also operate in the 'classic' monochromatic mode, in an identical manner to the D11 and D22 instruments, with the twin detectors allowing an extended and continuous dynamic q -range of $q_{min}/q_{max} \sim 30$.

Figure 2 shows the first TOF measurement of a powder sample of Silver Behenate which has a large layer spacing of 58.4 Å, evidenced by the first Bragg ring at a $q = 0.108 \text{ \AA}^{-1}$ and is compared with an equivalent measurement made in monochromatic mode. Despite only the rear detector being available for this measurement the dynamic q -range in TOF mode is impressive while the absolute q and intensity are in good agreement. Optimisation of the 'pin-hole' resolution conditions for a SANS instrument requires careful consideration of the maximum sample size, source neutron guide size and distances for a

In 2005 the ILL began to consider the construction of a third Small-Angle Neutron Scattering (SANS) instrument, D33. Building upon the successes of its forerunners, D11 and D22, the D33 instrument specification developed with the aim of providing an intense SANS instrument, offering a massive simultaneous measurement of structural length scales (q -range), while improving capabilities for studies in magnetism. At a total (and coincidental) cost of 3.3 M€, construction of D33 in the ILL 7 guide hall took place over an 18 month period during 2011 and 2012. At 15h30 on 20 June 2012 D33 switched on for the first time for scientific commissioning followed rapidly by the first user experiments. Here we describe the performance and characteristics following instrument commissioning during the second half of 2012.

given instrumental resolution. The overall size of D33 has been down-scaled based upon these principles to an instrument size of 12.8m maximum collimation and 12.8m detector distance, where the guide size (30 x 30 mm) and detector resolution have all been down-sized to about 2/3 relative to an instrument such as D22. This limits the maximum sample size on D33 to about

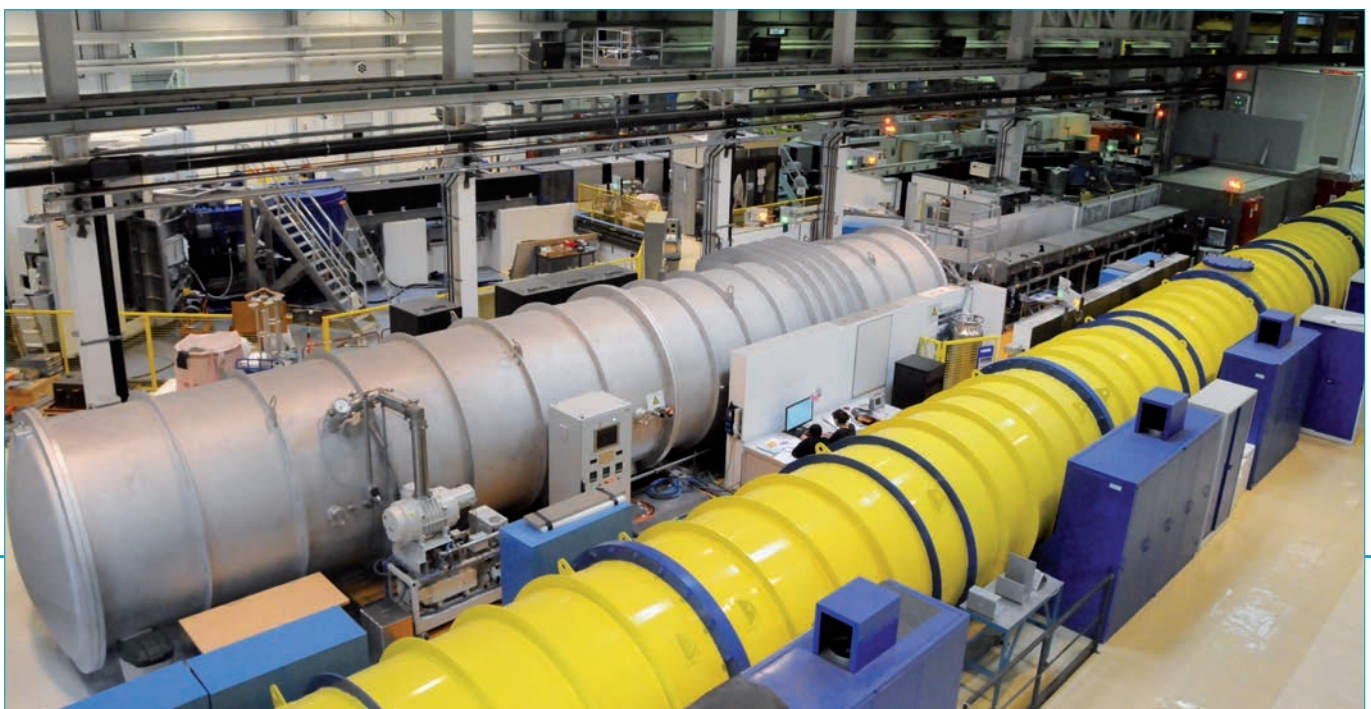


Figure 1: The D33 (metallic tube) and D11 (yellow tube) SANS instruments lying in the new extension of the ILL 7 guide hall.

15mm but gives resolution advantages when working in TOF mode, better optimises the instrument resolution for smaller samples, as well as saving the cost and space involved in building much larger instruments.

Figure 3 shows how the neutron flux at the sample position varies as a function of incoming beam angular resolution (source size /collimation length) for the ILL's SANS instruments, D11, D22 and D33. **Figure 3** shows that despite the long distance of D33 from the ILL's reactor (> 100m) and the reduced guide dimensions, D33's neutron flux for a given resolution is at least equal to, if not brighter than that of D22. The inset to **figure 3** shows how the neutron flux varies linearly as a function of TOF wavelength resolution and is comparable to monochromatic mode for a similar resolution. For example, TOF mode provides approximately the same neutron flux as monochromatic mode with a wavelength between 7 Å and 8 Å. In general, monochromatic mode is more suitable for high intensity studies over a limited *q*-range and the TOF mode more suitable for studies requiring a global overview over an extended *q*-range.

During the first reactor cycle of 2013 the final component of D33 to be installed, the front pannel-detector, will be commissioned marking the completion of D33. D33 will be

completed, commissioned, calibrated and competitive for full user operation with all options, including monochromatic and TOF modes of operation, twin detector arrays and polarisation and analysis capability. Demand for beamtime on D33 has already rivaled that of it's peers, D11 and D22 and abated the shortfall in SANS beamtime by increasing capacity by a factor of 1.5. The D33 team looks forward to many scientifically productive years of operation and improvements in the SANS technique.

ACKNOWLEDGEMENTS

Antonio Perillo-Marconne and Giuliana Manzin were the engineering project managers though the project. The instrument was designed and physically built for the most part by Cyril Amrouni, Michel Bonnaud and Mark Jacques. Many thanks also to all of the ILL services who took part in the design, construction and management of this project. The ILL directorate past and present are thanked for their continuing support of this project. Over now to you, the scientific user community!

Authors

C.D. Dewhurst, I. Grillo and M. Bonnaud (ILL)

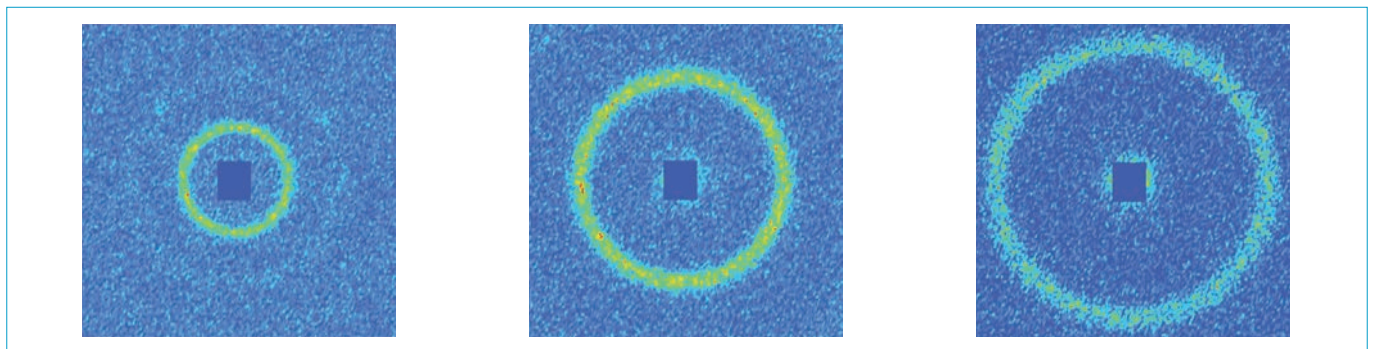


Figure 2a: TOF frames at wavelengths of 3 Å, 6 Å and 8 Å.

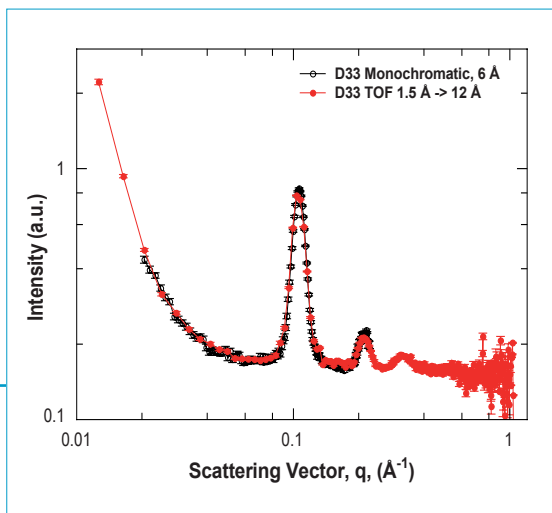


Figure 2b: Time-of-flight and monochromatic measurement of a Silver Behenate calibration sample.

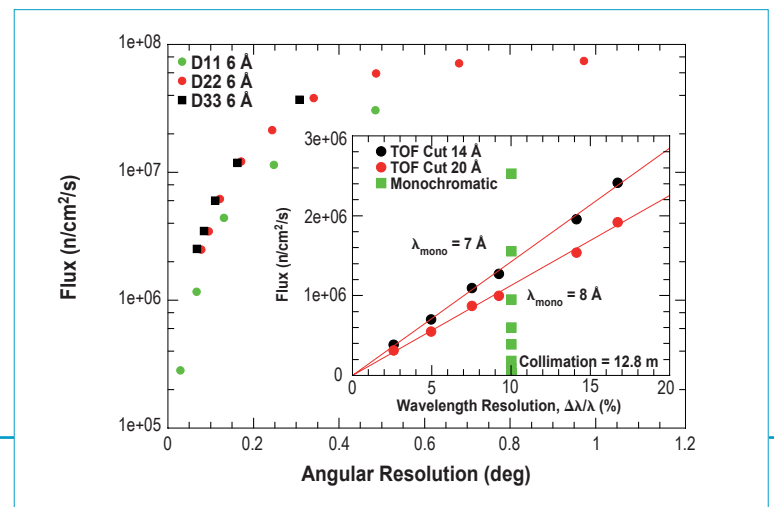


Figure 3: Neutron Flux at the sample position as a function of angular resolution for D11 (green), D22 (red) and D33 (black) SANS instruments. (Inset) Comparison of the neutron flux at the sample position in TOF (wavelength cut-offs of 14 Å and 20 Å) and monochromatic modes as a function of TOF wavelength resolution $\Delta\lambda/\lambda$.

New experimental techniques

Faster and more reliable overview of system dynamics using inelastic fixed-window-scan on backscattering instruments

In neutron spectroscopy, "elastic scans" or "elastic fixed-window-scans" (EFWS) are often used as a first step to obtaining an overview of changes in the dynamics of unknown systems under temperature or pressure. Intensity in incoherent neutron scattering is directly related to the self-correlation of a scattering particle, which is the probability of finding a particular particle displaced a certain distance after a given lapse of time. The Q -dependent elastic intensity measured therefore relates to the probability of still finding the observed scattering particle in a given volume, after a time delay corresponding to the spectrometer resolution.

For IN16 this observation time is about 2 nanoseconds. If the temperature is low enough, we can assume that all the scattering particles are frozen, which means they do not move within the time resolution. The intensity decay typically observed with increasing temperature is then directly related to the decrease in self-correlation.

This is a technique which allows easy detection of the dynamic precursors of phase transitions which can show up, for example, as an increase in the average mean square displacement of scattering atoms or molecules. These scans also help judge whether, and in what range of temperature, the relaxation time of the system being investigated enters the



Linear motor Doppler drive for IN16B (built by AEROLAS) with the monochromator plate without crystals mounted.

Spectroscopic investigations of small samples, often required for biology or high pressure research, and nano-confined systems have a great deal to gain from the new technique of inelastic fixed-window-scan on backscattering instruments.

A new generation of linear motor Doppler drives enables rapid switching between elastic and inelastic energy transfer channels, while continuously ramping up the temperature or pressure being applied to the sample.

This allows for much shorter counting times, safer interpretation of the popular elastic scan, or, on ILL's now almost complete IN16B instrument, perhaps even kinetic experiments.

nanosecond time range, or how fast relaxation changes with temperature, *i.e.* how large the activation energy is.

These sample parameter scans are particularly interesting for neutron backscattering, as they provide dramatically improved statistics. First, for solid samples the elastic signal is higher than for inelastic scattering, typically by a factor of 100. Secondly, on elastic scans, a backscattering spectrometer like IN16 spends all of its measuring time probing the elastic response of the sample. With normal backscattering spectroscopy however, measuring time is spread over a wider energy transfer range. These parameter scans are therefore frequently performed before engaging on a full spectroscopic study using backscattering or time-of-flight techniques.

There is now a new technique of *inelastic* fixed-window-scanning (IFWS) which provides the same level of statistical

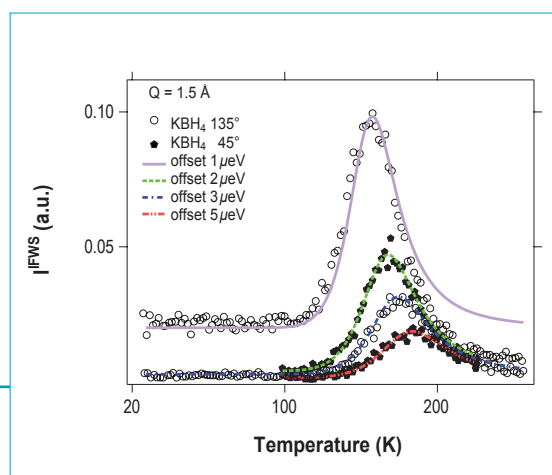


Figure 1: Inelastic fixed-window scan (IFWS) on KBH_4 at different energy offsets fitted with an Arrhenius activated relaxation process [3].

advantage, as nearly all the measuring time can be focused on one or several inelastic energy channels. Whilst the idea is not new [1], the technique has now become scientifically very interesting, as instrumentation has progressed.

Thanks to the new generation of Doppler drives using linear motors it is now possible to run different velocity profiles. For IFWS purposes the monochromator speed alternates periodically between constant velocities $\pm v$. It is even possible now to combine several inelastic and elastic channel measurements by switching between different Doppler velocities whilst continuously varying sample temperature or pressure [2].

The technique, besides improving statistical accuracy compared to full spectra measurements, also removes some of the uncertainties in the interpretation of elastic scans. These might be associated with the partial crystallisation or other elastic structural contributions of the sample, with changes in sample density or strong elastic contributions by the hosts when probing the dynamics of confined molecular guests. Such effects are either absent or have a different influence in IFWS; data interpretation is much safer, especially if EFWS and IFWS are combined.

The figures below provide three examples of applications for the new technique.

In the first example, **figure 1** shows the temperature-dependent IFWS on KBH_4 , which belongs to the class of potential light-weight hydrogen storage materials. The measured intensity shows a Q-independent distinct maximum in the temperature range where the relaxation rate corresponds to the energy of the chosen inelastic window. The lines in **figure 1** are fits assuming an Arrhenius temperature dependence of the relaxation process; they allow for a determination of the activation energy [3].

The second example concerns a glycerol-water mixture, and **figure 2** shows that the Q-dependence of the IFWS reveals whether detected quasielastic scattering originates from a

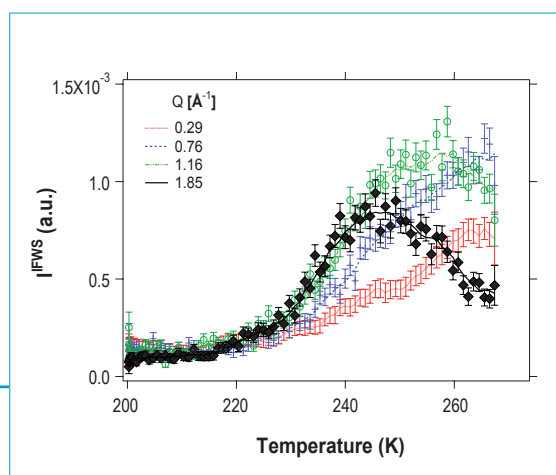


Figure 2: Inelastic fixed-window scan (IFWS) on a glycerol-water mixture showing a strong Q-dependence of the intensity maximum.

local or a diffusive process. In this example, for a fixed inelastic window energy the maximum is only clearly visible at high Q-values; it is outside the observed temperature range at low Q. This indicates strongly Q-dependent relaxation, as is the case for translational diffusion.

In the third example, **figure 3** shows measurements on ferrocene, where cyclopentadienyl rings undergo N-fold rotational jump diffusion [4]. EFWS and IFWS measurements and full energy spectra at selected temperatures were combined and simultaneously fitted with a rotational jump model. At $T=163\text{K}$, a phase transition leads to a sudden decrease of intensity visible in the IFWS.

With the high flux expected on the new backscattering spectrometer IN16B, IFWS will become even more powerful. It may then become possible to automatise data acquisition to a certain degree: it should soon become feasible to run the combination of elastic and inelastic fixed-window-scans described above, automatically evaluating the temperature or pressure dependence of these scans, before launching full spectroscopic runs at computer-selected temperatures or pressures.

Authors

B. Frick and **M. Appel** (ILL)
J. Combet (ILL and now Charles Sadron Institute, Strasbourg, France)
L. van Eijck (ILL and now TU Delft, The Netherlands)
A. Remhof (EMPA, Switzerland)
B. Stühn (TU Darmstadt, Germany)

References

- [1] H. Grapengeter, B. Alefeld and R. Kosfeld, *Colloid and Polymer Science*, 265 (1987) 226
- [2] B. Frick, J. Combet and L. van Eijck, *Nuclear Instruments & Methods In Physics Research A* 669 (2012) 7
- [3] A. Remhof *et al.*, unpublished IN16 data
- [4] M. Appel, ongoing PhD thesis work, unpublished

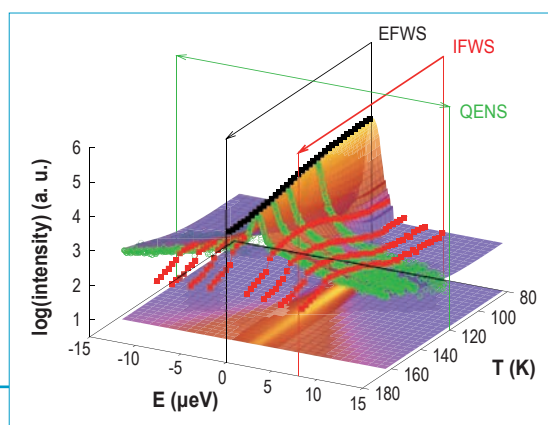


Figure 3: Inelastic (IFWS) and elastic fixed-window-scans (EFWS) combined with full spectroscopic runs (QENS) on ferrocene. The plotted surface represents a model fit for circular jump diffusion [4].

New experimental techniques

Terbium: "a new Swiss Army Knife" for cancer diagnosis and treatment

Systemic application of targeted radiopharmaceuticals results in specific accumulation of radioactivity in cancer cells. Depending on the decay properties of the isotope it can be used for nuclear imaging purposes or targeted radionuclide tumor therapy. Nuclear imaging involves positron (β^+)- or γ -radiation-emitting radiopharmaceuticals. The radiation emitted by diagnostic radioisotopes is detected outside the body using a positron emission tomography (PET) or single photon emission computed tomography (SPECT) scanner or a gamma-camera and allows not only diagnosis but possibly also the determination of the severity of a particular tumor type. Targeted radionuclide therapy makes use of the short-range radiation (α - and β^- -particles, Auger electrons) emitted by therapeutic radioisotopes to selectively destroy cancer cells.

With regard to the targeting vector many new designs are currently under development for a large variety of applications in oncology and other pathologies. This opens the possibility to select the best suitable radioisotopes at an early stage of the development allowing an overall optimisation of the radiopharmaceutical. Often such innovative radioisotopes are not commercially available and dedicated production methods have to be developed. Recently a method for large-scale production of non-carrier-added ^{161}Tb has been developed by radiochemists from TU Munich and PSI Villigen and irradiations at ILL and FRM2 enable supplying this isotope in a quality and quantity needed for clinical applications [1].

Overexpression of tumor markers (e.g. antigens, peptide receptors) which can be selectively targeted with biological vectors (e.g. antibodies or antibody fragments, peptides, vitamins) is a frequent characteristic of cancer cells. Such vectors can be derivatised in a way that they are accessible for conjugation of a payload, for instance a radioisotope.

Thus, receptor targeted radiopharmaceuticals consist of a radioactive isotope which is attached to a biological vector as a tumor targeting ligand (figure 1).

Here we report on a first preclinical study using this isotope together with other Tb isotopes produced at the on-line isotope separator ISOLDE at CERN, Geneva. Terbium is the only element in Mendeleev's table offering four clinically interesting radioisotopes (^{149}Tb , ^{152}Tb , ^{155}Tb and ^{161}Tb) with complementary nuclear decay characteristics covering all nuclear medicine modalities (figure 2).

Identical chemical characteristics of these radioisotopes allow the preparation of radiopharmaceuticals with identical pharmacokinetics useful for PET (^{152}Tb) and SPECT (^{155}Tb) and for radionuclide therapy using α -particles (^{149}Tb) and β^- /Auger electrons (^{161}Tb).

For this first in-vivo proof-of-principle study we employed a novel folate receptor targeting vector which was based on a folic acid conjugate with a DOTA chelator. The folate receptor is overexpressed in a variety of aggressively growing tumors including ovarian and other gynecological cancers as well as certain breast, renal, lung, colorectal and brain cancers, whereas its distribution in normal tissues and organs is highly limited. Folate vitamins show a rapid uptake but also a rapid renal elimination from the body, therefore it does not reside sufficiently long in the body to reach all cancer cells. Hence a new folate conjugate (indicated as cm09) was designed where folic acid is conjugated with an albumin binding entity that

Figure 1: Principle of targeted radiopharmaceuticals: a radioisotope is linked to a biological vector which binds to a target structure (e.g. antigen, receptor) expressed on cancer cells.

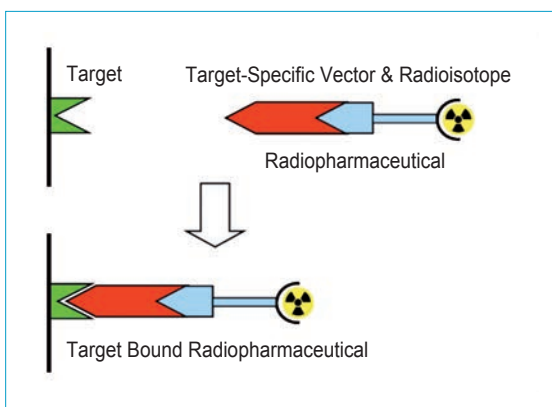
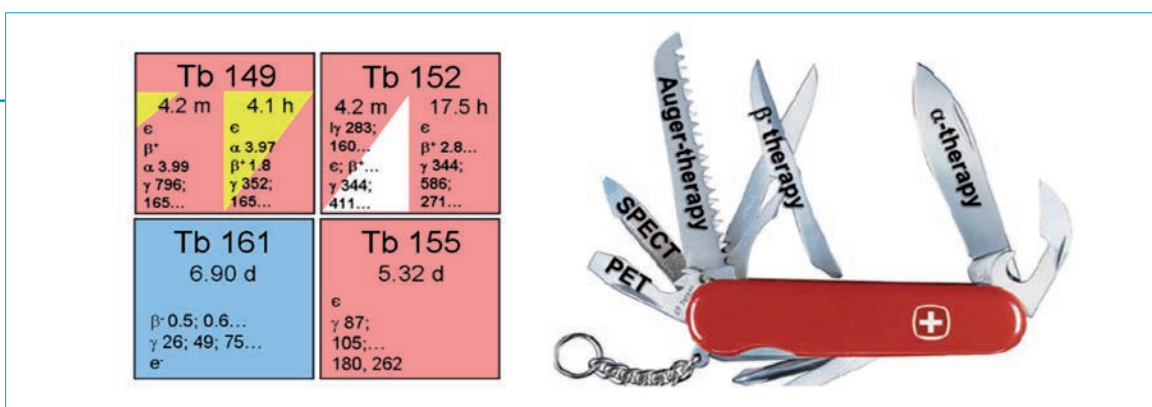


Figure 2: Terbium which comprises four medically interesting radioisotopes - the "Swiss Army knife" for diverse applications in nuclear medicine.



prolongs the circulation time in the blood. The Tb radioisotopes were stably coordinated by a DOTA-chelator which was linked to cm09 (**figure 3**).

^{161}Tb was produced by irradiations of enriched ^{160}Gd targets at ILL (V4 beam tube) and PSI (SINQ). The neutron-deficient Tb isotopes ^{149}Tb , ^{152}Tb and ^{155}Tb were produced by 1.4 GeV proton induced spallation in a tantalum target and separated with the isotope separation on-line method (ISOLDE/CERN). Purification of the isotopes was carried out by means of cation exchange chromatography at the PSI.

The carrier-free radioisotopes were used for labeling of cm09 which was then injected into KB tumor bearing nude mice. Excellent tumor-to-background ratios 24 h after injection allowed visualisation of tumor xenografts in mice using small-animal PET/CT (^{152}Tb -cm09) and small-animal SPECT/CT (^{155}Tb -cm09 and ^{161}Tb -cm09) (**figure 4**).

In vivo therapy experiments using ^{149}Tb -cm09 (α -therapy) and ^{161}Tb -cm09 (β -therapy) resulted in a marked delay in tumor growth or even complete remission (33 % for ^{149}Tb -cm09, 80 % for ^{161}Tb -cm09) and a significant increased survival in treated animals compared to untreated controls.

In contrast to clinically employed radioisotopes, ^{161}Tb has the particularity to emit besides β -particles also a significant fraction of Auger electrons. Auger electrons have usually low energies (few eV to few keV), short range in matter (nanometers) and are highly ionising due to high "linear energy transfer". When coupled to vectors that are selectively internalised into cancer cells, Auger emitters could provide thus a very efficient and selective cancer treatment.

Authors

C. Müller and **K. Zhernosekov** (PSI, Switzerland)

U. Köster (ILL)

K. Johnston (CERN, Switzerland)

H. Dorrer and **A. Türler** (PSI and University of Bern, Switzerland)

N.T. van der Walt (Cape Peninsula University of Technology, South Africa)

R. Schibli (PSI and ETH Zurich, Switzerland)

References

[1] S. Lehenberger *et al.*, Nucl. Med. Biol. 38 (2011) 917

[2] C. Müller *et al.*, J. Nucl. Med. 53 (2012) 1951

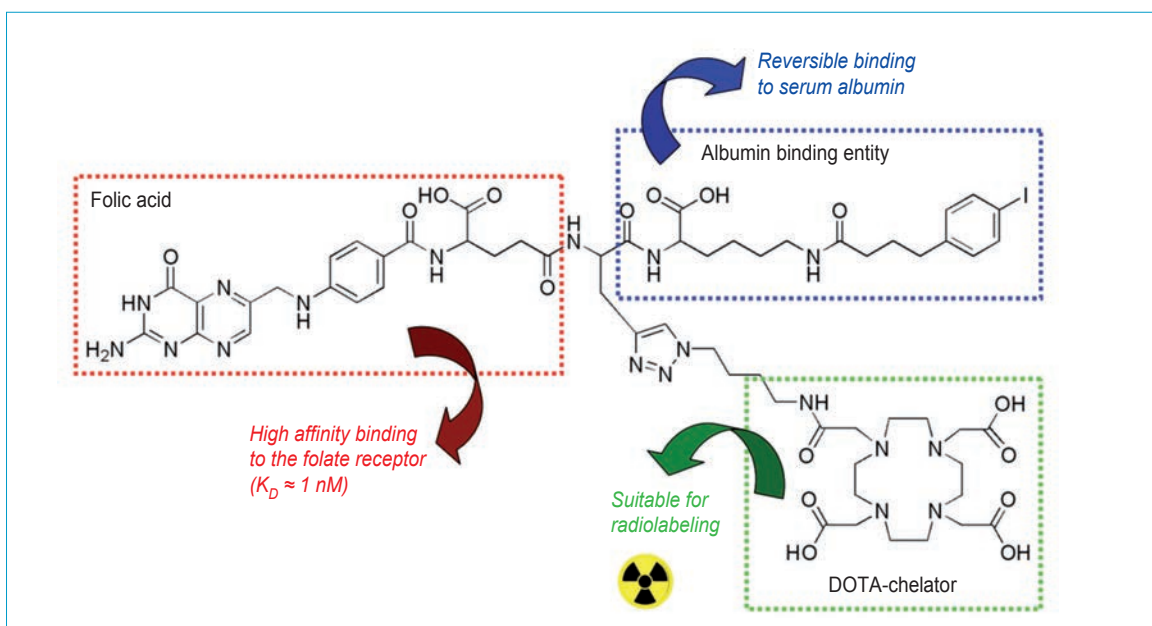


Figure 3: Chemical structure of Tb-cm09 comprising three functionalities: (red) folic acid as the targeting agent, (blue) an albumin binding entity to prolong blood circulation time and (green) a DOTA-chelator for stable coordination of the Tb-isotopes.

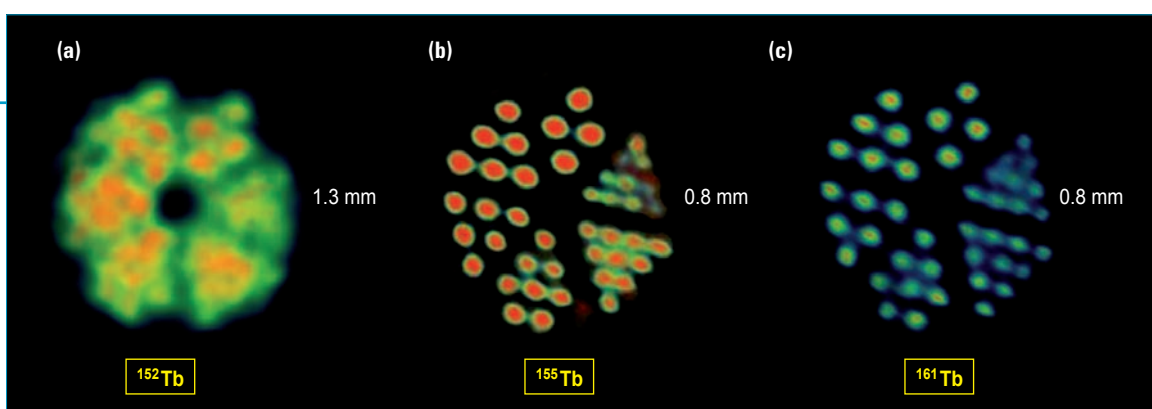


Figure 4: PET and SPECT images of Derenzo phantoms. **(a):** PET image of the β^+ emitter ^{152}Tb , **(c-d):** SPECT images of the diagnostic isotope ^{155}Tb and the therapeutic isotope ^{161}Tb .

Technical and computing developments

^{10}B multi-grid proportional gas counters for large-area thermal neutron detectors

The multigrid concept was introduced at the ILL in 2010. It consists of a gas vessel filled with grids stacked to make square or rectangular tubes [2]. Each grid is composed of blades coated with a neutron convertor material, typically ^{10}B or ^6Li . $^{10}\text{B}_4\text{C}$ was selected for its good mechanical properties. The tubes are equipped with an anode wire biased at positive high voltage. Any neutron captured by an atom of ^{10}B produces two ionising particles, a ^7Li and a α emitted in opposite directions. Only one of the two particles can escape the convertor film and ionise the gas; the other particle is absorbed in the substrate. Depending on the position and time resolution required, the number of readout channels can be minimised by gathering several sensing electrodes, either anode wires or cathode grids. By flushing the gas in the detector vessel during operation, low cost materials can be used to make the production of large-area neutron detectors economically viable. A multigrid detector designed for an instrument like IN5

Helium-3 (^3He) has been indispensable for many decades for the construction of high-efficiency detectors for neutron scattering research into condensed matter.

^3He is a by-product of 12-year tritium decay and its production has dramatically decreased in recent years, due to the (otherwise encouraging) reduction in military tritium stocks. If we are to meet the future demand for detectors, for new instruments at existing and emerging neutron scattering facilities worldwide, an alternative solution to helium-3 detectors will have to be found.

At the ILL we have built and tested a detector using dozens of 10-boron films as a neutron convertor. This "Multigrid" technique is being developed in collaboration with the European Spallation Source (ESS) under the auspices of the EU CRISP project [1].



Figure 1: Inside view of the IN6 Multigrid prototype. Each of the 6 columns contains 16 grids and 60 proportional counters.

would include 1 000 m² of ¹⁰B film, and 10 000 counter tubes; this is beyond our production capability and we are therefore working in collaboration with industrial partners in view of a technology transfer.

A Monte Carlo (MC) simulation programme has been developed to predict the detection efficiency, taking into account the scattering effect in the aluminium, and a 100 KeV energy cut for gamma suppression. According to this simulation, 1 µm of ¹⁰B₄C is the optimal coating thickness for 15 tubes (30 coatings) at 2.5 Å, leading to a maximum detection efficiency of 55 %.

Several prototypes were produced and tested between 2010 and 2012 to study this configuration. The coating was produced by magnetron sputtering [3]. A prototype containing grids with different coating thicknesses was tested on our monochromatic beamline at 2.5 Å. The results show a good match between the MC simulation and experimental results (we measured 53 % instead of 55 %). MC simulation can thus be used to predict detection efficiency at any wavelength. The gamma sensitivity measured with different gamma sources ranges from 10⁻⁵ to 5 10⁻⁵. This value can be improved by a factor 10 by using an energy cut at 150 keV, leading to a reduction in neutron detection efficiency from 53 % to 50 %. Ninety-six grids with 1 µm of ¹⁰B₄C were used in another prototype to make 15 rows of 4 tubes, with dimensions of 1 cm x 2 cm x 200 cm. A low operation voltage (+800 V on the anodes) can be used by filling the detector with 0.5 bar of Ar-CO₂ (90 %:10 %). The non-uniformity of the B₄C film thickness is of the order of 10 %; the variation in detector efficiency was reduced by mounting the blades in a specific order. This prototype was scanned with the Am-Be source mounted on a translation table; after correction for variations due to the electronics we measured a relative deviation in efficiency between the pixels of less than 0.5 %. This therefore establishes the feasibility of a 2 metre-long Multigrid. The 96 grids were then reassembled in 6 columns of 16 grids in a third prototype, in view of a future test on instrument IN6.

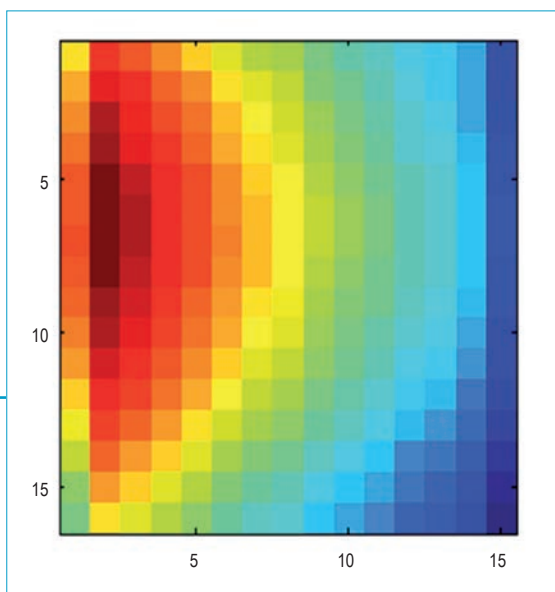


Figure 1 shows the mounting of the detector, and **figure 2** an image measured with an Am-Be source. The detector was scanned by the beamline in the direction parallel to the wires, and the position measured by a centre of gravity method. Preliminary results show good linearity and an average position resolution of 10 mm FWHM for grids of 20 mm height.

In conclusion, our tests of several prototypes show that the Multigrid concept allows large-area detectors to be produced with acceptable performances: the neutron detection efficiency is 50 % at 2.5 Å, combined with a gamma sensitivity of 10⁻⁶. This performance is equivalent to position-sensitive counters of 1" diameter filled with 1.5 bar of ³He. Monte Carlo simulation predicts a 65 % efficiency at 4.5 Å which is the typical wavelength on the IN5 instrument. The counting variation induced by the non-uniformity of the convertor thickness is negligible. Thanks to the small section of the tubes (10 mm in depth), and to the high granularity of the Multigrid, the time resolution and counting rate capability will be better than with standard ³He tubes.

The next step will be to optimise the electronics readout scheme and to continue the study on a real instrument before starting the production of a module measuring 300 cm x 80 cm.

Author

B. Guérard, on behalf of the ILL Detector Service

References

- [1] <http://www.crisp-fp7.eu/>
- [2] Patent n° 20110215251
- [3] C. Hoglund *et al.*, J. Appl. Phys. 111 (2012)104908. DOI: 10.1063/1.4718573

Figure 2:

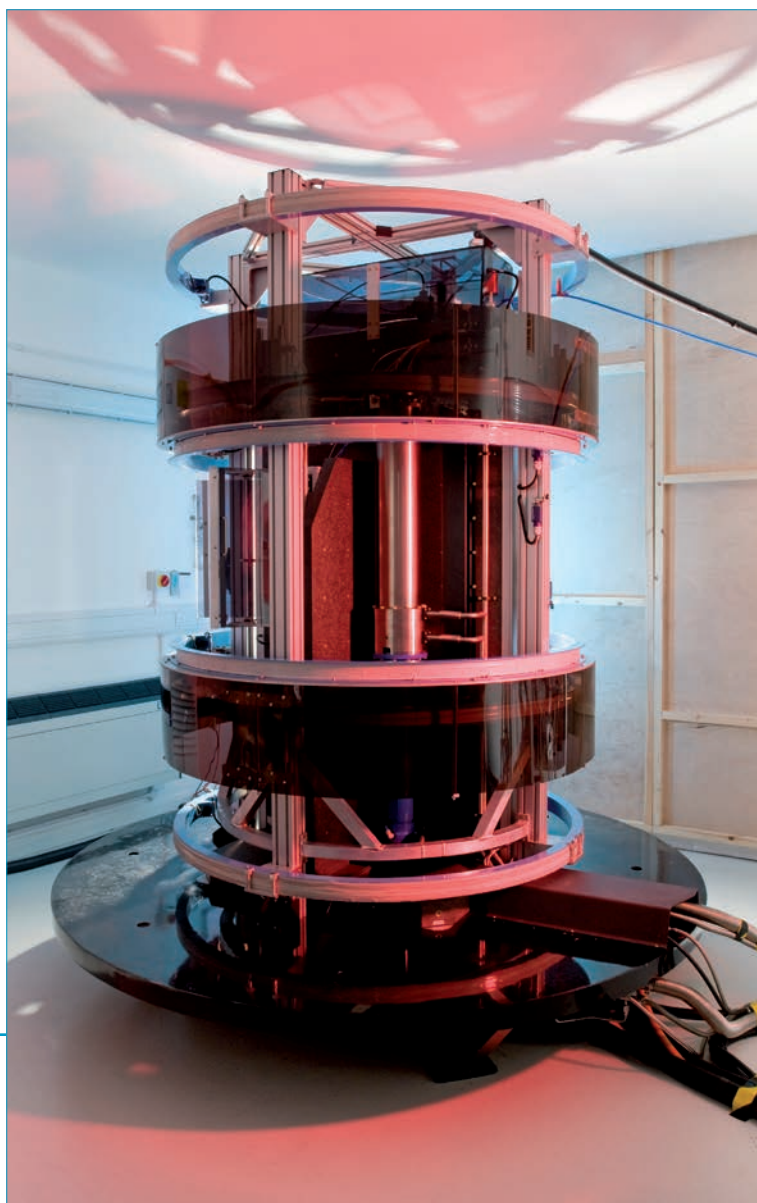
Image measured with the IN6 prototype and an Am-Be source. The horizontal scale corresponds to the grid number, and the vertical scale to the wire number (left = entrance window). The under-counting observed on wires 1 and 15 can be explained by the fact that the first and last B₄C-coated blades are missing.

Technical and computing developments

New-generation polarised ^3He filling stations developed at ILL

Polarised helium-3 neutron spin filters provide an elegant means of polarising neutron beams over the full spectrum of cold, thermal and hot neutrons [1]. We have been polarising ^3He gas using metastability-exchange optical pumping (MEOP) for over a decade at ILL [2]. A MEOP filling station known as Tyrex was commissioned in 2002 and now produces about 1.5 bar l/h of polarised ^3He gas [2]. Tyrex has so far produced more than 1000 bar.litre of polarised ^3He gas in all, allowing numerous neutron experiments to be performed at ILL.

To cope with the growing demand for ^3He spin filters, a new filling station with similar performances has now been designed and constructed at the ILL. Based on the experience acquired with Tyrex, the new station is more compact, with a vertical design to maximise the lifetime of the compressor (**figure 1**).



A new polarised helium-3 filling station has been developed at the ILL. Two of these stations have been constructed and recently delivered, the first to ISIS and the second to ANSTO. Thanks to ILL technology, instruments at ISIS and ANSTO may now soon be reaping the benefits of in-house produced state-of-the-art ^3He neutron spin filters.

All the components of the new station are optimised for high polarisation and reliability. The main advances include a compact polarisation stage, a new compressor, moveable magnetic coils and new automated control software.

The polarisation stage is now composed of six optical pumping cells (rather than five on Tyrex), filled with high purity low pressure ^3He gas. After excitation by an RF discharge of a few hundred volts, the ^3He atoms are optically pumped by three ytterbium lasers, one per pair of optical pumping cell (OPC). To reach a high degree of polarisation, each laser delivers 15 W of 1083 nm infra-red light. The geometry of the OPCs has also been optimised using software developed by the ^3He group. This software simulates the ^3He gas flow, pressures and polarisations in the OPCs for a chosen dynamic mode (filling mode), as a function of the geometry and size of the OPCs (**figure 2**). The optimum size was found to be 80 mm diameter and 1.2 m length for a total gas volume of 31 litres. Our calculations indicate that ^3He nuclear polarisation will be significantly higher than the 70 % requested in the specifications of our partners (ISIS and ANSTO).

Since the process is more efficient at low pressure (around 0.7 mbar), the polarised gas is transferred to a buffer cell and then compressed to the pressure required for neutron applications. The ^3He neutron spin filter cell is then filled with the polarised ^3He gas in the buffer cell. The polarised gas is transferred using an electric non-magnetic titanium compressor, in order to avoid magnetic field gradients which may depolarise the gas.

The MEOP set-up is placed within 6 large coaxial coils providing a homogeneous vertical magnetic field of 10 Gauss. The homogeneity of this field around the OPCs, compressor and buffer is kept at better than $2 \times 10^{-4} \text{ cm}^{-1}$ in order to maintain the level of polarisation.

All the filling station components (electric power system, piston compressor head, gas distribution) are monitored by a LabVIEW application [3]. A real-time automation device ensures system security and a user-friendly interface has been provided to facilitate operations (**figure 3**).

Figure 1:

The new-generation polarised ^3He filling station: a great technological achievement developed and constructed at the ILL.

The first neutron measurements were performed on instrument PF1B at ILL. We measured the neutron transmission of a neutron spin filter cell filled by the new station at four different wavelengths, for three cell filling states: polarised, unpolarised and empty. The results showed ^3He nuclear polarisation close to 70%. The new filling station was operational from Day one with no need for optimisation (for more details see [4]). In April 2012 a first station was successfully completed, transported and installed at ISIS. A second machine was installed at ANSTO in September 2012.

The two facilities are now neutron testing the filters produced by the new stations, with results showing ^3He nuclear polarisation always close to 70%. The preliminary results are therefore very promising and indicate that instruments at ISIS and ANSTO will soon be provided with in-house high-performance ^3He

neutron spin filters! The exceptional work of the ILL ^3He team combined with ILL expertise in polarised neutrons has produced a tremendous achievement.

Authors

P. Courtois, D. Jullien, E. Lelièvre-Berna, P. Mouveau, A. Petukhov, A. Rizzo, N. Thiery, C. Bougnet and S. Marty (ILL)

References

- [1] A.K. Petukhov *et al.*, Physica B 385-386 (2006) 1146
- [2] K.H. Andersen *et al.*, Physica B 356 (2005) 103-108
- [3] <http://www.ni.com/labVIEW/>
- [4] <http://intranet.ill.eu/fr/divisions/projets-et-techniques-dpt/son-servicedoptique-des-neutrons/3he-spin-filters>

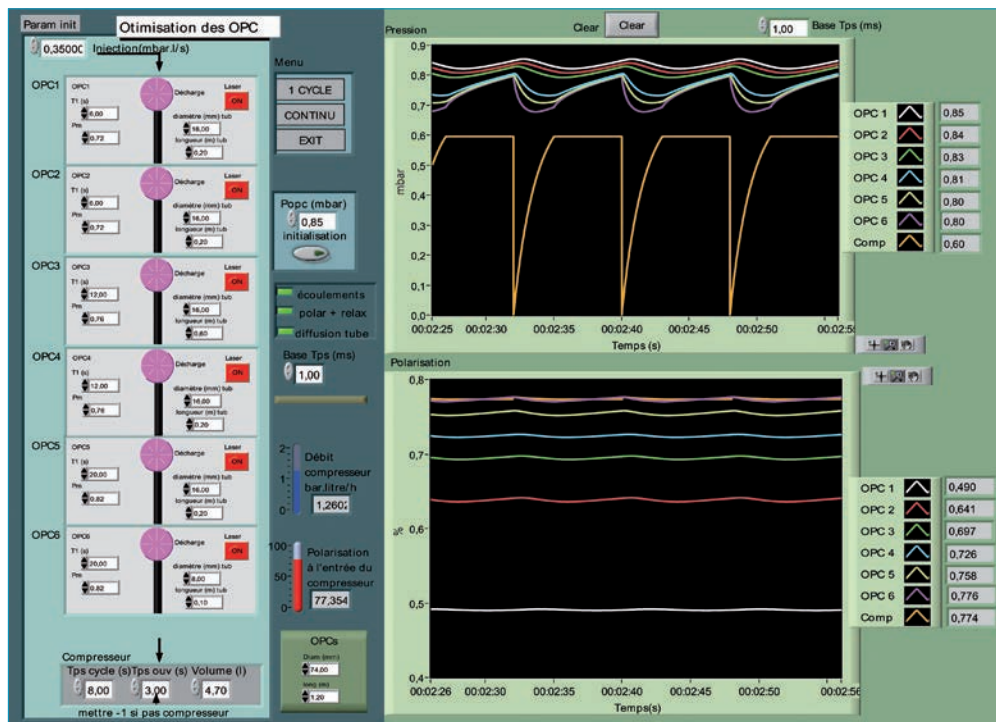


Figure 2: The in-house LabVIEW application simulating optimal OPC operation. Input parameters are (values of) pressure and discharge level of each OPC is entered (on the left). The top plot shows the pressure in each OPC as a function of time, i.e. the compressor cycles. ^3He gas polarisation for each OPC.

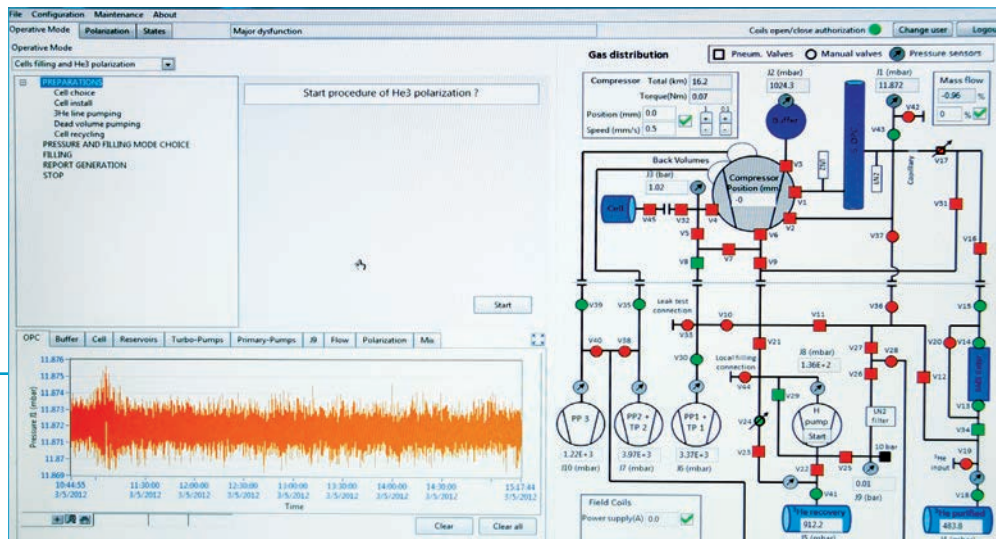


Figure 3: Efforts have been made to provide a user-friendly interface. All the filling station components can be monitored to optimise pressure and gas polarisation when producing the ^3He neutron spin filter.

Technical and computing developments

More neutrons, better science: two new neutron guides boost the ILL's instrument suite

DESIGN CONSIDERATIONS

The guide design developed over the last five years relies on the following principles:

- Collecting neutrons with large angular divergence from the moderator, followed by an increase of the guide cross section to create individual branches with lower divergence.
- Optimisation of each dedicated branch for a specific instrument instead of sharing a standard guide among successive instruments.

To ensure the full illumination of the guide and then its complete filling, the first guide units are optimised using high- m -index reflective coatings and specific shape. Both are defined by the source characteristics and distance between source and guide entrance. The primary section of the guide then expands progressively to reduce flux angular divergence and reflection losses. The guide can then fork into individual branches. To avoid the instrument to be directly exposed to the moderator, the primary section and individual branches are curved, thus minimising background problems. The radius of curvature must also be adjusted to the physical constraints of the guide halls (existing feed-through, walls, pillars in the hot cells, instruments...). This may be achieved by adapting the outer reflective surfaces of the guide using specific supermirror coatings.

Neutron guide technology has improved dramatically over the last 5 years.

Supermirrors with high reflectivity, new designs, and changes in manufacture are providing opportunities to significantly improve the ILL instrument suite.

Two recent achievements illustrate this and how the ILL's Experimental Halls Mechanical Service has developed its expertise: the construction of the brand-new quadruple supermirror guide H141/142/143/144 and the twin guide H112a/H112b.

At the end of the guide close to the instrument, the beam will be shaped to match the divergence acceptable by the instrument (focussing guide, collimation section). For example, the use of specific elliptical shapes with high- m supermirror coatings to enhance flux density ($n/s/cm^2$) by a factor of 2 to 4, and collimation system to reduce the flux divergence

If guides are to exceed 30-50m in length, high transport efficiency requires to reduce the number of neutron reflections inside the guide. This can be achieved by acting on guide geometry. Elliptical shapes are in theory highly efficient as reducing the number of reflexion to close to one, but the space and radiation constraints close to the neutron moderator make

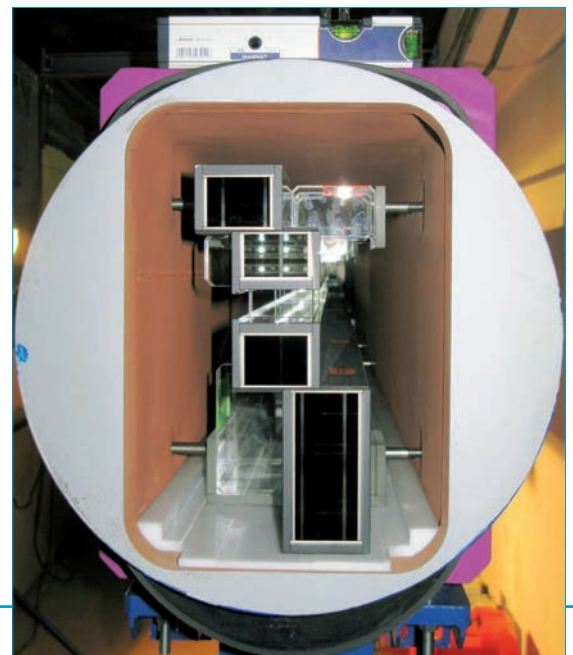
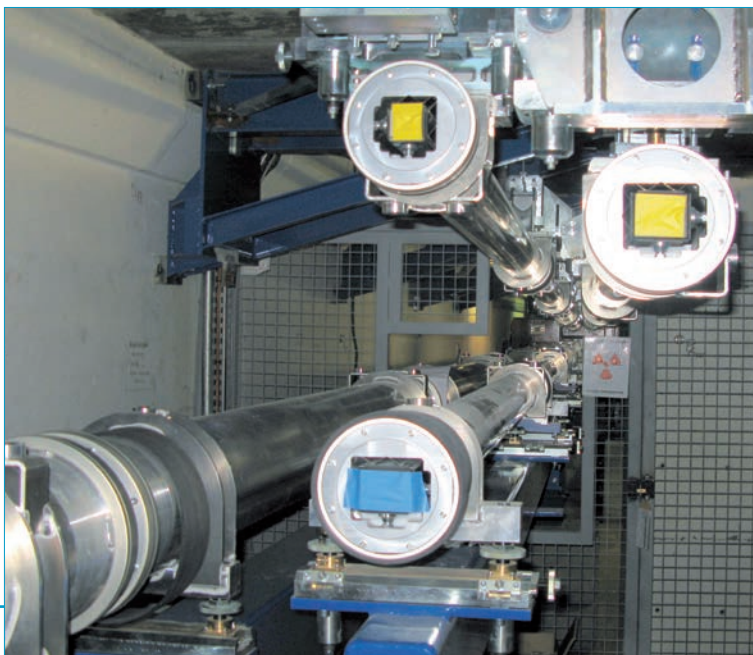


Figure 1: Quadruple guide H14: quad guide unit inside its housing (right), 2.5 m long individual guides in their aluminium housings (left).

them very difficult to implement. In practice, it is easier to use "ballistic" shapes to reduce significantly the number of reflection; these provide typical flux gains of 20-30 % at the guide exit compared to straight guides.

In addition to improving the collection of neutrons and their transport to the instrument, we have also been working on the engineering design. The new design is based on glass guides 2.5m in length (instead of 1m), mounted and pre-aligned within aluminium housings (see **figure 1**). Each of these units can be aligned from outside the housing, using a laser tracker system.

The new design provides several advantages:

- The guide is better aligned, as more alignment operations take place at the manufacturer, where precise geometrical controls can be easily achieved.
- The installation operation at ILL takes less time, as there are fewer guide units to install.
- The guides can be aligned and checked from outside the housings.
- Costs are lower, as standard aluminium tubes are used for the housing, and handling is easier (lower weight).

RESULTS ACHIEVED

The cold neutron guide H14 was commissioned in 1974 to supply neutrons to instrument IN11 on one branch and to IN12, T3, and LADI on the other.

The new H14 was commissioned in November 2011; it has now four independent branches, providing single end-of-guide positions for IN12, IN11, LADI, and the new SANS instrument D33.

Gold foil measurements on the new guide have confirmed the very good transport efficiency as predicted by the McStas simulations (**figure 2**). We obtain indeed the following gain factors, when these measurements are compared to the best historical measures of capture flux on the old H14 guide (following the 1985 upgrade of the vertical source and guide refurbishment):

- IN11⁽¹⁾: x 1.8 (coating upgraded to m=1.4)
- IN12⁽²⁾: x 2.2 (coating upgraded to m=2)
- LADI: x 1.4
- D33: x 1.15

Compared to the best H14 data of "modern times" (following the guide refurbishment in 2005/2006), the gain factors are:

- H14 primary guide: x 3.4
- IN11⁽¹⁾: x 3.1
- IN12⁽²⁾: x 3.5
- LADI: x 3.9

The second new guide, cold neutron guide H112, is a split and ballistic guide designed to feed the new backscattering spectrometer IN16B and an additional future instrument. It was commissioned in April 2012 and transports an m=2 cold neutron beam. Gold foil measurements have confirmed excellent performance, with the capture flux measured at 120 m from the source reaching 2.3×10^{10} n/s cm², a value surpassing even its big brother H113, an m=2 ballistic guide about 50 m shorter than H112: one of the highest value ever achieved in the world for a so long guide.

⁽¹⁾ At the neutron velocity selector.

⁽²⁾ At the secondary shutter.

Author

J. Beaucour (ILL)

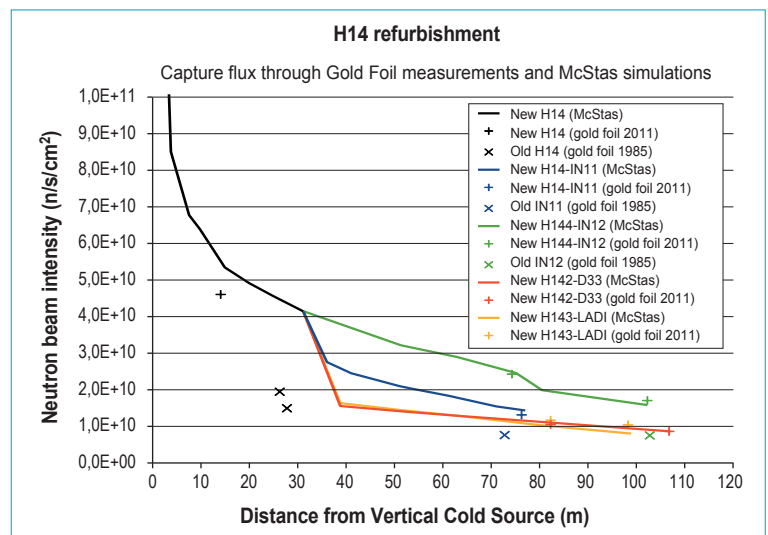


Figure 2: H14: McStas neutron transport calculation compared to gold foil measurements (capture flux).

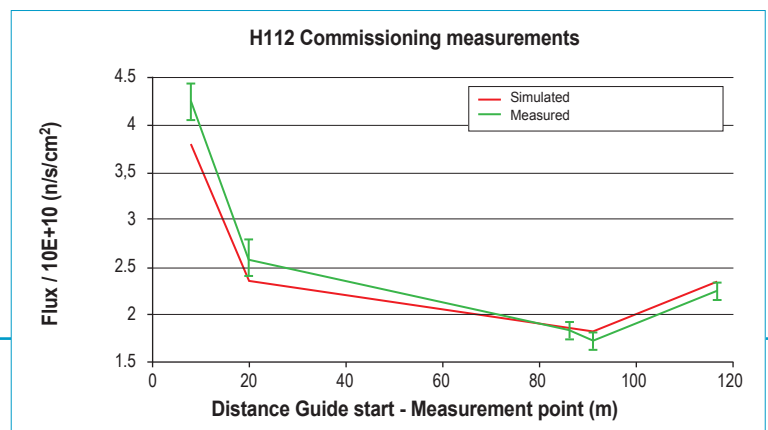


Figure 3:

H112: McStas neutron transport calculation compared to gold foil measurements (capture flux).

Technical and computing developments

NOMAD goes mobile

REMOTE INSTRUMENT CONTROL

Performing an experiment not only happens in the instrument cabin but also from the office, from another instrument, from the lab and from home. NOMAD architecture is heavily based on network technologies and the application can run without graphical interface or be controlled by several different interfaces. All this is made possible by the use of CORBA, acronym for Common Object Request Broker Architecture. CORBA makes the connection between two processes totally transparent whether they run on the same machine or on different ones. This technology together with the availability of powerful mobile devices pushed the Instrument Control Service (SCI) to increase the NOMAD's remote connectivity. The main goal of this new development was to offer an alternative graphic user interface (GUI) for NOMAD running on a tablet support.

Most of the new instruments have considerably increased their dimensions and the control room is today geographically distant from the sample area. All classical operations performed especially at the setup of a new experiment like manual sample and beam alignment or the configuration of the sample environment, becomes then tedious and extremely time consuming.

The commissioning of the new instruments in the M-1 phase of the Millennium Programme has shown the need to extend instrument control technology beyond the scope of classical desktop computers. This, together with the availability of reliable and powerful mobile devices such as smartphones and tablets, has triggered a new branch of development for NOMAD, the instrument control software in use at the ILL. Those devices, often considered only as recreational toys, can play an important role in simplifying life for instrument scientists and technicians.

After a series of benchmark tests performed on a number of different tablets, the SCI has selected the Android based ARCHOS 80 G9, offering an overall good price-to-performance ratio. The compact dimension and the light weight of the tablet, only 8" screen diagonal, offers to the user the possibility to access all functionalities using a single hand, transforming the tablet in a powerful remote control for the most common instrument's operations. The choice of Android as operating system was driven by the possibility to produce a Java application using most of the development already performed for the main NOMAD GUI.

Figure 1:
A tree view allows to select the desired axis and to access the new functionalities to manually control motion.



The interaction between the new remote interface and the server running on the instrument control computer takes place via a specific version of the CORBA protocol (JACORB). The porting of JACORB on Android has been achieved thanks to collaboration between the SCl and the official JACORB developer's team.

A DEDICATED NEW GUI

There is a fundamental consideration to be taken into account when designing a tablet based application, everything must be larger than normal. This includes things such as icons, buttons, text boxes, labels, etc. The first reason is that a tablet application is meant to be used on the 'go' and every element should be easily reachable. Second, the pointing device is often your finger and not a mouse. In order to enhance the user experience and to increase the functionalities of the new GUI, a set of dedicated screens has been developed. Those are not only better adapted to the reduced screen size of the tablet, but they also give access to options specifically developed for the mobile environment.

Figure 1 shows the new axis view in which the standard tree on the left side, allowing the choice of the desired motor, is seconded by a panel dedicated to the selected movement. Classical options like the positioning to a desired value are complemented by new possibilities like a fixed increment starting from the present position or the SeekBar. This last one allows controlling with a single finger the direction of the movement as well as the motor speed by simply moving the slide on the screen left or right. For security reasons, releasing the pressure on the slider will automatically stop the motion.

The new GUI also provides access to sample environment controls. **Figure 2** depicts the screen available to control the orange cryostat, in use at the ILL to hold samples at temperatures as low as 1.5 K. All the basic functionalities relevant for the control of such a device have been included in the interface allowing the user to select the proper PID values, temperature limits, cold valve parameters and other options. The generation of a complex sequence of instrument operations will not be included in the interface since the tablet is not meant to replace the desktop GUI for running the experiment.

WHAT NEXT

So far the ANDROID version of NOMAD has been successfully tested on three different instruments. Despite the fact the overall performances and the user feedback are more than satisfactory one technical aspect needs a deeper investigation. The loss of the WiFi connection during the execution of a command, always possible in a complex environment like the experimental areas of the ILL, should be further secured to avoid dangerous situations. On the development side, the set of tablet oriented screens and functionalities will be further enhanced. A portable rate meter including automatic peak detection is already in preparation as well as a new configuration manager for the sample environment.

Authors

P. Mutti, F. Cecillon, A. Elaazzouzi, Y. Legoc, J. Locatelli, H. Ortiz and **J. Ratel** (ILL)

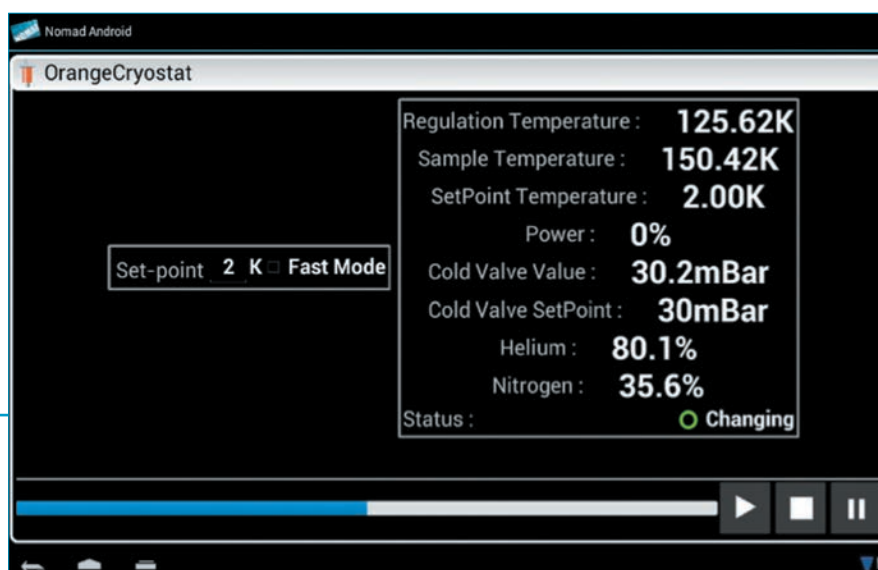


Figure 2: Example of the Orange Cryostat control screen.

User programme
Beamtime statistics
Instrument list



The ILL User Support team is dedicated to helping all visiting researchers to make the most of its facilities. If you are coming to the ILL to carry out experiments, the User Office is here to give you the organisational and administrative support you need to successfully perform your experiments.

Neutron beams and instrument facilities are free of charge for proposers of accepted experiments. Scientists affiliated to the Institute's member countries will also, in general, be assisted with necessary travel and daily subsistence for a limited period. The User Support Team makes all arrangements for accommodation and will process claims for expenses after you have completed your experiment.

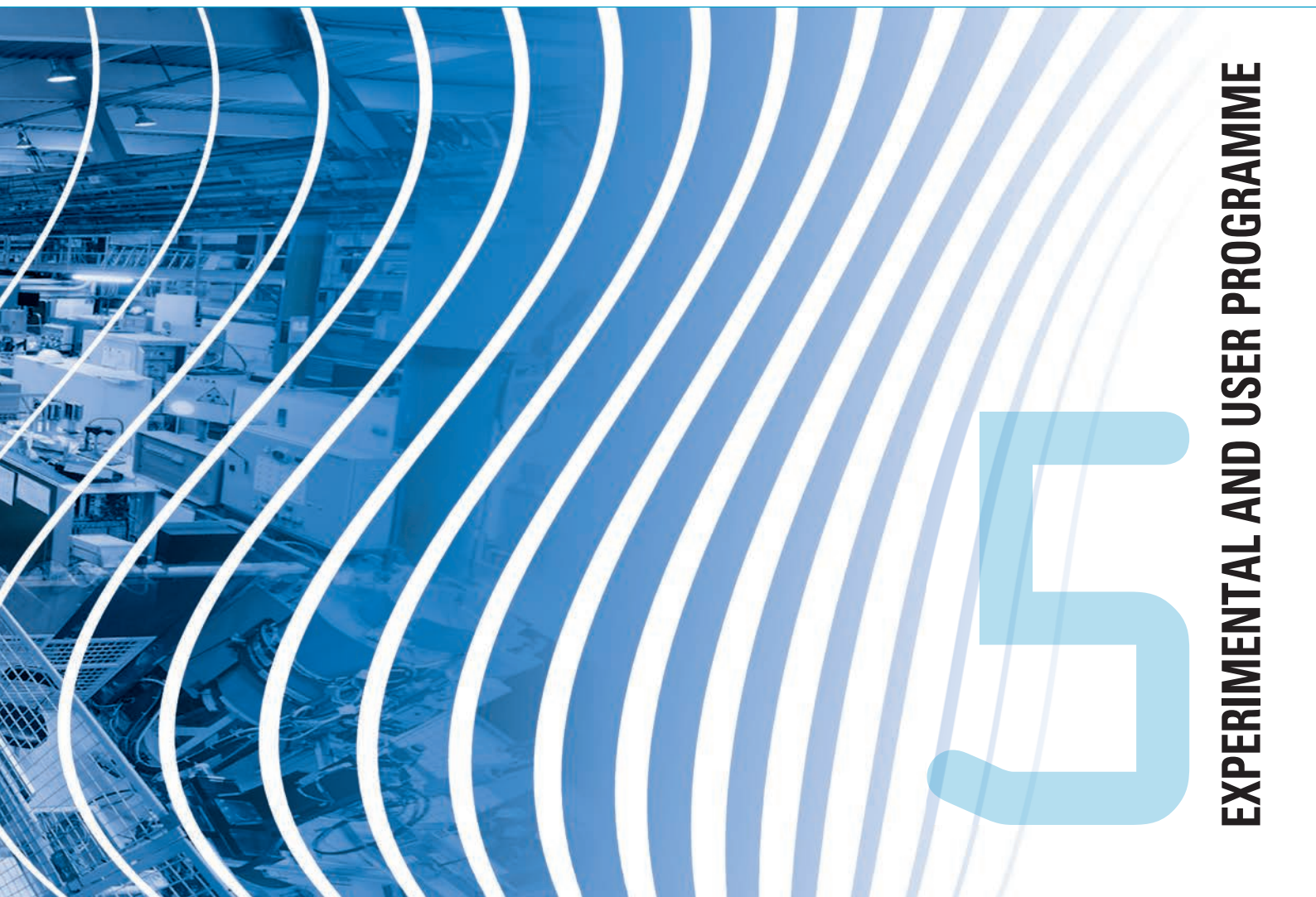
If you would like more information about the Institute's facilities, application for beamtime, user support and experimental programme, please visit our web-site.

<http://www.ill.eu/users>

5

ILL Annual Report 2012

EXPERIMENTAL AND USER PROGRAMME

90
91

EXPERIMENTAL AND USER PROGRAMME

User programme

THE ILL VISITORS CLUB

All administrative tools for our scientific visitors are grouped together and directly accessible on the web, thanks to the Visitors Club. All information is presented in a user-friendly environment. After having logged in with your own personal identification⁽¹⁾, you will have direct access to all the available information which concerns you. Users with particular responsibilities have privileged access to other tools, according to their role. The ILL Visitors Club includes the electronic proposal and experimental reports submission procedures, and electronic peer review of proposals. Additional electronic services have also been put in place: acknowledgement of proposals, subcommittee results, invitation letters, user satisfaction forms and so on.

PROPOSAL SUBMISSION

There are different ways of submitting a proposal to the ILL:

- Standard submission - twice a year - via the Electronic Proposal System (EPS).
- Long-Term Proposals - once a year - via the Electronic Proposal System (EPS).
- EASY access system (EASY) throughout the year.
- Director's Discretion Time (DDT) throughout the year.
- Special access for proprietary research and industrial users.

Submission of a standard research proposal

Applications for beamtime should be submitted electronically, via our Electronic Proposal Submission system (EPS), available on the Visitors Club web-site. Proposals can be submitted to the ILL twice a year, usually in February and in September. The web system is activated two months before each deadline.

Submitted proposals are divided amongst the different colleges (see box below) according to their main subject area.

Proposals are judged by a Peer Review Committee of the Subcommittees of the ILL Scientific Council. Subcommittee members are specialists in relevant areas of each College and they evaluate the proposals for scientific merit and recommend to the ILL Management the award of beamtime to the highest-priority proposals.

Before the meeting, the subcommittee receives a report on the technical feasibility and safety of a proposed experiment from the appropriate College at the ILL. Two proposal review rounds are held each year, approximately eight weeks after the deadline for submission of applications.

There are normally 4 reactor cycles a year, each of which lasts 50 days. Accepted proposals submitted by February will receive beamtime in the second half of the year and those submitted by September, in the first half of the following year. More detailed information on application for beamtime and deadlines is given on our website at

<http://www.ill.eu/users/applying-for-beamtime/>

Easy Access System

The Easy Access System (EASY) grants diffraction beamtime to scientists from ILL member countries, who need a rapid structural characterisation of samples and data analysis. Access is open all year long, and it does not go through the ILL standard proposal round and consequent peer review system.

The system offers one neutron day per cycle, on five instruments (D2B, D16 and OrientExpress) to perform very short experiments at room temperature. The users will not be invited to the ILL, but will send their samples to one of two designated ILL scientists, who will be responsible for the measurements and sample radiological control. The ILL will ship back the sample once the measurement is finished. You can apply for EASY beamtime on the Visitors Club. More information is available at

http://club.ill.eu/cvDocs/EASY_Guidelines.pdf

Long-Term Proposals

Users from ILL member countries can also apply for extended periods of beamtime, by submitting a Long-Term Proposal (LTP). Its purpose is to facilitate the development of instrumentation, techniques or software - which could be beneficial to the ILL community as a

THE ILL SCIENTIFIC LIFE IS ORGANISED INTO 10 COLLEGES

College 1	Applied Metallurgy, Instrumentation and Techniques
College 2	Theory
College 3	Nuclear and Particle Physics
College 4	Magnetic Excitations
College 5A	Crystallography
College 5B	Magnetic Structures
College 6	Structure and Dynamics of Liquids and Glasses
College 7	Spectroscopy in Solid State Physics and Chemistry
College 8	Structure and Dynamics of Biological Systems
College 9	Structure and Dynamics of Soft-Condensed Matter

whole - through the award of beamtime over several cycles. The total amount of beamtime that may be allocated to LTPs on any particular instrument is capped at 10 %, and beamtime is not awarded to LTPs to perform science beyond essential testing.

LTPs can be submitted once a year at the autumn proposal round using the specific LTP application form. The primary criterion for acceptance of a LTP is the excellence of the science that it will ultimately enable. The length of LTP projects is expected to be 3 years typically, with continuation approved at the end of each year, based on an annual report; a final report is also required at the end of the project. More details are given at

<http://www.ill.eu/users/applying-for-beamtime/>

Submission of a proposal to the Director's Discretion Time

This option allows a researcher to obtain beamtime quickly, without going through the peer-review procedure. DDT is normally used for 'hot' topics, new ideas, feasibility tests and to encourage new users. Applications for Director's Discretion Time can be submitted to the Head of the Science Division, Prof. Helmut Schober, at any time.

Experimental reports

Users are asked to complete an experimental report on the outcome of their experiments. The submission of an experimental report is compulsory for every user who is granted ILL beamtime. Failure to do so may lead to rejection in case of application for beamtime for a continuation proposal.

All ILL experimental reports are archived electronically and searchable via the web server as PDF files (under <http://club.ill.eu/cv/>). Experimental reports for experiments performed in 2012 are included in the CD-ROM of this year's Annual Report.

COLLABORATIVE RESEARCH GROUP INSTRUMENTS

The ILL provides a framework in which Collaborating Research Groups (CRGs) can build and manage instruments at the ILL to carry out their own research programmes. CRGs represent a particularly successful form of long-term international scientific collaboration. They are composed of scientists from one or two research disciplines, and often multinational, carrying out a joint research programme centred around a specific instrument. CRGs enjoy exclusive access to these instruments for at least half of the beamtime available. The CRGs provide their own scientific and technical support and cover the general operating costs of these instruments. If there is demand from the user community

and the resources are available, the beamtime reserved for ILL can be made accessible to users via the subcommittees.

There are currently three different categories of CRG instruments:

- CRG-A in which the external group leases an instrument owned by the ILL. They have 50 % of the beamtime at their disposal and for the remaining 50 % they support ILL's scientific user programme.
- The CRG-B category owns their instrument and retains 70 % of the available beamtime, supporting the ILL programme for the other 30 %.
- Finally, CRG-C instruments are used full time for specific research programmes by the external group, which has exclusive use of the beam.

SUPPORT LABORATORIES

The opportunities we offer to our users extend beyond the privileges of access to the world's leading suite of neutron instruments. The ILL - in collaboration with the ESRF and other institutes - is actively responding to the needs of scientists unfamiliar with neutron techniques and in need of training and support facilities. New support facilities have been already set up on the ILL site. For more information see the chapter "More than simply neutrons", p. 104.

ACCESS FOR INDUSTRIAL USERS

Besides academic research, ILL's instruments are used by a wide range of industries from pharmaceutical and chemical companies to materials and process engineering, energy and environment sectors. Neutron techniques are of particular interest in the industrial context as they provide unique and essential informations at the atomic and molecular level.

The Business Development Office (BDO) is the single point of contact for industry to use ILL neutrons scattering instruments. The Business Development Office will match the needs of industrial customers, direct them towards the best technique and scientists and takes care of the administrative procedures. The BDO will provide to industrial customers a fast proprietary access and confidentiality under specific contract giving access to any of the world leading scientific instruments of the ILL. The BDO may also set dedicated R&D partnerships for technological research with consortium including academic and industrial partners.

Contact: Jérôme Beaucour, beaucour@ill.eu

⁽¹⁾ If you are not yet registered in the Visitors Club and you wish to join it, you can register directly at <http://club.ill.eu/cv/>

User and beamtime statistics

THE ILL USER COMMUNITY

The ILL welcomed 1356 users in 2012, including 348 from France, 213 from Germany and 252 from the UK (figure 1). Many of our visitors were received more than once (for a total of 1993 user visits).

We value feedback from our users as an indicator of how well our facility is fulfilling their needs and to initiate actions when this is not the case (see figure 2).

The User Satisfaction Form is a means of finding out what our users think of the facility. Users who have just finished an experiment at the ILL are asked to complete the questionnaire on the Visitors Club and give us their views on different topics. User comments are made available to managers for their information and actions when appropriate.

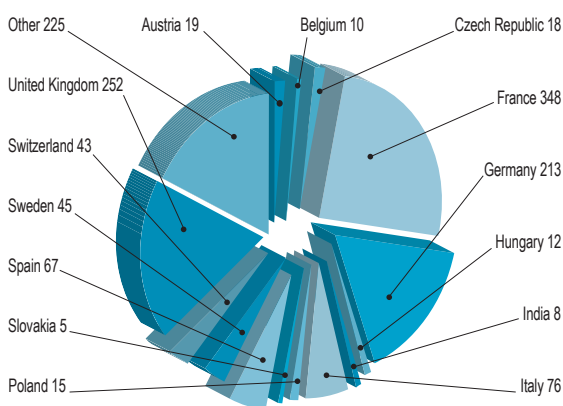


Figure 1: National affiliation of ILL users in 2012.

INSTRUMENTS

The instrumental facilities at the ILL are shown in the schematic diagram on page 98. The list of instruments as of December 2012 is summarised below. Besides the 28 ILL instruments, there are 9 CRG - instruments (marked with an asterisk *):

- Powder diffractometers: D1B*, D2B, D20, SALSA.
- Liquids diffractometer: D4.
- Polarised neutron diffractometers: D3, D23*.
- Single-crystal diffractometers: D9, D10.
- Large scale structures diffractometers: D19, LADI.
- Small-angle scattering diffractometers: D11, D22, D33.
- Low momentum-transfer diffractometer: D16.
- Reflectometers: SuperADAM*, D17, FIGARO.
- Diffuse scattering and polarisation analysis spectrometer: D7.
- Three-axis spectrometers: IN1-LAGRANGE, IN8, IN12*, IN14, IN20, IN22*.
- Time-of-flight spectrometers: BRISP*, IN4, IN5, IN6.
- Backscattering and spin-echo spectrometers: IN10, IN11, IN13*, IN15, IN16.
- Nuclear physics instruments: PN1, PN3.
- Fundamental physics instruments: PF1, PF2, S18*.

LADI and IN15 have a special status, since they are joint ventures of the ILL with other laboratories: in the case of LADI with EMBL and for IN15 with FZ Jülich and HZB Berlin. Cryo-EDM is a CRG-C instrument and is not available as a 'user' instrument. Details of the instruments can be found on the web at <http://www.ill.eu/instruments-support/instruments-groups/>

BEAMTIME ALLOCATION AND UTILISATION FOR 2012

During 2012, the reactor operated for 3 cycles - during which the proposals accepted in the November 2011 and April 2012 rounds where scheduled - representing 148 days of neutrons (see § Reactor Operation, p. 102).

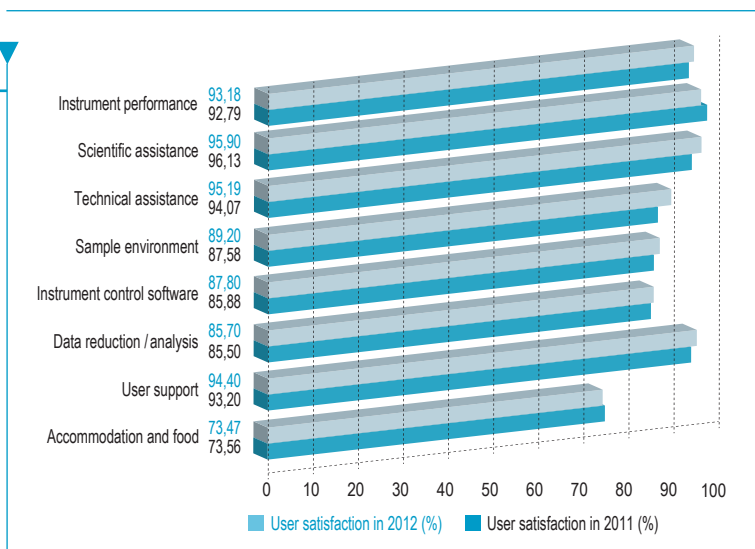


Figure 2: User satisfaction survey results for 2012, compared with those obtained in 2011.

Overall, the Subcommittees of the Scientific Council examined 1386 proposals requesting 8659 days for 2012, out of which 794 proposals received beamtime, allocating 4358 days of beamtime on the different instruments. A total of 869 experiments were scheduled. The distribution of accepted proposals amongst the different research areas and colleges is given in **figure 3**.

In 2012, the member countries of the ILL were: France, Germany, UK, Austria, Belgium, the Czech Republic, Hungary, Italy, Poland, Slovakia, Spain, Sweden, Switzerland and India.

Table 1 gives the beamtime distribution amongst the different member countries (request and allocation in 2012).

In calculating the statistics of beamtime per country, the attribution is based on the location of the laboratory of the proposers, not their individual nationality. For a proposal

involving laboratories from more than one member country, the total number of days is divided amongst the collaborating countries, and weighted by the number of people for each country. Local contacts are not counted as proposers except when they are members of the research team.

The beamtime requested by and allocated to scientists from ILL, ESRF or EMBL is allocated to the member countries according to a weighting system based on the fractional membership of the country of the institute concerned. When a proposal involves collaboration with a non-member country, the allocated time is attributed entirely to the collaborating member country (or countries), and weighted by the number of people for each member country.

Proposals for which all proposers are from non-member countries therefore do not appear in this table.

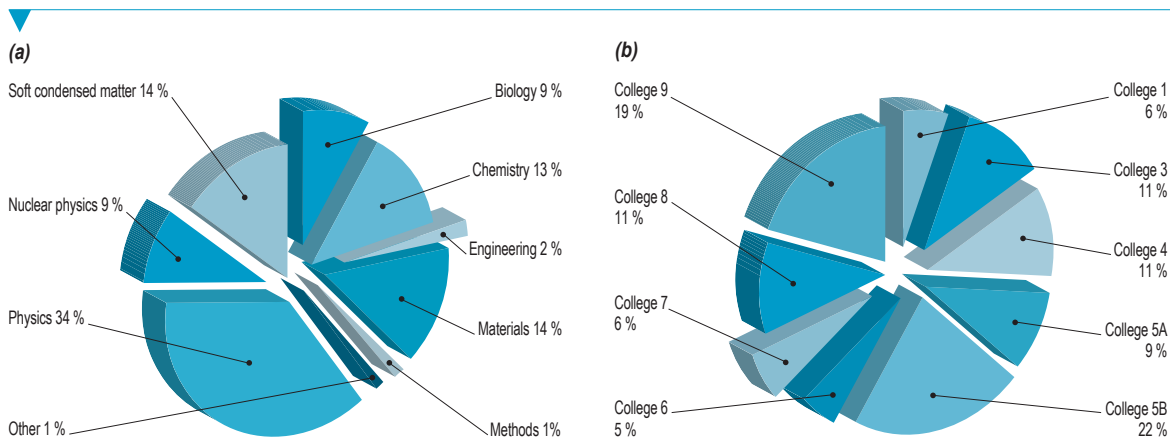


Figure 3: Beamtime allocation in 2012: distribution amongst the different research areas (a) and colleges (b).

Table 1: Distribution amongst the Associate and Scientific-Member countries of beamtime requested and allocated in 2012 during the Subcommittees of the Scientific Council. Proposals from purely non-member countries do not appear in this table; this is why the total request and allocation looks different in **Table 2** (p. 97).

Country	Requested days	Requested in %	Allocated days	Allocated in %
AT	166,26	1,92	124,33	2,85
BE	43,31	0,50	25,54	0,58
CH	413,99	4,78	193,51	4,42
CZ	143,97	1,66	69,28	1,61
DE	2143,34	24,73	1036,84	23,89
DK	57,73	0,66	13,78	0,33
ES	450,04	5,19	204,43	4,72
FR	2194,12	25,36	1295,47	29,61
GB	1747,73	20,18	910,17	20,90
HU	56,42	0,65	36,16	0,82
IN	347,41	4,01	98,40	2,28
IT	528,00	6,11	211,74	4,83
PL	141,06	1,63	72,82	1,65
SE	200,22	2,32	106,08	2,42
SK	19,75	0,23	14,43	0,33
Total	8659,17	100,00	4357,92	100,00

User and beamtime statistics

A more complete view of beamtime use is given in **table 2**. Request and allocation of beamtime as well as the number of scheduled experiments refer to standard submissions to the subcommittee meetings. The effective number of days given to our users takes into account also Director's Discretion Time and CRG time for CRG instruments.

INSTRUMENT PERFORMANCE

Table 2 also gives a summary of instrument performance for 2012. For each cycle, a record is kept of any time lost from the total available beamtime and the reasons for the lost time are analysed for all the instruments. The table gives a global summary for the year.

Overall 4351 days were made available to our users in 2012 on ILL and CRG instruments, which represents about 77.5 % of the total days of operation. 202 days were used by ILL scientists to carry out their own scientific research. About 12 % of the total beamtime available on the ILL instruments was allowed for tests, calibrations, scheduling flexibility, minor breakdowns recuperation and student training.

Beam days delivered for science in 2012 amount to 4553 (used for users and internal research).

In 2012, 356 out of 5613 days were lost due to various malfunctions, which represent about 6 % of the total available beamtime. The breakdown by reasons for beamtime losses is shown in **figure 4b**.

Detailed comments on the larger beamtime losses (above 25 days) are as follows:

- PN1 could operate only one target during the first cycle because of the impossibility of changing target on the H9 side;
- GAMS-5 could not operate during the second cycle because its target changer was blocked;
- GAMS-6 was not operational during the third cycle because the PN3 instrument team was involved in the running of the EXOGAM experiment (*p. 117*).

In addition, the instruments IN12 was only partially available in 2011, because of their dismantling remounting, and consequent commissioning and test time (*p. 115*).

Author

G. Cicognani (ILL)

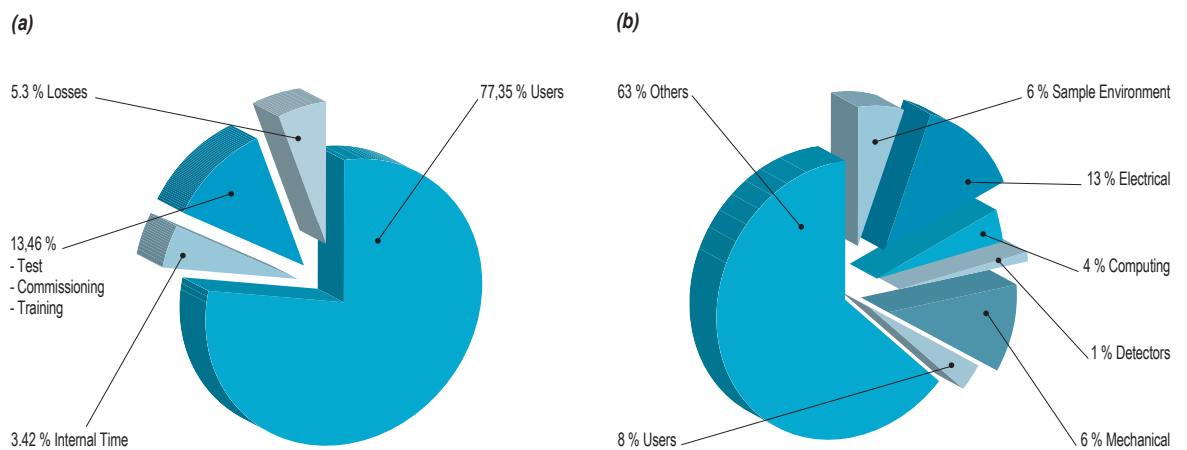


Figure 4: (a) Use of ILL beamtime (b) Reasons for beamtime losses.

REQUEST, ALLOCATION AND INSTRUMENT PERFORMANCE FOR 2012

Instrument	Days requested	Days allocated*	Number of scheduled experiments	Available days	Days used for users**	Days lost	Days for commissioning/test/training	Days for internal research
BRISP	125	54	5	148	129	1	18	0
D10	374	119	27	148	141	3	0	4
D11	272	143	51	148	104	1	43	0
D16	279	114	40	148	115	6	22	5
D17	257	118	30	148	120	10	11	7
D19	272	134	30	148	132	3	6	7
D1B	145	97	26	148	134	4	10	0
D20	318	123	56	148	133	6	2	7
D22	423	116	49	148	110	2	31	5
D23	210	71	23	148	132	0	16	0
D2B	317	80	39	148	134	3	4	7
D3	189	116	16	148	124	2	10	12
D33	80	40	14	148	34	16	87	11
D4	168	65	18	77	67	2	6	2
D7	203	121	19	148	127	4	17	0
D9	267	123	19	148	132	3	9	4
FIGARO	224	115	41	148	119	4	16	9
IN1	159	48	9	71	41	10	20	0
IN10	48	64	6	148	78	2	4	64
IN11	96	45	7	148	82	3	63	0
IN12	44	22	4	44	14	0	27	3
IN13	118	65	10	148	122	4	18	4
IN14	288	122	19	148	135	4	7	2
IN15	324	81	13	148	111	5	29	3
IN16	356	123	23	148	124	7	10	7
IN20	205	116	16	148	117	4	18	9
IN22	83	51	9	148	145	3	0	0
IN4	204	130	34	148	121	10	9	8
IN5	352	142	36	148	114	25	8	1
IN6	202	130	35	148	141	2	5	0
IN8	224	116	18	148	108	1	34	5
LADI	118	70	7	148	98	0	50	0
PF1B	925	762	46	148	138	3	3	4
PF2/5	145	113	9	148	113	0	33	2
PN1	211	128	12	148	75	45	28	0
PN3 - GAMS 5	217	122	8	148	94	54	0	0
PN3 - GAMS 6	76	45	4	93	0	93	0	0
S18	138	134	19	148	140	7	1	0
SALSA	255	77	16	148	121	2	15	10
SUPERADAM	107	75	6	148	132	2	14	0
Total	9018	4530	869	5613	4351	356	704	202
Percentage of the total available beamtime					77,50 %	6,30 %	12,50 %	3,60 %

Table 2: Beamtime request/allocation (via standard subcommittees and DDT together) by instrument and instrument performance. CRG instruments are in blue.

* 'days allocated' refers to only those days reviewed by the subcommittees (i.e., excluding CRG days and DDT).

** 'days used' refers to the total number of days delivered to users (i.e., including CRG days for CRGs and DDT).

PF2 consists of different set-ups where several experiments are running simultaneously. The values given are averages for these positions.

D4 and IN1 share the same beam port and cannot be run simultaneously.

Instrument list

INSTRUMENT LIST - DECEMBER 2012

ILL INSTRUMENTS

D2B	powder diffractometer	operational
D3	single-crystal diffractometer	operational
D4 (50% with IN1)	liquids diffractometer	operational
D7	diffuse-scattering spectrometer	operational
D9	single-crystal diffractometer	operational
D10	single-crystal diffractometer	operational
D11	small-angle scattering diffractometer	operational
D16	small momentum-transfer diffractometer	operational
D17	reflectometer	operational
D19	single-crystal diffractometer	operational
D20	powder diffractometer	operational
D22	small-angle scattering diffractometer	operational
FIGARO	horizontal reflectometer	operational
IN1 (50% with D4)	three-axis spectrometer	operational
IN4	time-of-flight spectrometer	operational
IN5	time-of-flight spectrometer	operational
IN6	time-of-flight spectrometer	operational
IN8	three-axis spectrometer	operational
IN10	backscattering spectrometer	to be dismantled
IN11	spin-echo spectrometer	operational
IN14	three-axis spectrometer	operational
IN16	backscattering spectrometer	operational
IN20	three-axis spectrometer	operational
PF1	neutron beam for fundamental physics	operational
PF2	ultracold neutron source for fundamental physics	operational
PN1	fission product mass-spectrometer	operational
PN3 - GAMS	gamma-ray spectrometer	operational
SALSA	strain analyser for engineering application	operational
VIVALDI	thermal neutron Laue diffractometer	on hold

CRG INSTRUMENTS

SuperADAM	reflectometer	CRG-B operational
BRISP	Brillouin spectrometer	CRG-B operational
CRYO EDM	installation for the search for the neutron electric dipole moment	CRG-C operational
D1B	powder diffractometer	CRG-A operational
D23	single-crystal diffractometer	CRG-B operational
GRANIT	gravitation state measurement	CRG under construction
IN12	three-axis spectrometer	CRG-B operational
IN13	backscattering spectrometer	CRG-A operational
IN22	three-axis spectrometer	CRG-B operational
S18	interferometer	CRG-B operational

JOINTLY FUNDED INSTRUMENTS

LADI (50%)	Laue diffractometer	operated with EMBL
IN15	spin-echo spectrometer	operated with FZ Jülich and HZB Berlin
GRANIT	gravitation state measurement	operated with LPSC (UJF, CNRS)

TEST AND CHARACTERISATION BEAMS

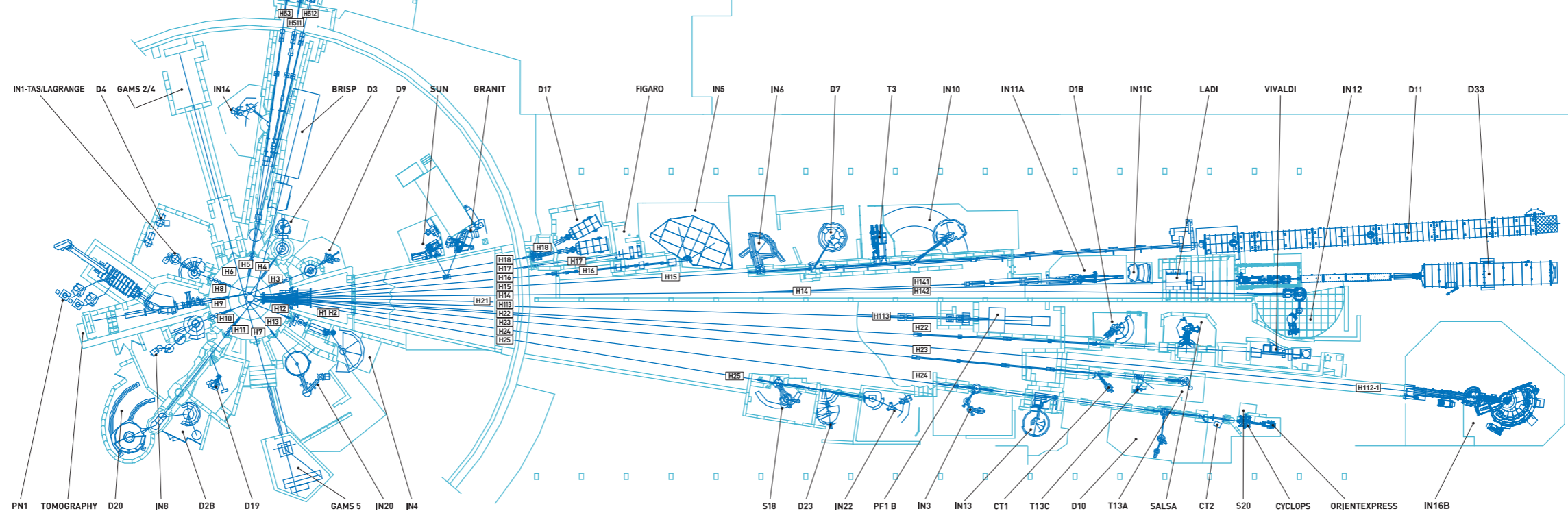
CT1, CT2	detector test facilities
CYCLOPS	Laue diffractometer
TOMOGRAPHY	neutrography
OrientExpress	Laue diffractometer
T3	neutron optics test facility
T13A, C	monochromator test facility
T17	cold neutron test facility

INSTRUMENT LAYOUT - JANUARY 2013

Neutron guide hall / ILL 22

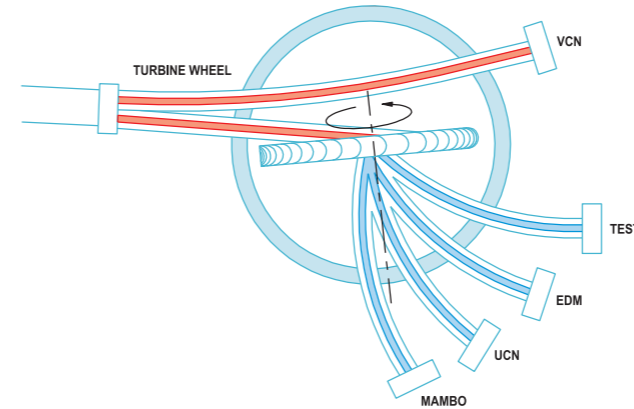


Reactor hall / Inclined guide H4



Reactor hall ILL 5 / Experimental level (C)

Reactor operational level (D)



Neutron guide hall / ILL 7 - Vercors side (WEST)

Neutron guide hall / ILL 7 - Chartreuse side (EAST)



INSTRUMENT LIST - DECEMBER 2012

This ILL High Flux Reactor (HFR) produces the most intense neutron flux in the world: 1.5×10^{15} neutrons per second per cm^2 , with a thermal power of 58.3 MW. The reactor operates 50-day cycles, with each cycle of operation followed by a shutdown period during which the fuel element is changed and a number of checks are carried out. Occasional longer shutdowns allow for equipment maintenance. There normally are 4 reactor cycles per year, supplying 200 days of neutron flux for scientific use.

“... the importance and quality of the safety evaluation report corresponds well to the specifications and enables to perform an analysis of the robustness of your installations ...”

Following the nuclear accident at Fukushima, Japan, the French nuclear safety authority (ASN) decided to launch additional safety assessments on all French nuclear bases (INBs), including the ILL. This additional safety review will have an impact on the Institute and will affect its budget over the next years.

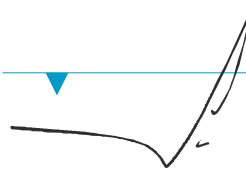


The studies performed by the reactor division teams analysed the behaviour of the ILL reactor under extreme conditions: the earthquake scenarios envisaged would have caused major damage to a town like Grenoble and would have led to the failure of all the dams on the river Drac, leaving the centre of town under 10 metres of water. On 15 September 2011, ILL submitted the results of its analyses to the IRSN (*Institut de Radioprotection et de Sûreté Nucléaire*) and the ASN. On 16 November 2011, the permanent group of experts for nuclear reactors replied with its conclusions: the ILL's proposals have been completely accepted. The precise plan of work has been well received by the Safety Authority. On 6 August 2012, the ASN wrote us:

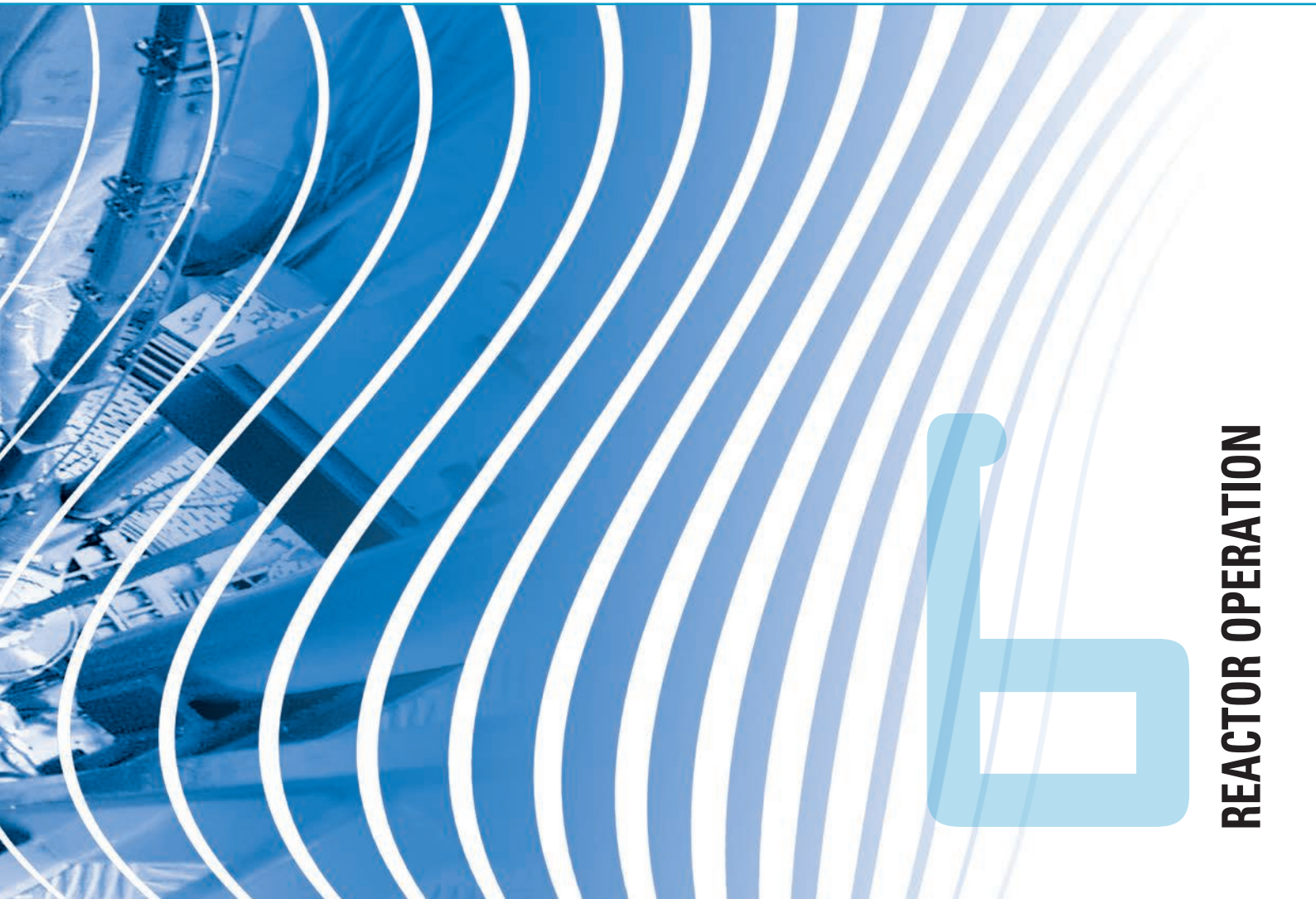
"First of all, I would like to stress the importance and quality of the safety evaluation report you submitted on 15 September 2011. It corresponded well to the specifications and enabled to perform an analysis of the robustness of your installations and of your plans for improvements."

We have now been putting the plans into operation since 2012. You will probably know that a major seismic reinforcement

programme (the so called REFIT programme) has already been carried out at the ILL, ending in 2007. The 2011 studies demonstrated the robustness of the reactor against the maximum physically expectable earthquake, cumulated with the possibility of the loss of the 4 dams upstream on the river Drac. This implies reinforcement of elements traversing the reactor containment and the construction of a new emergency reactor control room for the crisis management teams from which all the emergency safety circuits can be controlled. The civil work of building which will house the emergency control room is already achieved. The whole work is scheduled to be carried out over 5 years (from 2012 to 2016), with no major perturbation to the ILL user programme, and its total cost is estimated at 12 M€.



Hervé Guyon
Head of Reactor Division



3 cycles were planned in 2012, and overall 148 days of scientific activity were provided (**table 1**).

During the second cycle the reactor had to be shut down, as smoke was detected in the room housing the control rod system. The problem was identified as the overheating of an electronic component and the reactor was re-started after a delay due to xenon poisoning.

THE KEY REACTOR COMPONENTS PROGRAMME

In order to ensure reactor safety and reliability over the years to come, the DRe has been pursuing its "Key Reactor Components programme", with the aim of ensuring that the reactor's most important technical components are regularly replaced and improved. The programme started in 2005 and will continue until at least 2017, the date of the next ten-year safety review of our installations.

The main operations planned under this programme are:

- replacement of the beamtubes,
- upgrade of the out-of-pile part of the horizontal cold source, including its instrumentation and control system,
- manufacture of the hafnium safety rods,
- upgrade of the control systems on the safety circuits,
- procurement of backup cells for the cold sources.

OPERATIONS CARRIED OUT DURING THE 2012 REACTOR SHUTDOWNS

- despatch of 6 spent fuel elements to La Hague,
- procurement of 2 spare core cooling pumps,
- installation of the (non-automated) emergency core reflood system. The automated system will only be brought into operation once we have 12 months' experience with the new instrumentation (two different techniques for level measuring in the reactor block),
- bringing into service of the emergency 'tsunami' diesel generator,
- start of manufacture of a prototype hafnium safety rod (currently produced using a silver-indium-cadmium alloy),
- final seismic reinforcements (as defined by the latest requirements on seismic risk),
- replacement of the pressure sensors on the vertical cold source deuterium circuit,

- modifications to the makeup water circuit, to ensure that the two pumps play the same role, thus guaranteeing the highest levels of availability (redundance).

POST-FUKUSHIMA: ADDITIONAL SAFETY ASSESSMENT

The investigations carried out in 2011 and the subsequent discussions with the safety authority's expert groups in November successfully demonstrated that:

- the ILL has significant safety margins with respect to the risk of a design-basis earthquake,
- the loss of a single safety function would never result in an acute escalation of the danger (cliff-edge effect),
- the loss of both reactivity and confinement would never result in an acute escalation of the danger (cliff-edge effect),
- there are always at least two major barriers in place to prevent and mitigate the accidents to be feared,
- fusion under water would never result in a cliff-edge effect.

To comply with requirements following the Additional Safety Assessment, the ILL must ensure it is equipped with a "hard core", by:

- completing its installation of the emergency core reflood system and seismic depressurisation circuit,
- and installing a groundwater supply system, an emergency rod-drop system, and a new emergency reactor control room (PCS3).

The programme of work was defined and progressed as planned in 2012:

- test wells were carried out to define the dimensions of the 2 wells guaranteeing a long-term water supply,
- the structural engineering work for the PCS3 control room was finished - the building is dimensioned to resist an earthquake of 7.3 on the Richter scale on the Belledonne fault, and the breach of the 4 dams on the Drac river.

The ground floor of this building will accommodate the heavy water unit, required for preparing the transfers of heavy water between the ILL and Canada.

WORK PLANNED FOR THE 2012/2013 WINTER SHUTDOWN

The work involves both normal maintenance and pursuit of the operations resulting from the authorities' Safety Assessment.

Table 1

Cycle no.	Start of cycle	End of cycle	Number of days of operation	Number of days scheduled	Number of unscheduled shutdowns
165	07.06.12	01.08.12	55	55	0
166	28.08.12	14.10.12	45.6	47	1
167	24.10.12	09.12.12	46	46	0
Total			146.6	148	1

- introduction of a new automatic fire extinguisher system for electrical installations,
- preparation of the heavy water unit for the start of operations in May 2013,
- replacement of the absorber elements on safety rods 4 and 5,
- maintenance on the control rod mechanism,
- maintenance on the main secondary pumps,
- maintenance on the H9 canal safety valve,
- qualification of the core cooling pumps,
- equipping of the most important rotary machines with vibration measurement facilities.

RADIOACTIVE WASTE AND EFFLUENTS

The ILL's activities in 2012 generated waste and effluents respecting the regulatory limits applicable to our installation, as follows:

Authors

H. Guyon and **J. Tribolet** (ILL)

Evacuation of radioactive waste	Quantity
Decay bin (60 l)*	0
5 m ³ pre-concreted crate (low and intermediate level waste)	0
5 m ³ crate (low and intermediate level waste)	9
200 l drums of "incineratable" (laboratory waste)	61
HDPE drums 120 l (laboratory waste)	7
30 l cylinders (liquid)	3

** Waste stocked in these decay bins is still quite active and requires several years of interim storage before meeting ANDRA's specifications for processing as intermediate-level waste.*

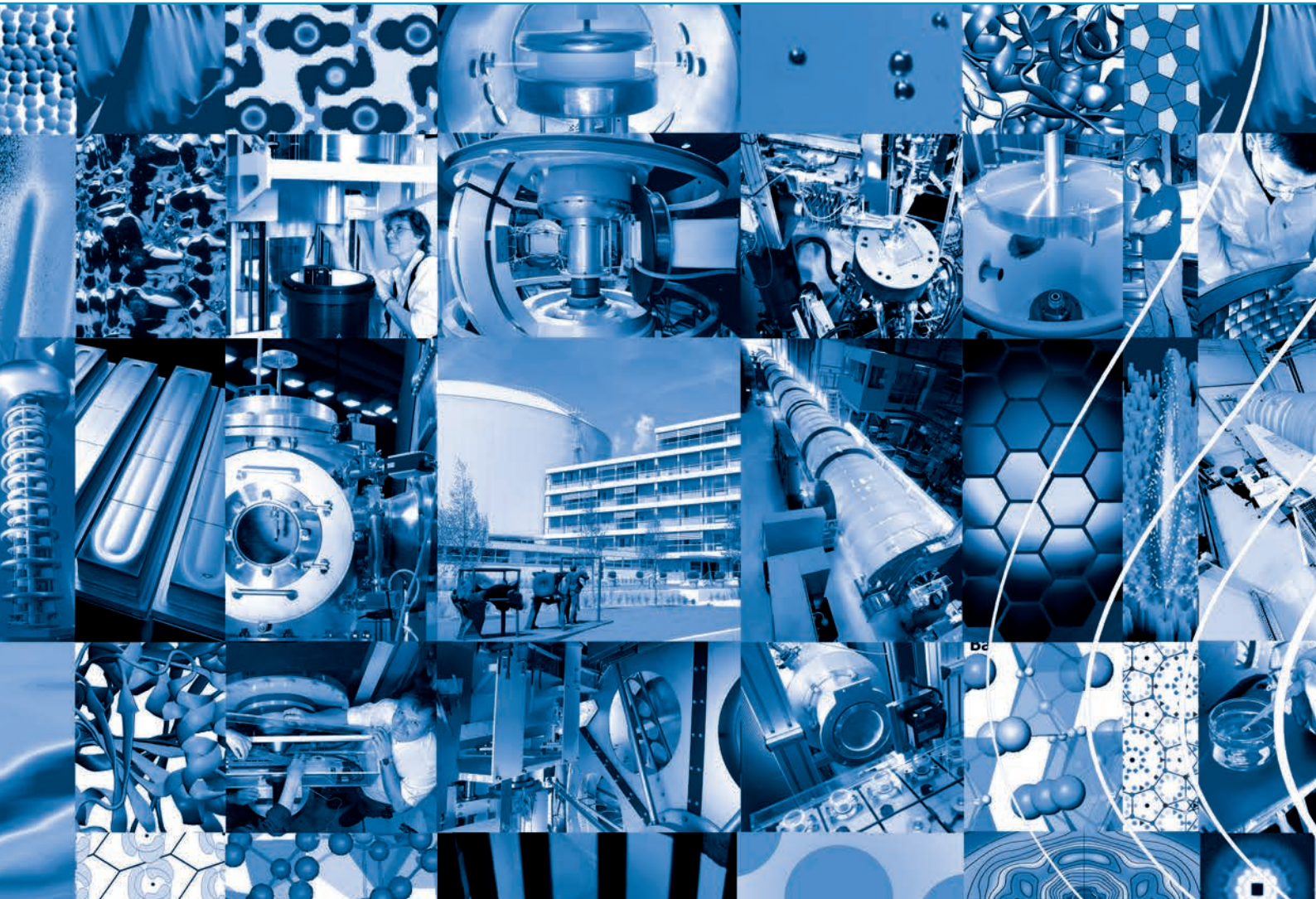
Gaseous effluents	Released in 2012 (TBq)
Tritium	12
Rare gas	0,88
Carbone 14	0,45
Iodine	0,0000014
Aerosols	0,00000031

Liquid effluents	Released in 2012 (TBq)
Tritium	0,37
Carbone 14	0,00027
Iodine	0,0000012
Other activation products	0,00011



The new PCS3 control room in construction.

Scientific support laboratories The EPN - Campus Grenoble and the future



In order to maintain their ranking on the international scene, European research institutes must optimise their resources and develop synergies at every level.

The ILL is firmly committed not only to build high-performance instruments but also to offer the best scientific environment to the user community and it has established successful collaboration with neighbouring institutes over the years. After the successful Partnership for Structural Biology, we have now launched a Partnership for Soft Condensed Matter.

In parallel, the ILL and the ESRF have been working on plans to transform our joint site into a research campus – the **European Photon and Neutron science campus**, or **EPN-campus for short** - with a truly international reputation, and launched an ambitious project to extend the facilities already offered by our international site. The new scientific and technological installations will be complemented with other more general improvements, such as a new Science Building, a new site entrance, a despatch and reception platform, a bigger restaurant and internal roadways.

The ILL is firmly committed not only to build high-performance instruments but also to offer the best scientific environment to the user community.

In addition, the ILL has teamed up with the other institutes located on the Polygone scientifique science park (where our Institute is located) for the GIANT partnership, a project which aims to develop our neighbourhood into a world-class science and technology park. The GIANT project aims to develop Grenoble's Polygone Scientifique into a world-class science and technology park.



Scientific support laboratories

PARTNERSHIP FOR SOFT CONDENSED MATTER

The final Agreement on the Partnership for Soft Condensed Matter (PSCM) between the Founding Partners, ILL and ESRF, has been signed in November 2012. It lays down the scientific and technical goals of the PSCM and develops and specifies the general organisational and operational framework of the PSCM. Laboratories within the PSCM will allow soft matter users to prepare and characterise samples before their experiments at both the ILL and ESRF and will facilitate the performance of complementary *in situ* measurements. The search for Collaborative Partners has started after the signature of the Agreement. By early 2013, the PSCM will be able to host 20 to 30 scientists and technicians both internal and from Collaborative Partners laboratories working in the new Science Building of the joint ESRF/ILL campus. In these laboratories, scientists will be able to prepare experiments with highly complex self-assembled and non-equilibrium soft matter systems in fields related to nanotechnologies, life sciences, environment as well as renewable energy.

Users wishing to use the facility in conjunction with neutrons or synchrotron radiation measurements should indicate this when submitting their request for beamtime.

Further details can be found at

<http://www.ill.eu/instruments-support/labs-facilities/pscm/>

PARTNERSHIP FOR STRUCTURAL BIOLOGY

The Partnership for Structural Biology (PSB) contains a powerful set of technology platforms that are contributed by the various partner institutes (ILL, ESRF, EMBL, IBS, and the unit for host-pathogen interactions). These platforms include advanced capabilities that complement the powerful neutron scattering facilities available to ILL users: synchrotron X-rays, electron microscopy, NMR, high-throughput methods (soluble expression and crystallisation), and a range of biophysical techniques such as isothermal calorimetry and surface plasmon resonance. A joint SANS/SAXS platform has been developed and there is also strong connectivity and collaboration between the ILL and ESRF crystallography groups involved in structural biology and related industrial efforts. The aim of the PSB is to enhance the interdisciplinary capabilities of each of the facilities co-located on the site.

Further details are provided on its website <http://www.psb-grenoble.eu/>. The Carl-Ivar Brändén building (CIBB), is the principal focus for the PSB and its partner organisations.

DEUTERATION LABORATORY

ILL's Life Science Group is located within the CIBB and contains the Deuteration Laboratory platform (D-LAB). The group is involved in a wide variety of externally funded programmes that exploit the capabilities of the PSB as well as promoting interdisciplinary structural biology (see <http://www.ill.eu/PSBLS>). The group also has a number of programmes for method development relating to sample preparation and data collection using crystallography, SANS, fibre diffraction and dynamics; it is therefore of central importance to the activities of biological work relating to all of the ILL instrument groups.

MATERIALS SCIENCE SUPPORT LABORATORY

The joint ILL-ESRF Materials Science Support Laboratory (MMSL) provides a range of support to our users, from advice with experiment proposals to advanced sample metrology. In particular, the Laboratory works with users to optimise the experimental methodology before the start of an experiment. This takes the form of standardised specimen mounting, digitisation of samples, definition of measurement macros and liaising with the instrument responsible. It is recommended that users arrive at the ILL a day or two prior to the start of an experiment to enable these off-line preparations to be performed. More information may be found on the MSSL's website <http://www.ill.eu/sites/mssl/>

C-LAB

The Computation-Lab offers support to ILL users for atomistic simulations using classical and *ab initio* methods. Typical applications for simulations are structure, phonons and (some) magnetism in crystals and structure and dynamics in (partially) disordered systems ranging from liquids and glasses to macro/bio-molecular systems. As samples become more complex, simulations can provide key, complementary information that will help to interpret experimental data and understand how systems behave. Scientists and thesis students at the ILL benefit from the software, hardware and expertise of the C-Lab and users can benefit via their local contacts. In order to improve access to simulations for users, they are now able to request simulation support for their neutron scattering experiments on the official ILL proposal forms by ticking the appropriate box. In 11 proposal rounds since Autumn 2007, there have been 390 requests, at an average of 35 requests per round, with the last round being a record with 55 requests.

For more information see ILL News N.47, June 2007 & N. 50, June 2009 (<http://www.ill.eu/html/quick-links/publications/ill-news/>).

Scientific support laboratories The EPN-Campus

The EPN-Campus

PROGRESS WITH THE 'CPER' PROJECT

The ILL and ESRF have launched an ambitious project to extend the facilities already offered by our international site. Under the French CPER (*Contrat de Projets entre l'Etat et la Région*), significant funding is available to finance it.

Work on all the new buildings currently being constructed on the site made excellent progress: the extension of ESRF and the new IBS (*Institut de Biologie Structurale*) building (see *Annual Report 2011*, p. 109) not to mention the Science Building.

Work started in early March on the **new Science Building**, which is to be located behind the ILL 7 guide hall. When completed, it will provide 5000 square metres of floor space across five levels – four floors of offices and labs etc. and one technical floor. There will be a link between the Science Building and ILL 7, equipped with a hand and foot contamination monitor. The building will also be accessible from the ESRF ring via a footbridge.

The building is due to be delivered in June 2013, and will be home to

- the Science Library
- the Partnership for Soft Condensed Matter

- the Materials Science Support Laboratory
- the Chemistry laboratory
- the Theory Group
- the Grenoble Technology Platform (large-scale instruments characterisation facility).

The CPER projects also include the new site entrance and restaurant extension. The interior of the common ILL-ESRF restaurant will be transformed to increase its capacity. The Theory Group and Science Library will move to the new Science Building to free up space on the first floor. The work will be split into three phases; during phase 2 (May to August 2013), the restaurant services will inevitably be impacted, however the utmost effort will be put into maintaining the best possible service.

The Theory Group and the Library will be accommodated temporarily in other ILL and ESRF premises until the Science Building is ready. The ESRF Works Council will move from ESRF 08 to its new premises on the first floor of the renovated building in summer 2013.

The **new site entrance** will be located on the Avenue des Martyrs, close to the new IBS building and a new tram B terminus.



The state of construction of the science building in November 2012.



The architect design for the new site entrance.

Grenoble and the future

Grenoble and the future

The Grenoble Innovation for Advanced New Technologies partnership, or '**GIANT**', is forging dynamic new links between higher education, research and industry, to foster technological breakthroughs for the future. The city of Grenoble has been supporting the project with the construction of a new 250 hectare town quarter in the neighbourhood of ILL.

A tram line is also being extended, with a new terminus which will serve the ILL well, as it will be only 300 metres from the future site entrance. It will take ca 10 mins to go from ILL to Grenoble railway station and 15 mins to the town centre. The current plans are for the tram to be up and running for the end of 2014.

Authors

G. Cicognani and **F. Vauquois** (ILL)



ILL workshops and schools in 2012

16-20 JANUARY

EMBO Small-Angle Scattering course.

24-27 JANUARY

5th ILL Annual School on Advanced Neutron Diffraction Data Treatment using the FullProf Suite.

1-3 FEBRUARY

2nd International REIMEI workshop.

12-13 MARCH

NMI3 kick-off meeting.

13-14 MARCH

2nd International ¹⁰B BF₃ Detectors' Workshop.

27-30 MARCH

MDANSE school 2012: Molecular Dynamics to Analyse Neutron Scattering Experiments.

13-16 MAY

NddB meeting: Establishing the Neutron Dynamics Data Bank.

21 MAY

Symposium in honour of Philippe Nozières.

27-31 MAY

International workshop on "Perspectives for Neutron Science in Novel and Extreme Conditions".

7-14 JUNE

11th European Summer School on "Scattering Methods Applied to Soft Condensed Matter".

9-11 JULY

NDS 2012, International Workshop on Neutron Delivery Systems.

3-5 SEPTEMBER

Colloquium in honour of Prof. K. Miyake (University of Osaka).

11-14 SEPTEMBER

Mc Phase 2012.

30 SEPTEMBER - 2 OCTOBER

BIOSAS workshop.

3-5 OCTOBER

Structural Dynamics and Dynamical Structures - A Symposium in honour of Joe Zaccai's Career.

26 OCTOBER

A Life of Refinement – 50 years of Neutron Scattering, Colloquium in honour of Alan Hewat.

13 NOVEMBER

Laue Day - 100 years of crystal diffraction symposium.

10-12 DECEMBER

Workshop on Gamma Ray Optics.

Short reports on the ILL workshops can be found on the ILL News (June and December 2012 issues)
<http://www.ill.eu/top-links/publications/ill-news/>

Workshops websites can be found at
www.ill.eu/news-events/past-events/





ILL Annual Report 2012

WORKSHOPS AND EVENTS

110
111

ILL chronicle 2012

4 MARCH - 4 APRIL

HERCULES, the Higher European Research Course for Users of Large Experimental Systems.

5 MARCH

Visit of Richard Banati (distinguished Researcher Fellow) from ANSTO.

16 APRIL

Clip session of the ILL PhD students.

24 - 27 APRIL

Meetings of the ILL Scientific Council and its Subcommittees.

2 - 3 MAY

Meeting of the Subcommittee on Administrative Questions (SAQ).

8 - 9 MAY

Dutch Research Council visit at ILL and ESRF.

13 - 14 JUNE

Meeting of the Steering Committee in Saclay (Paris).

22 JUNE

Visit of a delegation from the Direction Europe de la Recherche et Cooperation internationale (DERCI) of the CNRS accompanied by Nathalie Godet.

9 JULY

Visit of a delegation from the GIANT High level Forum (see <http://www.genevieve-fioraso.com/2012/07/23/high-level-forum-a-minatec-grenoble/>).

12 JULY

ILL takes over as Chair of EIROforum for a year.

20 JULY

Visit of a delegation from ENEA (Italian National Agency for new technologies, Energy and sustainable economic development).

4 - 5 SEPTEMBER

Visit and meeting of the UK Large Facilities Steering Group (LFSG).

12 SEPTEMBER

Visit of an Italian delegation from the CNR and National Research Council.

13 SEPTEMBER

Visit of the CEA Direction Recherche Technologique (DRT).

16 - 17 OCTOBER

Meeting of the Subcommittee on Administrative Questions (SAQ).

22 OCTOBER

Visit of Dan Shechtman, Nobel Prize for Chemistry in 2011.

6 - 9 NOVEMBER

Meetings of the ILL Scientific Council and its Subcommittees.

15 - 16 NOVEMBER

General Assembly of EIROforum DGs, with special guest Prof. Anne Glover, Chief Scientific Advisor of the President of the European Commission and Dr. Anneli Pauli, Deputy Director General of DG Research and Innovation of the European Commission.

21 NOVEMBER

Visit of Mrs Ana Arana Antelo (Head of European Commission Infrastructures Unit).

23 NOVEMBER

Visit of Dr Andris Sternberg of the Institute of Solid State Physics from Latvia.

28 - 29 NOVEMBER

Meeting of the Steering Committee in Grenoble.



Visits and events

- 1 - Clip session of the ILL PhD students on 16 April.
- 2 - On 12 September, Andrew Harrison (ILL Director, centre) and Francesco Sette (ESRF director, second on the right) welcomed a delegation from Italy headed by Prof. Luigi Nicolais (third on the right), President of the "*Consiglio Nazionale delle Ricerche*" (CNR).
- 3 - On 15 October, the ILL hosted the 3rd meeting of the NMI3 public relations network. This group aims to raising the visibility of neutron science and is working on a dedicated website, which should see the light in 2013.
- 4 - Celebration of the 10th Anniversary of EIROforum on 15 November: Andrew Harrison, the Director of the ILL, accompanied by Rolf Heuer, DG of CERN, Bruno Leibundgut, Head of the Directorate for Science at ESO, Mark McCaughrean, Head of ESA's Research and Scientific Support Department, Iain Mattaj, DG of the EMBL, Francesco Romanelli, EFDA Associate Leader for JET, Francesco Sette, DG of the ESRF, and Massimo Altarelli, Chairman and Managing Director of the European XFEL.
- 5 - On 17 February a group of students from the prestigious "*École Polytechnique*" came to visit ILL in the company of Robert Dautray (third on the right), one of the engineers who had worked on the construction of the high-flux reactor. They were accompanied during their visit by Duncan Atkins and Ingeborg Te Groen (first and second on the right, respectively).



A year in photos



ILL Annual Report 2012

WORKSHOPS AND EVENTS

112
113

6 - On 22 June, H el ene Langevin-Joliot entertained us with a lively conference on the life and work of her grandmother Marie Curie. From left: Trevor Forsyth (ILL), Philippe Nozi ere (Professor at the 'Coll ege de France'), H el ene Langevin, John White and Gerry Lander.

7 - On 3-5 October and 26 October and the ILL organised two colloquia in honour of Joe Zaccai and Alan Hewat, respectively, to celebrate their successful careers and acknowledge their contribution to neutron scattering science.

8 - New faces at the ILL management board: Charles Simon (right) is the new French Associate Director and Head of the Projects and Techniques Division; Manuel Rodriguez Castellano (left) is the new Head of Administration.

9 - On 21 May, the ILL celebrated the 80th birthday of Philippe Nozi eres with a symposium in his honour. Philippe Nozi eres, who is a member of the Academy of Sciences and Emeritus Professor at the 'Coll ege de France', has a long association with the ILL and the Grenoble area, where he has lived and worked for over 40 years.



100 years of crystallography

The year 2012 was the 100th year since the birth of crystallography - the central pillar of science supporting the exploration of matter over the last century: in fact, a century ago, the German scientist Max von Laue discovered that X-rays are diffracted by crystals. Ten years later, the neutron was discovered and its dual particle/wave behaviour paved the way to neutron scattering. To celebrate this important anniversary, a number of Grenoble scientists have come together to create the "100 years of crystallography" collective. ILL is of course very active in the group, together with the ESRF, CNRS, CEA, and Grenoble Universities (UJF and INP).

1 - Nobel Prize to quasicrystals

Dan Shechtman – who won the Nobel Prize in Chemistry in 2011 for the discovery of quasicrystals – was invited to the ILL on 22 October to give a seminar and visit our facility. Here is welcomed by Helmut Schober (center) and Charles Simon (left).

2 - Laue Day

To celebrate the 100th anniversary of crystal diffraction and to review recent developments in the field of condensed matter research using X-ray and neutron Laue diffraction, the ILL organised a science day - "Laue Day" - on 13 November.

3 - Marie-Hélène Lemée-Cailleau (ILL, one of the event organisers) with José Baruchel (ESRF).



A year in photos



ILL Annual Report 2012

WORKSHOPS AND EVENTS

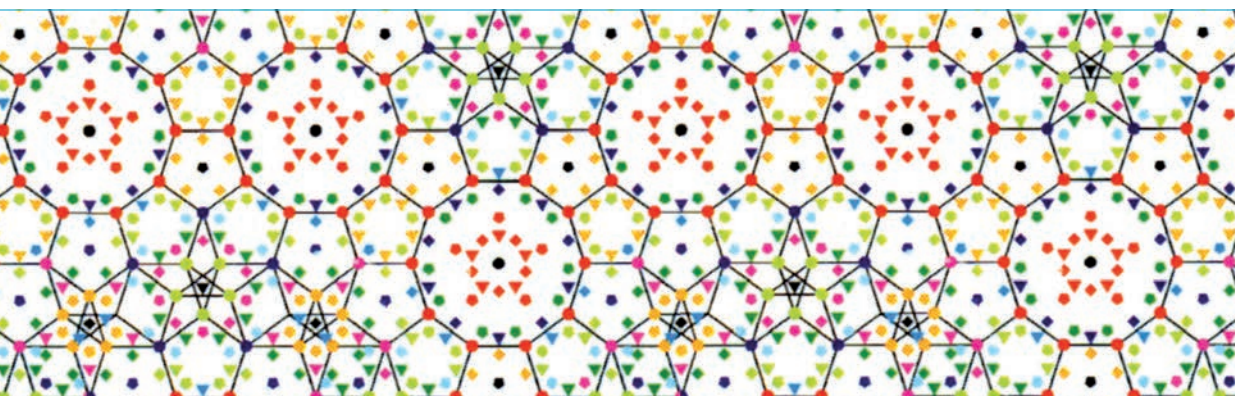
114
115

4 - Science Festival

La 'Fête de la Science' - which takes place every autumn in France – has the purpose of making science accessible to everybody, which is particularly important in Grenoble, where a large number of science institutes, technology-based companies and a university are located. The common ILL-ESRF stand this year was focused on crystallography and was organised and manned together with other local institutes.

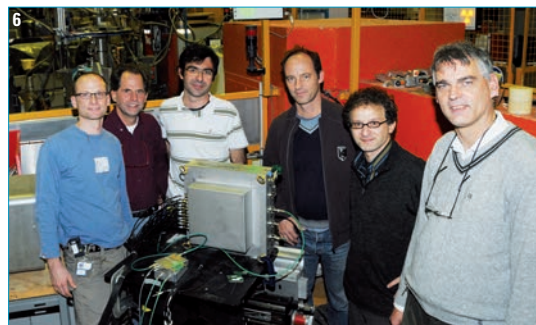
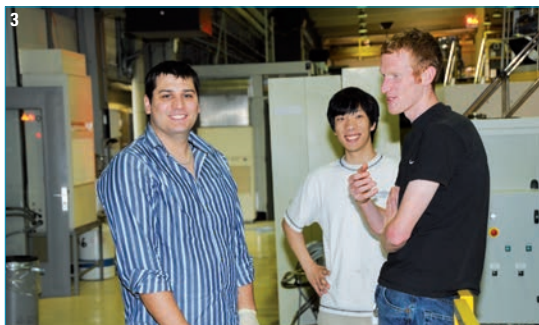
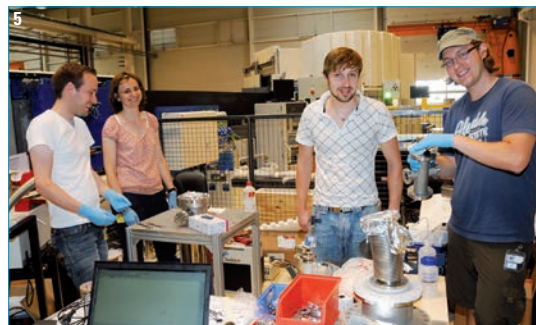
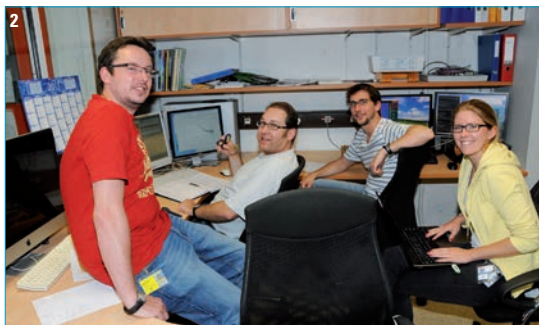
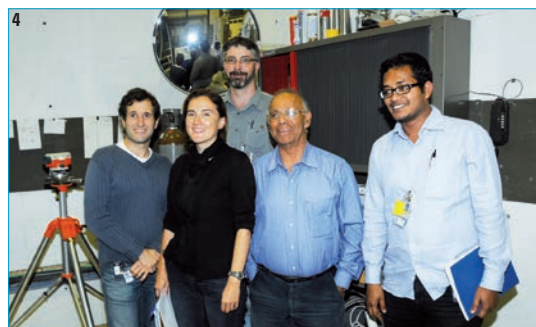
5 - Thanks to Serge Claisse for his photo recording of all these events (and many others)!

In collaboration with the Grenoble CCSTI science centre we have published a set of web pages on the crystallography centenary celebrations: www.100anscristallo-grenoble.com



Happy Users

- 1 - A happy team: the beam was switched on D33 on 20 June at 3h30 pm, and the flux was as good – if not better – than expected. From left: Gilles Rignon, Abdelali Elaazzouzi, Emmanuel Couraud, Charles Dewhurst, Michel Bonnaud, Cyril Amrouni, Isabelle Grillo, Martin Platz and Bruno Guérard
- 2 - From left: Jérôme Crassous (Lund University), Ralf Schweins (ILL), Marc Obiols-Rabasa and Sofi Nöjd (Lund University) on D11.
- 3 - From left to right: Craig James, Cheng Jing and Paul Brown (University of Bristol), happy users on FIGARO.
- 4 - From left to right: Antonio F. Moreira Dos Santos (SNS), Mark Loguillo (SNS), Karin Schmalzl, Tapan Chatterji (ILL), Shibabrata Nandi (Forschungszentrum Jülich) on D23.
- 5 - Alexander Wunderle (Mainz University), Gertrud Konrad (Vienna University of Technology), Jan Peter Karch and Christian Schmidt (Mainz University) on the aSPECT spectrometer.
- 6 - Final test of the prototype developed in the detector work package of the NMI3/FP7-1 project. From left to right: Martin Jurkovic (Heinz Maier-Leibnitz, München), Karl Zeitelhack (ZWE-FRM2 TU München), Davide Raspino (ISIS RAL, DIDCOT), Bruno Guérard (ILL), Riccardo Fabbri (Forschungszentrum Jülich) and Erik Schooneveld (STFC, UK).



A year in photos



ILL Annual Report 2012

WORKSHOPS AND EVENTS

116
117

EXILL – The EXOGAM Array at ILL

The combination of the intense cold neutron beam available at the PF1B position together with the high detection efficiency of the EXOGAM array of high purity Ge detectors (HPGe) has offered a unique opportunity for a set of experiments devoted to nuclear spectroscopy on stable isotopes as well as on exotic nuclei produced in the fission process of uranium and plutonium samples. A combination of 8 EXOGAM segmented clover detectors, 6 large volume GASP coaxial detectors and 2 LOHENGRIN clover detectors have been used to achieve large solid angle coverage around the sample (**figure 1**). All gammas from neutron capture on stable targets as well as fissile targets have been acquired in a trigger-less mode to preserve a maximum of information for further off-line treatment.

A CHALLENGE FOR THE ILL

The EXILL campaign of measurements has been a real challenge for the ILL. The numbers involved in the preparation and in the realisation of the experiment are impressive: a collaboration between 4 major laboratories (ILL, GANIL Caen and LPSC Grenoble in France, LNL Legnaro in Italy), more than 4 tons of very sensitive materials traveling to the ILL, 73 proposals for 2 reactor cycles involving a collaboration of more than 200 users, an array of segmented detectors consisting of 46 HPGe channels and 224 BGO detectors grouped in 14 channels used as active anti-Compton shielding, more than 4000 litres of liquid nitrogen to maintain the Ge crystals at cryogenic temperature, almost 2000 m of cables to provide high and low voltage and to collect all the signals from the detectors, a total acquisition rate of 700 000 events per second generating a data flux of about

10 Mbytes per second, more than 30 Tbytes of data collected in 44 days of operation, and this with negligible beam-time loss and one single detector failure (repaired on the fly).

AN EXTREMELY RICH DATA SET

The first of the foreseen two EXILL campaigns took place from 24 October until 9 December 2012. After an initial test and tuning phase during the first 5 days of beamtime the campaign lasted for a total of 44 days of almost continuous measurements. During this time 16 different target samples have been investigated, with the longest measuring time (22 days) devoted to γ -spectroscopy on fission products from $^{235}\text{U}(n, f)$. From a very preliminary evaluation of the ^{235}U data set we could count 950 billions of recorded events out of which 130 billions of proper triple γ coincidences. **Figure 2** shows a comparison between data from a previous EUROGAM 10 days experiment on ^{248}Cm spontaneous fission and our results collected in only 4 hours run for the same ^{92}Rb nucleus. The total statistic on this low-Z isotope is **a factor of 20 higher** than on previous experiments.

Authors

P. Mutti, A. Blanc, M. Jentschel, U. Köster, E. Ruiz-Martinez, T. Soldner and **W. Urban** (ILL)

F. Drouet, G. Simpson and **A. Vancraeyenes** (LPSC Grenoble, France)

G. de France, L. Menager and **J. Ropert** (GANIL, Caen, France)

C.A. Ur (INFN, Padova, Italy)

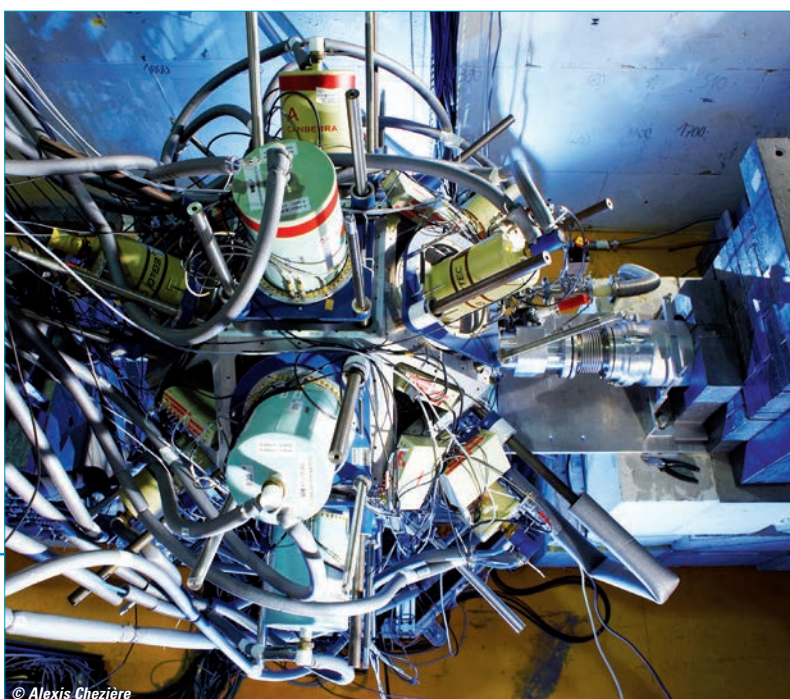


Figure 1: The EXILL set up on PF1B cold neutron beam consisting of 8 EXOGAM segmented clover detectors, 6 GASP high efficiency coaxial Ge detectors and 2 LOHENGRIN segmented clover detectors.

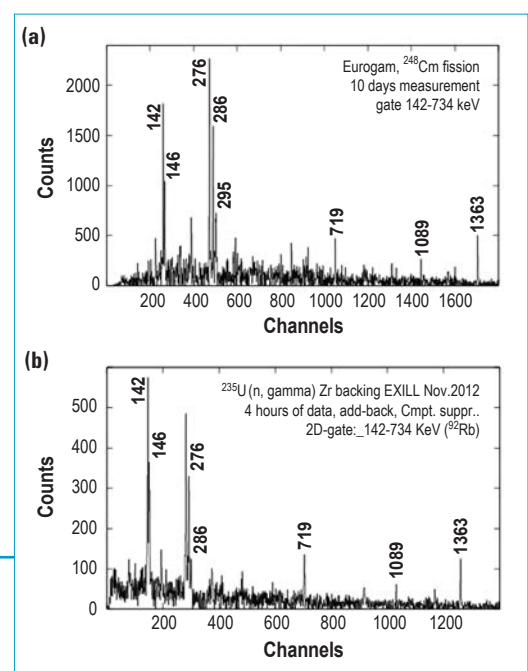


Figure 2: Comparison on the quality of data for low-Z isotope ^{92}Rb between (a) 10 days of EUROGAM data from ^{248}Cm spontaneous fission and (b) 4 hours of data collected with the EXILL set up from neutron-induced fission on ^{235}U .

Facts and figures

Organisation chart

When I took over as Head of the ILL's Administration Division in April 2012, I quickly discovered the high levels of competence and responsiveness of the ILL's administrative staff, as well as their clear motivation to provide a service of quality to ILL's other divisions and ultimately, of course, to the Institute's users. The Administration Division offers expertise ranging from human resource management, finance and purchasing to building construction and maintenance; it is supported by staff with legal experience, and the linguistic skills required in an Institute with three official languages, English, French and German. The Division is also responsible for preparing the working documents to be discussed by the ILL's official committees and for organising the meetings.

By signing the Protocol the three governments formally extend the Convention for a further ten-year period, thus confirming for users ILL's endurance in the neutron landscape for the years to come

The **Human Resources Service** plays a key role in maintaining relations both cordial and efficient with the staff representatives and the personnel as a whole, thus contributing to the high levels of motivation. In 2012 the Service made particular efforts to boost ILL's attraction to scientists and engineers, technicians and administrative staff, including students, from our Associate and Scientific Member countries. We are convinced that ILL has everything to gain by reinforcing its international in-house culture.

The Service was also deeply involved in the establishment of several agreements with the ILL's trade unions.

- The GPEC agreement (providing for a more forward-looking management of jobs and skills at ILL) was signed in December 2012. It concerns all staff members facing possible changes in their professional activity in the medium term. The aim is to facilitate professional mobility, whether in-house or external (secondment). This form of mobility is career-enhancing, and is also compatible with ILL's concern to ensure that the high level of specialist expertise held by critical staff members is passed on when they retire in the years to come. The integration of mobility and versatility in the workforce as a whole will ensure that the Institute is ready to meet the inevitable new challenges to be faced in research with neutrons.
- The ILL, like most of the other national or international research organisations, faced a very difficult budgetary situation in 2012. Despite this, the agreement reached on salaries at the end of the mandatory annual negotiations was a good one, thanks largely to the positive and realistic attitude of our staff representatives.
- As part of the effort to deal with the budgetary restrictions, the Human Resources Service held discussions during the year with the staff representatives on a "medium-term staff development plan". The plan sets out adjustments to minimise the impact of the budget cuts on ILL's operations and output.

Human Resources is also responsible for monitoring changes in social legislation and ensuring that these are properly implemented in ILL regulations. This particularly concerns pension arrangements, which underwent many changes in 2012 following the change of government.



Finance and Purchasing is a service with multiple responsibilities, including of course the ILL budget. In the light of the financial restrictions, budgetary management has become an increasingly complex art. The service was therefore very active in 2012. The year was also marked by work on a major upgrade of the financial control software, introduced primarily to improve and facilitate reporting, to the ILL's financial and governing committees, to Management, to the ILL divisions. This project will continue in 2013. The finance teams were also solicited by ILL's new audit arrangements; these were introduced in 2012 following a review of the ILL Statutes and the roles of ILL's external auditor and Audit Commission.

The Service's Purchasing Group was tested in 2012 by the procurement requirements of the post-Fukushima and Millennium Programmes. The group invested heavily, jointly with the divisions, in improving the return on our Associates' and Scientific Members' investment in the Institute, via purchasing on member country markets. Its work to identify and encourage suppliers in ILL countries led to an improvement in 2012 which is expected to continue in the future.

The Finance and Purchasing Service also successfully negotiated a number of highly strategic supply contracts in 2012, including those for highly enriched uranium, heavy water and electricity.

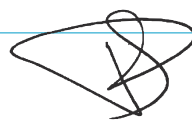
Our **Building and Site Maintenance Service** has been heavily solicited over recent years by the high level of building development on the *EPN Science Campus*, the site we share with the ESRF and the EMBL's Grenoble outstation. It is responsible for managing ILL's part in these projects and their coordination with GIANT activity on the *Presqu'île Scientifique* (p. 109). The new IBS building advanced well during 2012 and should be in use by the end of 2013 (p. 107). The arrival of IBS will increase the scientific opportunities offered by the Campus.

In 2012 the Service was particularly focused on

- the new Science Building, which has progressed well and should be delivered on schedule in 2013 - the building is fully funded by the French local authorities; it is to be shared with the ESRF for the development of scientific and technical partnerships and the hosting of joint services;
- collaboration with the DPT on the installation of new instruments and infrastructure;
- collaboration with the DRe to satisfy the technical requirements of the nuclear authorities following the Fukushima accident.

Finally, on **legal matters**, I should highlight the good progress we made in 2012 towards the signature by the French, British and German governments of the Fifth Protocol to the ILL's Intergovernmental Convention. By signing the Protocol the three governments formally extend the Convention for a further ten-year period, thus confirming for users ILL's endurance in the neutron landscape for the years to come. 2012 was also the year to prepare for the negotiation of our contracts with ILL's Scientific Members for the period 2014-2018.

My management team played a key role in managing these two topics so crucial for the ILL. My special thanks to them for this, and for their contributions to the ILL's different committees.



Manuel Rodriguez Castellano
Head of Administration

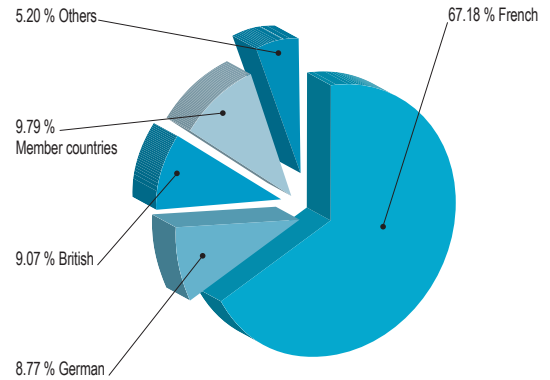


Facts and figures

STAFF ON 31/12/2012

- 490.5 people including 66 experimentalists in the scientific sector and 34 thesis students.
- 329.5 French, 43 German, 44.5 British, 48 scientific participating countries and 25.5 others.

Country		%
French	329.5	67.18
German	43	8.77
British	44.5	9.07
Member countries	48	9.79
Others	25.5	5.20
Total	490.5	100

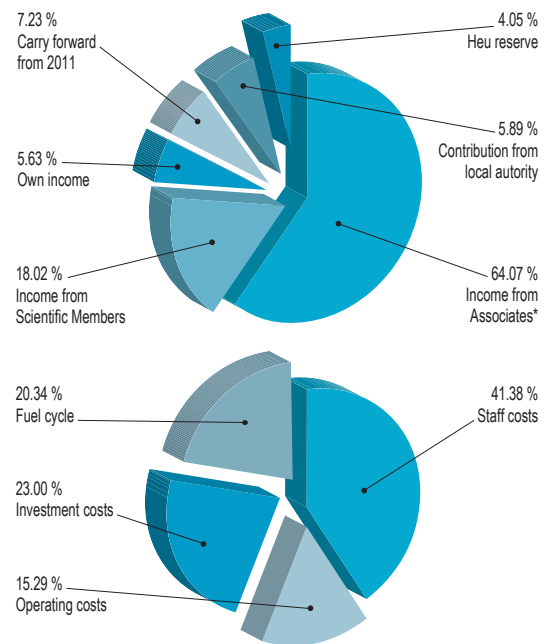


BUDGET 2012: 106 174 M€ (Excluding taxes)

Income	M€	%
Income from Associates*	68.022	64.07
Income from Scientific Members	19.133	18.02
Own income	5.978	5.63
Carry forward from 2011	7.672	7.23
Contribution from local authority	6.251	5.89
Heu reserve	4.300	4.05
Cash flow	-5.182	-4.88
Total	106.174	100.00

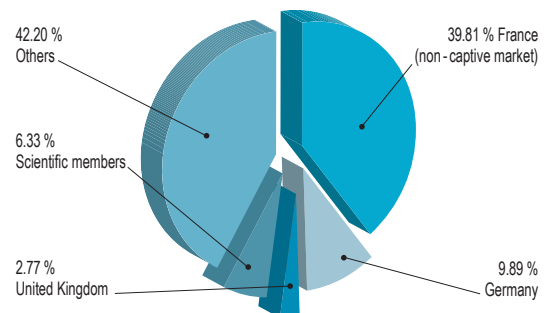
* Including Rex Fukushima expenses, Millennium Programme and Nuclear Tax.

Expenditure	M€	%
Staff costs	43.930	41.38
Operating costs	16.236	15.29
Investment costs	24.415	23.00
Fuel cycle	21.593	20.34
Total	106.174	100.00



PURCHASING STATISTICS (Figures 2012 to end September 2012)

Expenditure	M€	%
France (non - captive market)	10.63	39.81
Germany	2.64	9.89
United Kingdom	0.74	2.77
Scientific Members	1.69	6.33
Others	11	41.20
Total	26.7	100.00
France captif / market	16.57	-
Total captif / non captive	43.27	-



Facts and figures

9
ILL Annual Report 2012
ADMINISTRATIVE MATTERS
120
121

NAME

Institut Max von Laue - Paul Langevin (ILL).

FOUNDED

17 January 1967.

International Convention between France, Germany and UK (19/07/1974).

ASSOCIATES

France

Commissariat à l'Energie Atomique et aux Energies Alternatives (CEA).
Centre National de la Recherche Scientifique (CNRS).

Germany

Forschungszentrum Jülich (FZJ).

United Kingdom

Science & Technology Facilities Council (STFC).

COUNTRIES WITH SCIENTIFIC MEMBERSHIP

Spain

MINECO Ministerio de Economía y Competitividad.

Switzerland

Staatssekretariat für Bildung und Forschung (SBF).

Italy

Consiglio Nazionale delle Ricerche (CNR).

CENI (Central European Neutron Initiative)

Consortium, composed of:

- Austria: Österreichische Akademie der Wissenschaften.
- Czech Republic: Charles University of Prague.
- Hungary: Research Institute for Solid State Physics and Optics (RISP) / Budapest on behalf of the Hungarian Academy of Sciences (MTA).
- Slovak Republic: Comenius University Bratislava.

BELPOLSWENI (BELgian POLish SWEdish Neutron Initiative)

- Belgium: Belgian Federal Science Policy Office (BELSPO).
- Sweden: Swedish Research Council (SRC).
- Poland: Polish Academy of Sciences.

India

Bhabha Atomic Research Centre (BARC).
Interim scientific membership 01/01/2011 - 31/12/2014.

SUPERVISORY AND ADVISORY BODIES

- Steering Committee, meeting twice a year.
- Subcommittee on Administrative Questions, meeting twice a year.
- Audit Commission, meeting once a year, and statutory Auditor.
- Scientific Council with 9 Subcommittees, meeting twice a year.

REACTOR

58 MW, running 3 cycles in 2012 (with cycles of 50 days).

EXPERIMENTAL PROGRAMME

- 869 experiments (allocated by subcommittees) on 28 ILL - funded and 9 CRG instruments.
- 1356 visitors coming from 46 countries.
- 1386 proposals submitted and 794 accepted.



Organisation chart - January 2013



REVIEW PANELS (Chairs)

APPLIED METALLURGY, INSTRUMENTATION
AND TECHNIQUES

D. Hughes (WMG, University of Warwick, UK)

NUCLEAR AND PARTICLE PHYSICS

W. Korten (CEA Saclay, France)

MAGNETIC EXCITATIONS

E. Blackburn (Birmingham University, UK)

CRYSTALLOGRAPHY

R. Walton (Warwick University, UK)

MAGNETISM

R. Kremer (MPI Stuttgart, Germany)

STRUCTURE AND DYNAMICS
OF LIQUIDS AND GLASSES

D. Holland-Moritz (Institute of Materials Physics in Space,
Cologne, Germany)

SPECTROSCOPY IN SOLID STATE PHYSICS
AND CHEMISTRY

D. Djurado (CEA Grenoble, France)

STRUCTURE AND DYNAMICS
OF BIOLOGICAL SYSTEMS

C. Cardin (Reading University, UK)

STRUCTURE AND DYNAMICS
OF SOFT-CONDENSED MATTER

J. Cabral (London Imperial College, UK)

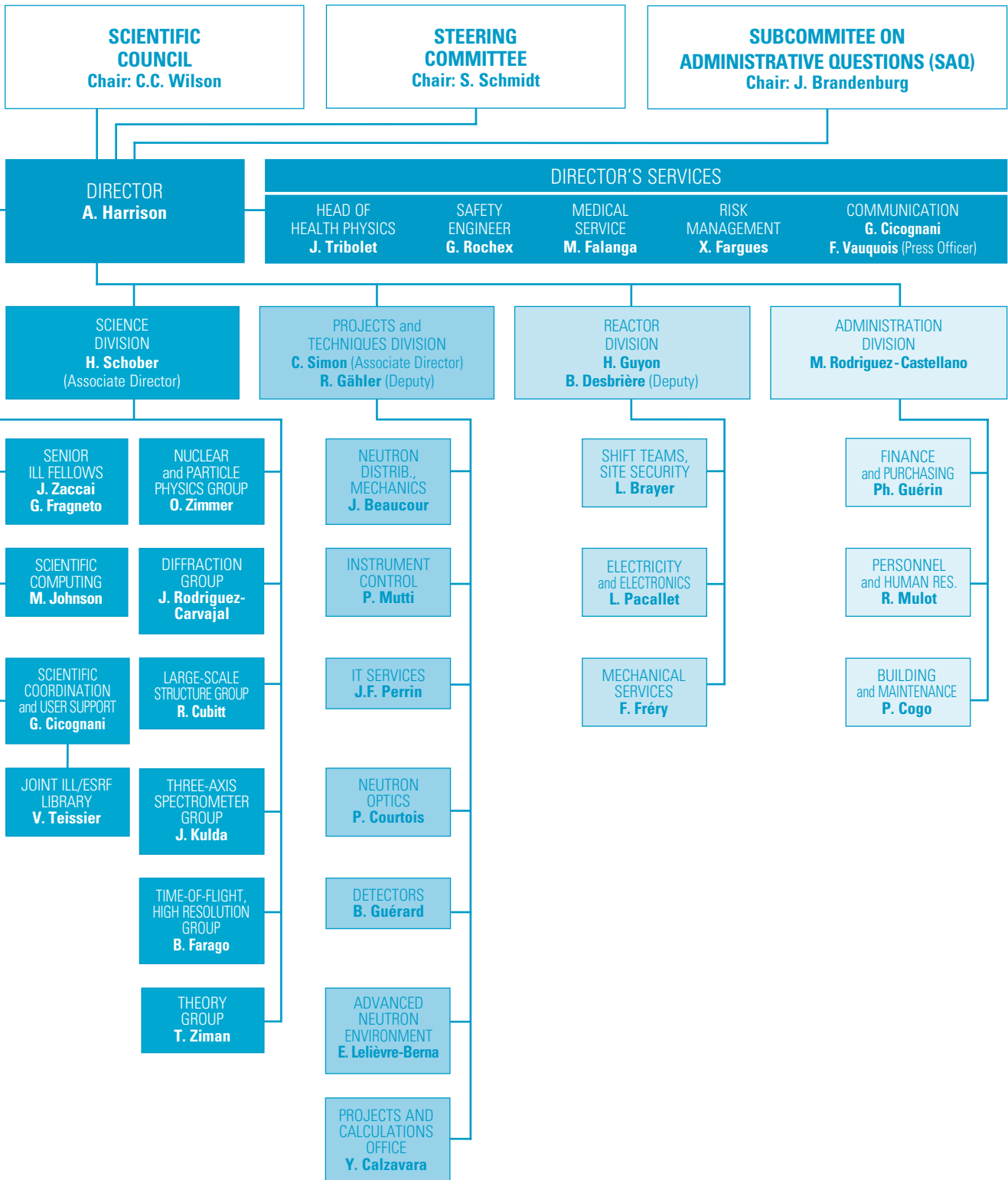
Organisation chart



ILL Annual Report 2012

ADMINISTRATIVE MATTERS

122
123



Publications in 2012

In 2012, the ILL received notice of 552 publications by ILL staff and users. They are listed in the CD-ROM of this year's Annual Report.

The distribution by subject is as follows:

Applied Physics, Instrumentation and Techniques	28
Biology	49
Crystallography	92
Liquids and Glasses	34
Magnetic Excitations	64
Magnetic Structures	86
Materials Science and Engineering	53
Nuclear and Particle Physics	37
Theory	13
Soft Matter	72
Spectroscopy in Solid State Physics and Chemistry	24

ILL PhD studentships

PhD students at ILL in 2012*	32
PhD theses completed in 2012	7

* Receiving a grant from ILL

Books published in 2012

